PREDICTION OF PHARMACOKINETIC BEHAVIOUR OF SOME DRUGS BY *INVITRO* STUDY

A THESIS SUBMITTED TO

THE MAHARAJA SAYAJIRAO UNIVERSITY OF BARODA
FOR THE AWARD OF DEGREE OF

"DOCTOR OF PHILOSOPHY"
(PHARMACY)

By
Ms. DIPTI BIPIN RUIKAR
Under the Guidance of
Prof. (Mrs.) SADHANA J. RAJPUT

Pharmacy Department,
Faculty of Technology and Engineering, Kalabhavan
The Maharaja Sayajirao University of Baroda
Vadodara – 390001, Gujrat.
April 2013

Pharmacy Department
Faculty of Technology and Engineering,
The Maharaja Sayajirao University of Baroda,
Post Box No. 51, Kalabhavan, Vadodara – 390 001, INDIA
Phone: (+91-0265)2434187 Fax: (0265)2423898/2418927.
E-mail: head-pharm@msubaroda.ac.in

Date:

CERTIFICATE

This is to certify that the thesis entitled, **"Prediction Of Pharmacokinetic Behaviour Of Some Drugs By *Invitro* Study"** submitted for the Ph.D. degree in Pharmacy by **Ms. Dipti Bipin Ruikar** (Registration Certificate No. 282) incorporates original research work carried by her under my supervision and no part of the thesis has been submitted for any other degree.

Prof. (Mrs.) Sadhana J. Rajput
Research Guide

Head
Pharmacy Department

Dean
Faculty of Technology and Engineering,
The M S University of Baroda

DECLARATION

In accordance with the University Ordinance No. FTE/1809 Ph.D., I State that the work presented in this thesis titled "**Prediction Of Pharmacokinetic Behaviour Of Some Drugs By *Invitro* Study** "*comprises of independent investigations carried out by me at the Pharmacy Department, Faculty of Technology & Engineering, The M. S. University of Baroda, Vadodara. Wherever references have been made to the work of others, it has been clearly indicated with the sources of information under the References in the individual chapters. The results of this work have not been previously submitted for any degree or fellowship.*

Ms. Dipti B. Ruikar

Certified and forwarded through Research Guide

Prof. (Mrs.) Sadhana J. Rajput
Pharmacy Department,
Faculty of Technology & Engineering,
The M. S. University of Baroda,
Kalabhavan, Vadodara – 390 001.

Acknowledgements

Today with humility, misty eyes and folded hands when I thank Almighty in these blissful moments, I am also expressing my innermost into words. Research is an arduous task that involves consistent and dedicated mind with persistent hard labour put into it. This can only be possible with His benediction and grace.

Language is the most eloquent vehicle of human expression, yet on occasions one finds it difficult to get appropriate words to express an emotion fully. Speech fails me when I fumble for words to articulate my heart felt and sincere gratitude to my worthy supervisor, ***Prof. (Mrs.) Sadhana J. Rajput,*** *whose continuous encouragement, invaluable guidance, constructive criticism, precious suggestions, crucial help, benevolent attention and tireless efforts enabled me to execute this project successfully. I will never forget the spirit of sincerity, devotion, dedication, moral certitude and ethics she has inculcated within me during this period.*

I express my sincere thanks to ***Prof. M. R. Yadav****, Head, Pharmacy Department, and my Resea rch colleague* ***Prafulla Sable*** *for providing me the potential new molecular entities to carry out project work.*

With great reverence, I also express my debt of gratitude to Prof. A. N. Mishra, Prof. S.H. Mishra, Dr. (Ms.) R. Mashru and Prof. (Mrs.) K. Sawant for their valuable suggestions and help whenever sought for.

I am immensely thankful to M/S Torrent Pharmaceuticals, Gandhinagar and Sun Pharmaceuticals Ltd., Baroda for providing me gift sample of APIs.

I am immensely thankful to AICTE, New Delhi for providing National Doctoral Fellowship (NDF).

I avail this rare opportunity to articulate my genuine appreciation to my most treasured friends, Abhishek Pathak, Diti Desai, Reshma Jain, Greeshma Patel & Prachi Bhamre who helped me as and when required without giving second thoughts. Thanks are also due to my friends Anita, Manjul and co researchers Kaustubh, Sandip, Kailash, Ahinesh, Anand for making this time memorable, with lots of cherished reminiscences to look at back. I am also grateful to my juniors Asiya & Bindiya for their help whenever needed. I am thankful to all those who have helped me in whatsoever manner during this work whom I might have missed inadvertently.

My heartiest thanks are due to all the non-teaching staff of G.H.Patel Building and Pharmacy Department, Kalabhavan.

I express my deepest sentiments of affection for my loving husband, and my daughter , PARI for their constant moral support.

Finally I would like the appreciate the endless love, care, patience and faith shown on me by my parents (RUIKAR) and in laws (DESHMUKH) who have stood behind me in every endeavor and have provide constant encouragement whatever be the situation.

Dipti B. Ruikar
alias
Mrs. Dipti Gajanan Deshmukh

Dedicated to my husband

GAJANAN

for his continuous encouragement

&

my darling daughter PARI……

INDEX

LIST OF FIGURES

LIST OF TABLES

List of Abbreviations

ADME	Absorption, Distribution, Metabolism, Excretion
ADMET	Absorption, Distribution, Metabolism, Excretion and Toxicity
ANOVA	Analysis Of Variance
ATV	Atorvastatin
AUC	Area Under Curve.
AUCc	Area Under Concentration-Time Curve
CHZ	Chlorzoxazone
CL	Total Body Clearance
Clh	Hepatic Clearance
Clint	Intrinsic Clearance
Clmet	Metabolic Clearance
CLP	Clopidogrel Bisulphate
Cmax	Peak Drug Levels
CYPs	Cytochrome P450s
DDI	Drug Drug Interaction.
DIC	Diclofenac
DMPK	Drug Metabolism Pharmacokinetic DMPK
EDTA	Ethylene Diamine Tetra Acetic Acid
EDTA	Ethylene Diamine Tetra Acetic Acid
EFV	Efavirenz
EMA	European Medicines Agency
FLX	Fluoxetine
FMOs	Flavin-Containing Monooxygenases
GLM	Glimepiride
HLM	Human Liver Micrososmes
HPLC	High Performance Liquid Chromatography
HPLC	High Performance Liquid Chromatography.
HTS	High Throughput Screening
IC_{50}	Concentration of inhibitor that causes 50% inhibition of an original enzyme activity.
IV	Intravenous
IVIVE	*In Vitro - In Vivo* Extrapolation
KET	Ketoconazole
Ki	Inhibition Constant
Km	Michaelis-Menten Constant
Kobs	Inactivation Rate Constant
LC-MS/MS	Liquid Chromatography-Tandem Mass Spectrometry
LLOD	Lower Limit Of Detection
LLOQ	Lower Limit Of Quatification
MgCl2	Magnesium Chloride
MM	Michaelis-Menten
NA	Not Applicable
NCE	New Chemical Entity
NIDDM	Noninsulin-Dependent Diabetes Mellitus

NME	New Molecular Entity
PDA	Photo Diode Array
PhRMA	Pharmaceutical Research And Manufacturers Of America Perspective
PIJ	Pineapple Juice
POJ	Pomegranate Juices
QC	Quality Control
NADPH	reduced Nicotinamide Adenine Dinucleotide Phosphate
Rs	Resolution Factor
RT	Retention Time
SD	Standard Deviation
SEM	Standard Error Of Mean
SMZ	Sulfamethoxazole
$\mathbf{T_{1/2}}$	Half-Life Of Enzyme Inactivation
Tmax	Time To Reach Cmax
UGTs	UDP-Glucuronyltransferases
USFDA	U.S. Food And Drug Administration
Vmax	Maximal Velocity
[S]	Substrate Concentration

Chapter 1
Introduction

Drug metabolism: The pharmacokinetics of an administered drug is determined by its properties, in which metabolism is a key component. The metabolism of a drug, i.e. its biotransformation, is a protection mechanism against chemical insults on the body through the generation of more hydrophilic compounds that can be readily excreted through kidneys and/or bile. Though essentially being a detoxification mechanism, it can also result in bioactivation of drugs with the generation of reactive or toxic species, which can become safety issue in the development of an NME (new molecular entity).

Drug metabolism is generally divided into two categories, functionalization (phase I) and conjugation reactions. In phase I polar functionalities are introduced or exposed, resulting in more hydrophilic compounds. This encompasses biotransformations such as oxidation and hydrolysis reactions, but also reductions. Phase I reactions introduce a functional group on the parent compound by oxidation, reduction or hydrolysis reactions, many of which are catalysed by the CYP system and require NADPH as a cofactor. These reactions usually create a handle for the conjugation of polar endogenous groups to the metabolite, e.g. glucuronic acid, sulfate, or amino acids, which further facilitate excretion from the body. Phase II reactions lead to the formation of a covalent linkage between a functional group of the parent drug or phase I metabolite and an endogenous compound. The conjugation reactions can also have the purpose of detoxification, e.g. conjugation with glutathione, or result in a termination of the effect via glucuronidation, sulfation, acetylation and methylation reactions. In addition to the protective detoxification function, biotransformation may also cause formation of active intermediate species, which, in certain situations, may elicit tissue lesions. [1-3]

The phase I reactions are often the rate limiting step for disposition of most drugs and of the phase I enzymes, the cytochrome P450s (CYPs) are essential catalysts for the metabolism of xenobiotics. The drug metabolizing enzymes are found mainly in the liver but are also present in virtually all tissues. An orally administered drug has to pass through the liver after being absorbed from the gastrointestinal tract; accordingly, the metabolism in this organ is one of the key limitations for the bioavailability of a compound.

Metabolic capacity can vary markedly between individuals, leading to differences in drug response and adverse effects among patients.[4] The variability in metabolic capacity is multifactorial; gender, polymorphism of drug-metabolizing enzymes, smoking, dietary factors and other drugs can all affect drug metabolism. Nowadays evaluation of ADMET (absorption, distribution, metabolism, excretion and toxicity) properties has become one of the most important issues in drug discovery. In other words, it is not sufficient that a drug possesses biological activity and therapeutic efficacy. If it has undesired ADMET properties, then this can lead to failure during the clinical phases.

Drug development: The drug development process involves several steps, from target identification and screening, lead generation and optimization, preclinical and clinical studies to final registration of a drug (Figure 1).[5] A study conducted in 2002[6] showed that the average development time of a **NME** up to the registration was 12 years, and its cost was approximately 900 million USD. In 1991, the major reason for failure of NMEs was due to inadequate metabolic and pharmacokinetic (PK) parameters. During the past years, pharmaceutical companies have invested and introduced a number of new approaches dedicated to improve the rate of success of development of new drugs. One of the new strategies is an *in vitro* approach for early determination and **prediction of drug metabolism of NMEs**.[7] The use of *in vitro* methods in drug metabolism studies has several advantages. First, it allows for determination of metabolic profiles of NME early in the drug discovery process, and, therefore, this information can be used to guide further modifications of NME in order to obtain favorable metabolic properties. Secondly, it is possible to use human enzymes, cells and liver fraction and consequently the data are more relevant and important for the human *in vivo* situation. The *in vitro* approach is cost and time effective. Due to introduction of the *in vitro* approach, the failure rate of NMEs related to inadequate metabolic and PK parameters had been reduced to approximately 10% in 2000.[6]

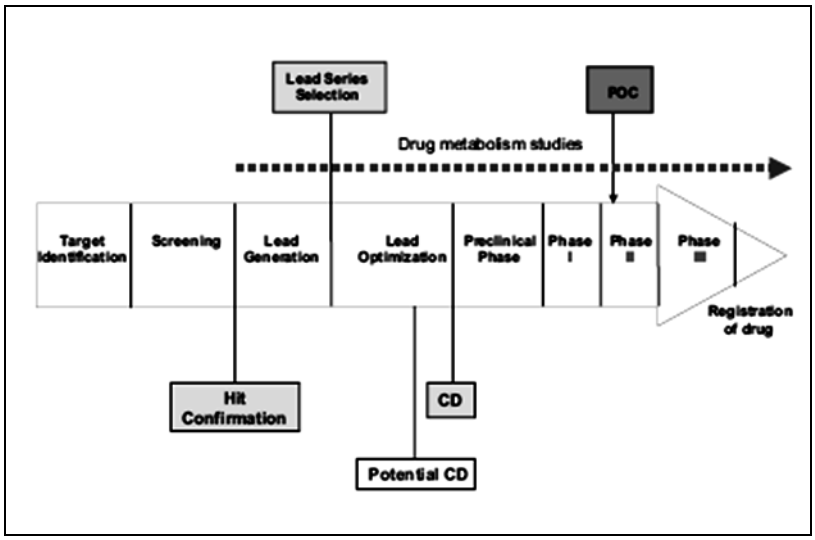

Figure 1.1 Schematic diagram of the drug discovery and development process. CD – candidate drug, POC – proof of concept.[5]

Pharmacokinetics interactions: Drug-drug interactions occur when one therapeutic agent either alters the concentration (pharmacokinetic interactions) or the biological effect of another agent (pharmacodynamics interactions). Pharmacokinetic drug-drug interactions can occur at the level of absorption, distribution, or clearance of the affected agent. Many drugs are eliminated by metabolism. The microsomal reactions that have been studied the most involve cytochrome P (CYP) 450 family of enzymes, of which a few are responsible for the majority of metabolic reactions involving drugs. These include the isoforms CYP1A2, CYP2C9, CYP2C19, CYP2D6, and CYP3A4.

Drug interactions are an important aspect of clinical drug treatment. Drug interactions can lead to severe side effects and such interactions have even resulted in early termination of drug development, refusal of approval and withdrawal from the market[8].Therefore, in addition to clinicians, the pharmaceutical industry and regulatory authorities have also paid increasing attention to drug-drug interactions. In pharmacokinetic drug interactions, the absorption, distribution, metabolism or excretion of a drug is altered due to the presence of other drug. Many clinically important pharmacokinetic drug interactions are based on inhibition or induction of CYP enzymes. The characteristics of various CYP enzymes and their involvement in the metabolism of commonly used drugs are now quite well established. This knowledge may provide a basis for better understanding and predictability of pharmacokinetic drug interactions.

Drug-drug interactions may have serious clinical consequences, and therefore, the potential of new chemical entities causing or being a victim of an interaction should be carefully studied. The interaction potential can be assessed using *in vitro* (laboratory), *in vivo* (animal and human study) and *in silico* (computational) methods. In early drug development, *in vitro* methods are used for assessing the metabolic pathways and for screening the interaction potential[9]. *In vitro* - *in vivo* extrapolation (IVIVE) is used for predicting the clinical drug-drug interactions of the compound. In case of signs of interaction potential based on *in vitro* studies or IVIVE, drug interaction studies are carried out. Drug-drug interactions have become an important issue in health care. It is now realized that many drug-drug interactions can be explained by alterations in the metabolic enzymes that are present in the liver and other extra-hepatic tissues. Many of the major pharmacokinetic interactions between drugs are due to hepatic cytochrome P450 enzymes being affected by previous administration of other drugs. After co-administration, some drugs act as potent enzyme inducers, whereas others are inhibitors. However, reports of enzyme inhibition are very much more common. Understanding these mechanisms of enzyme inhibition or induction is extremely important in order to give appropriate multiple-drug therapies. In future, it may help to identify individuals at greatest risk of drug interactions and adverse events.

When several drugs are used simultaneously or in sequence, there is always a risk of **metabolic interactions,** in case these compounds are metabolized by the same CYP enzyme or one compound affects the metabolism of the other compound. Many drug-drug interactions are metabolism based and mediated primarily via the cytochrome P450 (CYP) family of enzymes. The inhibition of these enzymes may have important clinical consequences such that inhibition of a CYP isoenzyme(s) by a xenobiotic (drug or food) may decrease the metabolic clearance of a co-administered drug resulting in elevated blood concentrations of the drug resulting in adverse drug effects or toxicity. As detailed in the FDA's Draft Guidance document for Drug-Drug Interactions (2006), the FDA has placed emphasis on evaluating the inhibition potential of a NME at an earlier stage in drug development in order to avoid developing compounds with the potential to yield adverse drug interactions.[10] Early assessment of an NME's ability to inhibit the activity of a particular CYP subtype can be achieved by conducting *in vitro* kinetic studies using

human liver microsomes and CYP isoform-specific model substrates and reactions. Also testing the effects of an NME on CYP-specific model activities and the effects of CYP-specific reference inhibitors on the metabolism of an NME in human liver microsomes *in vitro* gives information about the affinity of an NME for CYP enzymes and permits *in vivo* predictions about the behaviour of the NME in man (metabolic pathways, intrinsic clearance, etc.), which helps to design *in vivo* studies for revealing possible interactions . Thus prediction of metabolism-mediated drug interaction involves two strategies (i) Understanding whether an NME is an inhibitor for a particular P450 enzyme (ii) Understanding whether an NME is a substrate for a particular P450 enzyme.[11]

The determination of IC_{50} (the concentration causing 50% inhibition compared to the control activity) and Ki values (the affinity of the compound for the enzyme at the initial velocity conditions) for the studied compound produces information about the inhibitory effect of an NME on CYP isoforms, and enzyme kinetic studies can be made to evaluate the possibilities of drug-drug interactions. The Pharmaceutical Research and Manufacturers Of America Perspective (PHRMA) and U.S. Food and Drug Administration address the specific designs of the studies, and there is a desire by regulatory authorities to harmonize approaches and study designs to allow for a better assessment and to define a minimal best practice for *in vitro* and *in vivo* pharmacokinetic drug-drug interaction studies targeted to development.[10,12]

For the metabolism of most drugs, the **CYP superfamily** seems to be the most important enzyme family. Ten CYP isoforms are expressed in a typical human liver (CYP1A2, CYP2A6, CYP2B6, CYP2C8/9/18/19, CYP2D6, CYP2E1, andCYP3A4). Of these, six principle enzymes (CYP1A2, CYP2C8, CYP2C9, CYP2C19, CYP2D6 and CYP3A4) appear to be the most commonly responsible for the metabolism of most drugs and the associated drug-drug interactions. Identification of enzymes involved in the metabolism of the drug in question is one of the most important steps of drug metabolism studies during the drug discovery and development process, and it is useful for a better understanding of the possible role of genetic polymorphism in drug clearance and for prediction of potential metabolism-based drug-drug interactions.[13-16] The next important step of drug metabolism studies is the determination of enzyme kinetic parameters: Km, Vmax and CLint. The determination of enzyme kinetic parameters for the metabolic

reaction can be used for a better estimation of the NME pharmacokinetics in human and also to eliminate compounds with non-linear dose-exposure relationships.[17]

In order to investigate drug metabolism prior to human exposure, there are a number of options, ranging from *in vitro* screening with human enzymes to *in vivo* assessment in experimental animals. Although animal models can provide information about the biochemical potential for drug biotransformation (i.e. identifying the metabolite(s) that can be formed), such models may only indicate what is biologically possible, not what is biologically relevant for human drug exposure? This is due to the well documented inter-species differences in both expression and substrate specificity of drug metabolizing enzyme which give rise to species-differences in drug metabolism.[3] Thus human tissue systems have been developed to address the limitations enzymes and the enzymes that participate in the biotransformation of an NME are valuable information for the selection of lead compounds and for the planning of early clinical studies. On the basis of *in vitro* studies, a tentative prediction of the clearance and interaction potential of an NME can be made, and the first clinical studies can be based on these results of animal models of drug metabolism**. Many different models** for the prediction of drug metabolism and drug-drug interactions *in vitro* have been introduced recently. These systems consist of liver microsomes, hepatocytes and cell lines heterologously expressing drug-metabolising enzymes, liver slices and individually cDNA-expressed enzymes in host cell microsomes. One of the best characterized models is the use of the microsomal fraction derived from the human liver tissue samples called as Human liver microsomes (HLM).[18]

Advantages-Decreasing the use of test animals: *In vitro* models of drug metabolism are being increasingly applied in the drug discovery and development process as tools for predicting human pharmacokinetics and for the prediction of drug-drug interaction risks associated with new chemical entities. The use of *in vitro* predictive approaches offers several advantages including minimization of compound attrition during development, with associated cost and time savings, as well as minimization of human risk due to the rational design of clinical drug-drug interaction studies. Previously, great deals of preclinical studies have been accomplished by *in vivo* animal testing. The development and validation of *in vitro* methodologies have made it possible to give up animal testing

or to markedly decrease the number of animals used for some early ADME studies. This development is in line with the social awareness concerning animal rights and the demand for fewer animal studies. P450 affinity studies have increasingly utilized the possibility to substitute liver microsomes from specifically induced or control animals for human liver microsomes. This has led to the current situation, where the common protocol is to conduct affinity screening of an NME towards P450s participating in xenobiotic metabolism. Pharmacology and especially toxicology have traditionally been the areas where most of the test animals have been used principally to fulfill the regulatory requirements. Authorities strictly regulate toxicology testing, and it takes much more time to find appropriate *in vitro* tests for long-term toxicity studies. The *in vitro* methodology can already give a partial answer to those who are actively seeking to cut down the number of animals used for toxicity testing. For an NME, it is possible to conduct a metabolite search by liver preparations from the test species of choice. Using a pool of liver preparations, it is possible to avoid the use of live animals for metabolite searching. Also, the selection of test species for toxicity tests can be made by comparing the metabolite profiles produced by human liver microsomes and by microsomes from different test species. After identification of the formed metabolites, a comparison between the metabolites formed by human liver preparations and the test species can be done. This procedure can be used as an aid in selecting the species that most closely resemble humans in the metabolite profile. On the other hand, if the metabolic pathways differ considerably, this knowledge is still very useful in assessing the results of animal toxicity studies.[19]

High Throughput Screening (HTS): Assessment of physicochemical and pharmacological properties is now conducted at very early stages of drug discovery for the purpose of accelerating the conversion of hits and leads into qualified development candidates. In particular, *in vitro* absorption, distribution, metabolism and elimination (ADME) assays and *in vivo* drug metabolism pharmacokinetic (DMPK) studies are being conducted throughout the discovery process, from hit generation through to lead optimization, with the goal of reducing the attrition rate of these potential drug candidates as they progress through development. Because the continuing trend in drug discovery

has been to access ADME information earlier and earlier in the discovery process, the need has arisen within the analytical community to introduce faster and better analytical methods to enhance the 'developability' of drug leads. High-throughput *in vitro* ADMET (absorption, distribution, metabolism, excretion and toxicity) profiling has become an important common practice in the pharmaceutical industry to assess compound liability early in the drug discovery process. Liquid chromatography-tandem mass spectrometry (LC-MS/MS) is the bioanalytical method of choice for ADMET profiling assays that require compound-specific detection. However, the *in vitro* ADMET profiling environment, with its unique bioanalytical requirements of analyzing many samples generated from many discrete compounds in a high-throughput fashion, poses significant challenges for the traditional LC-MS/MS technology and process workflow, which were originally designed and optimized for single-compound bioanalysis. Recent advances such as automated MS/MS optimization, high-speed and multiplexed LC separation, and integrated software support have significantly increased the speed and quality of ADMET bioanalysis using LC-MS/MS. Emerging novel technologies in front-end sample introduction, ionization and mass analysis are expected to further push the current throughput limit and potentially transform the existing bioanalytical paradigm in the future. The HTS usually use protocol simplifications, microtiter plates (96-, 384- and 1536-well plate format) or incubations, and robotic system for pippeting of the samples (e.g. Packard MultiPROBE® II, SAGIANTM robotic system supplied by Beckman Coulter) combined with fluorescent substrates or high capacity LC/MS detection methods. Besides *in vitro* experiments, *in silico* modeling and simulation may also assist in the prediction for drug interactions.[20-21]

Determination of enzyme kinetic parameters: *In vitro* characterization of drug biotransformation generally begins with an enzyme kinetics analysis of metabolite formation rate using human liver microsomes. A typical enzyme kinetic analysis involving a mathematical description of reduced nicotinamide adenine dinucleotide phosphate (NADPH)-dependent biotransformation rate as a function of substrate concentration is based on the core assumptions that substrate consumption is minimal (typically less than 5%), and that product formation rate is linearly related to microsomal

protein concentration and duration of incubation. Normally, if the conversion of substrate to product is catalyzed by a single enzyme, the enzyme kinetics can be well described by a Michaelis-Menten (MM) equation (one-enzyme model) as follows [22-23]

$V_o = Vmax . S / (Km + S)$

where V_o is the rate of product formation (or substrate disappearance), S is the substrate concentration, Vmax is the maximal velocity of the reaction, and Km is the MM constant representing the concentration of substrate that results in half maximal velocity.

The Km value is an indicator of the affinity between an enzyme and a substrate and it can also reflect at which concentration of the substrate the enzymatic system will be saturated. Saturation of the enzymes may lead to non-linear kinetics of the drug candidate, which in turn may cause difficulties in prediction of dose and drug response. Michaelis-Menten plot presents the effect of a drug concentration [S] on the initial velocity [V] of an enzyme-catalyzed reaction. The drug concentration at which the initial velocity is half maximal is the Michaelis-Menten constant (Km). Lineweaver-Burk plot represents the linearization of the Michaelis- Menten hyperbola, also called "double-reciprocal" plot. 1/V is plotted *versus* 1/[S] and fitted to a straight line with linear regression. The Lineweaver-Burk plot is also useful in analyzing enzyme inhibition patterns, i.e. to distinguish between different types of inhibition.[24-25]

***In vitro* approaches in the prediction of metabolic clearance-**

- **Intrinsic clearance:** Intrinsic clearance (Clint) is the cornerstone for extrapolation of *in vitro* data to the *in vivo* situation. [26] Clint is a direct measure of enzyme activity toward a drug and is not influenced by other determinants such as hepatic blood flow or drug binding within the blood matrix. Clint acts as a proportional constant between rate of drug metabolism and drug concentration around the metabolic enzyme site (CE). If the process is consistent with a MM model, and if CE is less than 10% of the Km, Clint is equal to the Vmax/Km ratio. [27]

  i.e.: $Clint = Vmax / Km$

- **Prediction of *in vivo* metabolic clearance based on *in vitro* data:** In many cases, *in vivo* metabolic clearance (Clmet) can be predicted using *in vitro* drug

metabolism data based on the assumption that only the unbound drug can cross through the membranes, and that there is a homogenous distribution of enzymes within the liver.[28-29] Based on these assumptions, the hepatic clearance (Clh) can be predicted *in vitro* using the well-stirred model[30]:

$Clh = Q.E = Q.fu \ . \ Clint / (Q + fu\ Clint)$

or the parallel-tube model:

$Clh = Q.\ E = Q\ (1 - e^{-fu.Clint/Q})$

where Q is the hepatic blood flow (20 ml/min/kg)[31], E is the hepatic extraction ratio calculated as Clh/Q, Clint is the *in vivo* intrinsic clearance, and fu is the unbound fraction of a drug in the blood.

***In vitro* approaches in the prediction of drug-drug interactions-**

- **Determination of *in vitro* potency of inhibition:** In the case of reversible inhibition, the *in vitro* inhibitory potency of a given compound is quantified by determination of its IC_{50} and Ki values. The IC_{50} value is defined as a concentration of inhibitor that causes 50% inhibition of an original enzyme activity. The IC_{50} value can be determined by analyzing the relationship between inhibitor concentration and decrement in reaction velocity performed at a fixed substrate concentration (around Km).[32] The IC_{50} value is quite useful when comparing the inhibitory potencies of different candidate inhibitors of the same chemical class, but without any knowledge of the biochemical mechanism of inhibition. However, IC_{50} values have their own important limitations in the context of *in vitro-in vivo* scaling. IC_{50} value is dependent on the type of inhibitory mechanism. For example, IC_{50} is equal to the inhibition constant (Ki) only when the biochemical mechanism is noncompetitive or the substrate concentration used is much less than Km for competitive inhibition. If the substrate concentration approaches or exceeds Km, the IC_{50} value exceeds the competitive Ki.[33]. However, this limitation can be overcome by actual calculation of an *in vitro* Ki value based on a methodology involving coincubating varying concentrations of substrate with varying concentrations of a candidate chemical inhibitor. Ki, which expresses or is related to the affinity of a compound to an enzyme, is one of the key parameters for prediction of *in vivo* drug-drug

interactions resulting from metabolic inhibition. Ki can be estimated either graphically by using plotting methods or by nonlinear regression analysis. The Dixon plot relies on a linearized form of a nonlinear relationship of the inhibitor concentration versus the reciprocal of the rate of metabolite formation.[23] In the case of mechanism-based inactivation, time-, concentration- and NADPH dependent loss of enzyme activity is an important consequence of the processes. The important kinetic parameters for mechanism-based inactivation include the half-life of enzyme inactivation ($T_{1/2}$), the rate constant of inactivation (Kinact) and the concentration of inactivator that produces half the maximal rate of inactivation (KI). After preincubation of the microsomes with NADPH for an appropriate time in the presence or absence of various concentrations of an inhibitor, the $T_{1/2}$ and the apparent inactivation rate constant (Kobs) can be estimated from linear regression analysis of the natural logarithm of residual enzyme activity against the preincubation time. The KI and Kinact can be calculated from a double-reciprocal plot of the inactivation rate constant (Kobs) versus inhibitor concentration . The intercept on the ordinate gives 1/Kinact. If the line is extrapolated to the abscissa, the intercept gives -1/KI.[34] In addition to the linearized plots, KI and Kinact can also be estimated by fitting data to the following equation using nonlinear regression analysis.[35]

$T1/2 = 0.693 (1 + KI /I)/Kinact$

where I is the concentration of a mechanism-based inactivator.

- **Prediction of metabolic inhibition using an *in vitro-in vivo* scaling model:** Because of limitations of *in vivo* studies and problems in extrapolating the results of animal studies to humans, *in vitro* systems using human tissues have become widely used tools to predict potential drug-drug interactions in humans. The benefit of these studies is that *in vitro* data concerning the potential for drug-drug interactions can be obtained early in the drug development phase, thereby helping researchers to focus on *in vivo* interaction studies and the prediction of pharmacokinetic variability. Further details are discussed in literature review's section 2.11.1.

Clinical significance of drug-drug interactions involving CYP enzymes: In clinical practice, when two or more drugs are administered at the same or overlapping times, there is always a concern for drug-drug interactions. Although interactions can be pharmacokinetic or pharmacodynamic in nature, in many cases, the interactions have a pharmacokinetic basis. There are many underlying mechanisms responsible for pharmacokinetic interactions that can be understood in terms of alterations of CYP-catalyzed reactions. The major reasons for drug-drug interactions involving CYP enzymes are induction, inhibition, and possibly stimulation, with inhibition appearing to be the most important in terms of known clinical problems.[36] The inhibition of CYP enzymes can result in the undesirable elevation of plasma drug concentrations, leading to toxicity or therapeutic failure. A good understanding of the underlying mechanisms involving in such drug-drug interactions can avoid toxicity or therapeutic failure by a corresponding reduction or increment of the therapeutic doses of a targeted drug, or close monitoring of its plasma concentration whenever a precipitant compound is added to the therapeutic regime.

Clinical significance of drug-food interactions involving CYP enzymes: The opportunity for food drug interaction is an everyday occurrence. The interaction can be particularly important when total drug absorption is altered. In the early 1990s, it was reported that coadministration of grapefruit juice with felodipine or nifedipine, which are calcium channel antagonists, resulted in a large increase in the oral bioavailability of these drugs and an enhancement of their pharmacodynamic effects. Adverse experiences such as headaches, hypotension, facial flushing, and lightheadedness caused by these drugs were more frequently reported after the intake of grapefruit juice than after the intake of water. [37, 38] Fruit juice interacts with drugs that undergo substantial presystemic metabolism mediated by cytochrome P450. The mechanism of action probably involves competitive or irreversible (mechanism-based) inhibition of CYP's in the small intestine.[39] In recent years, there have been reports that citrus fruits as well as several other fruits have the potency to inhibit CYP activities in the liver and gut wall and thereby change the pharmacokinetics of certain drugs The inhibitory effect of a fruit is believed to depend on the fruit species and to be due to differences in the components of

the fruit.[37,40] These findings have led to conduct further studies on the interaction between other food items and the drugs metabolized by CYP's.

Glimepiride is a widely used medium to long-acting "third generation" sulfonylurea antidiabetic drug**.** It is completely metabolized by oxidative biotransformation to yield the major metabolite, cyclohexyl hydroxy methyl derivative (M1). Cytochrome P450 II C9 has been shown to be involved in the biotransformation of glimepiride to M1. The information on the contribution of CYP2C9 isoform to the metabolism of glimepiride seems to be based on unpublished data, and the experimental systems in which these results were obtained, have not been described. Hence GLM was chosen as a model substrate for CYP2C9.[41-43]

Sulfamethoxazole is a sulfonamide bacteriostatic antibiotic agent that interferes with folic acid synthesis in susceptible bacteria. Sulfonamides can potentiate the hypoglycemic effect of sulfonylurea agents when given in combination.[44] However, comprehensive studies on the inhibition of major CYP2C9 isoform by SMZ on the pharmacokinetics of glimepiride *in vitro* are not available. Hence *in vitro* evaluation of the pharmacokinetic alterations caused by sulfamethoxazole on glimepiride hydroxylation and prediction of the *in vivo* drug drug interaction from *in vitro* data was thought to be carried out.[45-46]

Interaction between **fruit juices** and drugs can have profound influence on the rate of drug absorption and metabolism. Hence the present study was focused to carry out *in vitro* assessment of pineapple and pomegranate juices on CYP2C9 mediated GLM metabolism *in vitro*.[47-48]

In vitro methods are commonly used to determine the CYP inhibitory potential of NMEs The potential influence of probe substrates and experimental conditions on the assessment of *in vitro* drug interactions has a significant impact on the drug development process and regulatory decisions. If an NME is an inhibitor of a specific CYP enzyme, it may have the potential to inhibit the metabolism of a substrate drug of that CYP enzyme.

Individual incubation approach is labor intensive, time consuming and not cost effective. Throughput can be increased by co-incubating a mixture of probe substrates with liver microsomes called as the **cocktail approach**, where the activities of several CYP isoforms can be assessed simultaneously by monitoring metabolite formation. Hence the

present study, describes simultaneous development and evaluation of cocktail substrate assay system for inhibition screening of the activities of **efavirenz (CYP2B6), diclofenac (CYP2C9), chlorzoxazone (CYPE1), atorvastatin (CYP3A4)** in human liver micrososmes by NME [synthesized in pharmaceutical chemistry laboratory of M.S.UNIVERSITY, Baroda, Gujrat]. Using selective marker reactions for the major CYP forms, prediction of the potential *in vivo* drug-drug interactions was carried out using reference inhibitor's and procured NME's.[49-50]

REFERENCES

1. Remmer H. The role of the liver in drug metabolism. *Am J Med* 49**:**617-629 (1970).

2. Brodie BB, Krishna G, Reid WD and Cho AK. Drug metabolism in man: past, present, and future.*Ann N Y Acad Sci* 179**:**11-18 (1971).

3. Murray M. Drug-mediated inactivation of cytochrome P450. *Clin Exp Pharmacol Physiol* 24**:**465-470(1997).

4. Wilkinson GR. Drug metabolism and variability among patients in drug response. *N Engl J Med* 2005;352:2211-21.

5. Pawel Baranczewski, Andrzej Stañczak, Kathrin Sundberg, Richard Svensson, Åsa Wallin, Jenny Jansson, Per Garberg, Hans Postlind. Introduction to *in vitro* estimation of metabolic stability and drug interactions of new chemical entities in drug discovery and development. Pharmacological Reports2006, 58, 453–472.

6. Kola I, Landis J: Can the pharmaceutical industry reduce attrition rates? Nat Rev: Drug Discov, 2004, 3, 711–715.

7. Plant N: Strategies for using *in vitro* screens in drug metabolism. Drug Discov Today, 2004, 9, 328–336.

8. Obach, R. S.; Baxter, J. G.; Liston, T. E.; Silber, B. M.; Jones, B. C.; Macintyre, F.; Rance, D. J.; Wastall, P.The prediction of human pharmacokinetic parameters from preclinical and *in vitro* metabolism data. Journal of Pharmacology and Experimental Therapeutics 1997**,** 283, 46-58.

9. Pelkonen O, Turpeinen M, Uusitalo J, Rautio A, Raunio H. Prediction of drugmetabolism and interactions on the basis of *in vitro* investigations. *Basic Clin Pharmacol Toxicol* 2005;96:167-75.

10. Draft guidance for industry: drug interaction studies—study design, data analysis,and implications for dosing and labeling. http://www.fda.gov/cder/guidance/6695dft.pdf.

11. Lei Zhang, Yuanchao (Derek) Zhang, Ping Zhao and Shiew-Mei Huang Predicting Drug–Drug Interactions: An FDA Perspective.The AAPS Journal, Vol. 11, No. 2, June 2009.

12. Bjornsson, T. D.; Callaghan, J. T.; Einolf, H. J.; Fischer, V.; Gan, L.; Grimm, S.; Kao, J.; King, S. P.; Miwa, G.; Ni, L. The conduct of *in vitro* and *in vivo* drug-drug interaction studies: a Pharmaceutical Research and Manufacturers of America (PhRMA) perspective. *Drug Metabolism and Disposition* **2003,** 31, 815-832.

13. Lewis DFV, Ito Y, Goldfarb PS: Structural modeling of the human drug-metabolizing cytochromes P450. Curr Med Chem. 13:2645-52, 2006.

14. Nebert DW, Russell DW. Clinical importance of the cytochromes P450. *Lancet* 2002;360:1155-62.

15. Nelson DR, Koymans L, Kamataki T, Stegeman JJ, Feyereisen R, Waxman DJ, Waterman MR, Gotoh O, Coon MJ, Estabrook RW, Gunsalus IC, Nebert DW. P450 superfamily: update on new sequences, gene mapping, accession numbers and nomenclature. *Pharmacogenetics* 1996;6:1-42.

16. Shimada T, Yamazaki H, Mimura M, Inui Y, Guengerich FP. Interindividual variations in human liver cytochrome P-450 enzymes involved in the oxidation of drugs, carcinogens and toxic chemicals: studies with liver microsomes of 30 Japanese and 30 Caucasians. *J Pharmacol Exp Th er* 1994;270:414-23.

17. Denisov IG, Makris TM, Sligar SG, Schlicting I: Structure and Chemistry of Cytochrome P450. Chem. Rev. 105:2253-2277, 2005.

18. Lewis DF and Pratt JM (1998) The P450 catalytic cycle and oxygenation mechanism. Drug Metab Rev 30:739-786.

19. Taavitsainen, Päivi, Cytochrome p450 isoformspecific *in vitro* methods to Predict drug metabolism and interactions (URL: http://herkules.oulu.fi/issn03553221/) University of Oulu, Finland 2001:53.

20. Kassel DB. Applications of high- throughput ADME in drug discovery. Curr Opin Chem Biol. 2004 Jun;8(3):339-45.

21. Roberts SA. High-throughput screening approaches for investigating drug metabolism and pharmacokinetics. Xenobiotica. 2001 Aug-Sep;31(8-9):557-89.

22. Segel IH (ed). Enzyme Kinetics. New York: John Wiley, 1975.

23. Schmider J, Greenblatt DJ, Harmatz JS, Shader RI. Enzyme kinetic modelling as a tool to analyse the behaviour of cytochrome P450 catalysed reactions: application to amitriptyline N-demethylation. Br J Clin Pharmacol 1996;41:593-604.

24. Houston JB, Kenworthy KE, Galetin A: Typical and atypical enzyme kinetics. In: Drug Metabolising Enzymes. Cytochrome P450 and Other Enzymes in Drug Discovery and Development. Ed. Lee JS, Obach RS, Fisher M B, Marcel Dekker Inc., New York, USA and FontisMedia S.A., Lausanne, Switzerland, 2003, 211–254.

25. Obach RS, Baxter JG, Liston TE, Silber BM, Jones BC, MacIntyre F, Rance DJ et al.: The prediction of human pharmacokinetic parameters from preclinical and *in vitro* metabolism data. J Pharmacol Exp Ther, 1997, 283, 46–58.

26. Pelkonen O, Mäenpää J, Taavitsainen P, Rautio A, Raunio H. Inhibition and Induction cytochrome p450 (CYP) enzymes. Xenobiotica 1998;28:1203-1253.

27. Houston JB.Utility of *in vitro* drug metabolism data in predicting *in vivo* metabolic clearance. Biochem Pharmacol 1994;47:1469-1479.

28. Iwatsubo T, Hirota N, Ooie T, Suzuki H, Shimada N, Chiba K, Ishizaki T, Green CE, Tyson CA, Sugiyama Y. Prediction of *in vivo* drug metabolism in the human liver from *in vitro* metabolism data. Pharmacol Ther 1997;73:147-171.

29. Lin Y, Lu P, Tang C, Mei Q, Sandig G, Rodrigues AD, Rushmore TH, Shou M. Substrate inhibition kinetics for cytochrome P450-catalyzed reactions. Drug Metab Dispos 2001;29:368-374.

30. Houston JB.Utility of *in vitro* drug metabolism data in predicting *in vivo* metabolic clearance. Biochem Pharmacol 1994;47:1469-1479.

31. Lin JH, Lu AY. Role of pharmacokinetics and metabolism in drug discovery and development. Pharmacol Rev 1997;49:403-449.

32. Rodrigues AD (ed). Drug-Drug Interactions. New York: Marcel Dekker, 2002.

33. Von Moltke LL, Greenblatt DJ, Schmider J, Wright CE, Harmatz JS, Shader RI. *In vitro* approaches to predicting drug interactions *in vivo*. Biochem Pharmacol 1998;55:113-122.

34. Kent UM, Yanev S, Hollenberg PF. Mechanism-based inactivation of cytochromes P450 2B1 and P450 2B6 by n-propylxanthate. Chem Res Toxicol 1999;12:317-322.

35. Lin JH, Lu AY. Inhibition and induction of cytochrome P450 and the clinical implications. Clin Pharmacokinet 1998;35:361-390.

36. Rodrigues AD (ed). Drug-Drug Interactions. New York: Marcel Dekker, 2002.

37. Bailey DG, Spence JD, Edgar B, Bayliff CD, and Arnold JM (1989) Ethanol enhances the hemodynamic effects of felodipine. *Clin Investig Med* **2:**357–362.

38. Bailey DG, Spence JD, Munoz C, and Arnold JM (1991) Interaction of citrus juices with felodipine and nifedipine. *Lancet* **337:**268–269.

39. Bailey DG, Dresser GK, Kreeft JH, Munoz C, Freeman DJ, and Bend JR (2000) Grapefruit felodipine interaction: effect of unprocessed fruit and probable active ingredients. *Clin Pharmacol Ther* **68:**468–477.

40. Guo LQ, Fukuda K, Ohta T, and Yamazoe Y (2000) Role of furanocoumarin derivatives on grapefruit juice-mediated inhibition of human CYP3A activity. *Drug Metab Dispos* **28:**766–771.

41. Langtry HD, Balfour JA. Glimepiride. A review of its use in the management oftype2diabetes mellitus. Drugs 1998; 55:563-84.

42. Stephen N. Davis: The role of glimepiride in the effective management of Type 2 diabetes. Journal of Diabetes and its Complications 18(6), 2004; 367–376.

43. Kirchheiner J, Roots I, Goldammer M, Rosenkranz B, Brockmöller J: Effect of genetic polymorphisms in cytochrome p450 CYP2C9 and CYP2C8 on the pharmacokinetics of oral antidiabetic drugs. Clinical Relevance Clin Pharmacokinet 2005, 44: 1209-1225.

44. Wilkinson, G. R. Drug metabolism and variability among patients in drug response. *New England Journal of Medicine* 2005, 352, 2211-2221.

45. Back DJ, Tjia JF, Karbwang J, and Colbert J (1988) *In vitro* inhibition studies of tolbutamide hydroxylase activity of human liver microsomes by azoles, sulphonamides and quinolines. Br J Clin Pharmacol 26:23–29.

46. Komatsu K, Ito K, Nakajima Y, Kanamitsu Si, Imaoka S, Funae Y, Green CE, Tyson CA, Shimada N,Sugiyama Y (2000a) Prediction of *in vivo* drug-drug interactions between tolbutamide and various sulfonamides in humans based on *in vitro* experiments. Drug Meta Dispos 28:475–481.

47. Dresser GK and Bailey DG (2003) The effects of fruit juices on drug disposition: a new model for drug interactions. Eur J Clin Investig 33: 10–16.

48. Fujita K. 2004 Food-drug interactions via human cytochrome P450 3A (CYP3A). Drug Metabol Drug Interact;20(4):195-217.

49. Rendic S and Di Carlo FJ (1997) Human cytochrome P450 enzymes: a status report summarizing their reactions, substrates, inducers, and inhibitors. Drug Metab Re29: 413– 580.

50. Allan E. Rettie1 and Jeffrey P. Jones, 2005.Clinical And Toxicological Relevance Of CYP2C9: Drug-Drug Interactions And Pharmacogenetics. Annu. Rev. Pharmacol. Toxicol. 45:477–94.

Chapter 2
Literature Review

2.1 Drug metabolism: It is a process of conversion of a lipophilic compound to more water soluble metabolites, which can be easily eliminated from the human and/or animal body.[1] It has a large impact on drug absorption, absorption, distribution, elimination and toxicity of NCEs. Since almost all drugs on the market are metabolized and inter-individual differences in activity of drug metabolic enzymes are responsible for different drug activities, it is easy to understand that drug metabolism has a key influence on the possible success of NCEs. Generally, drug metabolism can be divided into phase I and II. Phase I involves oxidation, reduction and hydrolysis reactions and is catalyzed by a number of enzymes, the most important being cytochrome P450 (CYP) and flavin-containing monooxygenases (FMOs).[1-3] The phase II metabolic enzymes, e.g. UDP-glucuronyltransferases (UGTs), sulfotransferases, catalyze conjugation reactions of lipophilic chemicals.

A key liability in transitioning a new chemical entity (NCE) to a development candidate is NCE-related inhibition of cytochrome P450 enzymes, a superfamily of heme-containing oxygenases that are the major route of first-pass metabolism for the majority of marketed drugs. The drawback of a drug/NCE that modulates CYP450 enzyme activity occurs when the compound is co-administered with another drug that relies on the same P450 enzyme for its metabolism. This could result in overdose of the second drug in the case of inhibition, or more rapid metabolism of one or both drugs accompanied by loss of efficacy in the case of enzyme induction. Screening for the inhibition of CYP450 enzymes is now routine in the early stages of evaluating NCEs. More than 90% of oxidative metabolic reactions (phase I) of drugs are catalyzed by enzymes of the P450 family.

2.2 Human cytochrome P450 (CYP450) enzyme system

The cytochrome P450 (CYP) family of heme monooxygenases comprises the most important group of phase I enzymes. The term cytochrome P-450 refers to a group of enzymes which are located on the endoplasmic reticulum. Cytochrome stands for hemoprotein, P stands for pigment as these enzymes are red because of their heme group and 450 refers to the maximum absorption wavelength of 450 nm in their reduced state in

the presence of carbon monoxide. In general, cytochromes are considered as heme-containing membrane-bound proteins with covalently bound sulfur from a cysteine residue as a proximal ligand.[4] In mammalian tissues, CYP enzymes are mainly expressed in the liver, but they are also located in the intestine, skin, lungs and kidneys. There are two main functional roles for CYP enzymes: metabolism of xenobiotics and biosynthesis of critical signaling molecules.

There are many members of the CYP superfamily currently known, and the numbers continue to grow. In humans, 57 cytochrome P450 genes arranged in 18 families have been identified, of which only the CYP1, CYP2 and CYP3 families seem to contribute to the metabolism of drugs.[5] CYP families are further divided into subfamilies and specific isoenzymes. All isoenzymes in the same family have at least 40% amino acid similarity, and those in the same subfamily have at least 55% amino acid similarity. Individual CYP enzymes are designated as shown in figure 1 by a family number (e.g. CYP2C8), a subfamily letter (CYP2C8) and a number for an individual enzyme within the subfamily (CYP2C8). At present almost 12,000 CYP genes have been identified and about sixty CYP genes are reported to exist in the human genome; humans have 18 CYP gene families, and 44 CYP gene subfamilies. [5-6] Of these sixty, it is estimated that more than 90% of human drug oxidation is attributable to six CYP is enzymes, CYP1A2, 2C9, 2C19, 2D6, 2E1 and 3A4.[7] Some CYPs are highly regio- and stereospecific in the oxygenation of substrate, whereas others such as the human liver CYP3A4 metabolize over 50% of the current marketed pharmaceuticals.[8] In other words, a drug can either be a substrate for only one CYP enzyme or it can be metabolized by several CYP enzymes. In general, the substrates for CYP metabolism are hydrophobic and poorly soluble in water. Extensive lists of the various substrates and corresponding CYP systems involved have been published. Figure 2 shows the most important CYP forms participating in the biotransformation of pharmaceutical agents.

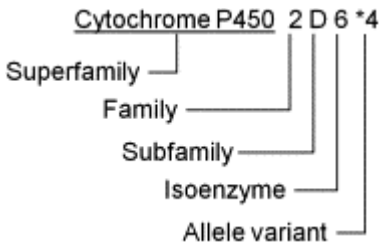

Figure 2.1. Nomenclature for the CYP enzymes and allelic forms.

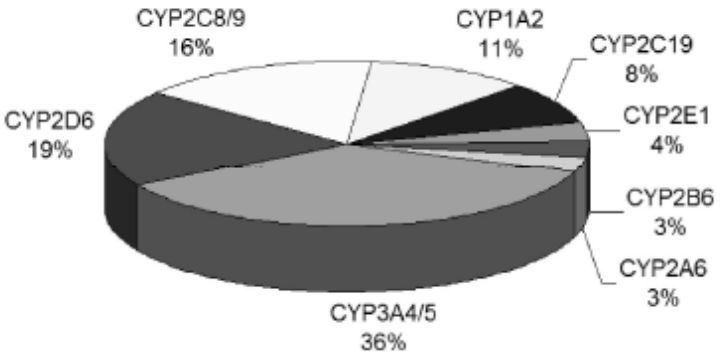

Figure 2.2. Proportion of drugs metabolised by CYP enzymes (modified from Wrighton and Steven).

The primary catalytic function of CYP enzymes is the addition of one oxygen atom from molecular oxygen (O_2) into various substrates and another oxygen atom is further reduced to water. An external reducing equivalent from NADPH (reduced nicotinamide adenine dinucleotide phosphate) is required.[9-10]

2.3 Cytochrome P450 Reductase and the CYP Catalytic Cycle[9-10]

The general cycle is presented in Figure 2.3. The CYP catalytic cycle is a multistep process where electrons are donated from the cofactor NADPH to the heme of the CYP in order for oxygen addition to occur on the substrate based on the net equation:

$$RH + NADPH + H^{+} + O2 \longrightarrow ROH + NADP^{+} + H2O \qquad (1)$$

where RH is the substrate and ROH is the product.

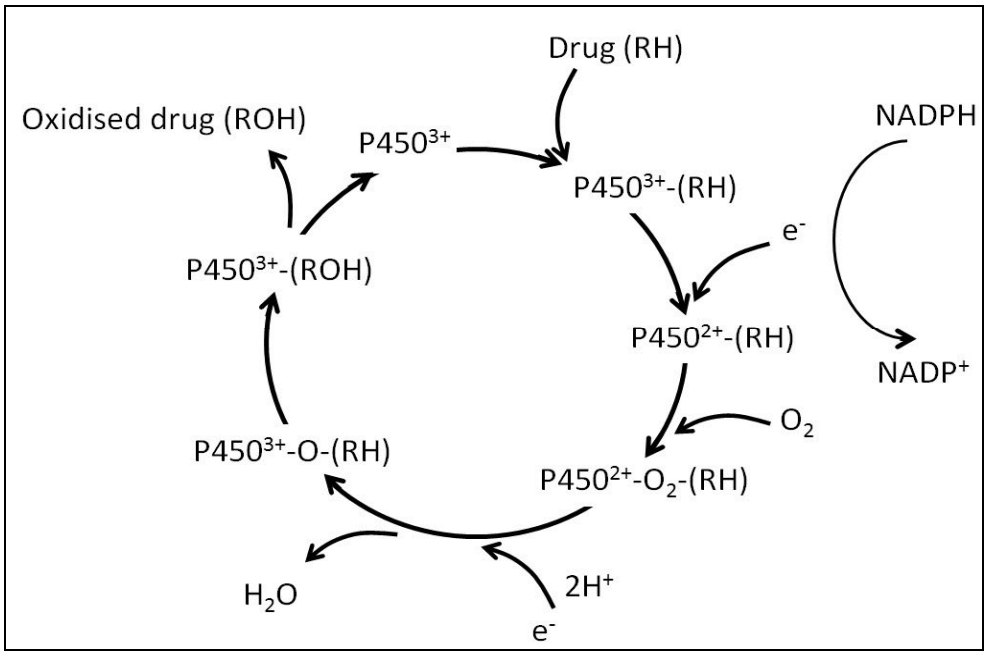

Figure 2.3. Basic catalytic cycle of cytochrome P450 enzymes. RH, drug; NADPH, reduced nicotinamide adenine dinucleotide phosphate; $NADP^+$, nicotinamide adenine dinucleotide phosphate; e-, electron; ROH, oxidized drug.

2.4 CYP enzymes

2.4.1 CYP1 –family

The CYP1-family consists of three members: CYP1A1, CYP1A2 and CYP1B1. Their expressions are all regulated by the aromatic hydrocarbon receptor (AHR). CYP1A1 is expressed in virtually every tissue of the body such as the lung, skin, larynx and placenta, and it is known for its capacity to activate compounds with carcinogenic properties.[11] CYP1A1 is detected after induction of polycyclic aromatic hydrocarbons (PAHs). There is also a positive association with increased risk of cancer and single nucleotide polymorphisms of the CYP1A1.[12-13] CYP1B is the next subfamily in the CYP1-family and it has only one member, CYP1B1. The *CYP1B1* gene is also transcriptionally activated by PAHs, with protein being expressed in variety of human cancers and it has been suggested that CYP1B1 may be a marker of tumorigenesis. [14]

2.4.1.1 CYP1A2

The CYP1A2 enzyme is expressed in the liver and accounts for about 12% of the total CYPcontent. The human *CYP1A2* gene is PAH-inducible in liver, gastrointestinal tract, nasal epithelium, and brain.[15] Several important drugs e.g. theophylline, tacrine, clozapine, olanzapine, phenacetin are predominantly metabolized by CYP1A2.[16] CYP1A2 is also important for the metabolism of endogenous substrates such as melatonin, estrone and estradiol, bilirubin and uroporphyrinogen.[17] and environmental toxins as well as for the activation of many environmental carcinogens including dietary heterocyclic amines, certain mycotoxins, tobacco-specific nitrosamines, and aryl amines.[18] Potent inhibitors of CYP1A2 include furafylline, fluvoxamine, ciprofloxacin, naphthoflavone and rofecoxib. Caffeine, phenacetin, melatonin and 7-ethoxyresorufin are the compounds most widely proposed as good specific probe substrates for use in *in vitro* testing. [16-19]

2.4.2 CYP2 –family

The CYP2 -family is one of the largest and most diverse families which play an important role in mammalian drug metabolism. The human *CYP2A* subfamily consists of three genes and two pseudogenes: CYP2A6, CYP2A7, CYP2A13, CYP2A7P(T) and CYP2A7P(C).[20] CYPs 2C8, 2C9, 2C18 and 2C19 share > 82% amino acid identity, but they only exhibit relatively little overlap of substrate specificity. CYP2C8, 2C9, and 2C19 proteins are primarily located in the liver, accounting for ~20% of total CYP contents, whereas CYP2C18 protein seems to be primarily expressed in the skin.[21] Members of the CYP2D family constitute only about 2-4% of total hepatic CYP content, however, they are responsible for the metabolism of 30% of commonly prescribed therapeutic compounds.

2.4.2.2 CYP2A6

In humans, there are three functional genes in the CYP2A subfamily*: CYP2A6, CYP2A7* and*CYP2A13*. CYP2A6 is the most important member: it metabolizes over 30 drugs from various therapeutic categories.[22] CYP2A6 is highly polymorphic and it is expressed in the human liver accounting for about 1-10% of total CYPs. CYP2A6 is also recognized

for its ability to metabolize nicotine and it is involved in the metabolism of a number of endogenous substances e.g. contributing to the metabolism of steroids with environmental compounds.[22-23] Several compounds inhibit CYP2A6 and several of them are mechanism-based (suicide) inhibitors e.g. selegiline, methoxsalen and isoniazid. The reversible inhibitors include pilocarpine andtranylcypromine.

2.4.2.3 CYP2B6

CYP2B6 was thought to be a minor member of the CYP family but recently it has attractedmore interest as its significance in the metabolism of xenobiotics has been appreciated. CYP2B6 is mainly expressed in the liver and it has been estimated to represent approximately 1-10% of the total hepatic CYP content.[24] It can be found also in various extrahepatic tissues including the kidney, skin, brain, intestine and lung, and it metabolises over sixty clinically used drugs and a number of procarcinogens and environmental compounds.[25] Some clinically used drugs that are metabolized by CYP2B6 include cyclophosphamide, tamoxifen, *S*-mephenytoin, bupropion and diazepam. Several inhibitors of CYP2B6 have been described including ticlopidine, clopidogrel, thioTEPA, memantine, and 2-phenyl-2-(1-piperidinyl) propane, clopidogrel, ticlopidine, mifepristone, duloxetine , phencyclidine and 17α-ethynylestradiol are mechanism-based inhibitors of CYP2B6.[26-28]

2.4.2.4 CYP2C8

CYP2C8 accounts for about 7% of total hepatic CYP contents and extrahepatic CYP2C8 mRNA has been detected in numerous tissues including the kidney, intestine, adrenal gland, brain, mammary gland, ovary, and heart, as well as in breast cancer tumours. It metabolizes ~5-8% of drugs. Its known substrates include paclitaxel, amodiaquine), rosiglitazone and its inhibitors are montelukast, quercetin, gemfibrozil. CYP2C8 is significantly induced by the prototypical inducers including rifampicin, phenobarbital, and dexamethasone.[29]

2.4.2.5 CYP2C9

CYP2C9 metabolizes approximately 20% clinical drugs. The majority of CYP2C9 substrates are acidic compounds such as several nonsteroidal anti-inflammatory drugs e.g. diclofenac and hypoglycaemic agents, as well as *S*-warfarin and phenytoin. This isoenzyme also participates in the oxidation of several important endogenous compounds such as progesterone, testosterone, 7 α-ethinylestradiol, all-transretinoic acid and arachidonic acid. Inhibitors of CYP2C9 include compounds such as sulfaphenazole and benzromarone and it is induced by rifampicin and barbiturates. CYP2C9 is highly polymorphic with more than 33 variants (*1B through to *34) and a series of subvariants of CYP2C9 have been reported (Wang B et al. 2009). A large interindividual variation has been noted. The most common allele is named CYP2C9*1, and it is considered as the wild-type allele. The variant *2 and *3 alleles are present in approximately 35% of Caucasian individuals. CYP2C9*2 was the first identified and is the most common allelic variant of CYP2C9, but it has a lesser impact on enzyme activity than CYP2C9*3.[29]

2.4.2.6 CYP2C19

CYP2C19 protein is mainly present in the liver, but significant activity has also been identified in the gut wall. CYP2C19 participates in the metabolism of many commonly used drugs, e.g. citalopram, diazepam, omeprazole, phenobarbital, proguanil and propranolol. Some proton pump inhibitors like omeprazole and lansoprazole are inhibitors of CYP2C19 are the antifungal drug fluconazole and antiplatelet drug ticlopidine. The most selective inhibitor of CYP2C19 is (-)-*N*-3-benzyl-phenobarbital. 2-4% of Caucasian and 10-25% of Asian populations are totally deficient in with CYP2C19, CYP2C19*2 and CYP2C19*3 being the most prevalent.[29]

2.4.2.7 CYP2D6

CYP2D6 represent only a few percent of the total human CYP content, but it is estimated to be involved in the metabolism of approximately 30% of the drugs from a wide variety of therapeutic indications. CYP2D6 has been identified also in human kidney, intestine, breast, lung, placenta and brain at low to moderate levels. CYP2D6 is perhaps the most

widely recognized polymorphic enzyme. The typical substrates for CYP2D6 are usually lipophilic base e.g. some antidepressants,antipsychotics, antiarrhythmics, antiemetics, s adrenoceptor antagonists (s-blockers) and opioids. Quinidine is most commonly used reference inhibitor. CYP2D6 is generally not regulated by many known environmental agents and is not inducible by the common known enzymeinducers such as steroids.[29]

2.4.2.8 CYP2E1

The highest levels of CYP2E1 enzyme are present in liver, where its expression predominates in the zone around the centrilobular vein. To lesser extent CYP2E1 is expressed also in extrahepatic tissues, such as lung, kidney, nasal mucosa, bone marrow, β cells in pancreas, brain ,breast and heart. CYP2E1 is also constitutively expressed in proliferating keratinocytes and epidermal cells and it can be detected also in the white cell fraction of peripheral blood from humans, rabbits and rats. CYP2E1 levels vary extensively due, in part, to pathophysiological conditions (including obesity and diabetes) and the enzyme is inducible by xenobiotics such as ethanol or volatile organic compounds. CYP2E1 catalyzes the metabolism of wide variety of endogenous substances and xenobiotics including therapeutic agents, procarcinogens, and low molecular weight solvents. In general, the majority of compounds are neutral with low molecular weights and relatively low log P values. CYP2E1 is mainly responsible formicrosomal ethanol oxidation. Fatty acids are very important endogenous substrates of CYP2E1 and they are converted preferentially to their (ω-1)-hydroxylated metabolites. The best known CYP2E1 inhibitors include clinically used drugs, e.g. disulfiram, as well as a herbicide 3-amino-1,2,4-triazole, which is a specific CYP2E1 inhibitor. Other CYP2E1 inhibitors are dilinoleylphosphatidylcholine (the major component of polyunsaturated phosphatydilcholines from soy beans) and diallylsulphide (which is a mechanism-based inhibitor found in Allium vegetables).[29]

2.4.3 CYP3 –family

The CYP3A subfamily of enzymes consists of four isoforms; CYP3A4, CYP3A5, CYP3A7and CYP3A43. CYP3A4 is present in the largest quantity of all the CYPs in the liver. CYP3A5 is a minor enzyme, which is expressed in the lungs and CYP3A7 is the major form of CYP in human fetal liver.

2.4.3.1 CYP3A4

CYP3A4 is expressed predominantly in the liver where it accounts for about 33% of the hepatic CYP enzyme content. CYP3A4 is the most abundant human hepatic CYP isoform responsible for the metabolism of almost 50% of known drugs. Therefore most drug interactions are a result of CYP3A4 inhibition. Among the substrates of CYP3A4, there are members of several important drug classes: antiarrhythmic agents, anxiolytics, HIV protease inhibitors, lipid-lowering agents, and strong opioids. CYP3A4 has large active site (~1368 A3) which enables the binding of multiple substrates and this might be the cause of atypical kinetics.[29]

2.5 Metabolic Stability

Metabolic stability is defined as the susceptibility of a chemical compound to biotransformation, and is expressed as *in vitro* half-life (t(1/2)) and intrinsic clearance (CL(int)). Determination of metabolic properties of a new chemical entity (NCE) is one of the most important steps during the drug discovery and development process. Nowadays, *in vitro* methods are used for early estimation and prediction of *in vivo* metabolism of NCEs. Using *in vitro* methods, it is possible to determine the metabolic stability of NCEs as well as the risk for drug-drug interactions (DDIs) related to inhibition and induction of drug metabolic enzymes. Based on these values, *in vivo* pharmacokinetic parameters such as bioavailability and *in vivo* half-life can be calculated. The drug metabolic enzymes possess broad substrate specificity and can metabolize multiple compounds. Therefore, the risk for metabolism-based DDIs is always a potential problem during the drug development process. For this reason, inhibition and induction *in vitro* screens are used early, before selection of a candidate drug. The *in vitro* data

obtained from a metabolic stability screen are used to predict and optimize the human pharmacokinetic parameters of NCEs during the drug discovery process. Additionally, during the drug development process the enzyme kinetic parameters (Km – Michaelis-Menten constant, Vmax – maximal velocity) are determined, which significantly contributes to a better understanding of the metabolism of NCEs. The Km value is an indicator of the affinity between an enzyme and a substrate and it can also reflect at which concentration of the substrate the enzymatic system will be saturated. Saturation of the enzymes may lead to non-linear kinetics of the drug candidate, which in turn may cause difficulties in prediction of dose and drug response.[30]

The hyperbolic curve obtained when plotting the rate of reaction against substrate concentration is shown in Figure 4 and can be described by Eq.2. This relationship is only valid using the initial velocity (*v0*), i.e. when the substrate concentration is not limiting (less than 10-20% of substrate consumed). As mentioned above it is also assumed that a single substrate and a single substrate-enzyme complex are involved and that no allosteric binding occurs. As can be seen from the plot, a linear relationship between rate of reaction and substrate concentration is observed at low substrate concentrations (1st order kinetics). At high concentrations no change in the rate of reaction is observed with increased substrate concentration, i.e. zero order kinetics is applicable, and the rate at this point is referred to as *Vmax*. At this phase, the enzyme's catalytic capacity is said to be saturated. The concentration at 50% of *Vmax* equals the *Km*-value, which can be used as a measure of the substrate's affinity for the enzyme.

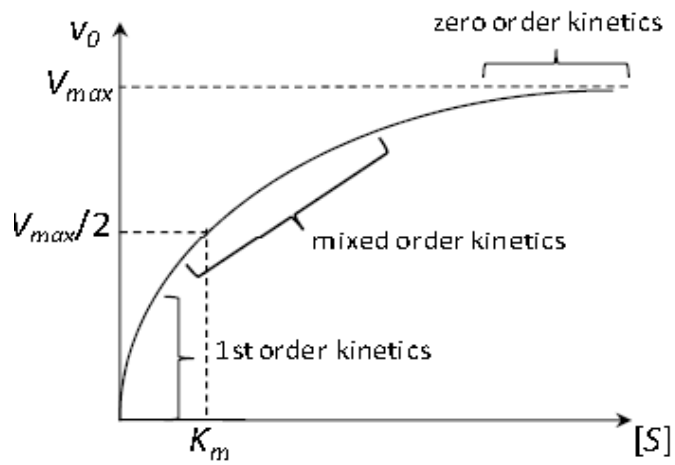

$$E + S \underset{k_{-1}}{\overset{k_1}{\rightleftharpoons}} ES \xrightarrow{k_2} E + P \qquad (2)$$

Figure 2.4. The concept of an enzyme catalyzed process & a graph describing the change in rate with substrate concentration for a reaction showing Michaelis-Menten kinetics.

2.6 P450 Probe Substrate Inhibition Assays.

General study outline and validation requirements: To determine whether an NME inhibits a particular P450 enzyme activity, changes in the metabolism of a P450-specific substrate (probe substrate) by human liver microsomes (or recombinant P450) with varying concentrations of NME are monitored. Potency of the inhibition and rank order of the inhibition of different P450 enzymes can be assessed by the determination of the *K*i or IC_{50} value (NME concentration, which reduced the metabolism of the P450 probe substrate by 50%). The concentration of P450 probe substrate used should be at or below its Michaelis-Menten constant (*K*m). Therefore, before performing *in vitro* P450 inhibition studies with NMEs, the test system (e.g., human liver microsomes) needs to be established, and kinetic parameters of the P450 probe substrate (*K*m, *V*max), as well as inhibition (*K*i or IC_{50}) by a typical P450 inhibitor (Table 1) determined and compared with reference values. Such a determination does not need to be repeated, unless the test

system is changed, e.g., from microsomes to recombinant P450. To determine the kinetic parameters for P450 probe substrate metabolism, or in general for any P450 substrate, the turnover of the substrate by the test system must first be optimized; turnover should be linearly dependent on time and less than 20% of the substrate should be consumed. It is desirable to utilize the lowest amount of protein in the incubation that yields readily quantifiable metabolite concentrations. A concentration of below 0.5 mg of microsomal protein per ml is suggested.[2]

2.7 Assay validation for probe substrate

At a minimum, the following experiments are needed to establish accurate kinetic parameters. First, a reaction time course experiment should be performed in which the incubation is conducted at a single concentration of protein near the lowest probe substrate concentration anticipated to be used in subsequent experiments, and isoform-specific metabolite formation measured at several time points. Second, the relationship between enzyme concentration and reaction velocity at an incubation time determined in the former experiment should be established. Thus, all subsequent *in vitro* incubations are performed using the condition that ensures linearity with time and enzyme concentration, conditions should also be such that less than 20% of the initial substrate is consumed. If studies are performed using a pool of samples from individual donors, e.g., pooled human liver microsomes, it should not be necessary to redefine these conditions for each individual lot of material, provided that substrate consumption is low. However, if the source of enzyme changes, for example from liver microsomes to expressed enzyme, then these experiments will need to be repeated. Once optimal conditions are obtained, e.g., incubation time, microsomal concentration, the substrate concentration dependence on the rate of metabolite formation is examined. The *K*m value is determined by nonlinear regression of a plot of enzyme activity versus substrate concentration. Substrate concentrations should span a range of at least 1/3 *K*m to 3 *K*m with at least six concentrations, to obtain an accurate measurement of *K*m value. In some cases, limitations of assay sensitivity or solubility of the substrate may prevent gathering of data over this range of concentrations, and caution should be applied to interpretation of the

data.

Once the *K*m of the probe substrate is established for the test system, an IC_{50} value of a known specific P450 inhibitor can be determined by using the probe substrate concentration at or below the *K*m. The determination of an IC_{50} or *K*i value can be used to verify the inhibition experiments by comparing the experimentally obtained IC_{50} or *K*i value with known literature values. The rate of the probe substrate turnover is assayed in the presence of various inhibitor concentrations, and the percentage of activity remaining (percentage of the original rate) with respect to inhibitor concentrations are plotted to derive an apparent IC_{50} value. To estimate the relationship between the IC_{50} and the *K*i value, the following equations may be used. When the probe substrate concentration is equal to the *K*m value, the concentration of inhibitor at which the activity of the enzyme reaction(s) is decreased by one-half (IC_{50}) will be the same as the *K*i value if the type of inhibition is noncompetitive or approximately twice the *K*i value for a competitive inhibitor ($Ki=IC_{50}/[1+(S)/Km]$) or an uncompetitive inhibitor ($Ki=IC_{50}/[1+Km/(S)]$). Actual calculation of a *K*i value can be determined as described below. [2]

Inhibition by NME: IC_{50} determination: The IC_{50} value for the inhibition of the P450 probe substrate can then be determined for NMEs, as described above for the specific P450 inhibitor. The concentration range of NME is based upon solubility of the compound and concentrations, which would cover, at least, the anticipated plasma concentration. Activities from the blank samples (assays with the substrate but without the inhibitor) should be compared with the historical data (data obtained previously for the same reaction conditions) for quality control purposes. In the case of major circulating metabolites, P450 inhibition studies may also be of importance. The term “major circulating metabolite” refers to 25% of the total drug related material in human circulation, as defined previously. [2]

Inhibition by NME: Ki determination: To examine the type of P450 inhibition, a *K*i value (i.e., dissociation constant for the enzyme inhibitor complex) may be determined for inhibitors where a clinical interaction is likely or possible.These *K*i values are determined from incubations of the NME with human liver microsomes and a P450-

selective substrate or with recombinant enzyme and a substrate, at several substrate and inhibitor (the NME) concentrations. The previous section, which described the establishment of reaction conditions to produce accurate kinetic parameters, should be used to guide the determination of the substrate concentrations used in the estimation of *K*i values. Furthermore, a preliminary IC_{50} determination guides the inhibitor concentrations used in these studies (inhibitor concentrations should encompass the IC_{50}). The rate of formation of the metabolite of interest in the presence and absence of inhibitor is determined. Using nonlinear regression analysis, the data obtained are used to determine whether the inhibition observed best fits various models of inhibition often including competitive, noncompetitive, mixed competitive/noncompetitive and uncompetitive types of inhibition. The model that best fits the data, determined by a number of statistical criteria, indicates the type of inhibition observed and the *K*i value for the NME. [2]

Table 2.1: Comparison of *in vitro* enzyme sources used in preclinical research.

Enzyme sources	Availability	Advantages	Disadvantages
Microsomes	Relatively good, from transplantations or commercial sources.	Easy to obtain. Also commercially available. Relatively inexpensive technique.	Contains only phase I DMEs and UDP-glucuronosyl transferases. Requires strictly specific substrates and inhibitors or antibodies for individual DMEs.
cDNA-expressed individual CYPs	Good, commercially available.	Can be utilised with HTS substrates. The role of individual CYPs in the metabolism of an NCE can be easily studied.	The effect of only one enzyme at a time can be evaluated.
Immortalised cell lines	Available at request, not many adequately characterised cell lines exist.	Non-limited source of enzymes.	The expression of most DMEs is poor or absent if characterised at all.
Primary hepatocytes	Relatively difficult to obtain, relatively healthy fresh tissue needed. Commercially available. Cryopreservation possible.	Contains the whole complement of DMEs. The induction effect of an NCE can be studied.	Requires specific techniques and well established procedures. The levels of many DMEs decrease rapidly during cultivation.
Liver slices	Relatively difficult to obtain, fresh tissue needed. Cryopreservation possible.	Contains the whole complement of DMEs and cell-cell connections. The induction effect ofan NCE can be studied.	Requires specific techniques and well established procedures.

2.8 CYP inhibition[29]

Inhibition denotes a decrease in enzyme activity. Determination of CYP inhibition is an important predictor of potential drug-drug interactions (DDIs). CYP enzyme inhibition can be either reversible or irreversible, the former being the more common type. Reversible inhibition is the most common mechanism responsible for documented drug interactions, competitive inhibition being the most important type.

2.8.1 Reversible inhibition[31]

Reversible inhibition can be divided into competitive, uncompetitive and mixed-type inhibition. In competitive inhibition, the binding of the inhibitor prevents the binding of the substrate to the active site of the enzyme. An inhibitor may bind to the same binding region or it may partly cover it. In particular when the substrate concentration is low, the inhibition is conspicuous. The equation (3) for competitive inhibition is shown below.

$$v_i = \frac{V_{max}[S]}{[S] + K_m\left(1 + \frac{[I]}{K_i}\right)}$$

Where vi is the observed velocity of the reaction, Vmax the maximum velocity, [S] the substrate concentration, Km the Michealis-Menten constant, [I] the free inhibitor concentration and Ki the inhibition constant. When inhibition is competitive, the apparent Km is increased but the Vmax is not affected by increased inhibitor concentrations.

In uncompetitive inhibition, the inhibitor does not bind to the free enzyme but instead to the enzyme-substrate complex and therefore the inhibition increases as the substrate concentration increases. The equation for uncompetitive inhibition is shown below. When inhibition is uncompetitive, both the Km and Vmax decrease. (Equation 4)

$$v_i = \frac{V_{max}[S]}{K_m + [S]\left(1 + \frac{[I]}{K_i}\right)}$$

Non-competitive inhibition is a special case of mixed type inhibition. In noncompetitive inhibition the inhibitor binds not to the active but to another site on the enzyme and which evokes conformational changes resulting in a reduced metabolic rate regardless of

substrate concentration. The equation for non-competitive inhibition is shown below. When inhibition is non-competitive, the Vmax is decreased but the Km remains unchanged. (Equation 5)

$$v_i = \frac{V_{max}[S]}{[S]\left(1+\frac{[I]}{K_i}\right) + K_m\left(1+\frac{[I]}{K_i}\right)}$$

2.8.2 Mechanism-based inhibition

Irreversible inhibition is also called mechanism-based inhibition or suicide inhibition. This involves the permanent inactivation of enzymes. Irreversible inhibitors are covalently or noncovalently bound to the target enzyme and dissociate so slowly from the enzyme, that in effect, the recovery requires resynthesis of the new enzyme molecules. Mechanism based inhibitors of CYP enzymes can be classified into two groups, namely irreversible and quasi-irreversible inhibitors. In the case of quasi-irreversible inhibitors, reactive intermediates coordinate with the heme prosthetic group leading to the formation of a catalytically inactive metabolite-inhibitor complex with the CYP enzyme. In irreversible inhibition, reactive intermediates metabolically generated from the inhibitors covalently react with an active site amino acid residue within the apoprotein and/or cause direct alkylation/arylation of the heme destruction.[32-33] There are many experimental compounds that have been shown to be mechanism-based inhibitors *in vitro* and several commonly used drugs have been described as being mechanism-based inhibitors *in vivo*. Experimentally, irreversible and reversible CYP inhibition can be differentiated through the examination of the inhibitory concentration (IC_{50}) at different time intervals; for irreversible inhibitors, the IC_{50} value changes over time, but for reversible inhibitors, the IC_{50} value remains independent of time.

2.9 Guidelines on the investigation of drug interactions

2.9.1 Drug Drug Interactions

DDIs are an important issue in clinical practice and drug development. The U.S. Food and Drug Administration (USFDA) first published its guidance for drug interactions in 1997, supplemented this information in 1999 and has published additional guidance in

2006, with a new draft issued in February 2011. The European Medicines Agency (EMA) also published guidance in 1995 and recently a new draft has been published.[34-35] The Pharmaceutical Research and Manufacturers of America Perspective (PHRMA) guidelines also address the specific designs of the studies, to define a minimal best practice for *in vitro* and *in vivo* pharmacokinetic studies targeted to the development. The intent is to define a minimal best practice for *in vitro* and *in vivo* pharmacokinetic drug-drug interaction studies targeted to development and to define a data package that can be expected by regulatory agencies in compound registration dossiers. According to these guidelines, pharmacokinetic interaction studies should generally be performed in humans.

Although animal models can provide information about the biochemical potential for drug biotransformation (i.e. identifying the metabolite(s) that can be formed), such models may only indicate what is biologically possible, not what is biologically relevant for human drug exposure? This is due to the well documented inter-species differences in both expression and substrate specificity of drug metabolising enzyme which give rise to species-differences in drug metabolism. Thus human tissue systems have been developed to address the limitations of animal models of drug metabolism. Many different models for the prediction of drug metabolism and drug-drug interactions *in vitro* have been introduced recently. One of the best characterized models is the use of the microsomal fraction derived from the human liver tissue samples called as Human liver microsomes (HLM).

The *in vitro* studies should be conducted before phase I clinical studies and those enzymes involved in metabolic pathways contributing to ≥25% of the oral clearance should be verified if possible *in vivo*. In the *in vitro* inhibition studies, the inhibition mechanisms (e.g. reversible or time dependent inhibition) and inhibition potency (e.g. Ki), are usually investigated using human liver tissues, e.g. human liver microsomes or cDNA-expressed enzymes under linear substrate metabolism and standardized assay conditions. A marker substrate is used to monitor the enzyme activity and known potent inhibitors should be included as positive controls in the study. A wide range of concentrations of the investigational drug should be included in these studies and Ki values should be determined. FDA and EMA have recommendations/guidelines about

which enzymes should be tested in inhibition studies. EMA has recommended that *in vitro* studies should be performed to investigate whether the investigational drug inhibits the CYP enzymes most commonly involved in drug metabolism. These presently include CYP1A2, CYP2B6, CYP2C8, CYP2C9, CYP2C19 CYP2D6, and CYP3A. It should also be evaluated if time-dependent inhibition is present.[36]

2.9.2 Drug Fruit Interactions[37-40]]

Potential interactions of foods and beverages with medications are of deep concern in clinical practice. It is well known that some kinds of fruit juice cause the pharmacokinetic alteration of medications. Interaction between fruit juices and drugs can have profound influence on the rate of drug absorption and metabolism.The possibility of an interaction between fruit juices and prescription drugs creates a dilemma for individuals who consume these juices for their health benefits. Fruit juices are more likely to inhibit drug metabolism *in vitro* than in humans.

Food interactions are usually studied in terms of fruit juices. It has been reported that some fruit juices like grapefruit, pineapple and pomegranate affect the oral bioavailability of drugs undergoing metabolism via CYP2C9 respectively.

In general, clinically important interactions are more likely to occur when the perpetrator is a significant modulator of a metabolic enzyme, or the therapeutic index of drug is narrow.While only a few clinically significant juice-drug interactions have been observed, invitro and animal studies suggests that fruit juices could influence the activities cytochrome P450 enzymes.

2.10 *In vitro* techniques for testing drug metabolism [41]

Cytochrome P450 is presented as a paradigm in order to illustrate the experimental techniques now available. Preclinical studies consist of animal studies (on the pharmacokinetics and pharmacodynamics of the compound, toxicological studies) and animal and human tissue-derived *in vitro* studies. Because of the problems in extrapolating the results of animal studies to humans, various *in vitro* methods have been developed by employing human tissue-derived systems. Also, the authorities have begun

to demand increasingly that the issues concerning metabolism and toxicity in test species compared to humans should be actively clarified in early preclinical tests. This is done by utilizing liver preparations from humans and trying to find the test species that most closely resemble human metabolism and the production of toxic intermediates. Such studies play a role in the drug development process as well as metabolism and safety assessment.

There are several approaches to preclinical metabolism studies. The enzyme sources in these studies are human-derived systems currently under rapid development and evaluation. These systems consist of liver microsomes, hepatocytes and cell lines heterologously expressing drug-metabolising enzymes, liver slices and individually cDNA-expressed enzymes in host cell microsomes. Each of these will be discussed briefly here. Table 1 shows a comparison of different human-derived *in vitro* methods.

There are many variables which need to be taken into account in measuring CYP inhibition potency. The choice of buffer strength and pH, divalent metals and organic solvents can all have effects on the outcome of *in vitro* drug interaction potential inhibitory effects (e.g. <0.5% final (v/v)), but this may cause precipitation of the inhibitor (or the substrate). The test inhibitor might be metabolized and there is the possibility that the metabolites can be more potent inhibitors than the parent substance. It is also advisable to use the lowest possible amount of protein in the incubation (below 0.5 mg of microsomal protein per ml is suggested) in order to avoid protein binding.

Human liver microsomes

Human liver microsomes are fractionated from subcellular organelles by differential ultracentrifugation. They are also very convenient, low in cost and easy to use. They are extremely popular and a widely used *in vitro* system for studying CYP kinetics. They contain a more complete complement of hepatic drug metabolizing enzymes which makes it a suitable tool for studying inhibitory interactions and CYP-catalysed metabolite formation. Microsomes are formed from smooth endoplasmic reticulum during tissue homogenisation. The selectivity of probe substrates for a particular CYP isoform is more important when multiple CYP enzymes are being evaluated simultaneously. The disadvantage is the incomplete representation of the *in vivo* situation, because only CYP

and UGT enzymes are represent.

Hepatocytes

Hepatocytes contain the full compartment of phase I and phase II enzymes, and the whole metabolite pattern can therefore be detected in incubations with it. Hepatocytes can also be used to assess drug interactions, but they are less commonly used for studies of human enzymes, because they are relatively difficult to obtain and difficult to preserve for later use.

cDNA-expressed enzymes

Drug-metabolising enzymes are available commercially as heterologously expressed enzyme systems. In these preparations, an individual enzyme is produced in the ER of an eucaryote host cell. The expression of human liver CYPs in different artificial systems has become easier due to the rapid development of recombinant DNA techniques. The systems employed for the production of cDNA-expressed CYPs include bacteria, yeast, mammalian cell lines and baculovirus systems. cDNA-expressed enzymes are a valuable tool in the search for the enzymes participating in the metabolism of an NCE. Because the enzymes are studied in isolation from other hepatic enzymes and because they lack the whole complement of hepatic enzymes, the *in vivo* predictive value of the data obtained from heterologously expressed enzyme systems has been debated. The disadvantage of expressed microsomal CYPs is that only a single enzyme at a time can be studied and the metabolic contribution of other enzymes is not represented.

Human liver S9 fractions

Liver S9 fractions are subcellular fractions that contain drug-metabolizing enzymes including the CYPs, flavin monooxygenases, and UDP-glucuronyltransferases. It is a major advantage that they contain both phase I and phase II activity. One disadvantage is the overall lower enzyme activity, 20-24 lower enzyme activity than in microsomes and expressed enzymes.

Liver slices

Liver slices resemble most closely the *in vivo* environment, because they contain the

entire complement of metabolizing enzymes and all cell types from the organ tissue and all the connections between the cells are present. Unfortunately liver slices are relatively difficult to obtain and the maintenance is demanding. In addition, loss of CYP catalytic activity can occur, thus metabolism studies are best performed using freshly cut slices. The thickness of a slice has to be minimal within the limits of the optimal number of cell layers and oxygen and nutrient transportation.

2.11 In Vitro – *In Vivo* Correlation (*IVIVC*)

2.11.1 Prediction of the clinical importance: In vitro testing of the inhibition of drug metabolism has extensively been used for the prediction of clinical drug-drug interactions since the mid-1990s. The kinetic values obtained from the in vitro studies of a chemical entity and an understanding of the inhibitor concentrations in clinical use ([I]) form the basis for this in vitro- *in vivo* extrapolation (IVIVE) process for interactions based on enzyme inhibition.[42]

The assessment of the inhibition potential for reversible inhibitors is based on the [I]/Ki ratio.[43] A value of < 0.1 usually indicates a low risk of interaction and a value of > 1 indicates a high risk. Based on the [I]/Ki ratio, the *in vivo* AUC ratio can be predicted also by using the following equation (Equation 6)

$$\frac{AUC_i}{AUC_c} = 1 + \frac{[I]}{K_i}$$

where AUCi is the area under concentration-time curve in inhibited phase and AUCc is the area under concentration-time curve in control phase. In order to forecast the interaction potential between the reversible inhibitor and the substrate, detailed information is required concerning the substrate metabolism by the enzyme. This can be expressed as the fraction metabolised by the inhibited enzyme (fm). The estimates of the fm can provide guidance related to the need of further studies. If human *in vivo* data indicate that CYP enzymes contribute > 25% to the total clearance of a drug, further studies are needed.[44] The drug-drug inhibition potential of a reversible inhibitor can be estimated by the following basic equation taking the fm into account (when the unbound fraction of the victim drug is low) (Equation 7)

$$\frac{AUC_i}{AUC_c} = \frac{1}{\frac{f_m}{\left(1+\frac{[I]}{K_i}\right)} + (1-f_m)}$$

2.11.2 Prediction of increase in Area under curve (AUC) of Glimepiride from In vitro metabolic data:[45]

As fractions of human tissues such as human liver microsomes and human hepatocytes have become more easily available for in vitro studies, attempts have been made to quantitatively predict *in vivo* drug metabolism or drug interactions in humans from in vitro data. In the case of a competitive or noncompetitive inhibition of drug metabolism, the degree of *in vivo* interaction can be evaluated from the [I] u /KI ratio, where [I] u is the unbound concentration around the enzyme and K i is the in vitro inhibition constant of the inhibitor. In clinical situations, the substrate concentration is usually much lower than Km and the maximum degree of interaction (R = area under the curve [AUC] (+ inhibitor) / AUC (control)) is expressed as R = 1 + [I] u /Ki , assuming that the substrate is eliminated from the body only by the inhibited pathway. Although Ki values can be determined by kinetic analyses of in vitro data using human liver microsomes or recombinant enzymes, it is usually impossible to directly measure [I]u in humans.

CYP2C9 mediated Glimepiride - Sulfamethoxazole interaction was studied for the prediction of clinical drug-drug interactions. Ki value for sulfamethoxazole (CYP2C9 Inhibitor) was determined by kinetic inhibition analysis of in vitro data using human liver microsomes. In the case of competitive or noncompetitive inhibition, the ratio of intrinsic metabolic clearance (CLint) in the presence and absence of the inhibitor can be described as follows assuming that the substrate is eliminated from the body only by the inhibited pathway (Equation 8)

$$\frac{\text{Clint}}{\text{Clint(i)}} = 1 + ([\text{Iu}]/\text{Ki})$$

It is usually impossible to directly measure Iu in humans. In the case of drugs that are transported into the liver by passive diffusion, Iu was assumed to be equal to the unbound

concentration in the liver at steady-state. Hence in order to avoid a false-negative prediction due to underestimation of [I] u , the maximum unbound concentration at the inlet to the liver, where the blood flow from the hepatic artery and portal vein meet (I in,max,u), as the maximum value of Iu was used. This method was thus proposed to be useful for predicting the maximal degree of inhibition.

According to the perfusion model the maximum concentration of inhibitor at the inlet to the liver (Iin,max) can be calculated as follows (Equation 9)

$$I_{in,max} = I_{max} + k_a \times Dose \times F_a / Q_h$$

where ka is the absorption rate constant, Dose is the amount of inhibitor administered, Fa is the fraction absorbed from gut to the portal vein, and Qh is the hepatic blood flow rate. Using the unbound fraction in the blood (fu) Iin,max,u is obtained as follows (Equation 10):

$$I_{in,max,u} = f_u \times I_{in,max}$$

In conclusion, the findings in the present study indicate that the [I] in,max,u / i ratios can be used to predict the possibility of drugs causing *in vivo* drug-drug interactions (Glimepiride – Sulfamethoxazole), in addition to [I] max,u /Ki or [I] max /Ki ratios.

2.12 Cocktail Assays

Evaluating CYP enzyme activities is traditionally performed for individual CYP isoforms. This approach is labor intensive, time consuming and not cost effective. Throughput can be increased by co-incubating a mixture of probe substrates with liver microsomes , and the activities of several CYP isoforms can be assessed simultaneously by monitoring metabolite formation. Success of this mixed-substrate incubation approach requires an analytical method that allows rapid quantitative determination of metabolites from multiple probe substrates, ideally in a single run. Liquid chromatography (LC) with ultraviolet (UV), fluorescence or mass spectrometry (MS) detection has been commonly used for quantitative determination of CYP probe substrates. Among different detection

methods, only LC/MS has been used for simultaneous analysis of multiple CYP probe substrates. LC/MS has the advantages of high sensitivity, selectivity and speed. However, LC/MS instrumentation is costly and may not be available for routine analysis in every research laboratory. In addition, LC/MS-based assays often require use of different ionization and ion detection modes due to the diverse structure of CYP probe substrate, which creates difficulty and complexity in developing LC/MS methods for simultaneous analysis. It has been reported that two sample injections and two runs (one for positive ion and one for negative ion) are needed to analyze the common probe substrates for major drug metabolizing human CYP enzymes. Fluorescence and UV are conventional and inexpensive detectors for LC. Fluorescence detectors are very sensitive but respond only to the few analytes that fluoresce [46]. In contrast, many compounds can absorb ultraviolet light. Therefore, LC with UV detection can be used for simultaneous analysis of multiple CYP probe substrates and metabolites. The drawback of UV detection is its relatively low sensitivity and selectivity. However, our preliminary results show that the sensitivity of LC/UV is sufficient for detection of CYP probe substrate metabolites resulting from normal microsomal incubations. Prior to this work, no report has been published using LC/UV for simultaneous analysis of substrate disappearance from multiple CYP probe substrates.

2.12.1 Cocktail CYP450 Inhibition assays [47-49]

In vitro P450 enzyme inhibition studies are routinely performed to evaluate the inhibitory potential of new chemical entity prior to their clinical use. Traditionally the evaluation of the P450 inhibitory potential has been performed separately for each single enzyme; this traditional enzyme screening is very time consuming, labor intensive, and cost ineffective. Recently, a substrate ‘cocktail’ strategy, in which a mixture of CYP substrates are added in a single human microsomal incubation have been developed for the definitive evaluation of inhibitory effects of drug candidates. *In vitro* methods are commonly used to determine the CYP inhibitory potential of NCEs. The CYP substrate cocktail assays employ a mixture of probe substrates to assess the inhibition of several CYP forms simultaneously. A compound being evaluated is co-incubated with a known

substrate for a specific CYP enzyme. The effect of the test compound on the metabolism of the substrate is then determined. The increased flux of NCEs into drug discovery due to combinatorial chemistry and high-throughput screening techniques has placed an increased demand for speed and efficiency for the CYP inhibition screening methodologies.

Inhibition assays for specific CYP enzymes using selective probe substrates and HLM have been developed for the definitive evaluation of inhibitory effects of new molecular entities. In this work, a LC/UV method has been developed for simultaneous and quantitative determination of substrate disappearance from several common CYP probe substrates for major drug metabolizing CYP isozymes (including CYP2B6, 2C9, 2E1 and 3A4) in a single run. This method has been used to quantify the probe substrate disappearance from human liver microsomal incubation of a mixture of probe substrates and the identification of interactions of NCEs (MCR 706 and MCR 742) with a specific CYP isozyme (e.g. inhibition of that isoenzyme) which can aid in predicting clinical drug interactions.

REFERENCES

1. Wilkinson GR. Drug metabolism and variability among patients in drug response. *N Engl J Med* 2005;352:2211-21.

2. Bjornsson TD, Callaghan JT, Einolf HJ, Fischer V, Gan L, Grimm S, Kao J, King SP, Miwa G, Ni L, Kumar G, McLeod J, Obach SR, Roberts S, Roe A, Shah A, Snikeris F, Sullivan JT, Tweedie D,Vega JM, Walsh J, Wrighton SA. Th e conduct of *in vitro* and in vivo drug-drug interaction studies: a PhRMA perspective. *J Clin Pharmacol* 2003;43:443-69.

3. Pelkonen O, Turpeinen M, Uusitalo J, Rautio A, Raunio H. Prediction of drug metabolism and interactions on the basis of *in vitro* investigations. *Basic Clin Pharmacol Toxicol* 2005;96:167-754.

4. Lewis DFV, Ito Y, Goldfarb PS: Structural modeling of the human drug-metabolizing cytochromes P450. Curr Med Chem. 13:2645-52, 2006.

5. Nebert DW, Russell DW. Clinical importance of the cytochromes P450. *Lancet* 2002;360:1155-62.

6. Nelson DR, Koymans L, Kamataki T, Stegeman JJ, Feyereisen R, Waxman DJ, Waterman MR, Gotoh O, Coon MJ, Estabrook RW, Gunsalus IC, Nebert DW. P450 superfamily: update on new sequences, gene mapping, accession numbers and nomenclature. *Pharmacogenetics* 1996;6:1-42.

7. Shimada T, Yamazaki H, Mimura M, Inui Y, Guengerich FP. Interindividual variations in human liver cytochrome P-450 enzymes involved in the oxidation of drugs, carcinogens and toxic chemicals: studies with liver microsomes of 30 Japanese and 30 Caucasians. *J Pharmacol Exp Th er* 1994;270:414-23.

8. Denisov IG, Makris TM, Sligar SG, Schlicting I: Structure and Chemistry of Cytochrome P450. Chem. Rev. 105:2253-2277, 2005.

9. Lewis DF and Pratt JM (1998) The P450 catalytic cycle and oxygenation mechanism. Drug Metab Rev 30:739-786.

10. Guengerich FP (2001) Common and uncommon cytochrome P450 reactions related to metabolism andchemical toxicity. Chem Res Toxicol 14:611-650.

11. Nebert DW, Dalton TP, Okey AB and Gonzalez FJ (2004) Role of aryl hydrocarbon receptor-mediatedinduction of the CYP1 enzymes in environmental toxicity and cancer. J Biol Chem 279:23847-23850.

12. Zhou ZW and Zhou SF. Application of mechanism-based CYP inhibition for predicting drug-drug interactions. *Expert Opin Drug Metab Toxicol* 5:579-605 (2009).

13. Shi X, Zhou S, Wang Z, Zhou Z and Wang Z (2008) CYP1A1 and GSTM1 polymorphisms and lung cancer risk in Chinese populations: a meta-analysis. Lung Cancer 59:155-163.

14. Murray GI, Melvin WT, Greenlee WF and Burke MD (2001) Regulation, function, and tissue-specific expression of cytochrome P450 CYP1B1. Annu Rev Pharmacol Toxicol 41:297-316.

15. Nebert DW, Dalton TP, Okey AB and Gonzalez FJ (2004) Role of aryl hydrocarbon receptor-mediated induction of the CYP1 enzymes in environmental toxicity and cancer. J Biol Chem 279:23847-23850.

16. Pelkonen O, Turpeinen M, Hakkola J, Honkakoski P, Hukkanen J and Raunio H

(2008) Inhibition and induction of human cytochrome P450 enzymes: current status. Arch Toxicol 82:667-715.

17. Gunes A and Dahl ML (2008) Variation in CYP1A2 activity and its clinical implications: influence of environmental factors and genetic polymorphisms. Pharmacogenomics 9:625-637.

18. Eaton DL, Gallagher EP, Bammler TK and Kunze KL (1995) Role of cytochrome P4501A2 in chemical carcinogenesis: implications for human variability in expression and enzyme activity. Pharmacogenetics 5:259-274.

19. Khojasteh SC, Prabhu S, Kenny JR, Halladay JS and Lu AY (2011) Chemical inhibitors of cytochrome P450 isoforms in human liver microsomes: a re-evaluation of P450 isoform selectivity. Eur J Drug Metab Pharmacokinet 36:1-16.

20. Honkakoski P and Negishi M (1997) The structure, function, and regulation of cytochrome P450 2A enzymes. Drug Metab Rev 29:977-996.

21. Zaphiropoulos PG (1997) Exon skipping and circular RNA formation in transcripts of the human cytochrome P-450 2C18 gene in epidermis and of the rat androgen binding protein gene in testis. Mol Cell Biol 17:2985-2993.

22. Rendic S and Guengerich FP (2010) Update information on drug metabolism systems--2009, part II: summary of information on the effects of diseases and environmental factors on human cytochrome P450 (CYP) enzymes and transporters. Curr Drug Metab 11:4-84.

23. Rendic S (2002) Summary of information on human CYP enzymes: human P450 metabolism data. Drug Metab Rev 34:83-448.

24. Lang T, Klein K, Fischer J, Nussler AK, Neuhaus P, Hofmann U, Eichelbaum M, Schwab M and Zanger UM (2001) Extensive genetic polymorphism in the human CYP2B6 gene with impact on expression and function in human liver. Pharmacogenetics 11:399-415.

25. Mo SL, Liu YH, Duan W, Wei MQ, Kanwar JR and Zhou SF (2009b) Substrate specificity, regulation, and polymorphism of human cytochrome P450 2B6. Curr Drug Metab 10:730-753.

26. Turpeinen M, Raunio H and Pelkonen O (2006) The functional role of CYP2B6 in human drug metabolism:substrates and inhibitors *in vitro, in vivo* and *in silico*. Curr Drug Metab 7:705-714.

27. Richter T, Murdter TE, Heinkele G, Pleiss J, Tatzel S, Schwab M, Eichelbaum M and Zanger UM (2004) Potent mechanism-based inhibition of human CYP2B6 by clopidogrel and ticlopidine. J Pharmacol Exp Ther 308:189-197.

28. Kent UM, Juschyshyn MI and Hollenberg PF (2001) Mechanism-based inactivators as probes of cytochrome P450 structure and function. Curr Drug Metab 2:215-243.

29. Laura Martikainenin (2011) *In Vitro* and *in Silico* Methods to Predict Cytochrome P450 Enzyme Inhibition. Publications of the University of Eastern Finland Dissertations in Health Sciences. 7-9.

30. Baranczewski P, Stańczak A, Sundberg K, Svensson R, Wallin A, Jansson J, Garberg P, Postlind H. Introduction to *in vitro* estimation of metabolic stability and drug interactions of new chemical entities in drug discovery and development. Pharmacol Rep. 2006 Jul-Aug; 58(4): 453-72.

31. Pelkonen O, Turpeinen M, Hakkola J, Honkakoski P, Hukkanen J and Raunio H (2008) Inhibition and induction of human cytochrome P450 enzymes: current status. Arch Toxicol 82:667-715.

32. Kalgutkar AS, Obach RS and Maurer TS (2007) Mechanism-based inactivation of cytochrome P450 enzymes: chemical mechanisms, structure-activity relationships and relationship to clinical drug-drug interactions and idiosyncratic adverse drug reactions. Curr Drug Metab 8:407-447.

33. VandenBrink BM and Isoherranen N (2010) The role of metabolites in predicting drug-drug interactions: focus on irreversible cytochrome P450 inhibition. Curr Opin Drug Discov Devel 13:66-77.

34. Boobis A, Watelet JB, Whomsley R, Benedetti MS, Demoly P and Tipton K (2009) Drug interactions. Drug Metab Rev 41:486-527.

35. The European Medicines Agency (EMA) (2010) Guideline on the Investigation of Drug Interactions (draft). http://www.ema.europa.eu/docs/en_GB/document_library/Scientific_guideline/2010/05/WC500090112.pdf

36. Zhang L, Reynolds KS, Zhao P and Huang SM (2010) Drug interactions evaluation: an integrated part of risk assessment of therapeutics. Toxicol Appl Pharmacol 243:134-145.

37. Muneaki Hidaka., Masashi Nagata., Yohei Kawano., 2008. Inhibitory effects of fruit juices on cytochrome P450 2C9 activity *in vitro*. Biosci. Biotechnol. Biochem. 72, 406.

38. Nagata, M., Hidaka, M., Sekiya, H., Kawano, Y.,Yamasaki, K., Okumura, M., and Arimori, K., 2007.Effects of pomegranate juice on human cytochrome P450 2C9and tolbutamide pharmacokinetics in rats. Drug Metab.Dispos., 35, 302.

39. Dresser GK and Bailey DG . The effects of fruit juices on drug disposition: a new model for drug interactions. Eur J Clin Investig *3, 2003. 3: 10*–16.

40. Fujita K. 2004 Food-drug interactions via human cytochrome P450 3A (CYP3A). Drug Metabol Drug Interact;20(4):195-217.

41. Päivi Taavitsainen. Cytochrome P450 isoform specific *in vitro* methods to predict drug metabolism and interactions (Dessertation 2010) (URL: http://herkules.oulu.fi/issn03553221/).

42. Kiyomi Ito 1 , Koji Chiba 2 , Masato Horikawa 3 , Michi Ishigami 4 , Naomi Mizuno 5 , Jun Aoki 6 , Yasumasa Gotoh 7 , Takafumi Iwatsubo 8 , Shin-ichi Kanamitsu 9 , Motohiro Kato 10 , Iichiro Kawahara 11 , Kayoko Niinuma 12 , Akiko Nishino 13 , Norihito Sato 14 , Yuko Tsukamoto 15 , Kaoru Ueda 16 , Tomoo Itoh 1 and Yuichi Sugiyama 17 Which Concentration of the Inhibitor Should Be Used to Predict *In Vivo* Drug Interactions From *In Vitro* Data? AAPS PharmSci 2002; 4 (3) article 20 (http://www.aapspharmsci.org).

43. Tucker GT, Houston JB, Hunag S-M. Optimising drug development: strategies to assess drug metabolism/transporter interaction potential—toward a consensus. Br J Clin Pharmacol 2001; 52: 107–17.

44. Huang SM, Strong JM, Zhang L, Reynolds KS, Nallani S, Temple R, Abraham S, Habet SA, Baweja RK, Burckart GJ, Chung S, Colangelo P, Frucht D, Green MD, Hepp P, Karnaukhova E, Ko HS, Lee JI, Marroum PJ, Norden JM, Qiu W, ahman A, Sobel S, Stifano T, Thummel K, Wei XX, Yasuda S, Zheng JH, Zhao H and Lesko LJ. (2008). New era in drug interaction evaluation: US Food and Drug Administration update on CYP enzymes, transporters, and the guidance process. *J Clin Pharmacol* 48:662-670.

45. Kanji, Komatsu., Kiyomi, Ito., Yukiko, Nakajima., Shin-ichi ,Kanamitsu., Susumu, Imaoka., Yoshihiko,Funae.,2000.Prediction of *in vivo* drug-drug interactions between tolbutamide and various sulfonamides in humans based on *in vitro* experiments. Drug Metab.Dispos., 28, 475.

46. Tianyi Zhang*, Yongxin Zhu Chandrani Gunaratna Simultaneous Determination of Metabolites from Multiple Cytochrome P450 Probe Substrates by Gradient Liquid Chromatography with UV Detection 2003 Current Separations 20:3, 87-91.

47. Kim MJ, Kim H, Cha IJ, Park JS, Shon JH, Liu KH, Shin JG. High-throughput screening of inhibitory potential of nine cytochrome P450 enzymes *in vitro* using liquid chromatography/ tandem mass spectrometry. Rapid Commun Mass Spectrom. 2005;19(18):2651-8.

48. Testino SA Jr, Patonay G. 2003 High-throughput inhibition screening of major human cytochrome P450 enzymes using an *in vitro* cocktail and liquid chromatography-tandem mass spectrometry. J Pharm Biomed Anal. Jan 1;30(5):1459-67.

49. Gao ZW, Shi XJ, Yu C, Li SJ, Zhong MK. 2007. Simultaneous determination of the inhibitory potency of compounds on the activity of five cytochrome P-450 enzymes using a cocktail probe substrates method. Yao Xue Xue Bao. Jun;42(6):589-94.

Chapter 3
Drug Profile

3.1 Glimepiride (GLM)

Glimepiride is a medium- to long-acting "third generation" sulfonylurea antidiabetic drug**.** The primary mechanism of action of glimepiride in lowering blood glucose appears to be dependent on stimulating the release of insulin from functioning pancreatic beta cells.

3.1.1 Pharmacodynamics and clinical use[1]

A mild glucose-lowering effect first appeared following single oral doses as low as 0.5-0.6 mg in healthy subjects. The time required to reach the maximum effect (i.e., minimum blood glucose level [Tmin]) was about 2 to 3 hours. In noninsulin-dependent (Type II) diabetes mellitus (NIDDM) patients, both fasting and 2-hour postprandial glucose levels were significantly lower with glimepiride (1, 2, 4, and 8 mg once daily) than with placebo after 14 days of oral dosing. The glucose-lowering effect in all active treatment groups was maintained over 24 hours.

Insulin release Sulfonylureas regulate insulin secretion by closing the ATP-sensitive potassium channel in the beta cell membrane. Closing the potassium channel induces depolarisation of the beta cell and results – by opening of calcium channels - in an increased influx of calcium into the cell. This leads to insulin release through exocytosis. Glimepiride binds with a high exchange rate to a beta cell membrane protein which is associated with the ATP-sensitive potassium channel but which is different from the usual sulfonylurea binding site.

Extrapancreatic activity The extrapancreatic effects are for example an improvement of the sensitivity of the peripheral tissue for insulin and a decrease of the insulin uptake by the liver.The uptake of glucose from blood into peripheral muscle and fat tissues occurs via special transport proteins, located in the cells membrane. The transport of glucose in these tissues is the rate limiting step in the use of glucose. Glimepiride increases very rapidly the number of active glucose transport molecules in the plasma membranes of muscle and fat cells, resulting in stimulated glucose uptake. Glimepiride increases the activity of the glycosyphosphatidylinositol-specific phospholipase C, which may be correlated with the drug-induced lipogenesis and glycogenesis in isolated fat and muscle

cells. Glimepiride inhibits the glucose production in the liver by increasing the intracellular concentration of fructose-2,6-bisphosphate, which in its turn inhibits the gluconeogenesis

General

In healthy persons, the minimum effective oral dose is approximately 0.6 mg. The effect of glimepiride is dose-dependent and reproducible. The physiological response to acute physical exercise, reduction of insulin secretion, is still present under glimepiride. There was no significant difference in effect regardless of whether the medicinal product was given 30 minutes or immediately before a meal. In diabetic patients, good metabolic control over 24 hours can be achieved with a single daily dose. Although the hydroxy metabolite of glimepiride caused a small but significant decrease in serum glucose in healthy persons, it accounts for only a minor part of the total drug effect.

3.1.2 Pharmacokinetics and clinical use[1]

Absorption. After oral administration, glimepiride is completely (100%) absorbed from the GI tract. Studies with single oral doses in normal subjects and with multiple oral doses in patients with NIDDM have shown significant absorption of glimepiride within 1 hour after administration and peak drug levels (Cmax) at 2 to 3 hours. When glimepiride was given with meals, the mean Tmax (time to reach Cmax) was slightly increased (12%) and the mean Cmax and AUC (area under the curve) were slightly decreased (8% and 9%, respectively).

Distribution. After intravenous (IV) dosing in normal subjects, the volume of distribution (Vd) was 8.8 L (113 mL/kg), and the total body clearance (CL) was 47.8 mL/min. Protein binding was greater than 99.5%.

Metabolism. Glimepiride is completely metabolized by oxidative biotransformation after either a parenteral or oral dose. The major metabolites are the cyclohexyl hydroxy methyl derivative (M1) and the carboxyl derivative (M2). Cytochrome P450 II C9 has been shown to be involved in the biotransformation of glimepiride to M1. M1 is further metabolized to M2 by one or several cytosolic enzymes. M1, but not M2, possesses about

1/3 of the pharmacological activity as compared to its parent in an animal model; however, whether the glucose-lowering effect of M1 is clinically meaningful is not clear.

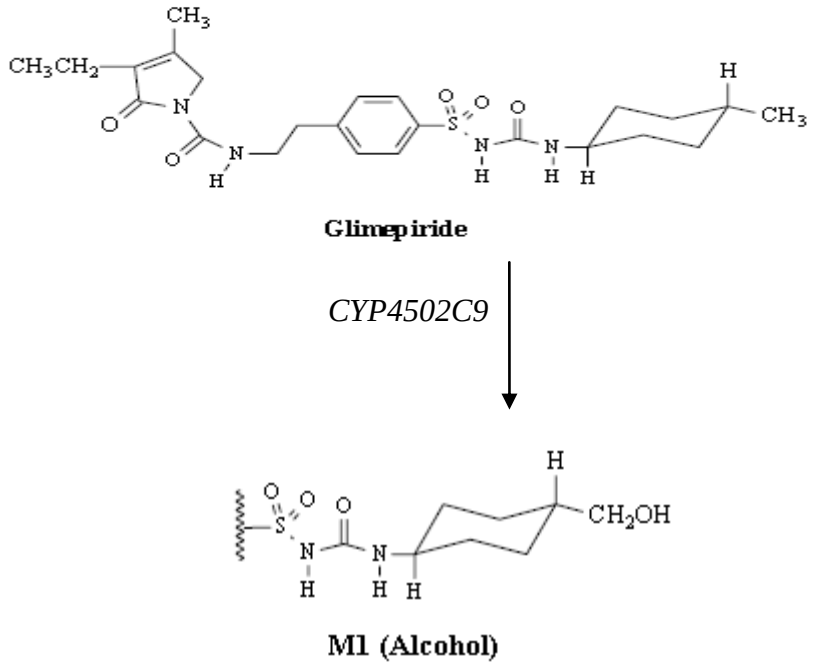

Figure 3.1. Metabolism of Glimepiride

Excretion. When 14C-glimepiride was given orally, approximately 60% of the total radioactivity was recovered in the urine in 7 days and M1 (predominant) and M2 accounted for 80-90% of that recovered in the urine. Approximately 40% of the total radioactivity was recovered in feces and M1 and M2 (predominant) accounted for about 70% of that recovered in feces. No parent drug was recovered from urine or feces. After IV dosing in patients, no significant biliary excretion of glimepiride or its M1 metabolite has been observed.

Although, GLM has been shown to undergo hepatic oxidative biotransformation via CYP450 system[4,5] and its metabolism also has been reported using CYP specific species of seven CYP2C9 variants found in Japanese subjects, oxidative biotransformation by *in vitro* studies using HLM has not been demonstrated. [6]

In vitro studies of glimepiride with HML have suggested the possibility of drug interaction with atorvastatin and rosuvastatin.[7] However, the information on the contribution of CYP2C9 isoform to the metabolism of glimepiride seems to be based on unpublished data, and the experimental systems in which these results were obtained, have not been described. Prior to this thesis, no published studies have been available on the effects of CYP2C9 inhibitors on the pharmacokinetics of glimepiride *in vitro.*

3.1.3 Pharmacokinetic Parameters[1]:

The pharmacokinetic parameters of glimepiride obtained from a single-dose, crossover, dose-proportionality (1, 2, 4, and 8 mg) study in normal subjects and from a single- and multiple-dose, parallel, dose-proportionality (4 and 8 mg) study in patients with Type 2 diabetes are summarized in below:

Table 3.1: Pharmacokinetic Parameters of glimepiride.

	Volunteers	**Patients with Type 2 diabetes**	
	Single Dose Mean±SD	**Single Dose (Day 1) Mean±SD**	**Multiple Dose (Day 10) Mean±SD**
Cmax (ng/mL)			
1mg	103 ± 34 (12)	-----	-----
2mg	177 ± 44 (12)	-----	-----
4mg	308 ± 69 (12)	352 ± 222 (12)	309 ± 134 (12)
8mg	551± 152 (12)	591 ± 232 (14)	578 ± 265 (11)
Tmax (h)	2.4 ± 0.8 (48)	2.5 ± 1.2 (26)	2.8 ± 2.2 (23)
CL/f (mL/min)	52.1 ± 16.0 (48)	48.5 ± 29.3 (26)	52.7 ± 40.3 (23)
Vd/f (L)	21.8 ± 13.9 (48)	19.8 ± 12.7 (26)	37.1 ± 18.2 (23)
T1/2 (h)	5.3 ± 4.1 (48)	5.0 ± 2.5 (26)	9.2 ± 3.6 (23)

( ) = No. of subjects.
CL/f=Total body clearance after oral dosing.
Vd/f=Volume of distribution calculated after oral dosing.

Table 3.2: Physicochemical properties of Glimepiride[1-3]

Chemical structure	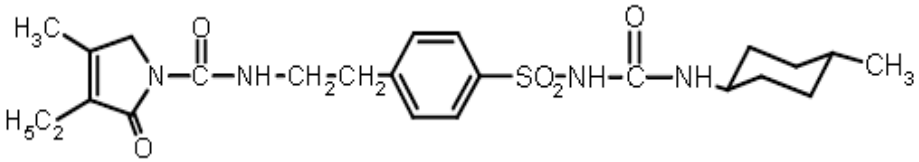
IUPAC name	3-ethyl-4-methyl-*N*-(4-[*N*-((1*r*,4*r*)-4-methylcyclohexylcarbamoyl)sulfamoyl]phenethyl)-2-oxo-2,5-dihydro-1*H*-pyrrole-1-Carboxamide
Molecular formula	$C_{24}H_{34}N_4O_5S$
Molecular weight	490.617 g/mol
Physical Properties **Appearance** **Solubility** **Melting point**	 Glimepiride is a white to yellowish-white, crystalline, odorless to practically odorless powder. Glimepiride is practically insoluble in water. 207°C
Drug category	Antidiabetic agent, Oral sulfonylurea
Mechanism of action	The primary mechanism of action of glimepiride in lowering blood glucose appears to be dependent on stimulating the release of insulin from functioning pancreatic beta cells. In addition, extra-pancreatic effects may also play a role in the activity of glimepiride.
Use	Used as an adjunct to diet and exercise in patients with non-insulin-dependent Type 2 diabetes mellitus whose hyperglycemia cannot be controlled by diet and exercise alone.

3.2 Drug studied with glimepiride *in vitro*

3.2.1 Sulfamethoxazole (SMZ)

Sulfamethoxazole is a sulfonamide bacteriostatic antibiotic agent that interferes with folic acid synthesis in susceptible bacteria. It is most often used as part of a synergistic combination with trimethoprim in a 5:1 ratio in co-trimoxazole. It is commonly used to treat urinary tract infections In addition it can be used as an alternative to amoxicillin-based antibiotics to treat sinusitis. It can also be used to treat toxoplasmosis and it is the drug of choice for *Pneumocystis pneumonia*, which affects primarily patients with HIV. In urine, approximately 20% of the sulfamethoxazole present is unchanged drug, 50-70% is the acetylated derivative, and 15-20% is the glucuronide conjugate. [8-9]

Hypoglycemia resulting from the combination of sulfonylurea and sulfonamides is a recognized drug interaction. Hypoglycemia induced by sulfonamides alone may be encountered less frequently. Because of their structural similarities to sulfonylureas, sulfonamides are liable to facilitate hypoglycemia by increasing insulin release in susceptible individuals. Sulfonamides can potentiate the hypoglycemic effect of sulfonylurea agents when given in combination.[10]

Whereas the pharmacokinetic interaction between sulphonylureas and CYP2C9 is well characterized in healthy subjects, data are lacking on the clinical significance of these interactions in the everyday treatment setting.

In previous *in vitro* studies, sulfamethoxazole has been shown to inhibit tolbutamide hydroxylation (a CYP2C9 marker reaction) with an apparent *K*i value of about 250 µM.[11-12] However, it seems that there are no published *in vitro* studies investigating the effects of sulfamethoxazole on major CYP2C9 isoform activities of glimepiride hydroxylation in human liver microsomes.

Hence the present research work evaluates the use of glimepiride as a model substrate and sulfamethoxazole as an inhibitor for CYP2C9 *in vitro* using human liver microsomes and establishes *in vivo* clinical significance of potential CYP2C9 mediated drug-drug interaction of glimepiride with sulfamethoxazole from *in vitro* data.

Table 3.3: Physicochemical properties of Sulfamethoxazole.[8-9]

Chemical structure	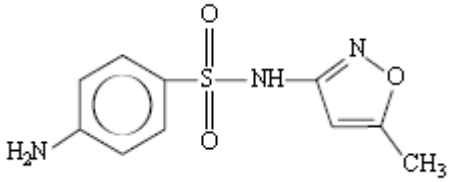
IUPAC name **Molecular formula** **Molecular weight**	4-amino-*N*-(5-methylisoxazol-3-yl)-benzenesulfonamide $C_{10}H_{11}N_3O_3S$ 253.279 g/mol
Physical Properties **Appearance** **Solubility** **Melting point**	White to slightly off-white crystalline powder. Practically insoluble in water. Soluble in methanol. 168-172 °C
Drug category	sulfonamide bacteriostatic antibiotic.
Mechanism of action	Sulfamethoxazole interferes with folic acid synthesis in susceptible bacteria. Its use has been limited by the development of resistance and it is used mainly as a mixture with trimethoprim.
Uses	Sulfamethoxazole is an antibacterial drug which has been used since the 1960s in the treatment of various systemic infection in humans and other species. The main use has been in the treatment of acute urinary tract infections. It has also been used against gonorrhoea, meningitis and serious respiratory tract infections (*Pneumocystis carinii*) and prophylactically against susceptible meningococci.

3.3 Fruit Juices studied with glimepiride *in vitro*[13-17]

Interaction between fruit juices and drugs can have profound influence on the rate of drug absorption and metabolism. The possibility of interaction between fruit juices and prescription drugs creates a dilemma for individuals who consume these juices for their health benefits. CYP2C9 makes up about 18% of the cytochrome P450 protein in liver microsomes. Very few reports are available on the inhibition of CYP2C9 activity by fruit juice or extract. Hence it is important to evaluate the effect of fruit juice on CYP2C9 activity.

Food interactions are usually studied in terms of fruit juices. It has been reported that some fruit juices like grapefruit, pineapple and pomegranate affect the oral bioavailability of drugs undergoing metabolism via CYP450 respectively. Normally grape fruit juice is used for drug food interaction studies which interacts with drugs that undergo substantial presystemic metabolism mediated by CYP3A4.[17] Glimepiride undergoes hepatic metabolism via CYP2C9 invivo[6].PIJ and POJ have strong affinity towards CYP2C9 as compared to grapefruit juice. Hence pineapple and pomegranate juice were chosen as food for CYP2C9 interaction study.

Pineapple (*Ananas comosus, Bromeliaceae)* and Pomegranate *(Punica granatum, Punicaceae)* are consumed around the world and has been used as traditional medicine for a variety of therapeutic purposes. Both the pineapple root and fruit may be eaten or applied topically as an anti-inflammatory or as a proteolytic agent while Pomegranate fruit shows potential antioxidant activity such as inhibition of low density lipoprotein oxidation and decrease in cardiovascular diseases. Based on these findings the fruits have high demand which allows for possible drug fruit interaction.

The present study was focused to determine whether **pineapple and pomegranate juices** would inhibit the CYP2C9-mediated drug metabolism of glimepiride. Drug fruit interaction is not yet reported with glimepiride. So it was planned to study the interaction of glimepiride as a model substrate with pineapple and pomegranate juices.

However, because information concerning the influence of pineapple and pomegranate juices on the pharmacokinetics of CYP2C9 substrates is limited, it was necessary to reach

to a definite conclusion about the effect of these juices on the pharmacokinetics of medications that are mainly metabolized by CYP2C9. To address the issue, the effect of pineapple and pomegranate juices on another CYP2C9 substrate glimepiride, *in vitro* was studied. The inhibitory effect of pineapple and pomegranate juices on glimepiride metabolism by human liver microsomes was determined.

3.4 MCR-706 and MCR-742: New Molecular Entities synthesized in Pharmaceutical Chemistry Laboratory of M.S.University, Baroda, Gujrat)[18-19]

Estrogens are essential regulators of many physiological processes including maintenance of the female sexual organs, the reproductive cycle and numerous neuroendocrine functions. Along with these normal physiological functions, these hormones also play crucial roles in some disease states, particularly in breast cancer, where through binding to their target receptor, they promote proliferation of breast cancer cells. Production of estrogens takes place in many tissues throughout the body including the ovaries, adipose tissue, muscle, liver, breast tissue and malignant breast tumors. In premenopausal women the ovaries are the main source of circulating estrogens while in the postmenopausal women the main source is adipose tissue and muscle. Aromatase (CYP19) is the cytochrome P450 enzyme responsible for the conversion of androgens including androstenedione and testosterone, to the estrogen products, estrone and estradiol Expression of aromatase is highest in or near the breast tumor cells . Aromatase has been a particularly attractive target for inhibition in the treatment of hormone-dependant breast cancer since the aromatization of androgen substrates is the terminal and rate limiting step in estrogen biosynthesis. Inhibition of aromatase is an efficient approach for the prevention and treatment of breast cancer.

Besides attempts to develop novel nonsteroidal compounds, there is a focus on the development of steroidal compounds as potential aromatase inhibitors also. Treatment with aromatase inhibitors is generally well tolerated with low incidence of serious side effects. However short-term events like hot flushes, vaginal dryness, musculoskeletal pain and headache have been observed. Accordingly there is need for new, potent, more selective and less toxic CYP19 inhibitors. Eventually new aromatase inhibitors could also

be superior to the current compounds regarding the acquirement of resistance. Hence novel pyrazole and 4-phenylthia derivatives **MCR-706 and MCR-742** have been synthesized as **aromatase inhibitors in Pharmaceutical Chemistry Laboratory of M.S. University, Baroda, Gujrat.** The synthesized compounds were expected to show noticeable aromatase inhibiting activity. Therefore it was envisaged to study the pharmacokinetic behavior of these NME's *in vitro*.

According to literature [18-19] both the synthesized compounds were evaluated for their aromatase inhibiting activity. The assay was performed by monitoring the enzyme activity by measuring the concentration of ^{3}H2O formed from [1β-^{3}H] androstenedione as a substrate during its aromatization by the enzyme. The literature revealed that aromatase inhibitory activity for compound MCR-706 having pyrazole ring at 2, 3 position showed the highest activity as compared to the compound MCR-742.Both the compounds being strong aromatase inhibitors are covered by patent application no. Appl/3309/MUM/2010.

3.4.1 Drugs studied with MCR-706 and MCR-742

During the drug-candidate screening and development process, investigators often conduct two types of *in vitro* drug metabolism studies to assess the potential for CYP450-based drug interactions. One type of study characterizes the metabolic pathway of the new drug and the potential for other drugs to modify the metabolism of the new drug. The other type of study evaluates the potential for the new drug to alter the metabolism of other drugs.

Predicting the potential for the new drug to alter the metabolism of other drugs usually relies on the evaluation of the effect of the new drug on the rate of a probe reaction that represents a specific P450 enzyme activity. An ideal probe substrate is the one with a simple metabolic scheme, so that the formation rate of a metabolite specifically reflects the activity of one distinct P450 enzyme. Preferably, the metabolite formed does not undergo sequential metabolism. The reaction should be selective, with at least 80% of the formation of a metabolite being carried out by a single enzyme. In addition to the above-mentioned scientific criteria, the following practical criteria are relevant: the commercial availability of the assayed molecular species (i.e., parent drug and the metabolite); the

availability of an assay that is sensitive, rapid, and simple; and reasonable *in vitro* experimental conditions. The *in vitro* probe reaction is a useful tool to screen for potential *in vivo* drug interactions. Due to genetic variation, the influence of environmental or hormonal factors, as well as intrinsic limitations of *in vitro* systems, the quantitative prediction of *in vivo* drug interactions for an individual patient remains a challenge. However, with the rapid growth of our knowledge and technology in drug metabolism and disposition, quantitative prediction may be achievable in the future. The conduct of high-quality *in vitro* studies is the first step toward this goal.[20]

The potential influence of probe substrates and experimental conditions on the assessment of *in vitro* drug interactions has a significant impact on the drug development process and regulatory decisions. The *in vivo* drug interaction guidance published by the Food and Drug Administration in 1999 (www.fda.gov/cder/guidance) indicates that investigators may use *in vitro* drug interaction data to conclude that a new drug does not inhibit a specific P450 activity.

Table 3.4: Physicochemical properties of NCE's[18,19]

Drug	MCR 706	MCR 742
Chemical structure	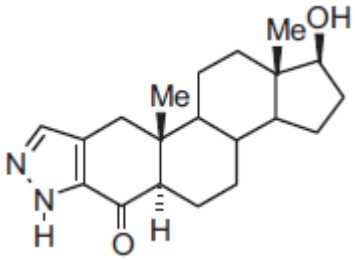	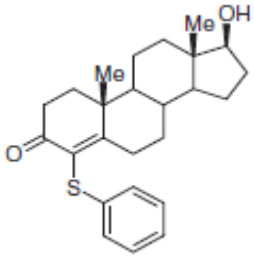
IUPAC name	17β-Hydroxy-4-oxo-5α-androstano [2,3-d] pyrazole.	17β-Hydroxy-4-phenylthia-4-androsten-3-one.
Molecular formula	$C_{20}H_{32}N_2O_2$	$C_{25}H_{32}O_2S$
Molecular weight	344.50 g/mole	396.60 g/mole
Physical properties		
Appearance	White crystalline powder.	White crystalline powder.
Solubility	Soluble in methanol.	Soluble in methanol.
Melting point	245-249.5°C	159-161°C
Spectral data	**UV** (MeOH): 270nm (logЄ4.31), UV (Alk. MeOH): **IR** (KBr): 3388, 3258, 3319, 2944, 1634, 1545, 1447, 1259, 1074, 959. **^{1}H NMR**: δ12.5 (s, 1H); 7.24(s, 1H); 3.51–3.55 (t, 1H); 2.70–2.74 (d, 1H); 2.51–2.53 (dd, 1H), 2.20– 2.24 (d, 1H); 1.19–1.38 (m,6H);0.92–1.18(m,4H);0.68(s,3H);0.64(s,3H)	**UV** (MeOH): 270nm (logЄ3.67), **IR** (KBr): 3499, 1689, 1609, 1532 and 744. **^{1}H NMR**: 7.11-7.15 (m, 2H); 7.00-7.04(m, 3H); 3.55–3.60 (t, 1H); 1.22 (s, 3H) and 0.74 (s, 3H).
Category	Aromatase Inhibitor	Aromatase Inhibitor

3.5 Selection of Probe substrates

3.5.1 Efavirenz (CYP2B6 mediated efavirenz 8-hydroxylation)

CYP2B6 enzyme system plays an important role in the metabolism of a growing list of frequently prescribed drugs and other chemicals but, it has been studied less because of unavailability of a specific and safe substrate reaction marker that will allow prediction of *in vivo* activity from *in vitro* studies. Efavirenz (EFV), being a substrate, an inhibitor and an inducer of cytochromes P450 (P450s) exhibits multiple interactions with the P450 system. The utility of efavirenz as a novel substrate probe of CYP2B6 has been tested. Efavirenz 8-hydroxylation is a specific *in vitro* reaction marker of CYP2B6 and may have utility as a phenotyping tool to study the role of this enzyme in human drug metabolism. The product label of efavirenz [21] implicate CYP3A and CYP2B6 in efavirenz metabolism, but there have been no published data that comprehensively address the contribution of these or any other enzymes *in vitro* or *in vivo*. All these data suggest that P450s (most likely CYP2B6) other than CYP3A might be responsible for the human metabolism of efavirenz.

All these Cytochrome P450 (P450) 2B6 is the main enzyme catalyzing the major clearance mechanism of efavirenz, 8-hydroxylation to 8-hydroxyefavirenz, *in vitro*. However, information on the clinical relevance of this enzyme has been generally limited because of the lack of suitable *in vivo* substrate probe. Bupropion 4-hydroxylation has been increasingly used as an *in vitro* and *in vivo* probe of activity, but its *in vivo* utility has important limitations.[22] Efavirenz has been proposed to be an alternative probe of CYP2B6 activity to evaluate the clinical relevance of this enzyme.[23] Hence Efavirenz may serve as an effective probe of CYP2B6 activity *in vitro* and *in vivo*.[24]

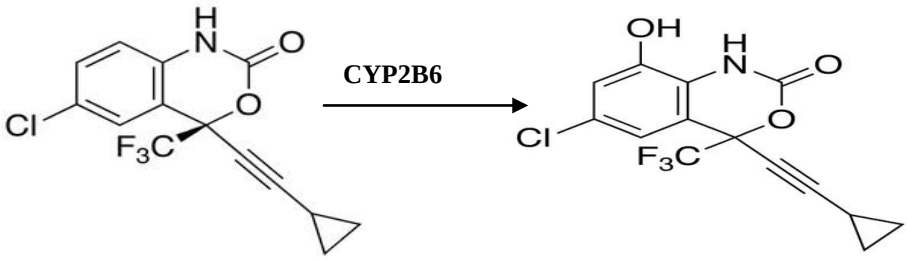

Efavirenz **8-Hydroxy Efavirenz**

Figure 3.2. Metabolism of Efavirenz

3.5.2 Diclofenac (CYP2C9 mediated diclofenac 4-hydroxylation)

Cytochrome P450 2C is the second most abundant subfamily of P450 enzymes and is responsible for metabolism of almost 20% of the drugs currently available in the market. CYP2C9 is an important member of the subfamily, serving as the primary metabolic pathway of the narrow therapeutic index drugs warfarin and phenytoin. Diclofenac (DIC) is the commonly employed substrate probes for determining CYP2C9 activity in human liver micrososmes.[25] DIC has the advantage that CYP2C9 catalyzes its metabolism with a high turnover number. Also this is beneficial in allowing for facile, economical HPLC-UV assays to be employed for routine screening *in vitro*. It is a potential probe to quantify CYP2C9 activity in humans.[26] Oxidation of the aromatic rings of DIC is mediated by cytochromes P450. Hydroxylation of the dichlorophenyl ring is catalyzed specifically by CYP2C9 to produce 4 hydroxydiclofenac as the major metabolite.[27-28]

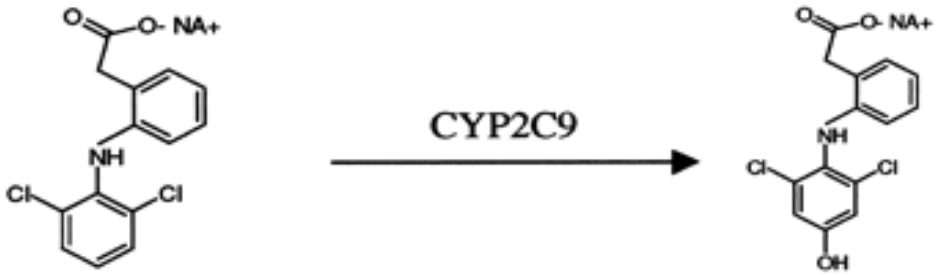

Diclofenac **4´-OH-Diclofenac**

Figure 3.3 Metabolism of Diclofenac

3.5.3 Chlorzoxazone (CYP2E1 mediated chlorzoxazone 6-hydroxylation)

Cytochrome (CYP) P450 2E1 is clinically and toxicologically important and it is constitutively expressed in the liver and many other tissues. Chlorzoxazone (CHZ), a muscle-relaxing drug, is metabolized by carbon-hydroxylation at position 6**.** After ingestion, chlorzoxazone is rapidly absorbed and extensively metabolized. In HLMs, 6-OH-chlorzoxazone is the sole metabolite formed, which makes the assay highly specific. Literature evidence indicates that chlorzoxazone 6-hydroxylation is the current preferred probe reaction for CYP2E1, but it is important to use high substrate concentrations that reflect low-affinity enzyme (i.e., CYP2E1) activity toward this reaction.[29-30]

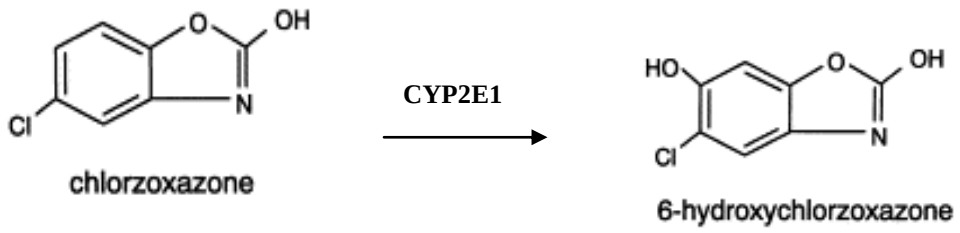

Figure 3.4 Metabolism of Chlorzoxazone

3.5.4 Atorvastatin (CYP3A4 mediated atorvastatin hydroxylation)

Atorvastatin (ATV) is a 3-hydroxy-3-methylglutaryl-coenzyme A (HMG-CoA) reductase inhibitor that is mainly metabolized by cytochrome P450 (CYP) 3A4. A recent study showed that the lipid-lowering effect of statins is affected by the CYP3A5 polymorphism. Therefore, it was investigated whether CYP3A5 contributes to the metabolism of atorvastatin. The intrinsic clearance (CL(int)) rates of atorvastatin hydroxylation by CYP3A4 indicates that CYP3A4 is the major P450 isoform responsible for atorvastatin metabolism. These results suggest that atorvastatin is preferentially metabolized by CYP3A4 rather than by CYP3A5**.** Hence atorvastatin may serve as an effective probe of CYP3A4 activity *in vitro* and *in vivo*.[34]

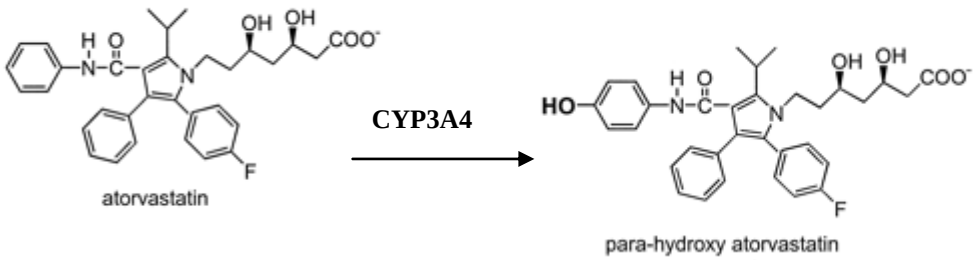

Figure 3.5 Metabolism of Atorvastatin

Table 3.5: Physicochemical properties of Efavirenz (EFA)[21,38-39], Diclofenac sodium (DICLO Na)[40-43], Chlorzoxazone (CHLRZX)[31-33] and Atorvastatin calcium (ATORVA Ca^{2+})[35-37]

Drug	EFV	DIC	CHZ	ATV
Chemical structure	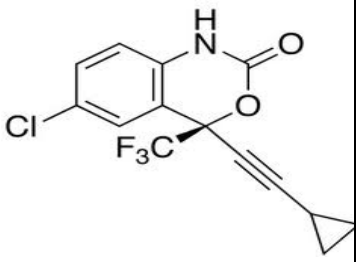	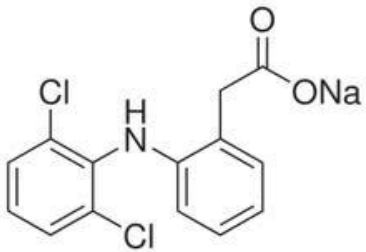	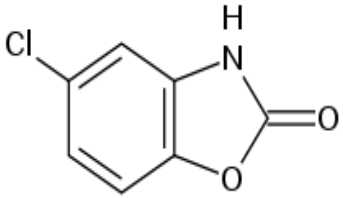	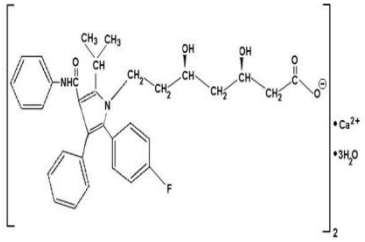
IUPAC name	(4*S*)-6-chloro-4-(2-cyclopropylethynyl)-4-(trifluoromethyl)-2,4-dihydro-1*H*-3,1-benzoxazin-2-one	2[(2, 6-dichloro phenyl) amino] benzene acetic acid sodium salt	5-chloro-3*H*-benzooxazol-2-one	[R-(R*, R*)]-2-(4-fluorophenyl)-β, δ-dihydroxy-5-(1-methylethyl)-3-phenyl-4-[(phenylamino) carbonyl]-1H-pyrrole-1-heptanoic acid, calcium salt (2:1) trihydrate
Molecular formula	$C_{14}H_9ClF_3NO_2$	$C_{14}H_{10}Cl_2NNaO_2$	$C_7H_4ClNO_2$	$(C_{33}H_{34}FN_2O_5)_2Ca{\bullet}3H_2O$
Molecular weight	315.675 g/mole	318.13 g/mole	169.565 g/mole	1209.42 g/mole
Physical prop. Appearance	White powder	White crystalline powder	White powder	White to off-white crystalline powder, soluble in methanol
Solubility	Soluble in methanol	Soluble in methanol	Soluble in methanol	
Melting point	139-141°C	284°C	191-192 °C	176-178 °C

Drug	EFV	DIC	CHZ	ATV
Drug Category	Non-nucleoside reverse transcriptase inhibitor (NNRTI)	Nonsteroidal anti-inflammatory drug (NSAID)	Centrally acting muscle relaxant	Synthetic lipid-lowering agent.
Mechanism of action	Efavirenz inhibits the activity of viral RNA-directed DNA polymerase (i.e., reverse transcriptase).	The primary mechanism responsible for its anti-inflammatory, antipyretic, and analgesic action is thought to be inhibition of prostaglandin synthesis by inhibition of cyclooxygenase (COX).	Chlorzoxazone acts at the level of the spinal cord and subcortical areas of the brain where it inhibits multi synaptic areas involved in producing and maintaining skeletal muscle spasm of varied etiology, thus relieving painful musculoskeletal conditions. It also has sedative property.	Atorvastatin is a selective, competitive inhibitor of HMG-CoA reductase, the rate-limiting enzyme that converts 3-hydroxy-3-methylglutaryl-coenzyme
Uses	Efavirenz is used as part of highly active antiretroviral therapy (HAART) for the treatment of a human immunodeficiency virus (HIV) type 1	DIC is used to treat pain, inflammatory disorders, and dysmenorrhea.	Painful muscle spasm associated with musculo - skeletal conditions.	The primary uses of atorvastatin is for the treatment of dyslipidemia and the prevention of cardiovascular disease.

REFERENCES

1. Product monograph: Amaryl® Glimepiride Oral Hypoglycemic (Sulfonylurea); Sanofi-aventis Canada Inc., July 2009.

2. Langtry HD, Balfour JA. Glimepiride. A review of its use in the management of type2diabetes mellitus. Drugs 1998; 55:563-84.

3. Stephen N. Davis: The role of glimepiride in the effective management of Type 2 diabetes. Journal of Diabetes and its Complications 18(6), 2004; 367–376.

4. Kirchheiner J, Roots I, Goldammer M, Rosenkranz B, Brockmöller J: Effect of genetic polymorphisms in cytochrome p450 CYP2C9 and CYP2C8 on the pharmacokinetics of oral antidiabetic drugs. Clinical Relevance Clin Pharmacokinet 2005, 44: 1209-1225.

5. Suzuki K, Yanagawa T, Shibasaki T, Kaniwa N, Hasegawa R, Tohkin M: Effect of CYP2C9 genetic polymorphisms on the efficacy and pharmacokinetics of glimepiride in subjects with type 2 diabetes. Diabetes Res Clin Pract 2006, 72: 148-54.

6. Keiko M, Noriko H, Emiko S, Masahiro T, Su-Ryang K, Nahoko K, Noriko K, Ryuichi H, Kazuki Y, Kei K, Toshiyuki M, Yoshiro S, and Jun-ichi S: Substrate-Dependent Functional Alterations of Seven CYP2C9 Variants Found in Japanese Subjects. *Drug metab Dispos* 2009, 37: 1895-1903.

7. Galani VJ, Vyas M. *In vivo* and *In vitro* drug interaction study of glimepiride with atorvastatin and rosuvastatin. Journal of Young Pharmacist.2010;2(2):196-200.

8. Martindale, *The extra pharmacopoeia*, 30th ed, p. 208.

9. Sulfamethoxazole: 723-46-6 (CAS DataBase Reference).

10. Zeliha Hekimsoy, Sevinç Biberoğlu, Abdurrahman Çömlekçi, Oktay Tarhan, Cem Mermut, and Kadir Biberoğlu. Trimethoprim/sulfamethoxazole-induced hypoglycemia in a malnourished patient with severe infection Eur J Endocrinol 1997 136 304-306.

11. Back DJ, Tjia JF, Karbwang J, and Colbert J (1988) *In vitro* inhibition studies of tolbutamide hydroxylase activity of human liver microsomes by azoles, sulphonamides and quinolines.Br J Clin Pharmacol 26:23–29.

12. Komatsu K, Ito K, Nakajima Y, Kanamitsu Si, Imaoka S, Funae Y, Green CE, Tyson CA, Shimada N, Sugiyama Y (2000a) Prediction of *in vivo* drug-drug interactions between tolbutamide and various sulfonamides in humans based on *in vitro* experiments. Drug Metab Dispos 28:475–481.

13. Muneaki Hidaka., Masashi Nagata., Yohei Kawano., 2008. Inhibitory effects of fruit juices on cytochrome P450 2C9 activity *in vitro*. Biosci. Biotechnol. Biochem. 72, 406.

14. Nagata, M., Hidaka, M., Sekiya, H., Kawano, Y.,Yamasaki, K., Okumura, M., and Arimori, K., 2007.Effects of pomegranate juice on human cytochrome P450 2C9and tolbutamide pharmacokinetics in rats. Drug Metab.Dispos., 35, 302.

15. Muneaki Hidaka, Manabu Okumura, Ken-ichi Fujita, Tetsuya Ogikubo, Keishi Yamasaki, Tomomi Iwakiri, Nao Setoguchi and Kazuhiko Arimori.2005. Effects of pomegranate juice on human cytochrome p450 3a (cyp3a) and carbamazepine pharmacokinetics in rats. Drug Metab Dispos. vol. 33 no.5 644-648.

16. Dresser GK and Bailey DG (*2003*) The effects of fruit juices on drug disposition: a new model for drug interactions. Eur J Clin Investig 33: 10–16.

17. Fujita K. 2004 Food-drug interactions via human cytochrome P450 3A (CYP3A). Drug Metabol Drug Interact;20(4):195-217.

18. Yadav MR, Sabale PM, Giridhar R, Zimmer C, Haupenthal J, Hartmann RW. Synthesis of some novel androstanes as potential aromatase inhibitors. Steroids 2011;76:464–70.

19. Yadav MR, Sabale PM, Giridhar R, Zimmer C, Hartmann RW. Steroidal carbonitriles as potential aromatase inhibitors. Steroids 2011; 77 (2012) 850–857.

20. Rae yuan, soraya madani, xiao-xiong wei, kellie reynolds, and shiew-mei huang, 2002. Drug Administration guidance.Evaluation of cytochrome p450 probe substrates commonly used by The Pharmaceutical industry to study *in vitro* drug interactions. Drug metabolism and disposition Vol. 30, No. 12 DMD 30:1311–1319.

21. Product Information of Efavirenz (Sustiva), Bristol-Myers Squibb Company, April 2002.

22. Kharasch ED, Mitchell D, and Coles R (2008) Stereoselective bupropion hydroxylation as an *in vivo* phenotypic probe for cytochrome P4502B6 (CYP2B6) activity. *J Clin Pharmacol*48:464–474.

23. Bryan A. Ward, J Christopher Gorski, David R. Jones, Stephen D. Hall, David A. Flockhart, and Zeruesenay Desta,2003. The Cytochrome P450 2B6 (CYP2B6) Is the Main Catalyst of Efavirenz Primary and Secondary Metabolism: Implication for HIV/AIDS Therapy and Utility of Efavirenz as a Substrate Marker of CYP2B6 Catalytic Activity. JPET, Vol. 306, No. 1 306:287–300.

24. Evan T. Ogburn, David R. Jones, Andrea R. Masters, Cong Xu, Yingying Guo, and Zeruesenay Desta, 2010.Efavirenz Primary and Secondary Metabolism *In Vitro* and *In Vivo*: Identification of Novel Metabolic Pathways and Cytochrome P450. 2A6 as

the Principal Catalyst of Efavirenz 7-Hydroxylation.Drug Metabolism And Disposition Vol. 38, No. 7 38:1218–1229.

25. Rendic S and Di Carlo FJ (*1997*) Human cytochrome P450 enzymes: a status report summarizing their reactions, substrates, inducers, and inhibitors. *Drug Metab Rev 29: 413*– 580.

26. Allan E. Rettie1 and Jeffrey P. Jones, 2005.Clinical And Toxicological Relevance Of CYP2C9: Drug-Drug Interactions And Pharmacogenetics. Annu. Rev. Pharmacol. Toxicol. 45:477–94.

27. R. Menassé, P. R. Hedwall, J. Kraetz, C. Pericin, L. Riesterer, A. Sallmann, R. Ziel and R. Jaques Pharmacological Properties of Diclofenac Sodium and Its Metabolites 1978,7: 5-16.

28. Carlos Rogério Tonussi, Sérgio H. Ferreira, Mechanism of diclofenac analgesia: direct blockade of inflammatory sensitization. European Journal of Pharmacology, 1994, 251:173–179.

29. Ono S, Hatanaka T, Hotta H, Tsutsui M, Satoh T, and Gonzalez FJ ,1996. Chlorzoxazone is metabolized by human CYP1A2 as well as by human CYP2E1. Pharmacogenetics 5:143–150.

30. Peter R, Bocker R, Beaune PH, Iwasaki M, Guengerich FP, and Yang CS ,1990). Hydroxylation of chlorzoxazone as a specific probe for human liver cytochrome P-450IIE1. Chem Res Toxicol 3:566–573.

31. Amide Pharmaceutical, Inc. Chlorzoxazone tablets prescribing information. Little Falls, NJ: 2002 Apr.

32. United State Pharmacopoeia XXVII22, Rockville, MD: United States Pharmacopoeia Convention INC; 2004, 441.

33. Reynolds JEF. Chlorzoxazone. *Martindale's The Extra Pharmacopoeia* (31 ed) London: Royal Pharmaceutical Society, 1996; 1518-1519.

34. Park JE, Kim KB, Bae SK, Moon BS, Liu KH, Shin JG.Source CJ, 2008. Contribution of cytochrome P450 3A4 and 3A5 to the metabolism of atorvastatin. Xenobiotica. Sep; 38(9):1240-51.

35. "Atorvastatin Calcium". Drugs.com. Retrieved 3 April 2011.

36. Budawari S., The Merck Index, Merck and Co., Inc., Whitehouse Station, NJ, 1996, 23rd ed., 893;8280.

37. Malhotra HS, Goa KL. Atorvastatin: an updated review of its pharmacological properties and use in dyslipidaemia. Drugs. 2001;61(12):1835-81.

38. Cespedes, MS; Aberg, JA (2006). "Neuropsychiatric complications of antiretroviral therapy.". *Drug safety: an international journal of medical toxicology and drug experience* 29 (10): 865–74.

39. Ren J, Bird LE, Chamberlain PP, *et al.* (2002). "Structure of HIV-2 reverse transcriptase at 2.35-A resolution and the mechanism of resistance to non-nucleoside inhibitors". *Proc Natl Acad Sci USA* 99 (22): 14410–15.

40. Merck Index: 2001, *An Encyclopedia of Chemicals, Drugs, and Biologicals*, 13th edn., Merck Research Laboratories, Whitehous Station, NJ.

41. Reynolds JEF, ed. Martindale: the extra pharmacopeia. 28th ed. London: The Pharmaceutical Press; 1989:250.

42. Windholz M, ed. The Merck index. 10th ed. Rahway, NJ: Merck & Co, Inc; 1983:447-8.

43. Fowler PD. Voltarol: diclofenac sodium. *Clin Rheum Dis*. 1979; 5:427-64.

Chapter 4
Objectives Of The Study

Adequate assessment of the safety and effectiveness of a drug includes a description of its metabolism and the contribution of metabolism to overall elimination. For this reason, the development of sensitive and specific assays for predicting the pharmacokinetic behavior of drug and its important metabolites is critical to the study of metabolism and drug-drug interactions. Keeping those views in mind the present investigation was undertaken for prediction of the pharmacokinetics of drugs *in vitro.*

- To investigate the formation kinetics of the metabolites from parent drug *in vitro* (using glimepiride as a model substrate).

- To predict the specific enzymes involved in its metabolic pathway and possible metabolism based Drug/Drug interactions (using sulfamethoxazole as a substrate inhibitor) *in vitro* in terms of enzyme inhibition by using liver microsomes.

- To determine the kinetics of enzyme inhibition (IC_{50} and Ki value).

- To estimate whether the interaction is pharmacologically significant or insignificant by AUC (HPLC Analysis).

- To predict the possible metabolism based Drug/Food interactions *in vitro* by using human liver microsomes. i.e, the effect of fruit juices (pineapple and pomegranate) on CYP2C9 activity as well as the comparative evaluation of the inhibitory potencies of fruit juices affecting glimepiride's metabolism.

- Development of cocktail probe substrate assay system for inhibition screening of CYP2B6 (Efavirenz), 2C9 (Diclofenac), 3A4 (Atorvastatin), 2E1 (Chlorzoxazone) by MCR-706 and MCR-742. (New Molecular Entities synthesized in pharmaceutical chemistry laboratory of M.S.UNIVERSITY, Baroda, Gujrat)

Chapter 5

In vitro oxidative biotransformation of Glimepiride as a model substrate for CYP450

Glimepiride (GLM) was chosen as a model substrate in order to determine the kinetic parameters for *in vitro* metabolism via human liver micrososmes (HLM). It was aimed to optimize the turnover of the substrate by GLM in relation to incubation time and HLM concentration in such a way that it was linearly dependent on time and less than 20% of the substrate was consumed which utilized the lowest amount of the HLM. Further it was also aimed to determine pharmacokinetic parameters for GLM e.g. K_m and V_{max} values. Linearity of enzyme reactions in microsomal incubations was assessed by monitoring the effect of incubation time (from 5 to 60 min) and HLM concentration (from 0.2 to 0.75 mg/ml) on metabolite formation of GLM. The ideal conditions for turnover of GLM were justified using 3^3 factorial design. F value was calculated to confirm the omission of insignificant terms from the full-model to derive a reduced- model polynomial equation. The regression equation was used to develop a contour plot that showed turnover rate within the limits of this design. The optimized reaction velocity data was extrapolated to carry out the kinetic studies *in vitro* to generate a saturation curve for the determination of K_m and V_{max} values.

5.1 EXPERIMENTAL

5.1.1 Chemicals and Reagents

GLM was received as a gift sample from Cadila Healthcare Ltd., Ahmedabad, India. Nicotinamide Adenine Dinucleotide Phosphate, reduced tetra sodium salt (NADPH) and magnesium chloride ($MgCl_2$) were purchased from Himedia laboratories, India. Ethylene diamine tetra acetic acid (EDTA), dipotassium hydrogen phosphate and potassium dihydrogenphosphate were purchased from S.d Fine-Chem Limited, India. Methanol and Acetonitrile of HPLC grade were purchased from Spectrochem India. All other chemicals and reagents used in this study were of analytical grade.

5.1.2 Microsomal Source

A pool of the 50 HLM (0.5 ml at 20 mg/ml), mixed gender, in a suspension medium of 250 mM sucrose was obtained from Xenotech LLC., USA and stored at -80°C in a deep freezer. The frozen microsomes were thawed by placing the vial under cold running water and kept in an ice water bath until use. The total CYP450 content, protein

concentrations, and specific activity of each CYP450 isoforms were as supplied by the manufacturer.

5.1.3 *In vitro* incubation conditions

To define the optimal conditions for incubation and HPLC analysis, GLM (10 – 30 µMole) was incubated with HLM for 10 to 60 min across a range of microsomal enzyme concentrations (0.25 – 0.75 mg/ml). Briefly the incubation mixtures consisted of 50mM phosphate buffer (pH 7.4), 10 mM $MgCl_2$, 1 mM EDTA, 1 mM NADPH and 0.5 mg/ml of microsomal protein. In all experiments, GLM was dissolved and diluted serially in methanol and then alcohol was removed by evaporating to dryness. GLM was reconstituted in potassium phosphate buffer (50 mM, pH 7.4) .The tubes were placed into an ice bath and 5 µl of HLM was added and vortexed. Tubes (duplicate) containing the reaction mixture in phosphate buffer and NADPH solution were allowed to equilibrate separately in a shaker incubator at 150 rpm for 5 minutes at 37°C. The reaction was initiated by adding 20 µl of NADPH immediately to the tubes and incubation carried out for 30min. The reaction was terminated by the addition of 100 µl ice cold acetonitrile. The tubes were centrifuged at 10,000 rpm (4°C; 10min), and aliquots of the supernatant were directly injected into an HPLC system.

5.1.3.1 HPLC separation and detection of GLM metabolite (M_1)

Control incubations were carried out without HLM, NADPH to confirm metabolism. Wherever necessary the volume was made up to 200 µl with buffer.

5.1.4 Factorial design and optimization

Based on the results obtained in the preliminary experiments, drug concentration, HLM concentration and incubation time were found to be major variables affecting metabolism of GLM. Hence 3^3 factorial design was applied to find the optimized conditions for carrying out a reaction time course experiment for GLM's oxidative biotransformation. In all the experiments NADPH concentration was 1mM and buffer concentration was 50 mM. In this experimental design, GLM in the presence of HLM was incubated in 27 different combinations.

Effect of Variables

To study the effect of variables, different batches were prepared by using 3^3 factorial design. Drug concentration (X1), incubation time (X2) and HLM concentration (X3) were selected as three independent variables. The independent variable and their levels are shown in Table 5.1. The turnover rate (Y1%) was taken as a response parameter as the dependent variable. These three factors were evaluated each at 3 levels and experimental trials were performed for all 27 possible combinations as reflected from Table 5.2. The values of the factors were transformed to allow easy calculation of co-efficient in polynomial equation. Interactive multiple regression analysis and F statistics were utilized in order to evaluate the response. The regression equation for the response was calculated using the following equation-

Response: $Y1\ (\%) = \beta_0 + \beta_1 X1 + \beta_2 X2 + \beta_3 X3 + \beta_4 X1^2 + \beta_5 X2^2 + \beta_6 X3^2 + \beta_8 X1X2 + \beta_9 X1X3 + \beta 10X2X3 + \beta_{11}\ X1X2X3$

where Y1 (%) is turnover rate and indicates the quantitative effect of the independent variables X1 , X2 and X3, which represent the drug concentration, incubation time and HLM concentration respectively, β0 is the intercept while β1-β11 represents the regression coefficient of the system. To identify the significant terms, the variables having p value > 0.05 in the full model were discarded and then the reduced model was generated for the independent variables.

The multiple regression was applied using Microsoft excel 2007 in order to deduce the factors having a significant effect on the enzymatic reaction and the best fitting mathematical model was selected. Two dimensional contour plot and three dimensional response surface plot resulting from the equations were obtained by the NCSS software.

Table 5.1: Factors, their levels, and coded values

	Levels		
Variables	Low	Medium	High
Drug concentration (X1)	10 µmole	20 µmole	30 µmole
Incubation time (X2)	10minutes	35 minutes	60 minutes
HLM concentration (X3)	0.25 mg/ml	0.5 mg/ml	0.75 mg/ml
Coded values	-1	0	+1

Table 5.2: Different batches with their experimental coded level of variables for full factorial design.

Batch no.	X_1	X_2	X_3	X_1^2	X_2^2	X_3^2	X_1X_2	X_1X_3	X_2X_3	$X_1X_2X_3$	% Turnover rate ± (SEM)†
1	-1	-1	-1	1	1	1	1	1	1	-1	5.01(0.44)
2	-1	-1	0	1	1	0	1	0	0	0	6.5(0.21)
3	-1	-1	1	1	1	1	1	-1	-1	1	8.9(0.41)
4	-1	0	-1	1	0	1	0	1	0	0	8.92(0.25)
5	-1	0	0	1	0	0	0	0	0	0	19.91(0.69)
6	-1	0	1	1	0	1	0	-1	0	0	18.01(0.48)
7	-1	1	-1	1	1	1	-1	1	-1	1	33.4(0.76)
8	-1	1	0	1	1	0	-1	0	0	0	37.69(0.91)
9	-1	1	1	1	1	1	-1	-1	1	-1	38.81(0.56)
10	0	-1	-1	0	1	1	0	0	1	0	4.4(0.84)
11	0	-1	0	0	1	0	0	0	0	0	6.1(0.58)
12	0	-1	1	0	1	1	0	0	-1	0	8.45(0.76)
13	0	0	-1	0	0	1	0	0	0	0	8.05(0.51)
14	0	0	0	0	0	0	0	0	0	0	18.91(0.62)
15	0	0	1	0	0	1	0	0	0	0	15.05(0.65)
16	0	1	-1	0	1	1	0	0	-1	0	31.75(0.53)
17	0	1	0	0	1	0	0	0	0	0	38.45(1.03)
18	0	1	1	0	1	1	0	0	1	0	38.15(0.89)
19	1	-1	-1	1	1	1	-1	-1	1	1	3.8(0.75)
20	1	-1	0	1	1	0	-1	0	0	0	5.24(0.92)
21	1	-1	1	1	1	1	-1	1	-1	-1	7.91(0.72)
22	1	0	-1	1	0	1	0	0	0	0	7.56(0.55)
23	1	0	0	1	0	0	0	0	0	0	19.08(0.78)
24	1	0	1	1	0	1	0	0	0	0	14.32(0.43)
25	1	1	-1	1	1	1	1	-1	-1	-1	30.56(0.67)
26	1	1	0	1	1	0	1	0	0	0	35.91(0.48)
27	1	1	1	1	1	1	1	1	1	1	36.42(0.34)

†n = 2

5.1.5 HPLC Instrumentation

The HPLC system consisted of Shimadzu LC 20 AT pump and SPD 20A UV detector, a rheodyne 7725 fixed injector loop (20 µl), Thermo scientific C18 Hypersil BDS column (4.6 x 250 mm, 5 µm) and a Phenomenex C18 guard column (4×3mm). Data acquisition and integration was performed using Spinchrome software (Spincho biotech, Vadodara).

5.1.6 Preparation of standard and quality control sample

Stock solution of GLM was prepared by dissolving precisely weighed 25 mg of GLM in 25 ml of methanol in a volumetric flask to yield a concentration of 2mM. The stock solution was stored at 4℃until use. GLM **working solution** (200 µM) was prepared by transferring 1.0 ml from GLM stock solution to 10 ml volumetric flask and diluted to the mark with MeOH. For the preparation of **calibration standards**, a series of working solutions of GLM were produced by adding appropriate amount of GLM to HLM-free incubation solution to yield 5,10, 20, 30, 40, 50, 60, 70, 80, 100 and 120 µM of GLM. Among them, 5, 50 and 100 µM of GLM were used as **quality control (QC) samples.**

5.2 METHOD DEVELOPMENT

5.2.1 Selection and Optimization of chromatographic condition:

To optimize the chromatographic conditions, the effect of chromatographic variables such as composition of mobile phase, pH of mobile phase and flow rate were studied. The resulting chromatograms were recorded and the chromatographic parameters such as capacity factor, asymmetric factor, resolution and theoretical plates were calculated. The conditions that gave the best resolution, symmetry and theoretical plate were selected for estimation.

5.2.2 Effect of ratio of mobile phase:

A working standard solution containing 10 μg mL^{-1} of GLM was analyzed using mobile phase of varied ratios of ACN and Buffer and the respective chromatograms were recorded. A composition of 0.1% Formic acid (pH adjusted to 3.5 with sodium hydroxide): ACN:: **55:45** (%v/v) showed symmetric sharp peak with acceptable retention time (9.3min) at ambient temperature with flow rate of 1 ml/min.(Figure 5.1).

Table 5.3: Optimization of mobile phase

Mobile phase		Flow Rate	GLM	
			RT	Peak Shape
Column - BDS Hypersil C8 Column; Thermoquest; 250 mm × 4.6 mm; 5µ				
ACN : Water ; 1% TEA (pH – 2.5 adjusted with OPA)	50:50	1	6.247	Broad
	70:30	1	6.00	Not Good
ACN: 0.1 M Pot. Phosphate Buffer (pH – 3 adjusted with OPA)	70:30	1	7.793	Fronting
ACN: 0.1 M Pot. Phosphate Buffer (pH – 3.5 adjusted with OPA)	48:52	1	19.82	Fronting Broad
Methanol : Water; 1%TEA (pH 3.5 adjusted with OPA)	50:50	1	-	No peak up to 45 min
ACN: 0.1 M Ammonium acetate (pH – 4.5 adjusted with acetic acid)	60:40	1	12.327	Broad
ACN: 0.05 M sodium dihydrogen phosphate ; (pH – 3 adjusted with OPA)	55:45	1	5.890	Not good
ACN: 0.1% Formic acid (pH – 3.5 adjusted with NaOH)	65:35	1	9.858	Fronting; Broad
	80:20	1	7.28	

Column - Phenomenex C18 Column; 250 mm × 4.6 mm; 5µ				
ACN: 0.1% Formic acid (pH – 3.5 adjusted with NaOH)	50:50	1	12.67	Bifurcated
	70:30	1	9.85	Tailing
Column - BDS Hypersil C18 Column; Thermo; 250 mm × 4.6 mm; 5µ				
ACN: 0.1 M Ammonium acetate (pH – 4.5 adjusted with acetic acid)	60:40	1	11.327	Broad
ACN: 0.05 M sodium dihydrogen phosphate ; (pH – 3 adjusted with OPA)	55:45	1	6.590	Bifurcated
ACN: 0.1% Formic acid (pH – 3.5 adjusted with NaOH)	50:50	1	11.86	Sharp
	55:45	**1**	**9.3**	**Sharp**
	60:40	0.5	16.25	Sharp
		0.6	15.82	Sharp
		0.7	14.070	Sharp
		0.8	13.497	Sharp
	65:35	1	8.9	Sharp

5.2.3. Result & discussion of method development:

Various columns were tried but HYPERSIL BDS C_{18} (250mm X 4.6 mm i.d., 5 µm particle size) column showed better resolution. Quantitation of GLM was achieved with UV detection at 228 nm based on its λ_{max}. To optimize the HPLC parameters, several mobile phase compositions with different column and different flow rate were tried. Various buffers e.g. Potassium phosphate buffer, Sodium phosphate buffer, Ammonium acetate buffer and formic acid at different pH with different ion pair reagents and with

different composition with ACN were tried. After trying various mobile phases as described in Table 5.3, finally the mobile phase ACN: 0.1% Formic acid (pH- 3) (55:45; v/v) was selected as it ideally resolved the metabolite peak (M_1) with retention time (RT) 3.6 min and GLM peak at 9.3 min (Figure 5.4). The studies suggested that a mobile phase at acidic pH value might favor the peak shape of GLM on column to achieve a reasonable retention and resolution.

Table 5.4: Optimized HPLC parameters for GLM

Column	HYPERSIL BDS C_{18} (250mm X 4.6mm i.d., 5µm particle size)
Mobile Phase	ACN: 0.1% Formic acid (pH adjusted to 3.5 with sodium hydroxide):: 55:45 (%v/v)
Flow rate	1 ml/min
Retention time	9.3min
Detector - Detection Wavelength	UV Detector – 228 nm
Needle wash	ACN: 0.1% Formic acid (55:45)
Temperature	Ambient

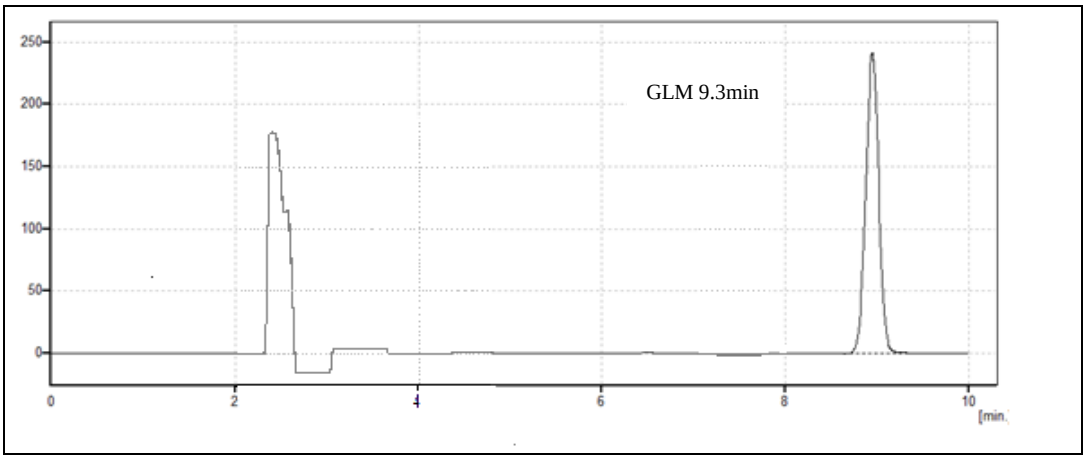

Figure 5.1. HPLC chromatogram of GLM

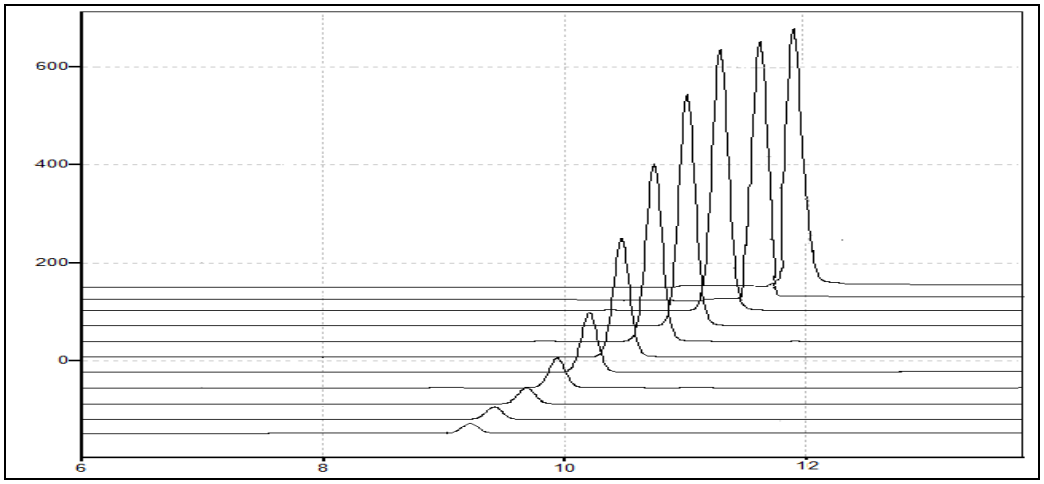

Figure 5.2. Overlay chromatogram of GLM (5-120 µM)

5.3 METHOD VALIDATION

The method validation assays were carried out according to the currently accepted U.S. Food and Drug Administration (FDA) bioanalytical method validation guidance.

5.3.1 Linearity and Range:

Calibration curve for the assay was constructed by analyzing the eleven concentrations of GLM mentioned above. The peak area of GLM (*Y*) was measured and plotted against the concentration (*X*) of GLM. The calibration curve constructed was linear over the concentration range of 5-120 μM for GLM with correlation co-efficient, slope and intercept values of 0.999, 11.53 and 2.29 respectively (Figure 5.3)**.** The results show that good correlation existed between the peak area and concentration of the analyte.

Table 5.5: Linearity data for GLM

Sr No.	GLM (μM)	Peak area
1	5	58.80±0.411
2	10	115.02 ±0.189
3	20	230.81±0.534
4	30	336.83±1.603
5	40	466.41±0.717
6	50	589.79±0.424
7	60	690.91±1.391
8	70	818.09±0.382
9	80	938.09±0.423
10	100	1159.09±0.911
11	120	1371.35±0.760

*Average of three experiments

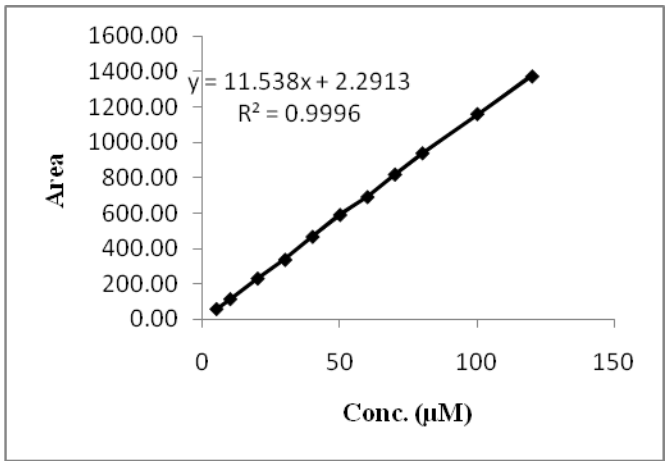

Figure 5.3. Linearity plot of GLM

5.3.2 Precision:

In order to evaluate the intra-day precision, samples were analyzed for each concentration on the same day. The inter-day precision was evaluated on three consecutive days. The assays for both intra- and inter-day precision were performed by using the three QC samples of GLM (5, 50 and 100 µM). Precision was determined by repeated analyses of the group of standards on one batch (n =3). The concentration of each sample was determined using the calibration curve prepared and analyzed on the same batch.

Table 5.6: Intra-day precision for estimation of GLM

GLM (µM)	Peak Area			MEAN	%RSD
	Set 1	Set 2	Set 3		
5	58.45	56.23	57.89	57.523	2.01
50	589.417	581.55	583.89	584.95	0.69
100	1154.26	1149.69	1160.24	1154.73	0.46
				Average % RSD	1.05

Table 5.7: Inter-day precision for estimation of GLM

GLM (µM)	Peak Area			MEAN	%RSD
	Day 1	Day 2	Day 3		
5	56.52	51.23	55.87	54.54	5.29
50	585.72	582.25	582.65	583.54	0.33
100	1149.26	1150.62	1154.67	1151.52	0.24
				Average % RSD	1.95

5.3.3 LLOD and LLOQ

The lower limit of detection (LLOD) and the lower limit of quatification LLOQ were determined as the concentrations at signal-to-noise ratios of 3 and 10, respectively. Calibration curve was repeated for 3 times and the standard deviation (SD) of the intercepts was calculated. Then LLOD and LLOQ were measured as follows.

LLOD=3.3 * SD/slope of calibration curve

LLOQ=10 * SD/slope of calibration curve

SD = Standard deviation of intercepts

The values of LLOD and LLOQ are given in **Table 5.4.3.1.**

Table 5.8: LLOD and LLOQ GLM

Parameter	GLM (µM)
SD	± 1.80
LLOD	0.514
LLOQ	1.558

5.3.4 Specificity:

The specificity of the HPLC method was illustrated by the complete separation of metabolite of GLM (M_1) from GLM. Typical chromatograms obtained following the *in vitro* incubation procedure are shown in Figure 5.4. The resolution factor (*R*s) from *in vitro* metabolism product was above 2.0, which ensured complete separation of metabolite from its substrates GLM.

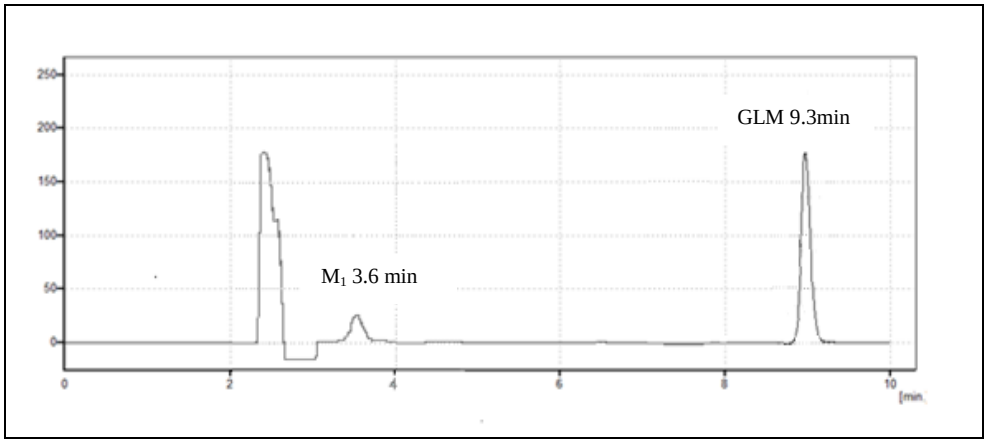

Figure 5.4. HPLC chromatogram of GLM metabolite (M_1, 3.6min) and GLM (9.3min)

5.3.5 System suitability:

Following parameters were evaluated for system suitability of HPLC method.

Table 5.9: System suitability parameters for GLM

Parameters	Data obtained	
	M_1	GLM
Theoretical plates per meter± RSD	515620±0.853	243650±0.451
Retention time	3.6min	9.3min
Capacity factor	1.12	2.85
Symmetry factor/Tailing factor	0.913	1
Resolution	--	11.601

5.3.6 Recovery:

Accuracy of the method was confirmed by recovery study from HLM-free incubation solution at 3 level of standard addition (80%, 100%, and 120%).

Table 5.10: Recovery studies of GLM from HLM incubation mixture

Spiked amount (%)	Theoretical Content ($\mu g\ mL^{-1}$)	*Recovery (%) ± S.D.
80	40	99.67 ± 0.24
100	50	99.43 ± 0.85
120	60	100.65 ± 0.31

*Average of three experiments

5.3.7 Stability:

Freeze and thaw stability:

QC microsomes samples at three concentration levels were stored at the storage temperature (−70°C) for 24 h and thawed unassisted at room temperature. When completely thawed, the samples were refrozen for 24 h under the same conditions. The freeze–thaw cycles were repeated twice, and the samples were analyzed after three freeze (−70°C)-thaw (room temperature) cycles;

Short-term temperature stability:

QC samples at three concentration levels were kept at room temperature for a period that exceeded the routine preparation time of the samples (around 6 h)

Long-term stability:

QC samples at three concentration levels kept at low temperature (−70°C) were studied for a period of one week.

Table 5.11: Data showing stability of GLM in HLM (n=2)

GLM QC samples (µM)	Freeze and thaw stability	Short term stability	Long term stability
5	95.5 ± 4.6	98.56 ± 2.1	110 ± 2.8
50	101.25 ± 2.5	97.63 ± 1.5	107.5 ± 2.2
100	99.56 ± 3.8	100.54 ± 1.2	101.4 ± 3.7

5.4 *IN VITRO* METABOLISM OF GLM USING HLM

5.4.1 Detection of GLM metabolite (M_1):

Control incubations were carried out without HLM, NADPH to confirm metabolism. Wherever necessary the volume was made up to 200 µl with buffer. The figure 5.5 (a-c) suggest that NADPH as a cofactor is necessary for HLM to carry out the *in vitro* metabolism of GLM. Addition of NADPH to the incubation medium generates metabolite M_1 at RT 3.6min suggesting that GLM undergoes *in vitro* hydroxylation.

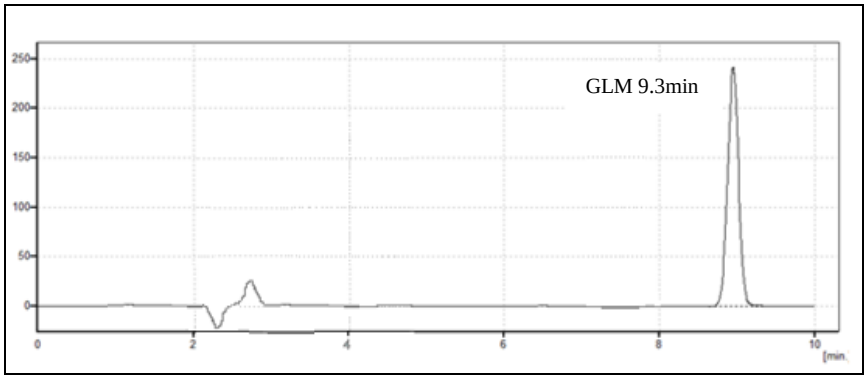

Figure 5.5a. GLM in NADPH free incubation medium (with HLM)

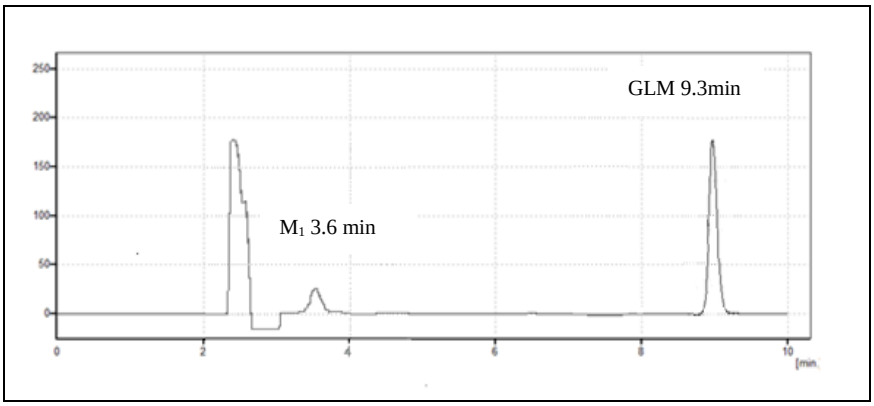

Figure 5.5b. GLM in microsomal incubation medium (with HLM & NADPH)

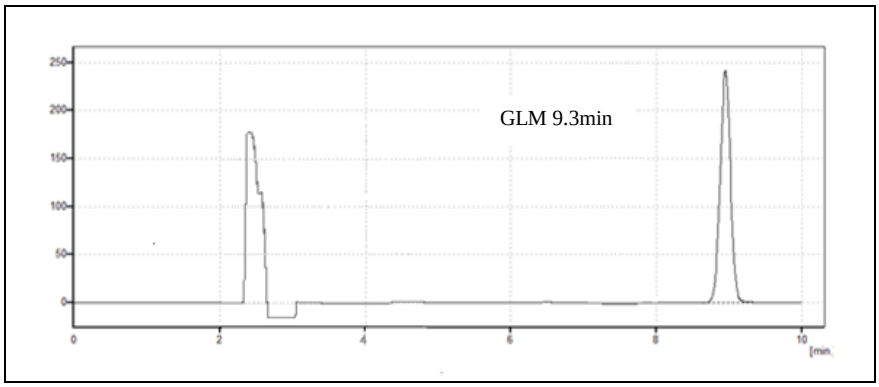

Figure 5.5c. GLM in HLM free incubation medium (with NADPH)

5.4.2 Determination of K_m and V_{max} for GLM metabolism by nonlinear and linear transformations

Preliminary experiments showed that the substrate depletion was linear with respect to both time over 50 min and liver microsomal protein concentration (0.3-0.65 mg/ml) at 37°C. Thus a 30 min incubation time and 0.5 mg/ml microsomal protein concentration was selected for kinetic studies.

The studies were performed by incubating eight concentrations of GLM (0-100 µMole) in duplicate with HLM. For the determination of the apparent Michaelis-Menten constant (K_m) and the maximal velocity of the reaction (V_{max}), plots in relation to the substrate concentration were derived using GraphPad Prism 5 software. A number of ways of re-arranging the Michaelis-Menten equation ($V=V_{max}$ [S] / K_m + [S]) have been devised to obtain linear relationships which permit more precise fitting to the experimental points, and estimation of the values of K_m and V_{max}. Hence data for reaction velocities was also

evaluated by double reciprocal plot (Lineweaver-Burk equation, $1/V = K_m/V_{max} * 1/[S] + 1/V_{max}$). The intersection points were determined graphically using Microsoft Excel 2007.

Table 5.12: Michaelis-Menten kinetics data for GLM *in vitro* incubation with HLM

Substrate conc. Cs (µM)	Peak area 0 min As	Peak area 30 min Au	Cu_{30min}= Au*Cs/As	C=Cs_{0min}-Cu_{30min}	*C/30min/0.5 (µM/min/mg protein)
2	31	28.066	1.811	0.189	0.013
4	58.459	47.024	3.218	0.782	0.052
6	78.06	57.727	4.437	1.563	0.104
8	96.842	71.089	5.873	2.127	0.142
20	228.246	190.934	16.731	3.269	0.218
50	624.417	558.108	44.690	5.310	0.354
75	931.941	853.715	68.705	6.295	0.420
100	1287	1205.41	93.660	6.340	0.423

*Average of two experiments

Table 5.13: Graphpad Prism data observations

Michaelis-Menten Kinetics Best-fit values	
Vmax (µM/min/mg protein)	0.5594
Km(µM)	28.9
SD	
Vmax (µM/min/mg protein)	±2.97
Km(µM)	±0.017
Goodness of Fit	
Degrees of Freedom	6
R^2	0.9905
Absolute Sum of Squares	0.001796
Analyzed	8

Table 5.14: Lineweaver Burk kinetics data for GLM *in vitro* incubation with HLM

Substrate conc. Cs (µM)	**$1/Cs_{(\mu M)}$**	**Velocity V**	**$1/V_{(\mu M/min/mg\ protein)}$**
6	0.167	0.1042	10.939
8	0.125	0.1418	7.051
20	0.050	0.2180	4.588
50	0.020	0.3540	2.825
75	0.013	0.4197	2.383
100	0.010	0.4226	2.366

*Average of two experiments

Table 5.15: Lineweaver Burk Kinetics observations

Lineweaver Burk Kinetics Best-fit values	
Vmax (µM/min/mg protein)	0.571
Km(µM)	29.41
SD	
Vmax (µM/min/mg protein)	±1.25
Km(µM)	±0.020

5.4.3 Data Analysis

In the present study, the disappearance of GLM in the medium incubated at 37°C with HLM in the presence of the NADPH was determined as the percentage of the initial amount of GLM in the medium without incubation. The obtained results were expressed as the turnover rate in percentage wherever necessary. Substrate disappearance velocity was calculated as [($C_{0,\ initial}$ - $C_{s,\ t\ min}$) / incubation time /CYP concentration], where $C_{0,\ initial}$ is the substrate concentration at time 0 min and $C_{s,\ t\ min}$ is the substrate concentration after 10, 35, 60 min incubation with 0.25, 0.5 and 0.75mg/ml protein concentration. Metabolite formation velocity (V) was calculated as ($C_{s,\ t\ min}$ / incubation time / CYP concentration), where Cs, t min was the metabolite concentration after a 10, 35, 60 min incubation.

5.4.4 Intrinsic clearance

Intrinsic clearance (Clint) is the cornerstone for extrapolation of *in vitro* data to the *in vivo* situation. Clint is a direct measure of enzyme activity toward a drug and is not influenced by other determinants such as hepatic blood flow or drug binding within the blood matrix. Clint acts as a proportional constant between rate of drug metabolism and drug concentration around the metabolic enzyme site (CE). If the process is consistent with a MM model, and if CE is less than 10% of the Km, Clint is equal to the Vmax/Km ratio[1].

i.e.: Clint = Vmax / Km

The obtained Km and Vmax values from MM plot were substituted in the above equation to get the Clint data.

5.5 RESULTS

5.5.1 Reaction linearity optimization by factorial design:

Linearity of enzyme reactions in the *in vitro* human liver microsomal incubations was assessed by monitoring the effect of incubation time (from 10 to 60 min) and protein concentration (from 0.25 – 0.75 mg/ml) on metabolite formation of GLM. Using 3^3 factorial design as shown in Table 5.2, 27 batches were prepared varying three independent variables such as drug concentration (X1), incubation time (X2) and HLM concentration (X3). The turnover rates as response are recorded in Table 5.2. The results of the regression output and response of full model and reduced model are represented in Table 5.16. The equations for full and reduced model are given below

Full model

$$Y=16.522-0.903X1+14.707X2+2.891X3-0.042X1^2+6.541X2^2-3.107X3^2-0.288X1X2-0.263X1X3+0.468X2X3+0.02875X1X2X3 \quad (1)$$

Reduced model

$$Y=16.522+14.707X2+2.891X3+6.541X2^2-3.107X3^2 \quad (2)$$

As the model was generated by taking only the significant terms from the full model, the results are deduced by interpreting the reduced model. The positive sign for coefficient of X2 and X3 in equation 1 shows that the rate of metabolism increases with increase in incubation time and HLM concentration.

The results of the Analysis of variance (ANOVA) of the second order polynomial equation are given in Table 5.17**.** F statistics of the result of ANOVA of full and reduced model confirmed omission of non-significant terms of equation 1. Since the calculated F value (0.6841) was less than the tabled F value (2.74) ($\alpha = 0.05$, V1 = 6 and V2 = 16), it was concluded that the neglected terms do not significantly contribute in the prediction. The goodness of fit of the model was checked by the determination coefficients (R^2). In this case, the values of the determination coefficients (adj R^2) were very high (>90%),

which indicates a high significance of the model. All the above considerations indicate an adequacy of the regression model.

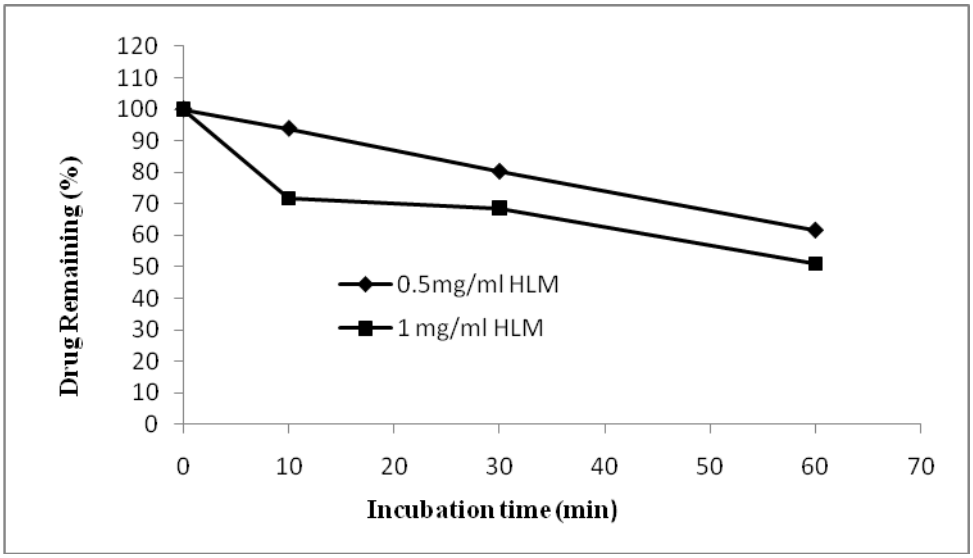

Fig. 5.6 Effect of time and protein concentration on metabolism of GLM (20µM) after incubation with human liver microsomes at 37°C.

Table 5.16. Response of Full Model and Reduced Model.

	Turnover rate (%)			
	Full model		Reduced model	
Response	X coefficient	P value	X coefficient	P value
X1	-0.903	0.093963003	-	-
X2	14.707	2.935912E-15†	14.708	1.92E-19
X3	2.891	3.72138E-05†	2.921	4.63E-06
$X1^2$	-0.042	0.962269567	-	-
$X2^2$	6.541	1.39313E-06†	6.541	9.21E-08
$X3^2$	-3.107	0.0027451†	-3.107	0.001253
X1X2	-0.288	0.648852013	-	-
X1X3	-0.263	0.706627127	-	-
X2X3	0.468	0.46193583	-	-
X1X2X3	0.028	0.970329444	-	-
Intercept	16.522	7.07592E-11	16.49481481	5.84E-15

†significant terms at $p > 0.05$

Table 5.17. Analysis of variance (ANOVA) for full and reduced models of GLM metabolism.

	DF	SS	MS	*F*†	R	R^2	Adj. R^2
Regression							
FM	10	4380.932	438.0932	94.570	0.9916	0.9834	0.9730
RM	4	4361.916	1090.479	257.590			
Error							
FM	16	74.119(E1)	4.632				
RM	22	93.134(E2)	4.233				

†SSE2-SSE1 = 93.134 – 74.119 = 19.015
No. of the parameters omitted = 6
MS of error (full model) =4.632
F calculated = (SSE2 –SSE1/no. of parameters omitted)/MS of error (full model) = (19.015/6)/4.632 = 0.684189
Tabled *F* value = 2.74 (α = 0.05, V1 = 6 and V2 = 16)
Where DF indicates degrees of freedom; SS sum of square; MS mean sum of square and *F* is Fischer's ratio.

5.5.2 Contour Plot

Contour plots are a diagrammatic representation of the values of the response. They are helpful in explaining the relationship between independent and dependent variables. The reduced models were used to plot two dimension contour plot at a fixed level of 0 for X1 respectively, and the values of X2 and X3 were computed between -1 and +1 at predetermined values of the turnover rate.

Figure 5.7(a-c) shows the contour plot drawn at -1, 0 and +1 level of X_1, for a prefixed turnover rate of GLM ranging from 4.0% to 34.6%. The plot was found to be linear for approximate values of 17.60%, 21.00% and 24.40% whereas the approximate values of 10.80%, 14.20% and 17.60% showed somewhat linearly curved segments. The approximate values 7.40% and 34.60% showed inconsistent segments signifying nonlinear relationship between X_2 and X_3 variables. It was determined from the contour that maximum turnover of about 34.60% could be obtained with X_2 range at 54.4 to 60 min and X_3 at 0.4 to 0.8 mg/ml of protein concentration. As per the PhRMA and USFDA guidelines, it was observed that up to 20% metabolism of the substrate within the limits of this design could be obtained with incubation time (X_2) from 24 to 50 min and protein

concentration (X3) from 0.3 to 0.65 mg/ml. Hence for further study, 0.5mg/ml protein and 30 min incubation time was optimized.

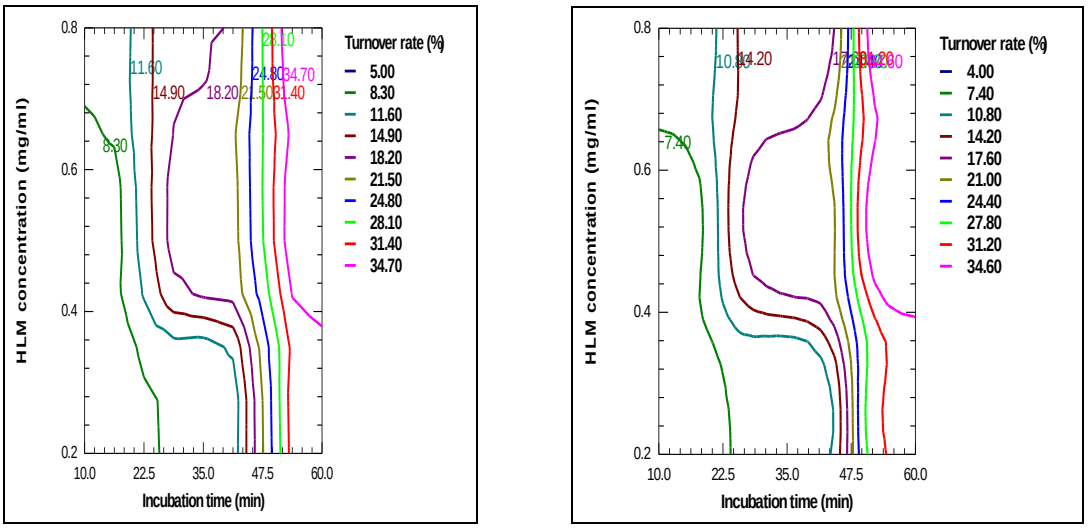

(a) **(b)**

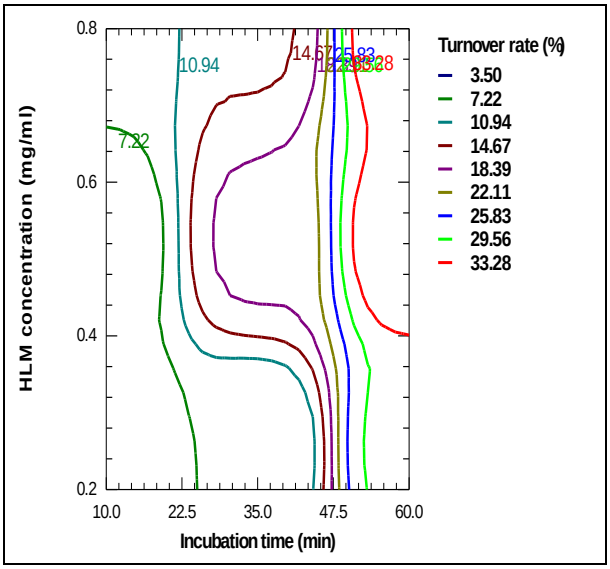

(c)

Figure 5.7.Contour plots for GLM oxidative biotransformation: (a) effect on turnover rate at -1 level of drug concentration (X1) (b) effect on turnover rate at 0 level of X1(c) effect on turnover rate at +1 level of X1.

5.5.3 Response surface plot

Three dimensional response surface plot generated by NCSS software represented in Figure 5.8, depicts the turnover rate of GLM as a substrate. It shows an increase in turnover of the substrate with increase in the protein concentration and incubation time.

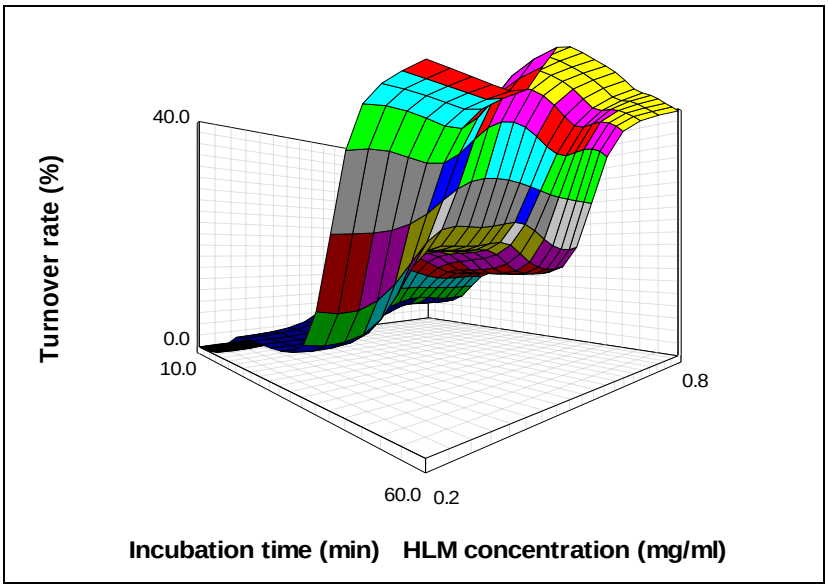

Figure 5.8. Response surface plots for GLM oxidative biotransformation showing effect on turnover rate at 0 level of X1.

5.5.4 Determination of K_m and V_{max} for GLM metabolism by nonlinear and linear transformations.

GLM metabolism in the presence of HLM followed Michaelis-Menten kinetics. K_m and V_{max} values obtained by nonlinear least squares regression method were found to be 28.9 ± 2.97 µMole and 0.559 ± 0.017 µMole/min/mg protein respectively (Figure 5.9). From Lineweaver-Burk plot the K_m and V_{max} values were found to be 29.411 ± 1.25 µMole and 0.571 ± 0.020 µMole/min/mg protein respectively (Figure 5.10). Thus the values obtained with nonlinear as well as a linear transformation of the data were found to be in close agreement with each other. Each data point represents an average of at least two parallel incubations.

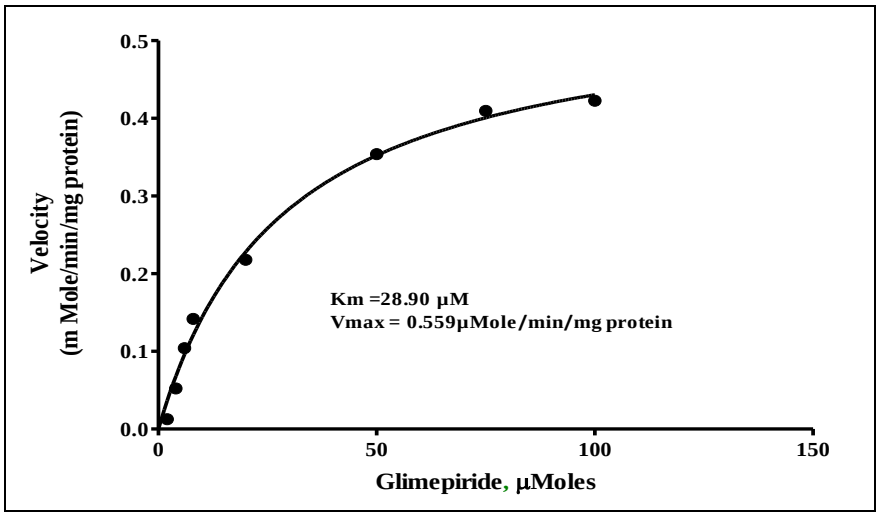

Figure 5.9. Michaelis Menten plot for GLM oxidative biotransformation in HLM.

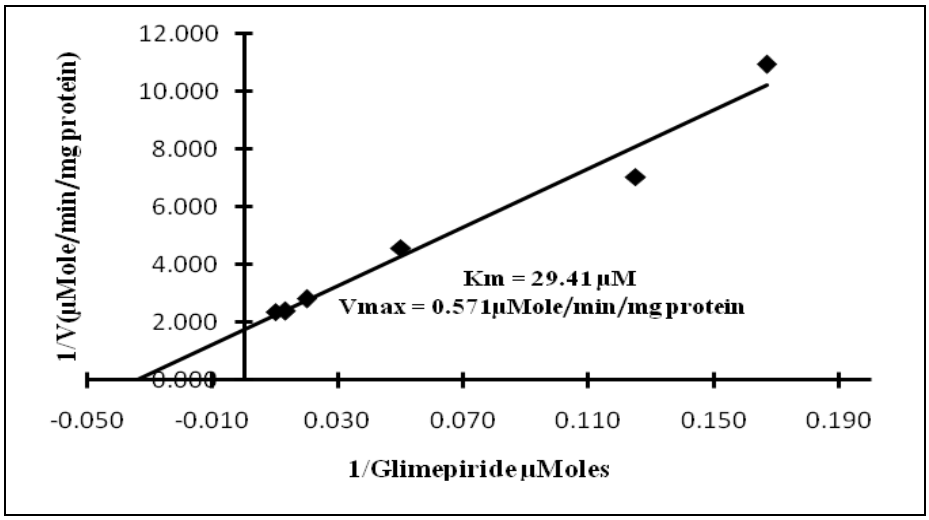

Figure 5.10. Lineweaver Burk plot for GLM oxidative biotransformation in HLM.

5.5.5 Intrinsic clearance

Intrinsic clearance was obtained by substituting the Km and Vmax values.

Clint = Km/Vmax = 0.559/28.9= 0.019 µl/min/mg.

5.6 DISCUSSION

P450 reaction phenotyping is defined as a set of experiments that aim to define which human cytochrome P450 enzyme(s) is involved in a given metabolic transformation. Such data are useful in the prediction of pharmacokinetic drug-drug interactions and interpatient variability in drug exposure. Any prolonged incubation in a closed *in vitro* system such as liver microsomes can cause formation of secondary metabolites from the primary metabolites of a drug. Inactivation or denaturation of enzymes can become significant over time in the *in vitro* systems. Thus it is of critical importance that initial velocity conditions are defined.

The present study conclusively demonstrates the use of a 3^3 factorial design in the optimization of initial velocity conditions affecting turnover of GLM. The derived reduced polynomial equation, contour plot and response surface plot aid in predicting the values of selected independent variables. Contour plots obtained by applying a computerized optimization process suggested a level of 30 minute incubation time (X2) and 0.5mg/ml protein (X3) as an ideal condition. At this level the turnover rate (%Y) was found to be ranging from 18.91% to 19.91%. Thus the rate of GLM disappearance was linear at the chosen concentrations of substrate using the assay conditions and detection system. However, a decrease in the level of incubation time and protein concentration below the selected level, typically yield nonlinear initial velocities of enzyme activity.

Once the optimal conditions (30 min incubation time, 0.5mg/ml HLM) were obtained, the substrate concentration dependence on the rate of metabolite formation was examined. The K_m (28.9 ± 2.97 µMole) and V_{max} (0.559 ± 0.017 µMole/min/mg protein) values were determined by nonlinear regression of a plot of enzyme activity versus substrate concentration. A Clint value of 0.019 µl/min/mg was obtained which suggests a direct measure of enzyme activity. The Michaelis constant, K_m accounts for the concentration of substrate at which half the active sites are filled. Thus, K_m provides a measure of the substrate concentration required for significant catalysis to occur. V_{max} is the rate at which substrate will be converted to product once bound to the enzyme. A substrate concentration around or below the K_m is ideal for determination of competitive inhibitor

activity. Hence further inhibition studies are needed to confirm the performance of GLM's oxidative biotransformation *in vitro*.

5.7 CONCLUSION

This study examines the effects of the main control factors and attempts to enhance the turnover rate of GLM's oxidative biotransformation by optimizing these factors using full factorial design. It was possible to optimize the turnover of the candidate drugs within the limits of developed assay design such that all subsequent *in vitro* incubations can be performed using the condition that ensures linearity with time and HLM concentration, and less than 20% of the initial substrate is consumed. Thus the precise information about the effects of each factor on metabolism can be used to flexibly adjust the system performance.

The best estimates of K_m and V_{max} values were obtained with linear as well as nonlinear transformation for the enzymatic assay of GLM under initial velocity conditions. The Cl_{int} value as predicted after *in vitro* studies was found to be 0.019 µl/min/mg suggesting a direct measure of enzyme activity towards glimepiride. The low Km value of GLM (28.9 µMole) as compared to literature value of tolbutamide (50 µMole) for CYP2C9 suggest that enzyme has a high affinity for the substrate GLM. Thus GLM can be used as a alternative probe substrate for CYP2C9 reaction phenotyping of new molecular entities.

5.8 REFERENCE

1. Pelkonen O, Mäenpää J, Taavitsainen P, Rautio A, Raunio H. Inhibition and Induction cytochrome P450 (CYP) enzymes. Xenobiotica 1998;28:1203-1253.

Chapter 6

In vitro Evaluation of the Pharmacokinetic Alterations Caused by Sulfamethoxazole on Glimepiride Hydroxylation: Prediction Of The In vivo Drug Drug Interaction From In vitro Data.

Accumulating evidence indicates that CYP2C9 ranks amongst the most important drug metabolizing enzymes in humans[1-4]. Due to the role of CYP2C9 in drug metabolism, it is important to evaluate the kinetic behavior of CYP2C9 substrates and their potential to undergo inhibiton with concomitant drugs. Hypoglycemia resulting from the combination of sulfonylurea and sulfonamides is a recognized drug interaction. The aim of this work was to investigate the effect of inhibition of CYP2C9 on the pharmacokinetics of glimepiride (GLM), with Sulfamethoxazole (SMZ) as model inhibitor of CYP2C9. The present study investigates and compares the impact of GLM as a substrate and SMZ as inhibitor on *in vitro* kinetic parameters, namely K_m, V_{max}, IC_{50} and Ki. Thus the clinical significance of potential CYP2C9-mediated drug–drug interaction of GLM with SMZ in presence of human liver microsomes was established. The overall metabolism of GLM in presence and absence of SMZ was determined as disappearance of parent drug from an incubation mixture using HPLC with UV detection at 228nm. Further the studies conducted by using constant concentration of SMZ on the MM kinetics of glimepiride were used to assess the nature of inhibition.

6.1 EXPERIMENTAL

6.1.1 Chemicals and Reagents

SMZ was received as a gift sample from M/s Natco Pharma Ltd, Hyderabad. All other chemicals and reagents used in this study were of analytical grade and were procured as described under section 5.1.1.

6.1.2 Microsomal Source

A pool of the 50 HLM (0.5 ml at 20 mg/ml), mixed gender, was procured and processed as described under section 5.1.2.

6.1.3 Preparation of standard and working solutions

For GLM: Stock solution of GLM was prepared by dissolving a precisely weighed 25 mg of GLM in 25 ml of methanol in a volumetric flask to yield a concentration of 2mM. The stock solution was stored at 4℃ until use. GLM **second stock solution** (200 µM) was prepared by transferring 1.0 ml from GLM stock solution to 10 ml volumetric flask

and diluted to the mark with MeOH. A solution of 10µM was prepared by transferring 10µl GLM second stock solution to the incubation tubes for inhibition experiments. Similarly a series of working solutions were produced by adding appropriate amount of GLM to incubation solution to yield 2,4, 6, 8, 20, 50, 80, 100,120, 160 and 200 µM of GLM for MM kinetics.

For SMZ: Stock solution of SMZ was prepared by dissolving a precisely weighed 25 mg of SMZ in 25 ml of methanol in a volumetric flask to yield a concentration of 4mM. The stock solution was stored at 4℃ until use. A series of working solutions were produced by adding appropriate amount of SMZ to the incubation solution to yield 30, 50, 100, 300, 500, 700, 900 and 1100 µM of SMZ for inhibition experiment.

6.1.4 Analytical method for GLM *in vitro* metabolism

Briefly the incubation mixtures consisted 1M phosphate buffer (pH 7.4), 10mM $MgCl_2$, 1mM EDTA, 10 mM NADPH and 0.5mg/ml of microsomal protein. The concentration of glimepiride was 10µM. Tubes (duplicate) containing the reaction mixture in phosphate buffer and NADPH solution (10mM) were allowed to equilibrate in a shaker incubator at 150 rpm for 5 minutes at 37°C. Preliminary experiments showed that the substrate depletion was linear with respect to time over 30 min and liver microsomal protein concentration of 0.5mg/ml at 37°C. The reaction was initiated by addition of NADPH (preincubated for 5 min) and procedure as described in section 5.1.3 was followed. Wherever necessary volume was made up to 200µl with buffer.

6.1.5 Determination of K_m and V_{max} for GLM metabolism by nonlinear and linear transformations

The procedure of determination of K_m and V_{max} for GLM metabolism is described in section 5.4.2 while the observations are described in Table 5.12 and Table 5.14.

6.1.6 Inhibitory effect of SMZ on CYP2C9 activity was determined by studying following parameters:

6.1.6.1 IC_{50} Determination

The potential inhibitory effect of the SMZ on the activity of human CYP2C9 was evaluated using developed model substrate reaction for CYP2C9 (GLM,10 µM to

hydroxyglimepiride) and method as follows: Varying concentrations of SMZ (0–110 mM) were coincubated with fixed concentration (10 µM) of the model substrate GLM. The reaction mixture was added to the tubes and mixed vigorously for 5 seconds and procedure as described in section 5.1.3 was followed. The inhibitory effect of SMZ on glimepiride metabolism was expressed as a percentage of the residual activity compared with the control in absence of inhibitor (Table 6.1). Each assay was performed in duplicate.

Table 6.1: Inhibitory effect of varying concentrations of SMZ on 10µM GLM (IC_{50} determination)

SMZ (µM)	Substrate conc. Cs (µM)	Peak area 0 min As	Peak area 30 min Au	Cu_{30min}= Au*Cs/As	C=Cs_{0min}-Cu_{30min}	*C/30min/0.5 (µM/min/mg protein)	*Residual Activity (%)
0	10	121.49	101.272	8.336	1.664	0.111	100
30	10	121.49	102.762	8.458	1.542	0.103	92.630
50	10	121.49	104.844	8.630	1.370	0.091	82.333
100	10	121.49	107.142	8.819	1.181	0.079	70.966
300	10	121.49	109.562	9.018	0.982	0.065	58.997
500	10	121.49	112.81	9.286	0.714	0.048	42.932
700	10	121.49	116.28	9.571	0.429	0.029	25.769
900	10	121.49	117.365	9.660	0.340	0.023	20.403
1100	10	121.49	118.339	9.741	0.259	0.017	15.585

*Average of two experiments

Table 6.2: Inhibitory effect of varying concentrations (log) of SMZ (IC_{50} determination)

SMZ (µM)	SMZ log conc. Cs (µM)	*Residual Activity (%)
0	0	100
30	1.4771	92.630
50	1.6990	82.333
100	2.0000	70.966
300	2.4771	58.997
500	2.6990	42.932
700	2.8451	25.769
900	2.9542	20.403
1100	3.0414	15.585

*Average of two experiments

6.1.6.2 Ki Determination

The method is primarily used as a means of readily obtaining K_i. the reciprocal of the initial velocity (i.e.1/*V*) is plotted against a series of inhibitor concentrations [I], at constant substrate concentration, [S]. When this is done for a number of values of [S], the resulting lines intersect at a point corresponding to K_i. The value of [I] at which this occurs is to the left of the ordinate (for competitive inhibition) and corresponds to $-K_i$ [5-6] Exact inhibition constants (*K*i) were determined from **Dixon plots** obtained by co incubating various concentrations of the inhibitor, SMZ (0, 5,10,30 and 50 mM), with 5 and 10µM GLM in the presence of pooled human liver microsomes and an NADPH-generating system(Table 6.3, 6.4). All incubations were carried out as described before. Before the addition of substrate, the incubation mixture was preincubated for 5 min at

37°C, then allowed to proceed for 30 min, and then terminated as described earlier. *K*i value was calculated by traditional graphical method.

Table 6.3: Inhibitory effect of varying concentrations of SMZ on 5µM GLIM (Ki determination)

SMZ (µM)	Substrate conc. Cs (µM)	Peak area 0 min As	Peak area 30 min Au	Cu_{30min}= Au*Cs/As	C=Cs_{0min}-Cu_{30min}	*C/30min/0.5 (µM/min/mg protein)
0	**5**	52.14	37.695	3.615	1.385	0.092
50	**5**	52.14	40.824	3.915	1.085	0.072
100	**5**	52.14	42.006	4.028	0.972	0.065
300	**5**	52.14	44.523	4.270	0.730	0.049
500	**5**	52.14	46.517	4.461	0.539	0.036

*Average of two experiments

Table 6.4: Inhibitory effect of varying concentrations of SMZ on 10µM GLIM (Ki determination)

SMZ (µM)	Substrate conc. Cs (µM)	Peak area 0 min As	Peak area 30 min Au	Cu_{30min}= Au*Cs/As	C=Cs_{0min}-Cu_{30min}	*C/30min/0.5 (µM/min/mg protein)
0	**10**	121.49	101.272	8.336	1.664	0.111
50	**10**	121.49	104.844	8.630	1.370	0.091
100	**10**	121.49	107.142	8.819	1.181	0.079
300	**10**	121.49	109.562	9.018	0.982	0.065
500	**10**	121.49	112.81	9.286	0.714	0.048

*Average of two experiments

Ki value was also estimated using the following formula:

$$K_i = \frac{IC_{50}}{1 + \frac{[S]}{K_m}}$$

where,

IC_F is **half maximal inhibitory concentration (**functional strength of the inhibitor**),** [S] is fixed substrate concentration, K_m is the concentration of substrate at which enzyme activity is at half maximal and Ki is apparent inhibition constant (binding affinity of the inhibitor).

6.1.7 Effect of SMZ on enzyme kinetics of Glimepiride: Nature of inhibition

For the determination of the apparent Michaelis-Menten constant (K_m) and the maximal velocity of the reaction, (V_{max}), plots in relation to the substrate concentration were derived using Graph pad prism 5 software.The nature of inhibition (competitive or noncompetitive) was assessed by adding 500µM SMZ as inhibitor to varying concentrations of GLM as substrate spanning a range of 2 to 100µM.(Table 6.5)

Data for reaction velocities was also evaluated by double reciprocal plot (Lineweaver-Burk equation,). The intersection points were determined graphically using Microsoft Excel 2007.

Table 6.5: Michaelis-Menten kinetics data for GLM *in vitro* incubation (with 500 µM SMZ)

Substrate conc. Cs (µM)	Peak area 0 min As	Peak area 30 min Au	Cu_{30min}= Au*Cs/As	C=Cs_{0min}-Cu_{30min}	*C/30min/0.5 (µM/min/mg protein)
2	31	30.383	1.960	0.040	0.003
4	58.459	42.353	2.898	1.102	0.073
6	78.06	62.119	4.775	1.225	0.082
8	96.842	73.58	6.078	1.922	0.128
20	228.246	197.191	17.279	2.721	0.181
50	624.417	564.983	45.241	4.759	0.317
75	931.941	860.192	69.226	5.774	0.385
100	1287	1211.883	94.163	5.837	0.389

*Average of two experiments

6.1.8 HPLC Conditions

A validated HPLC method with UV detection was used to measure glimepiride and its metabolite in microsomal incubates. Aliquots of the supernatants of the centrifuged incubates were injected into HPLC. The HPLC system consisted of Shimadzu LC 20 AT pump and SPD 20A UV detector,a rheodyne 7725 fixed injector loop(20µl).The separation consisted of a Thermo scientific C18, Hypersil BDS column (250 x 4.6 mm), particle size 5µ and a Phenomenex C18 guard column (4×3mm). Mobile phase was composed of 0.1% formic acid (pH 3) and acetonitrile (55:45) .The operating temperature was ambient and mobile phase was delivered at a flow rate of 1ml/min. Quantification was performed by determining the peak areas at 228nm. Under these chromatographic conditions, SMZ, GLM metabolite (M1) and GLM were eluted at 3.1min, 3.6 min and 9.3min respectively (Fig. 6.1).

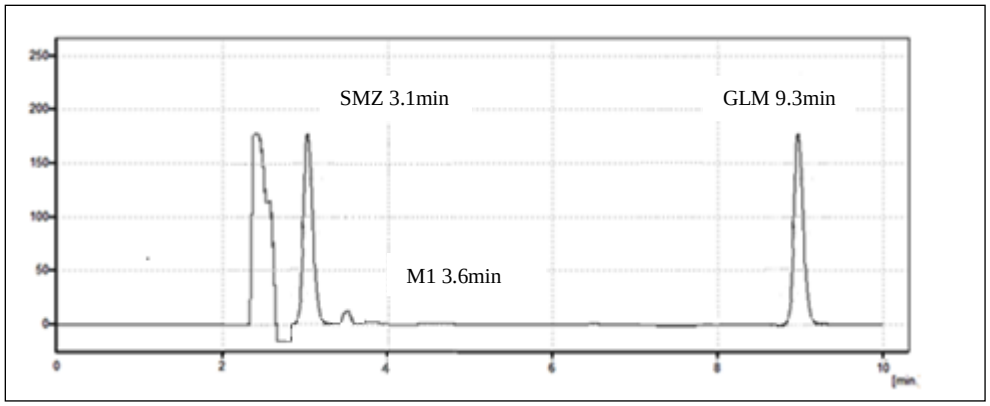

Figure 6.1: HPLC chromatogram of SMZ(3.1 min), GLM metabolite (M_1,3.6min) and GLM (9.3min)

6.1.9 Data analysis

In the present study, the disappearance of GLM in the medium incubated at 37°C with HLM in the presence of the NADPH was determined as the percentage of the initial amount of GLM in the medium without incubation. The obtained results were expressed as the turnover rate in percentage wherever necessary. Substrate disappearance velocity was calculated as [($C_{0,\ initial}$ - $C_{s,\ t\ min}$) / incubation time /CYP concentration], where $C_{0,\ initial}$ is the substrate concentration at time 0 min and $C_{s,\ t\ min}$ is the substrate concentration 30 min incubation with 0.5 mg/ml protein concentration.

The apparent kinetic parameters i.e K_m, Vmax and IC_{50} for CYP2C9 catalyzed reaction in human liver microsomes were assessed with Graphpad Prism 5 software using nonlinear least square regression analysis. All the results were expressed as arithmetic mean ± SD.

6.2 RESULTS

6.2.1 Determination of K_m and V_{max} for GLM metabolism by nonlinear and linear transformations

GLM metabolism in the presence of HLM followed Michaelis-Menten kinetics. K_m and V_{max} values obtained by nonlinear least squares regression method were found to be 28.9 ± 2.97 µMole and 0.559 ± 0.017 µMole/min/mg protein respectively (Figure 5.9, Table 5.13). From Lineweaver-Burk plot the K_m and V_{max} values were found to be 29.411 ± 1.25 µMole and 0.571 ± 0.020 µMole/min/mg protein respectively (Figure 5.9, Table 5.15). Thus the values obtained with nonlinear as well as a linear transformation of the data were found to be in close agreement with each other. Each data point represents an average of at least two parallel incubations.

6.2.2 Inhibitory effect of SMZ on CYP2C9 Activity

6.2.2.1 IC_{50} Determination

To evaluate the inhibitory effect of SMZ on CYP2C9 activity, GLM hydroxylation was carried out in the presence and absence of inhibitor using liver microsomes. Fig. 6.2, illustrates the effect of SMZ on CYP2C9 catalyzed GLM hydroxylation in liver microsomes. With concentrations ranging from 50 to 500 µMole, SMZ exhibited a selective inhibitory effect on CYP2C9 mediated glimepiride metabolism with an apparent IC_{50} value of 400 µMole.

.

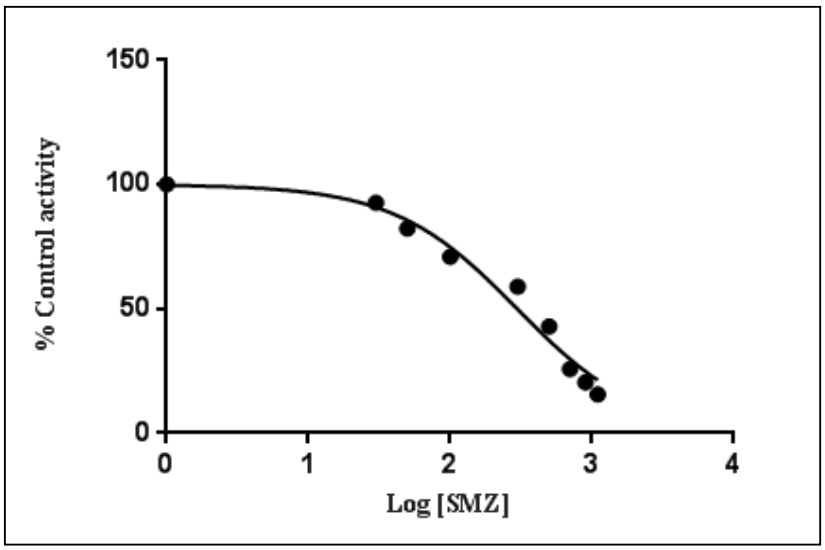

Figure 6.2: The inhibitory effect of SMZ (log conc.) on GLM hydroxylation

6.2.2.2 Ki Determination

Exact inhibition constants (*K*i) were determined from **Dixon plots** (Fig. 6.3) obtained by co incubating various concentrations of the inhibitor, SMZ (0, 5,10, 30 and 50 mM), with 5 and 10µM GLM in the presence of pooled human liver microsomes and an NADPH-generating system. From the Dixon plot analysis using human liver microsomes, the *K*i value of SMZ for GLM hydroxylation was found to be 290µMole. The reciprocal of the initial velocity (i.e.1/*V*) was plotted against a series of inhibitor concentrations [I], at constant substrate concentration, of 5 and 10 µMole and Ki value was obtained by intersecting lines (Table 6.6). The value of 290µMole was obtained to the left of the ordinate for SMZ as inhibitor which suggested competitive inhibition and corresponds to $-K_i$.

Table 6.6: Data for Dixon plot obtained by plotting the reciprocal of the initial velocity (i.e.1/*V*) against a series of inhibitor concentrations [SMZ], at constant substrate concentration, [GLM]

SMZ conc. (µM)	Activity GLM(5µM) (µM/min/mg protein)	1/v Activity GLM(5µM) (µM/min/mg protein)$^{-1}$	Activity GLM(10µM) (µM/min/mg protein)	$1/v_1$ Activity GLM(10µM) (µM/min/mg protein)$^{-1}$
0	0.092	12.005	0.111	9.017
50	0.072	13.793	0.091	10.948
100	0.065	15.435	0.079	12.701
300	0.049	20.536	0.065	15.278
500	0.036	27.818	0.048	20.995

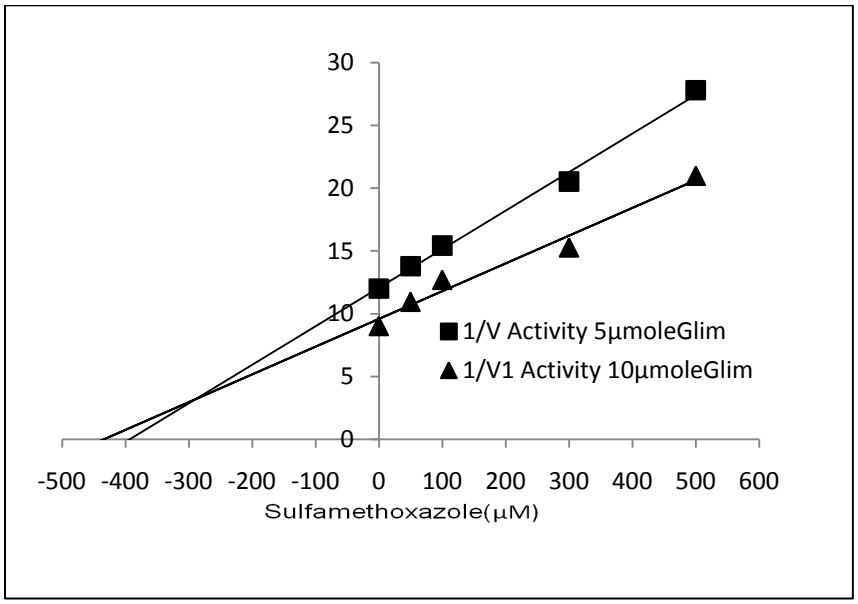

Figure 6.3: Dixon plots showing effect of SMZ (0, 5,10, 30 and 50 mM) when coincubated with 5 µM and 10µM GLM in the presence of pooled HLM.

Ki value was also estimated using the following formula

$$K_i = \frac{IC_{50}}{1 + \frac{[S]}{K_m}}$$

Where, IC_{50} is **half maximal inhibitory concentration (**functional strength of the inhibitor**) =** 400 µMole

[S] is fixed substrate concentration = 10µMole

K_m is the concentration of substrate at which enzyme activity is at half maximal = 28.90µMole

Ki is Apparent inhibition constant(binding affinity of the inhibitor) which was found to be **297.17µMole** after substituting the respective values.

Thus the Ki value obtained by graphical method and equation was found to be in close agreement with each other.

6.2.3 Effect of SMZ on enzyme kinetics of Glimepiride: Nature of inhibition

As shown in Fig. 6.4 the *in vitro* findings suggested the competitive nature of inhibition as K_m was increased (32.26 µMole) and V_{max} (0.526 µMole/min/mg protein) almost remained unaffected (Table 6.7)

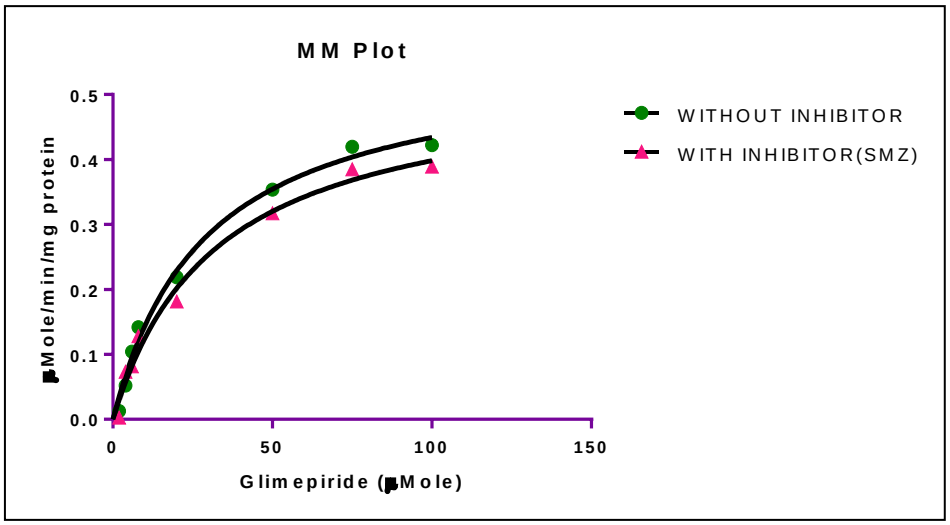

Figure 6.4: Effect of SMZ on MM kinetics of Glimepiride.

Table 6.7: Michaelis-Menten Kinetics Best-fit values

Michaelis-Menten Kinetics Best-fit values	
V_{max} (µM/min/mg protein)	0.571±1.25
K_m(µM)	29.41±0.020
with 500 µM SMZ	
V_{max} (µM/min/mg protein)	0.526
K_m(µM)	32.26
SD	
V_{max} (µM/min/mg protein)	±0.031
K_m(µM)	±4.31
Goodness of Fit	
Degrees of Freedom	6
R^2	0.9905
Absolute Sum of Squares	0.001796
Analyzed	8

Data for reaction velocities (Table 6.8) was also evaluated by plotting the reciprocal of the initial velocity (i.e.1/*V*) against the reciprocal of a series of substrate concentration (i.e.1/GLM) at constant inhibitor concentrations [500 µM SMZ] compared with the control in absence of inhibitor (Lineweaver-Burk equation). As shown in Fig. 6.5, the intersection points were determined graphically using Microsoft Excel 2007. From Lineweaver-Burk plot the K_m was found to be increased from 29.411 to 32.258 µMole but V_{max} remained almost unaffected i.e., 0.525µMole/min/mg protein in presence of 500µM SMZ as inhibitor (Table 6.9). Thus the values obtained with nonlinear as well as a linear transformation of the data were found to be in close agreement with each other.

Table 6.8: Data for Lineweaver Burk plot

Sr. No.	1/GLM (µM)	1/V0 (No Inhibitor)	1/V1 (500 µMole Inhibitor)
1.	0.167	10.966	12.907
2.	0.125	7.051	8.867
3.	0.050	4.588	5.512
4.	0.020	2.825	3.152
5.	0.013	2.326	2.598
6.	0.010	2.366	2.570
7.	-0.200	--	--

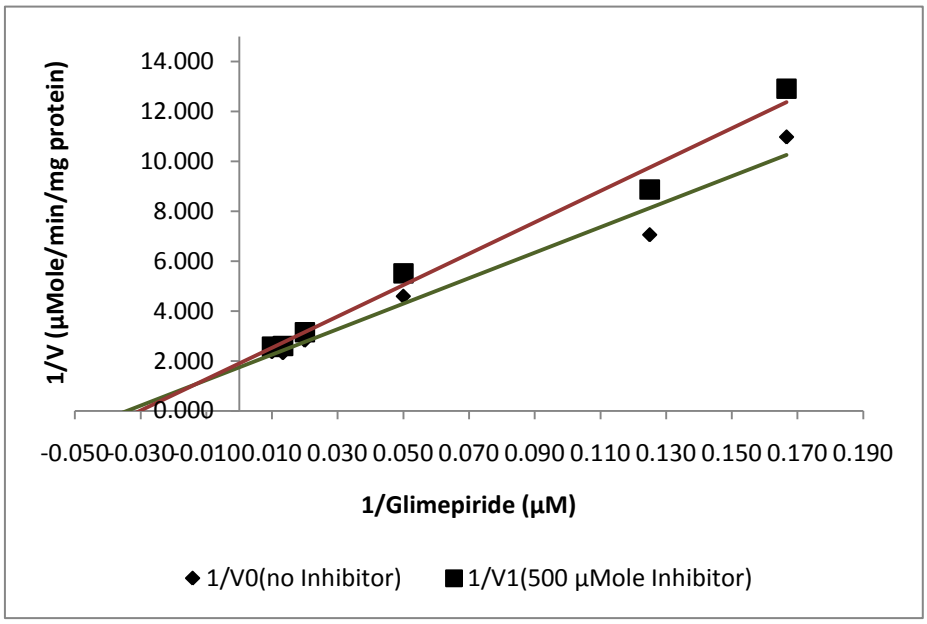

Figure 6.5. Lineweaver Burk plot obtained by co-incubating GLM(0-100 µMole) with HLM in the presence and absence of SMZ (500 µMole).

Table 6.9: K_m and V_{max} data obtained by Lineweaver Burk plot

1.	K_m (Lineweaver-Burk plot)	**No Inhibitor**	1/0.034=29.411 µMole
		500 µMole SMZ (Inhibitor)	1/0.031=32.258 µMole
2.	V_{max} (Lineweaver-Burk plot)	**No Inhibitor**	1/1.75=0.571 µMole
		500 µMole SMZ (Inhibitor)	1/1.90=0.525 µMole

6.2.4. Prediction of Increase in AUC of Glimepiride from *In Vitro* Metabolic Data: *IVIVC*

As fractions of human tissues such as human liver microsomes and human hepatocytes have become more easily available for *in vitro* studies, attempts have been made to quantitatively predict *in vivo* drug metabolism or drug interactions in humans from *in vitro* data. In the case of a competitive or noncompetitive inhibition of drug metabolism, the degree of *in vivo* interaction can be evaluated from the [I] u /Ki ratio, where [I] u is the unbound concentration around the enzyme and Ki is the *in vitro* inhibition constant of the inhibitor. Although Ki values can be determined by kinetic analyses of *in vitro* data using human liver microsomes, it is usually impossible to directly measure [I]u in humans.

In the case of drugs that are transported into the liver by passive diffusion, [I]u may be assumed to be equal to the unbound concentration in the liver sinusoid at steady-state. In order to avoid a false-negative prediction due to underestimation of [I]u , the maximum unbound concentration at the inlet to the liver, where the blood flow from the hepatic artery and portal vein meet ([I] in,max,u), as the maximum value of [I]u was used.[7-8] This method was thus proposed to be useful for predicting the maximal degree of inhibition.

According to the perfusion model the maximum concentration of inhibitor at the inlet to the liver ([I]in,max) can be calculated as follows :

$$[I]in,max = [I]max + ka \times Dose \times Fa / Qh \quad (1)$$

where ka is the absorption rate constant, Dose is the amount of inhibitor administered, Fa is the fraction absorbed from gut to the portal vein, and Qh is the hepatic blood flow rate. The reported literature[9] [I]max value of 217 and ka x Dose x Fa / Qh value of 244 for SMZ as inhibitor was used for the calculations.

$$[I]in,max = 217 + 244 \quad (2)$$
$$= 461$$

Using the unbound fraction in the blood (fu) which is reported to be 0.35[9] for SMZ, [I]in,max,u was obtained as follows:

$$[I]in,max,u = fu \times [I]in,max \quad (3)$$
$$= 0.35 \times 461$$
$$= 161.35$$

In clinical situations, the substrate concentration is usually much lower than K_m and the hence maximum degree of interaction (R = area under the curve [AUC] (+ inhibitor) / AUC (control)) is expressed as

$$R = 1 + [I]u / Ki \quad (4)$$
$$= 1 + 161.35/290$$
$$= 1.542$$

where *K*i is the dissociation constant for the enzyme–inhibitor complex obtained by co incubating various concentrations of the inhibitor, SMZ (0, 5, 10, 30 and 50 mM), with 5 and 10µM GLM in the presence of pooled human liver microsomes and an NADPH-generating system. [From the Dixon plot analysis, the *K*i value of SMZ for GLM hydroxylation was found to be 290µMole (Refer sec. 6.3.2.2)]. The AUC of GLM was predicted to increase about 1.5-fold by co administration of SMZ, suggesting the risk of hypoglycemia.

6.3 DISCUSSION

With concentrations ranging from 30 to 1100 µMole, SMZ exhibited a selective inhibitory effect on CYP2C9-mediated GLM-hydroxylation with an apparent IC_{50} value of 400 µMole and Ki value of 290 µMole. The pattern of inhibition was found to be competitive as K_m value was increased (32.26 ±4.31 µMole) and V_{max} (0.526 ± 0.031) almost remain unaffected as predicted by Michaelis Menten plot and Lineweaver Burk plot. Also the Ki value obtained by Dixon plot to the left of the ordinate (-290 µMole) suggests competitive inhibition. The results indicate that, SMZ when used at concentrations lower than 500 µMole, can be used as selective inhibitor of CYP2C9 for *in vitro* studies. In addition, even with a concentration reaching 1000 µMole, sulfamethoxazole is a very selective inhibitor of CYP2C9.

IVIVC findings suggest that AUC of GLM was increased around or more than 1.5 fold by SMZ**.** This predicted increase in plasma concentration of GLM is high, suggesting the risk of hypoglycemia when SMZ is coadministered with GLM.

6.4 CONCLUSION

In this study, we systematically evaluated the inhibitory effects of sulfonamides on GLM metabolism mediated by CYP2C9. Caution must be exercised when extrapolating the effects of inhibitor from *in vitro* to *in vivo* conditions. Sulfonamides can potentiate the hypoglycemic effect of sulfonylurea agents when given in combination. Hence coadministration of sulfamethoxazole with glimepiride (to avoid hypoglycemic attack) should be monitored. The study demonstrated that GLM and SMZ can be used as a probe substrate and selective inhibitor of CYP2C9 respectively, which can provide a reliable *in vitro* approach for kinetic studies. The literature kinetic parameters [10] of tolbutamide-sulfamethoxazole interaction (K_m= 50µMole, IC_{50}=544µMole,Ki= 271µMole) were found to be consistent to some extent with our laboratory findings.

This interaction study predicts that coadministration of sulfamethoxazole with glimepiride and CYP2C9 substrates with narrow therapeutic ranges such as phenytoin (an antiepileptic) and warfarin (an anticoagulant) should be monitored closely as sulfonamides can potentiate the hypoglycemic effect of sulfonylurea agents when given in combination.

6.5 REFERENCES

1. Vikas K, Dan R, Chad W, Timothy T, Jan L. W: Enzyme source effects on CYP2C9 kinetics and inhibition. Drug metab Dispos 2006, 34: 1903-1908.
2. Dermot F, James T Steve T, Robert J: Prediction of CYP2C9-mediated drug-drug interactions: a comparison using data from recombinant enzymes and human hepatocytes. Drug metab Dispos 2005, 33: 1700-1707.
3. Dayong Si, Ying W, Yi-Han Zhou, Yingjie G, Juan W, Hui Z, Ze-Sheng Li, and J. Paul F: Mechanism of CYP2C9 Inhibition by flavones and flavonols. Drug metab Dispos 2009, 37: 629-634.
4. Vikas K, Jan W, Dan R, Chad J, Lee A, Timothy T: CYP2C9 Inhibition: Impact of probe selection and pharmacogenetics on *in vitro* inhibition profiles. Drug metab Dispos 2006, 37: 1966-1975.
5. Tarundeep K, Harold B, Michael M: Estimation of *k*i in a competitive enzyme-inhibition model: Comparisons among three methods of data analysis. *Drug metab Dispos* 1999, 27: 756-762.
6. M. Dixon: The determination of enzyme inhibitor constants. *Biochem. J.*1953, 55: 170-171.
7. Hayley S. , Kiyomi I, Aleksandra G, Brian J: Prediction of *in vivo* drug–drug interactions from *in vitro* data: impact of incorporating parallel pathways of drug elimination and inhibitor absorption rate constant. Br J Clin Pharmacol 2005 , 60: 508–518.
8. Larry C, Timothy G: Predicting *in vivo* drug interactions from *in vitro* drug discovery data. Drug Discov 2005, 4: 825-833.
9. Kanji K, Kiyomi I, Yukiko N, Shin-Ichi K, Susumu I, Yoshihiko F, Carol E, Charles A , Noriaki S, Yuichi S: Prediction of *in vivo* drug-drug interactions between tolbutamide and various sulfonamides in humans based on *in vitro* experiments. Drug metab Dispos 2000, 28: 475-481.
10. Xia Wen, Jun-Sheng Wang, Janne T. Backman, Jouko Laitila, And Pertti J. Neuvonen:

11. Trimethoprim and sulfamethoxazole are selective inhibitors of CYP2C8 and CYP2C9, respectively**.** Drug metab Dispos 2002, 30: 631-635.

Chapter 7

In vitro assessment of Pineapple and Pomegranate juice on CYP2C9 mediated Glimepiride metabolism in vitro

There is limited information on the effect of fruits on human cytochrome P450 (CYP) 2C9 activity. GLM was used as a substrate for CYP2C9, since this drug is metabolised to cyclohexyl hydroxy methyl derivative (M1) by CYP2C9. The objective of this study was to determine the effect of pineapple (PIJ) and pomegranate (POJ) juices on CYP2C9 mediated metabolism of GLM *in vitro* using human liver microsomes. The study focused on comparative evaluation of the inhibitory potencies of fruit juices like PIJ and POJ on CYP2C9-mediated drug metabolism of GLM *in vitro* using human liver microsomes.

7.1 EXPERIMENTAL

7.1.1 Chemicals and Reagents

All chemicals and reagents used in this study were of analytical grade and were procured as described under section 5.1.1.

7.1.2 Microsomal Source

A pool of the 50 HLM (0.5 ml at 20 mg/ml), mixed gender, was procured and processed as described under section 5.1.2.

7.1.3 Fruit Juices

PIJ and POJ fruits were obtained from the local commercial source. Fruit juice was obtained by squeezing the edible portion of the fruit, centrifuged , and filtered to remove the residues. All samples were used within 1 hour after they were squeezed and filtered.

7.1.4 Preparation of standard and working GLM solutions

The procedure mentioned in section 6.1.3 was followed to prepare GLM solutions.

7.1.5 Analytical method for GLM *in vitro* metabolism

The procedure described in section 6.1.4 was followed.

7.1.6 Inhibitory effect of fruit juices on CYP2C9 Activity: IC_{50} determination

Appropriate amounts of PIJ juice (1, 2, 3.5, 5 and 7.5µl) and POJ juice (1, 3, 5, 7 and 10 µl) were added to fresh tubes containing 10 µM GLM. The reaction mixture described above was added to the tubes and mixed vigorously for 5 seconds and procedure described under 5.1.3 was followed. The inhibitory effects of PIJ and POJ juice on GLM metabolism was expressed as a percentage of the residual activity compared with the control in absence of fruit juices (Table 7.1-7.2). Each assay was performed in duplicate.

Table 7.1: Inhibitory effect of varying concentrations of PIJ on 10µM GLIM.

PIJ (µl)	Substrate conc. Cs (µM)	Peak area 0 min As	Peak area 30 min Au	Cu_{30min}= Au*Cs/As	C=Cs_{0min}-Cu_{30min}	*C/30min/0.5 (µM/min/mg protein)	*Residual Activity (%)
0	10	107.524	99.029	9.210	0.790	0.053	100
1	10	108.133	102.899	9.516	0.484	0.032	61.266
2	10	107.789	104.587	9.703	0.297	0.020	37.600
3.5	10	107.887	106.512	9.873	0.127	0.008	16.132
5	10	108.785	107.567	9.888	0.112	0.007	14.172
10	10	108.789	107.79	9.908	0.092	0.006	11.623

*Average of two experiments

Table 7.2: Inhibitory effect of varying concentrations of POJ on 10µM GLIM.

POJ (µl)	Substrate conc. Cs (µM)	Peak area 0 min As	Peak area 30 min Au	Cu_{30min}= Au*Cs/As	C=Cs_{0min}-Cu_{30min}	*C/30min/0.5 (µM/min/mg protein)	*Residual Activity (%)
0	10	108.789	99.029	9.103	0.897	0.060	100
1	10	109.102	101.56	9.309	0.691	0.046	77.053
3	10	108.856	103.52	9.510	0.490	0.033	54.638
5	10	108.759	104.222	9.583	0.417	0.028	46.498
7	10	108.789	105.42	9.690	0.310	0.021	34.518
10	10	108.989	106.155	9.740	0.260	0.017	28.984

*Average of two experiments

7.1.7 Effect of Fruit juices on MM kinetics of GLM

For the determination of the apparent Michaelis-Menten constant (K_m) and the maximal velocity of the reaction, (V_{max}), plots in relation to the substrate concentration were derived using Graph pad prism 5 software.The nature of inhibition (competitive or noncompetitive) of fruit juices on GLM metabolism was assessed by adding 5µl (2.5% v/v) PIJ and 7µl (3.5% v/v) POJ juices separately as inhibitor to varying concentrations of GLM as substrate spanning a range of 2 to 100µM.(Table 7.3-7.5)

7.1.8 HPLC Conditions

A validated HPLC method with UV detection described in section 5.2.3 was used to measure GLM and its metabolite in microsomal incubates.

7.1.9 Data analysis

In the present study, the disappearance of GLM in the medium incubated at 37°C with HLM in the presence of the NADPH was determined as the percentage of the initial amount of GLM in the medium without incubation. The obtained results were expressed as the turnover rate in percentage wherever necessary. Substrate disappearance velocity was calculated as [($C_{0,\ initial}$ - $C_{s,\ t\ min}$) / incubation time /CYP concentration], where $C_{0,\ initial}$ is the substrate concentration at time 0 min and $C_{s,\ t\ min}$ is the substrate concentration 30 min incubation with 0.5 mg/ml protein concentration.

The apparent kinetic parameters i.e K_m and V_{max} for CYP2C9 catalyzed reaction in human liver microsomes were assessed with Graphpad Prism 5 software using nonlinear least square regression analysis and IC_{50} values for the inhibition of the P450 activities were assessed with Microsoft Excel 2007. All the results were expressed as arithmetic mean ± SD.

7.2 RESULTS

7.2.1 Inhibitory effect of fruit juices on CYP2C9 Activity

To evaluate the inhibitory effect of fruit juices on CYP2C9 activity, GLM hydroxylation was carried out in the presence and absence of fruit juices using liver microsomes. As shown in Figure 7.1, the inhibitory effect of PIJ and POJ juices on CYP2C9 activity depended on the amount of respective juices added to the reaction mixture. The mean IC_{50} value obtained for PIJ and POJ juice was found to be 1.50 ± 0.23 µl (0.75% v/v) and 4.25 ± 0.53µl (2.12% v/v) respectively. At concentrations 0.5% v/v the percentage inhibition was 61.26% and at 1.5% v/v it was 22.42% for PIJ juice. Similarly for POJ juice, at concentrations 0.5% v/v the percentage inhibition was 77.05% and at 1.5% v/v it was 53.98%.Amongst the fruit juices evaluated PIJ juice showed strong CYP2C9 inhibitory activity than POJ juice.

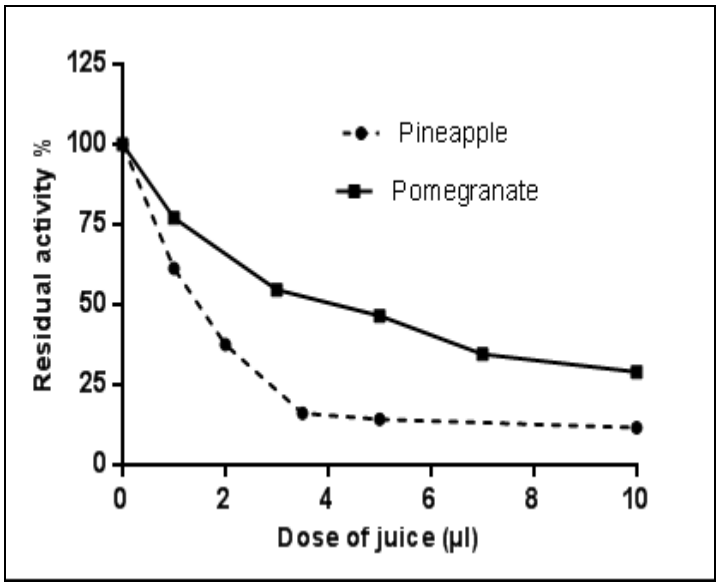

Figure 7.1 The inhibitory effect of PIJ and POJ juices on CYP2C9 activity.

The bar graph (Figure 7.2) represents the comparative evaluation of the inhibitory potencies of PIJ and POJ juices on CYP2C9-mediated drug metabolism of GLM *in vitro* using human liver microsomes. It reflects that PIJ juice is more inhibitory in nature than POJ.

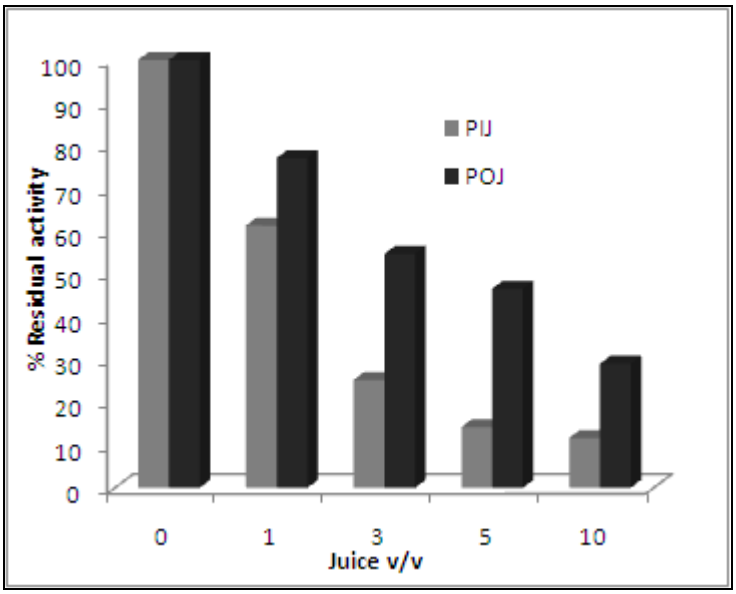

Figure 7.2 Bar graph representing the comparative evaluation of the inhibitory potencies of PIJ and POJ on CYP2C9-mediated drug metabolism of GLM.

7.2.2 Effect of Fruit juices on MM kinetics of GLM

As shown in Figure 7.3, the *in vitro* findings suggested the competitive nature of inhibition as K_m was increased (47.50 µMole) and V_{max} (0.492 µMole/min/mg protein) almost remained unaffected for PIJ juice. Similarly for POJ juice K_m was increased (34.00µMole) and V_{max} (0.509µMole/min/mg protein) almost remained unaffected.(Table 7.6-7.8)

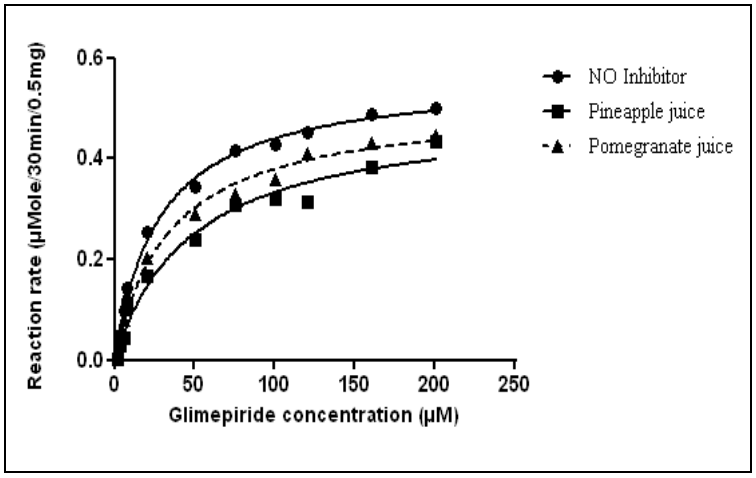

Figure 7.3. Effect of PIJ and POJ on MM kinetics of GLM.

Table 7.3: Michaelis-Menten kinetics data for GLM *in vitro* incubation.

The observation table is same as described under Table 5.12

Table 7.4: Michaelis-Menten kinetics data for GLM *in vitro* incubation (with 5µl PIJ).

Substrate conc. Cs (µM)	Peak area 0 min As	Peak area 30 min Au	Cu_{30min}= Au*Cs/As	C=Cs_{0min}-Cu_{30min}	*C/30min/0.5 (µM/min/mg protein)
2	30.44	29.933	1.967	0.033	0.002
4	60.88	53.981	3.547	0.453	0.030
6	72.629	64.899	5.361	0.639	0.043
8	99.899	79.01	6.327	1.673	0.112
20	249.899	218.63	17.497	2.503	0.167
50	629.61	584.422	46.411	3.589	0.239
80	999.991	942.371	75.390	4.610	0.307
100	1277.41	1216.322	95.218	4.782	0.319
120	1408.216	1353	115.295	4.705	0.314
160	1939.395	1870	154.275	5.725	0.382
200	2284.5	2210	193.478	6.522	0.435

*Average of two experiments

Table 7.5: Michaelis-Menten kinetics data for GLM *in vitro* incubation (with 5µl POJ).

Substrate conc. Cs (µM)	Peak area 0 min As	Peak area 30 min Au	Cu_{30min}= Au*Cs/As	C=Cs_{0min}-Cu_{30min}	*C/30min/0.5 (µM/min/mg protein)
2	30.44	28.284	1.858	0.142	0.009
4	60.88	52.181	3.428	0.572	0.038
6	72.629	58.076	4.798	1.202	0.080
8	99.899	75.535	6.049	1.951	0.130
20	249.899	211.812	16.952	3.048	0.203
50	629.61	574.897	45.655	4.345	0.290
80	999.991	938.26	75.061	4.939	0.329
100	1277.41	1208.506	94.606	5.394	0.360
120	1408.216	1336.11	113.856	6.144	0.410
160	1939.395	1861.052	153.537	6.463	0.431
200	2284.5	2208.065	193.308	6.692	0.446

*Average of two experiments

Table 7.6: Michaelis-Menten Kinetics Best-fit values for GLM.

V_{max} (µM/min/mg protein)	0.564
K_m(µM)	27.98
SD	
V_{max} (µM/min/mg protein)	± 0.015
K_m(µM)	± 2.772
Goodness of Fit	
Degrees of Freedom	9
R^2	0.994
Absolute Sum of Squares	0.002
Analyzed	11

Table 7.7: Michaelis-Menten Kinetics Best-fit values (with 5µl PIJ).

V_{max} (µM/min/mg protein)	0.492
K_m(µM)	47.5
SD	
V_{max} (µM/min/mg protein)	± 0.038
K_m(µM)	± 10.99
Goodness of Fit	
Degrees of Freedom	9
R^2	0.974
Absolute Sum of Squares	0.006
Analyzed	11

Table 7.8: Michaelis-Menten Kinetics Best-fit values (with 5µl POJ).

V_{max} (µM/min/mg protein)	0.5092
K_m(µM)	34
SD	
V_{max} (µM/min/mg protein)	± 0.02185
K_m(µM)	± 4.964
Goodness of Fit	
Degrees of Freedom	9
R^2	0.9873
Absolute Sum of Squares	0.003364
Analyzed	11

7.3 DISCUSSION

Very few reports are available regarding food-drug interactions by fruit juices. In this study we investigated that PIJ as well as POJ juice affected the CYP2C9 activity *in vitro* which suggests the possible interaction of juices with substrates of CYP2C9 in humans.

The addition of 10 µl (5% v/v) of PIJ juice (PIJ) resulted in almost complete inhibition. On the other hand POJ juice (POJ) had less CYP2C9 inhibitory capacity. At concentrations 0.5% v/v the percentage inhibition was 61.26% and at 1.5% v/v it was 22.42% for PIJ juice. Similarly for POJ juice, at concentrations 0.5% v/v the percentage inhibition was 77.05% and at 1.5% v/v it was 53.98%.

PIJ juice was found to be a potent inhibitor of human CYP2C9 as compared to POJ juice. In human liver microsomes, the mean 50% inhibitory concentrations (IC_{50}) for PIJ and POJ versus CYP (GLM hydroxylation) were 1.50 ± 0.233 µl and 4.25 ± 0.532µl respectively. Thus, POJ does not significantly alter metabolism of GLM as compared to PIJ which suggests its beneficial effects in subjects with type 2 diabetes.

Inhibition constants (IC_{50}) from *in vitro* studies can been used for quantitative forecasting of pharmacokinetic food-drug interactions. From the comparative study or results of K_m and V_{max} for GLM alone (27.98 ± 2.77 µM, 0.564 ± 0.015 µM/min/mg protein), K_m, V_{max} and IC_{50} for GLM in presence of PIJ (47.50 ± 10.99 µM, 0.492 ± 0.038 µM/min/mg protein, 1.50 ± 0.23 µl (0.75% v/v)) and GLM in presence of POJ (34.00 ± 4.96 µM, 0.50 ± 0.021 µM/min/mg protein, 4.25 ± 0.53µl (2.12% v/v)), it was observed that PIJ exerts significant competitive inhibitory effect than POJ on GLM metabolism.

One of the ways to control diabetes mellitus is through the diet and it is here that POJ juice can play a part. The low inhibitory potential of POJ towards GLM *in vitro* metabolism suggests beneficial effects in subjects with type 2 diabetes. POJ juice may be considered as a healthy fruit juice and awaits additional clinical research to further strengthen for its unique antidiabetic effect. Several reports are present on the hypoglycemic activity of flowers, seeds, and juice of POJ.[1-3]

According to literature[4-6], POJ and extracts of the seed oils and flowers have been recently proven to be powerfully helpful in management of insulin resistance and glucose

metabolism. When taking POJ, research shows that subjects tend to have improved insulin efficiency, reduced insulin resistance, improved lipid metabolism and control and improved blood sugar control. These results are remarkable help for diabetics. One surprising finding[4] was that the sugars contained in POM juice although similar in content to those found in other fruit juices did not worsen diabetes disease parameters in patients but in fact reduced the risk for atherosclerosis. This is because in most juices, sugars are present in free and harmful forms but in POJ juice however the sugars are attached to unique antioxidants, which make these sugars protective against diabetes and atherosclerosis.

Although our *in vitro* evidence in favor of using POJ juice for diabetics is very promising, extensive studies are required to fully understand its possible contribution to human health before recommending its regular consumption.

7.4 CONCLUSION

This study demonstrated that the metabolism of GLM was altered by PIJ and POJ. Addition of 10 µl (5% v/v) of pineapple juice resulted in almost complete inhibition. Amongst the fruits evaluated, PIJ showed strong inhibition towards CYP2C9 activity while POJ appears to make minor contributions to the oxidative metabolism of GLM. Caution must be exercised when extrapolating the effects of inhibitor from *in vitro* to *in vivo* conditions. In addition, the effects of fruit juices on pharmacokinetics of drugs *in vitro* may not be consistent with those in humans. Therefore further investigations in humans are necessary to elaborate our findings.

The *in vitro* drug fruit interaction study predicts that pineapple juice is more inhibitory in nature as compared to pomegranate juice. Hence coadministration of juices should be closely monitored in diabetic patients.

7.5 REFERENCES

1. Katz SR, Newman RA, Lansky EP. 2007. *Punica granatum*: heuristic treatment for diabetes mellitus. J Med Food 10(2):213–7.

2. Huang THW, Peng G, Kota BP, Li GQ, Yamahara J, Roufogalis BD, Li Y. 2005. Anti-diabetic action of *Punica granatum* flower extract: activation of PPAR-g and identification of an active component. Toxicol App Pharmacol 207:160–9.

3. Li Y, Wen S, Kota BP, Peng G, Li GQ, Yamahara J, Roufogalis BD. 2005. *Punica granatum* flower extract, a potent alpha-glucosidase inhibitor, improves postprandial hyperglycemia in Zucker diabetic fatty rats. J Ethnopharmacol 99:239–44.

4. Aviram M, Dornfeld L. 2001. Pomegranate juice consumption inhibits serum angiotensin-converting enzyme activity and reduces systolic blood pressure. Atherosclerosis 158(1):195–8

5. Bagri P, Ali M, Aeri V, Bhowmik M, Sultana S. 2009. Antidiabetic effect of *Punica granatum* flowers: effect on hyperlipidemia, pancreatic cells, lipid peroxidation and antioxidant enzymes in experimental diabetes. Food Chem Toxicol 47:50–4.

6. Basu A, Penugonda K. 2009. Pomegranate juice: a heart-healthy fruit juice. Nutr Rev 67(1):49–56.

Chapter 8

Part I: Simultaneous method development of cocktail substrate assay system for Efavirenz (CYP2B6), Diclofenac (CYP2C9), Chlorzoxazone (CYPE1), Atorvastatin (CYP3A4)

Part II: Evaluation of cocktail substrate assay system for inhibition screening of CYP2B6, CYP2C9, CYP2E1 & CYP3A4 by MCR-706 and MCR-742.

Chapter 8

Part I: Simultaneous method development of cocktail substrate assay system for Efavirenz (CYP2B6), Diclofenac (CYP2C9), Chlorzoxazone (CYPE1), Atorvastatin (CYP3A4)

This chapter follows a description of the HPLC-UV method developed for simultaneous evaluation of the activities of four cytochrome P450's (CYP2B6, CYP2C9, CYP2E1, and CYP3A4) in human liver microsomes. The developed isocratic LC/UV method can offer new analytical possibilities which provides sufficient sensitivity and linear concentration range for the analysis of probe substrate and its metabolites with good resolution from *in vitro* individual incubations as well as cocktail incubations. Hence can be used to improve throughput and cost-effectiveness in preclinical drug studies. The four-specific probe substrates include efavirenz (CYP2B6), diclofenac (CYP2C9), chlorzoxazone (CYPE1), and atorvastatin (CYP3A4).

8.1 EXPERIMENTAL

8.1.1 Chemicals and Reagents

GLM and Atorvastatin(ATV) were received as gift samples from Cadila Healthcare Ltd., Ahmedabad, India. Diclofenac(DIC) sodium was obtained as the gift sample from Alembic Pharma, Baroda, Gujarat, India. Pharmaceutical grade of Chlorzoxazone(CHZ) was kindly supplied as gift sample from Uni Drugs Innovative Pharma Technologies Ltd., Indore and Efavirenz(EFV) was obtained from Torrent Pharmaceuticals, Gujarat, India. Nicotinamide Adenine Dinucleotide Phosphate, reduced tetra sodium salt (NADPH) and magnesium chloride ($MgCl_2$) was purchased from Himedia laboratories, India. Ethylene diamine tetra acetic acid (EDTA), dipotassium hydrogen phosphate and potassium dihydrogenphosphate were purchased from S.d Fine-Chem Limited, India. Methanol and Acetonitrile of HPLC grade were purchased from Spectrochem India. All other chemicals and reagents used in this study were of analytical grade.

8.1.2 Microsomal Source

A pool of the 50 HLM (0.5 ml at 20 mg/ml), mixed gender, was procured and processed as described under section 5.1.2.

8.1.3 Preparation of standard and quality control sample

Stock solution, 1mg/ml of EFV, DIC, CHZ, ATV were prepared individually by dissolving 5mg,5.35mg, 5mg and 10.34mg of the drugs in 5 ml of methanol in a volumetric flask to yield a concentration of 3.17mM, 3.37mM, 5.9mM, 0.895mM. The stock solution was stored at 4℃until use. **Working solution**, 0.1mg/ml were prepared by transferring 1.0 ml from stock solution to 10 ml volumetric flask and diluted to the mark with MeOH.

For the preparation of **DIC calibration standards**, a series of working solutions were produced by adding appropriate amount to HLM-free incubation solution to yield 11.23, 22.46, 33.70, 44.93, 56.16, 67.40, 78.63, and 89.86 μM of DIC. Among them, 11.23, 44.93 and 78.63 μM of GLM were used as quality control (QC) samples.

For the preparation of **CHZ calibration standards**, a series of working solutions were produced by adding appropriate amount to HLM-free incubation solution to yield 19.70, 39.40, 59.10, 78.85, 98.50, 118.2, 137.9, and 157.6 μM of CHZ. Among them, 19.70, 78.85 and 137.9μM of GLM were used as quality control (QC) samples.

For the preparation of **ATV calibration standards**, a series of working solutions were produced by adding appropriate amount to HLM-free incubation solution to yield 5.96, 11.93, 17.90, 23.86, 29.83, 35.80, 41.76, and 41.73 μM of ATV. Among them, 5.96, 23.86 and 41.76 μM of GLM were used as quality control (QC) samples.

For the preparation of **EFV calibration standards**, a series of working solutions were produced by adding appropriate amount to HLM-free incubation solution to yield 10.56, 21.13, 31.70, 42.26, 52.03, 63.40, 73.96, and 84.53 μM of EFV. Among them, 10.56, 42.26 and 73.96 μM of GLM were used as quality control (QC) samples.

8.1.4 HPLC Instrumentation

Chromatography was performed on Shimadzu (Shimadzu Corporation, Kyoto, Japan) chromatographic system equipped with Shimadzu LC-20AD pump and Shimadzu PDA-M20A Diode Array Detector. Samples were injected through a Rheodyne 7725 injector valve with fixed loop of 20 μl. Data acquisition and integration was performed using LC

Solution software (Shimadzu Corporation, Kyoto, Japan). Compounds were separated on a Phenomenex Luna C18 column (150 mm × 4.6 mm i.d, 5-µm particle) associated with a Phenomenex C18 guard column (4×3mm) under reversed-phase partition chromatographic conditions. The mobile phase consisted of 20 mM ammonium formate buffer of pH 3.2 containing 0.1% formic acid and acetonitrile. (52:48). The substrate disappearance rate for CYP2C9 (diclofenac 4'-hydroxylation) and CYP2E1 (chlorzoxazone 6-hydroxylation), was quantified at 230 nm while for CYP2B6 (efavirenz 8-hydroxylation) and CYP3A4 (atorvastatin *o*-hydroxylation) was quantified at 247 nm.

8.1.5 HPLC separation and detection of metabolites (M_1, M_2, M_3, M_4):

Control incubations were carried out without HLM, NADPH to confirm metabolism. Wherever necessary the volume was made up to 200 µl with buffer.

8.1.6 *In vitro* incubation conditions:

To define the optimal conditions for incubation and HPLC analysis, CHZ/ATV/DIC/EFV (5 – 150 µMole) were incubated with HLM for 10 to 60 min across a range of microsomal enzyme concentrations (0.25 – 1 mg/ml). Briefly the incubation mixtures consisted of 50mM phosphate buffer (pH 7.4), 10 mM $MgCl_2$, 1 mM EDTA, 1 mM NADPH and microsomal protein. In all experiments, CHZ/ATV/DIC/EFV were dissolved and diluted serially in methanol and then alcohol was removed by evaporating to dryness. CHZ/ATV/DIC/EFV were reconstituted in potassium phosphate buffer (50 mM, pH 7.4) .The tubes were placed into an ice bath and HLM was added and vortexed. Tubes (duplicate) containing the reaction mixture in phosphate buffer and NADPH solution were allowed to equilibrate separately in a shaker incubator at 150 rpm for 5 minutes at 37°C. The reaction was initiated by adding 20 µl of NADPH immediately to the tubes and incubation carried out for 30min. The reaction was terminated by the addition of 100 µl ice cold acetonitrile containing 40 mcg/ml of GLM as internal standard. . Then the samples were subjected to centrifugation on a cooling laboratory centrifuge (Sigma, 3K30; Germany) at 10,000 rpm (4°C; 10min), and aliquots of the supernatant were directly injected into an HPLC system.

8.2 METHOD DEVELOPMENT

8.2.1 Selection of probe substrates: A cocktail approach to measure the activity of several enzymes simultaneously is desirable because it can reduce both time and cost of analysis. However, the potential interference between substrates and their metabolites should be considered. The probes to be used in this cocktail approach were chosen based not only on their CYP specificity, but also on their availability and recommendations in regulatory guidance. The probe drugs and doses in this cocktail were chosen to be selective for individual CYP isoforms, with the expectation of no or minimal interference between probes.

It is important to select specific probe substrates for each P450 enzyme because multiple P450 enzymes are involved in the metabolism of a single drug. In this study, therefore, probe substrate for each P450 enzyme were selected based on a representative list of preferred and acceptable *in vitro* probe substrates recommended by FDA. The probe substrates selected for each P450 enzyme were as follows: EFV (CYP2B6), DIC (CYP2C9), CHZ (CYPE1), ATV (CYP3A4). CHZ, ATV, DIC, EFV met all the typical requirements to be used as probe substrate for the simultaneous evaluation of the activities of four cytochrome P450s (CYP2B6, CYP2C9, CYP2E1, and CYP3A4) in human liver microsomes. All the substrates were soluble in common solvent methanol, which was evaporated during analysis. All the substrates were stable during the analysis i.e., no additional interacting peaks of probe substrate were observed in chromatograms after cocktail incubation. All the peaks of probe substrate and their respective metabolites were well resolved.

8.2.2 Selection and Optimization of chromatographic conditions:

To optimize the chromatographic conditions, the effect of chromatographic variables such as composition of mobile phase, pH of mobile phase and flow rate were studied. The resulting chromatograms were recorded and the chromatographic parameters such as capacity factor, asymmetric factor, resolution and theoretical plates were calculated. The conditions that gave the best resolution, symmetry and theoretical plate were selected for estimation as shown in Table 8.1a and 8.1b.

Table 8.1a: Optimization of HPLC method

Column - BDS Hypersil C18 Column; Thermo Scientific (250 mm × 4.6 mm; 5µ)										
Isocratic Elution										
Mobile phase	Ratio	Flow Rate	CHZ		ATV		DIC		EFV	
			RT min	Peak Shape	RT Min	Peak shape	RT min	Peak shape	RT min	Peak Shape
Methanol:Water	50:50	1ml/ min	2.99	Tailing	15.52	broad	19.52	broad	No Peak upto 40min	--
Methanol: Phosphate buffer pH-3	50:50	1ml/ min	2.88	Tailing	14.23	Tailing	20.10	broad	No Peak upto 40min	--
	70:30	1ml/ min	2.83	Sharp	15.08	Tailing	18.15	broad	31.54	Broad
	75:25	1ml/ min	2.83	Sharp	14.23	Tailing	16.47	Bifurc ated	29.55	Broad
	80:20	1ml/ min	2.88	Tailing	13.70	Tailing	15.23	Bifurc ated	28.21	Broad
	90:10	1ml/ min	2.89	Broad	12.23	Tailing	14.22	Bifurc ated	25.13	Tailing
Methanol: Phosphate buffer pH-4.5	75:25	1ml/ min	2.63	Sharp	15.51	Tailing	20.12	Broad	35.01	Tailing
	80:20	1ml/ min	2.87	Sharp	13.73	Tailing	18.24	Broad	34.15	Broad
	90:10	1ml/ min	2.89	Tailing	13.17	Tailing	17.56	Tailin g	33.87	Broad
Acetonitrile: Phosphate buffer pH-3	60:40	1ml/min	4.01	Sharp	13.27	Merged with DIC peak	13.98	Merged with ATV peak	34.23	sharp
	70:30	1ml/min	2.52	Sharp	12.83	Broad	14.86	Sharp	32.01	Sharp

Table 8.1b: Optimization of HPLC method.

Column - Phenomenex Luna C18 column (150 mm × 4.6 mm i.d, 5-µm)										
Mobile phase	**Ratio**	**Flow Rate ml/min**	**CHZ**		**ATV**		**DIC**		**EFV**	
			RT min	**Peak shape**	**RT min**	**Peak Shape**	**RT min**	**Peak Shape**	**RT min**	**Peak Shape**
Methanol: Ammonium Formate (20mM)	55:45	1	3.10	Sharp	7.12	Broad	8.57	Broad	12.24	Sharp
	60:40	1	2.19	Tailing	6.48	Merged with DIC peak	6.31	Merged with ATV peak	7.13	Broad
ACN: Ammonium Formate	50:50	1	2.88	Tailing	6.23	Tailing	14.10	Broad	18.01	Broad
	55:45	1	3.1	tailing	3.99	Sharp	8.17	Tailing	10.98	Broad
	60:40	1	2.89	tailing	4.89	Tailing	6.10	Broad	5.28	Sharp
	40:60	1	5.11	Sharp	No peak upto 25min	--	No peak upto 25min	--	6.5	Sharp
ACN:Ammonium Formate 0.1% FA	50:50	0.8	2.63	Sharp	15.51	Tailing	20.12	Broad	35.01	Tailing
	55:45	0.8	3.51	Sharp	4.16	Sharp	8.37	Broad	11.62	Broad
	60:40	0.8	3.43	Tailing	5.89	Tailing	7.56	Merged with EFV peak	8.12	Merged with DIC peak
	40:60	0.8	6.5	Sharp	No peak upto 25min	--	No peak upto 25min	--	7.21	Sharp
ACN:Ammonium Formate 0.1% FA column oven 35°C	55:45	0.8	3.6	Sharp	7.21	Sharp	8.40	Sharp	11.74	Sharp
	52:48	**0.8**	**4.08**	**Sharp**	**9.76**	**Sharp**	**10.89**	**Sharp**	**15.58**	**Sharp**
	60:40	0.8	3.43	Sharp	5.89	Sharp	7.56	Merged with EFV peak	8.08	Merged with DIC peak
ACN:Ammonium Formate 0.1% FA column oven 30°C	52:48	0.8	5.18	Sharp	10.55	Sharp	11.38	Sharp	16.41	Sharp

Selection of Internal Standard (IS): To select a suitable internal standard for the analysis, eight drug substances, viz. Metaxolone, Ofloxacin, Valsartan, GLM, Lamivudine, Nevirapine, Atenolol, and Enalapril, were examined (Figure 8.1(a-h)). During the determination of the suitable candidates for **the internal standard**, it was found that the peaks of atenolol and enalapril did not appear when injected, by using the developed HPLC condition. Metaxolone and Ofloxacin peak coeluted with the solvent front while Nevirapine showed a relatively long retention time of 26 min. Valsartan's peak coeluted with ATV as it appeared at 9.65 min, which is very close to ATVs retention time. Similarly lamivudine's peak coeluted with CHZ as it appeared at 3.55 min, which is very close to CHZ's retention time. Therefore, GLM was selected as the internal standard of choice because its peak did not coelute with the solvent front of CHZ, ATV, DIC, EFV's peak. Furthermore, it showed an acceptable retention time (12.58 min) and a symmetrical peak. Among these, GLM 40 mcg/ml, (Figure 8.1h) met all the typical requirements of a compound to be used as an IS, i.e. it was stable during the analysis, readily available, was well resolved from CHZ, ATV, DIC, EFV, its peak shape was good (tailing factor at 230 nm 1.25, tailing factor at 247 nm 1.20), and its elution time (12.58 min) was shorter than that of last eluting analyte peak, EFV (15.58 min) saving run time per sample.

Higher column temperatures tend to lower mobile phase viscosities, which is desirable because a lower systemic pressure is produced. This will allow a lower linear velocity for the chromatographic system and produce a sharper peak. The heat will also provide some kinetic energy to the samples to propel them faster within the column, thereby decreasing the total analytical time. A column temperature of 35 °C was finally selected because it gave a faster retention time without compromising the peak area A higher temperature than this was not tested in order to preserve column life since high temperatures may be detrimental to the columns packing when used over time.

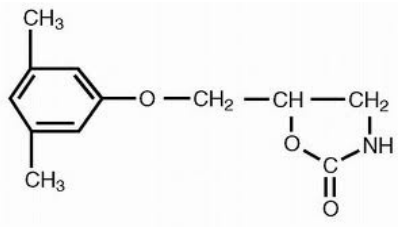

a. Metaxolone

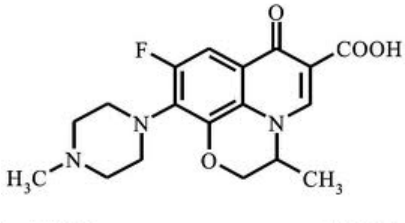

b. Ofloxacin

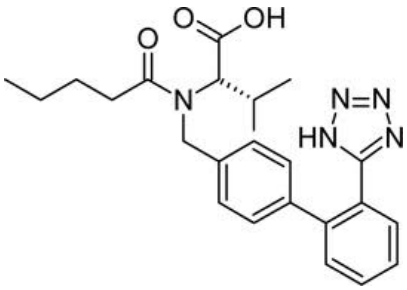

c. Valsartan

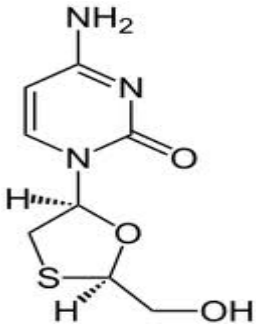

d. Lamivudine

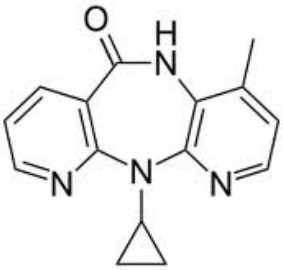

e. Nevirapine

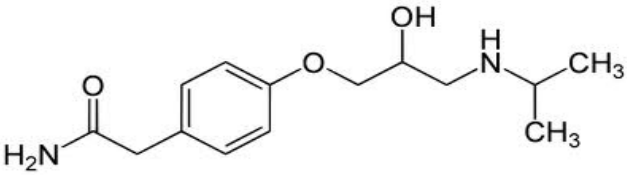

f. Atenolol

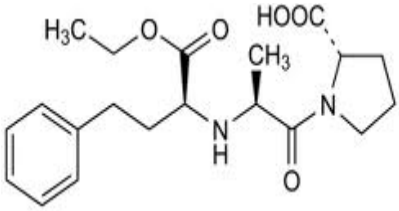

g. Enalapril

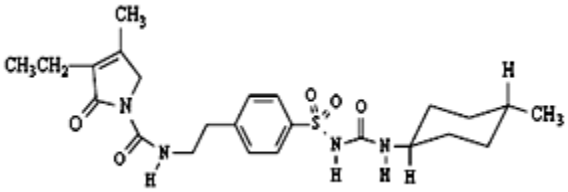

h.Glimepiride

Figure 8.1. Structures of Internal standards.

Increased flow rates tend to shorten retention time, but at the same time may contribute to band broadening and a decrease in the columns efficiency. Flow rates of 0.8 mL/min produced significantly larger peak areas than 1.0 mL/min did, hence was chosen as sharp and intense peaks were obatined.

Formic acid was used as a **volatile modifier** in the mobile phase to provide an acidic pH. In this experiment, formic acid (0.1%) was added because it decreased the band-broadening effect and ultimately improved chromatographic separation efficiency of structurally related compounds in a mixture.

The use of a **Photodiode UV detector (PDA)** is advantageous as it allows for the viewing and selection of wavelengths in real time. The sensitivity of HPLC method that uses UV detection depends upon proper selection of detection wavelength. An ideal wavelength is the one that gives good response for the drugs that are to be detected. From our analyses, we found that a broad-spectrum range such as 190-400 nm tends to be suitable for the analysis of probe substrates. In the present study individual drugs solutions of 20 µM of CHZ, ATV, DIC, EFV into an incubation mixture were injected into the HPLC system and the detection wavelength was selected from the spectra obtained from the PDA detector. Hence CHZ and DIC were analyzed at 230 nm while ATV and EFV were analyzed at 247 nm with appreciable signal intensities.

8.2.3 Result & discussion of method development:

Various columns were tried but Phenomenex C_{18} (150mm X 4.6 mm i.d., 5 µm particle size) column showed better resolution. Quantitation of CHZ and DIC was achieved at 230 nm while ATV and EFV were analyzed at 247 nm.. To optimize the HPLC parameters, several mobile phase compositions with different column and different flow rate were tried. Various buffers e.g. Potassium phosphate buffer, Ammonium formate buffer and formic acid at different pH with different composition of ACN and MeOH were tried. After trying various mobile phase as described in Table 8.1b. Finally, the mobile phase ACN: Ammonium Formate (0.1% FA):: 52:48 (%v/v) was selected because it was found to ideally resolve all the substrate and metabolite peaks.(Figure 8.4j & 8.4l).

The studies suggested that a mobile phase at acidic pH value might favor the peak shape of GLM on column to achieve a reasonable retention and resolution.

Table 8.2: Optimized HPLC parameters.

Column	Phenomenex C_{18} (150mm X 4.6mm i.d., 5µm particle size)
Mobile Phase	ACN: Ammonium Formate (0.1% FA):: 52:48 (%v/v)
Flow rate	0.8 ml/min
Internal standard	Glimepiride
Retention time (substrates)	4.08 min for CHZ, 9.76 min for ATV, 10.89 min for DIC, 15.58 min for EFV, 12.58 min for GLM.
Retention time (metabolites)	2.58 min for CHZ(M_1), 4.8 min for DIC(M_2), 7.9 min for ATV(M_3), 8.6 min for EFV (M_4).
Detector - Detection Wavelength	PDA Detector - 230 nm for CHZ and DIC - 247nm for ATV and EFV
Needle wash	ACN: Ammonium Formate (0.1% FA) (52:48)
Column Temperature	35°C

8.3 METHOD VALIDATION

The method validation assays were carried out according to the currently accepted U.S. Food and Drug Administration (FDA) bioanalytical method validation guidance.

8.3.1 Linearity and Range:

A standard mixture of 591/89.5/337/317µM CHZ/ATV/DIC/EFV was prepared by appropriately diluting 3.17/ 3.37/ 5.9/ 0.895mM individual standard with methanol. The standard mixture was used as a stock to prepare calibration standards (n=2) by spiking the analyte working solution into an incubation mixture with CHZ ranging from 19.7 to 157.6 µM, ATV ranging from 5.97 to 47.73µM, DIC ranging from 11.23 to 89.86µM and

EFV ranging from 10.56 to 84.53 μM. To each of these samples 40 μg/ml GLM as internal standard was added. Linear regression plots of peak-area ratios of CHZ/ATV/DIC/EFV to GLM versus concentration of CHZ/ATV/DIC/EFV were constructed as shown in Figure 8.2(a-d).

Quality control (QC) samples were prepared at low, medium and high concentrations of 19.7/5.96/11.23/10.56, 78.85/23.86/44.39/42.26 and 137.9/41.76/78.63/73.96 μM, for CHZ/ATV/DIC/EFV respectively.

The working solutions (200μL) for calibration and quality control contained the same components as for incubation except microsomal protein. The samples were incubated at 37 °C for 10 min without NADPH, followed by addition of 100 μL acetonitrile and NADPH to make the same exact matrix as from real microsomal incubations. The samples were centrifuged at 10,000 rpm (4°C; 10min), and aliquots of the supernatant (20μL) were directly injected into an HPLC system.

Table 8.3a: Linearity data for CHZ.

CHZ added (µL)	CHZ (µg/ml)	CHZ (µM)	Peak area CHZ	Peak area GLM (IS)	*Peak area of CHZ / Peak area of GLM
10	3.33	**19.7**	104614	539921	**0.194±0.08**
20	6.66	**39.4**	258157	540521	**0.478±0.23**
30	10	**59.1**	401014	532921	**0.752±0.36**
40	13.33	**78.85**	552132	542859	**1.017±0.87**
50	16.66	**98.5**	712955	539989	**1.320±0.91**
60	20	**118.2**	842767	541881	**1.555±0.98**
70	23.33	**137.9**	989677	540935	**1.830±0.56**
80	26.66	**157.6**	1109062	529921	**2.093±0.87**

*Average of two determinations

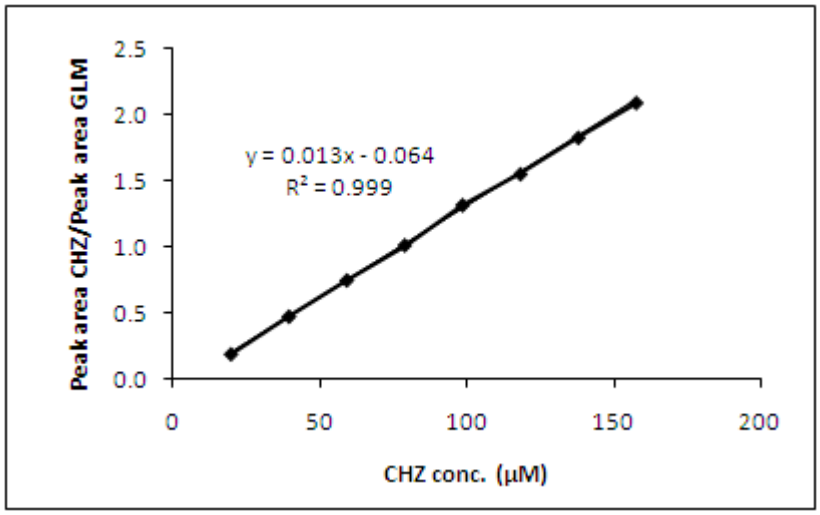

Figure 8.2a. Linearity plot of CHZ.

Table 8.3b: Linearity data for CHZ.

ATV added (µL)	ATV (µg/ml)	ATV (µM)	Peak area ATV	Peak area GLM (IS)	*Peak area of ATV / Peak area of GLM
10	3.33	**5.966**	305175	215168	**1.418±0.25**
20	6.66	**11.933**	748837	209687	**3.571±0.23**
30	10	**17.9**	1134338	216520	**5.239±0.91**
40	13.33	**23.86**	1565517	209915	**7.458±1.23**
50	16.66	**29.83**	2040393	211148	**9.663±0.62**
60	20	**35.8**	2411515	209428	**11.515±0.36**
70	23.33	**41.76**	2882685	215080	**13.403±0.55**
80	26.66	**47.73**	3284226	215964	**15.207±0.84**

*Average of two determinations

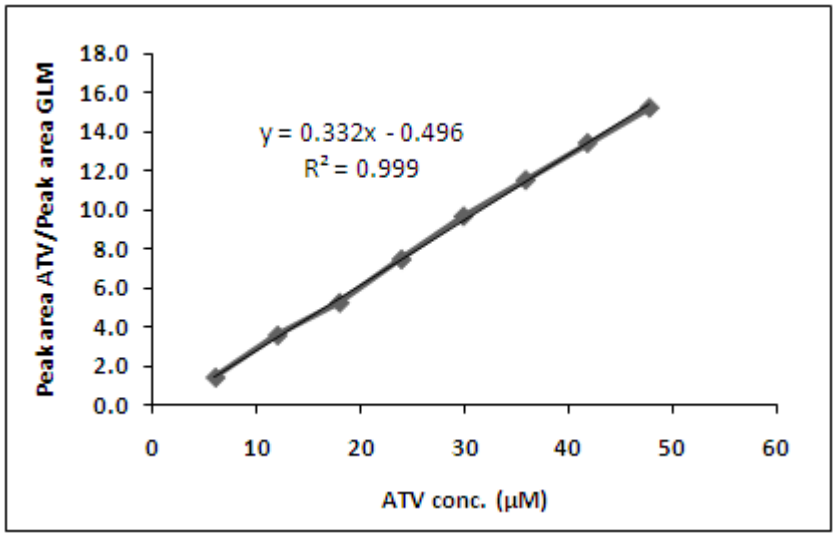

Figure 8.2b. Linearity plot of ATV

Table 8.3c: Linearity data for DIC

DIC added (µL)	DIC (µg/ml)	DIC (µM)	Peak area DIC	Peak area GLM (IS)	*Peak area of DIC / Peak area of GLM
10	3.33	**11.23**	145949	539921	**0.270±0.09**
20	6.66	**22.46**	358028	540521	**0.662±0.23**
30	10	**33.7**	542605	532921	**1.018±0.56**
40	13.33	**44.93**	758028	542859	**1.396±0.42**
50	16.66	**56.16**	992004	539989	**1.837±1.02**
60	20	**67.4**	1184883	541881	**2.187±0.25**
70	23.33	**78.63**	1389969	540935	**2.570±0.39**
80	26.66	**89.86**	1545037	529921	**2.916±0.87**

*Average of two determinations

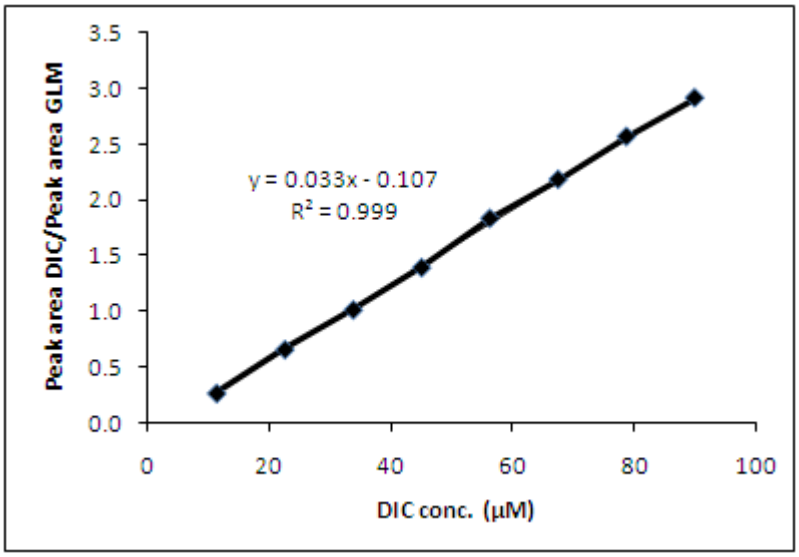

Figure 8.2c. Linearity plot of DIC

Table 8.4d: Linearity data for EFV

EFV added (µL)	EFV (µg/ml)	EFV (µM)	Peak area EFV	Peak area GLM (IS)	*Peak area of EFV / Peak area of GLM
10	3.33	**10.56**	195193	215168	**0.907±0.12**
20	6.66	**21.13**	485343	209687	**2.315±1.21**
30	10	**31.7**	742308	216520	**3.428±0.56**
40	13.33	**42.26**	986102	209915	**4.698±0.63**
50	16.66	**52.03**	1300541	211148	**6.159±0.88**
60	20	**63.4**	1582816	209428	**7.558±0.97**
70	23.33	**73.96**	1908621	215080	**8.874±1.23**
80	26.66	**84.53**	2153863	215964	**9.973±1.19**

*Average of two determinations

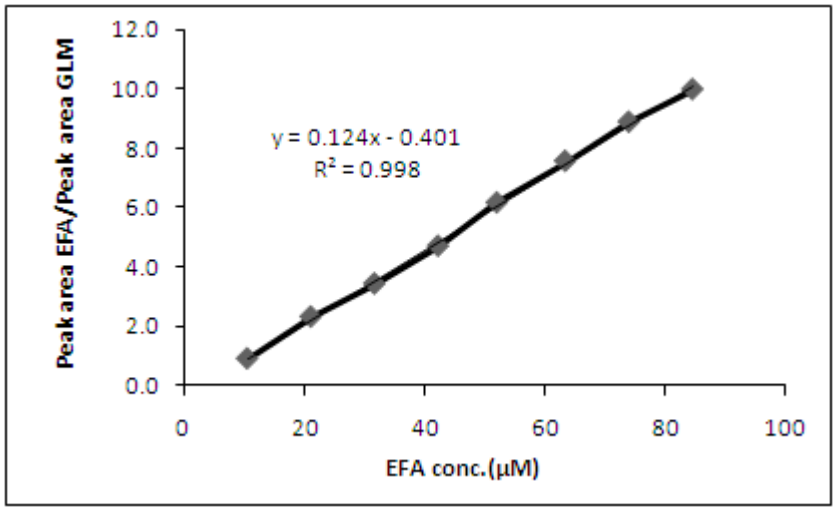

Figure 8.2d. Linearity plot of EFV

8.3.2 Accuracy

The ***accuracy*** of an analytical method describes the closeness of mean test results obtained by the method to the true value (concentration) of the analyte. The accuracy of the method was confirmed by recovery study analyzing the QC samples of CHZ/ATV/DIC/EFV at three concentrations (low, medium, and high) for five replicates on the same day.

8.3.3 Precision:

Precision was determined by repeated analyses of the group of standards on one batch (n =5). The assays for both intra- and inter-day precision were performed by using the three QC samples of GLM (5, 50 and 100 µM). Precision was calculated according to Relative Standard Deviation (RSD). The acceptable intraday and interday precision was set at ± 15%. The experiment was repeated 5 times in a day for Intra-day precision and on 3 different days for inter-day precision. The values confirm the precision of the method.

Table 8.4a: Intra-day precision for estimation of CHZ.

CHZ (µM)	**Peak area of CHZ / Peak area of GLM**					**MEAN**	**S.D ±**	**%RSD**
	Set 1	Set 2	Set 3	Set 4	Set 5			
19.7	0.198	0.210	0.20	0.208	0.21	0.203	0.009	4.219
78.85	1.05	0.99	1.1	0.98	0.98	1.002	0.079	7.903
137.9	1.79	1.85	1.82	1.84	1.84	1.868	0.099	5.291
						Average	0.062	5.804

Table 8.4b: Intra-day precision for estimation of ATV.

ATV (µM)	Peak area of ATV / Peak area of GLM					MEAN	S.D ±	%RSD
	Set 1	Set 2	Set 3	Set 4	Set 5			
5.96	1.21	1.16	1.08	1.39	1.15	1.198	0.117	9.759
23.86	7.45	7.55	7.58	7.18	6.95	7.342	0.270	3.677
41.76	13.40	12.86	12.54	12.95	13.21	12.992	0.331	2.545
						Average	0.239	5.327

Table 8.4c: Intra-day precision for estimation of DIC.

DIC (µM)	Peak area of DIC / Peak area of GLM					MEAN	S.D ±	%RSD
	Set 1	Set 2	Set 3	Set 4	Set 5			
11.23	0.27	0.35	0.31	0.24	0.30	0.288	0.022	7.528
44.39	1.41	1.38	1.50	1.45	1.42	1.432	0.045	3.177
78.63	2.58	2.63	2.65	2.58	2.60	2.608	0.031	1.194
						Average	0.032	3.966

Table 8.4d: Intra-day precision for estimation of EFV.

EFV (µM)	Peak area of EFV / Peak area of GLM					MEAN	S.D ±	%RSD
	Set 1	Set 2	Set 3	Set 4	Set 5			
10.56	0.90	0.98	0.87	0.83	0.91	0.898	0.055	6.170
42.26	4.69	4.55	4.58	4.62	4.63	4.614	0.053	1.153
73.96	8.87	8.85	8.81	8.79	8.79	8.822	0.036	0.412
						Average	0.048	2.578

Table 8.5a: Inter-day precision for estimation of CHZ (day 1)

CHZ (µM)	Peak area of CHZ / Peak area of GLM					MEAN	S.D ±	%RSD
	Set 1	Set 2	Set 3	Set 4	Set 5			
19.7	0.198	0.210	0.20	0.208	0.21	0.205	0.006	2.808
78.85	1.05	0.99	1.1	0.98	0.98	1.020	0.053	5.234
137.9	1.79	1.85	1.82	1.84	1.84	1.828	0.024	1.306
						Average	0.027	3.116

Table 8.5b: Inter-day precision for estimation of CHZ (day 2)

CHZ (µM)	Peak area of CHZ / Peak area of GLM					MEAN	S.D ±	%RSD
	Set 1	Set 2	Set 3	Set 4	Set 5			
19.7	0.18	0.22	0.24	0.22	0.23	0.218	0.023	10.460
78.85	1.08	0.97	1.05	0.95	0.98	1.006	0.056	5.561
137.9	1.97	1.85	1.75	1.83	1.84	1.848	0.079	4.268
						Average	0.052	6.763

Table 8.5c: Inter-day precision for estimation of CHZ (day 3)

CHZ (µM)	Peak area of CHZ / Peak area of GLM					MEAN	S.D ±	%RSD
	Set 1	Set 2	Set 3	Set 4	Set 5			
19.7	0.19	0.21	0.24	0.23	0.23	0.220	0.020	9.091
78.85	1.10	0.99	1.12	1.08	0.98	1.054	0.065	6.134
137.9	1.83	1.85	1.88	1.87	1.84	1.854	0.021	1.118
						Average	0.035	5.447

Table 8.6a: Inter-day precision for estimation of ATV (day 1)

ATV (µM)	Peak area of ATV / Peak area of GLM					MEAN	S.D ±	%RSD
	Set 1	Set 2	Set 3	Set 4	Set 5			
5.96	1.21	1.16	1.08	1.39	1.15	1.198	0.117	9.759
23.86	7.45	7.55	7.58	7.18	6.95	7.342	0.270	3.677
41.76	13.40	12.86	12.54	12.95	13.21	12.992	0.331	2.545
						Average	0.239	5.327

Table 8.6b: Inter-day precision for estimation of ATV (day 2)

ATV (µM)	Peak area of ATV / Peak area of GLM					MEAN	S.D ±	%RSD
	Set 1	Set 2	Set 3	Set 4	Set 5			
5.96	1.20	1.19	1.10	1.28	1.20	1.194	0.064	5.350
23.86	6.98	7.32	7.23	7.18	6.95	7.132	0.161	2.255
41.76	13.10	12.76	12.56	12.43	12.95	12.760	0.274	2.148
						Average	0.166	3.251

Table 8.6c: Inter-day precision for estimation of ATV (day 3)

ATV (µM)	Peak area of ATV / Peak area of GLM					MEAN	S.D ±	%RSD
	Set 1	Set 2	Set 3	Set 4	Set 5			
5.96	1.11	1.16	1.18	1.24	1.15	1.168	0.048	4.079
23.86	7.41	7.25	7.38	7.08	7.22	7.268	0.133	1.829
41.76	12.40	12.66	12.54	12.55	12.87	12.604	0.175	1.389
						Average	0.118	2.432

Table 8.7a: Inter-day precision for estimation of DIC (day 1)

DIC (µM)	Peak area of DIC / Peak area of GLM					MEAN	S.D ±	%RSD
	Set 1	Set 2	Set 3	Set 4	Set 5			
11.23	0.27	0.35	0.31	0.24	0.30	0.288	0.022	7.528
44.39	1.41	1.38	1.50	1.45	1.42	1.432	0.045	3.177
78.63	2.58	2.63	2.65	2.58	2.60	2.608	0.031	1.194
						Average	0.032	3.966

Table 8.7b: Inter-day precision for estimation of DIC (day 2)

DIC (µM)	Peak area of DIC / Peak area of GLM					MEAN	S.D ±	%RSD
	Set 1	Set 2	Set 3	Set 4	Set 5			
11.23	0.25	0.25	0.28	0.30	0.30	0.276	0.025	9.094
44.39	1.44	1.56	1.50	1.45	1.42	1.474	0.056	3.826
78.63	2.58	2.53	2.70	2.68	2.63	2.624	0.070	2.676
						Average	0.050	5.198

Table 8.7c: Inter-day precision for estimation of DIC (day 3)

DIC (µM)	Peak area of DIC / Peak area of GLM					MEAN	S.D ±	%RSD
	Set 1	Set 2	Set 3	Set 4	Set 5			
11.23	0.28	0.29	0.31	0.23	0.27	0.276	0.030	10.748
44.39	1.42	1.48	1.51	1.45	1.45	1.462	0.034	2.340
78.63	2.57	2.61	2.62	2.59	2.60	2.598	0.019	0.740
						Average	0.027	4.603

Table 8.8a: Intra-day precision for estimation of EFV(day 1)

EFV (µM)	Peak area of EFV / Peak area of GLM					MEAN	S.D ±	%RSD
	Set 1	Set 2	Set 3	Set 4	Set 5			
10.56	0.90	0.98	0.87	0.83	0.91	0.898	0.055	6.170
42.26	4.69	4.55	4.58	4.62	4.63	4.614	0.053	1.153
73.96	8.87	8.85	8.81	8.79	8.79	8.822	0.036	0.412
						Average	0.048	2.578

Table 8.8b: Intra-day precision for estimation of EFV (day 2)

EFV (µM)	Peak area of EFV / Peak area of GLM					MEAN	S.D ±	%RSD
	Set 1	Set 2	Set 3	Set 4	Set 5			
10.56	0.92	0.96	0.88	0.84	0.91	0.902	0.045	4.983
42.26	4.33	4.56	4.58	4.39	4.43	4.458	0.108	2.434
73.96	8.78	8.69	8.56	8.54	8.79	8.672	0.118	1.363
						Average	0.090	2.926

Table 8.8c: Intra-day precision for estimation of EFV (day 3)

EFV (µM)	Peak area of EFV / Peak area of GLM					MEAN	S.D ±	%RSD
	Set 1	Set 2	Set 3	Set 4	Set 5			
10.56	0.95	0.98	0.88	0.88	0.90	0.918	0.045	4.896
42.26	4.68	4.59	4.52	4.62	4.52	4.586	0.068	1.492
73.96	8.55	8.45	8.63	8.79	8.59	8.602	0.125	1.448
Average							0.079	2.612

8.3.4 LLOD and LLOQ

The lower limit of detection (LLOD) and the LLOQ were determined as the concentrations at signal-to-noise ratios of 3 and 10, respectively. Calibration curve was repeated for 3 times and the standard deviation (SD) of the intercepts was calculated. Then LOD and LOQ were measured as follows.

LLOD=3.3 * SD/slope of calibration curve

LLOQ=10 * SD/slope of calibration curve

SD = Standard deviation of intercepts

The values of LOD and LOQ are given in **Table 8.9.**

Table 8.9. LLOD and LLOQ data

Parameter	CHZ (µM)	ATV (µM)	DIC (µM)	EFV (µM)
SD	± 1.80	±2.5	±0.89	±1.45
LLOD(µM)	1.10	0.92	0.88	0.54
LLOQ(µM)	1.98	1.85	1.28	1.25

8.3.5 SPECIFICITY: The **specificity** was investigated by analyzing blank incubation medium and comparing the potential interferences at the LC peak region for each analyte of CHZ/ATV/DIC/EFV and GLM (IS), each in duplicate.

The specificity of the HPLC method was illustrated by the complete separation of metabolites of CHZ(M_1)/ATV(M_2)/DIC(M_3)/EFV(M_4) from CHZ/ATV/DIC/EFV cocktail incubations. Typical chromatograms obtained following the *in vitro* incubation procedure are shown in Figure 8.4(a-l). The resolution factor (*R*s) from *in vitro* metabolism product was above 2.0, which ensured complete separation of metabolite from its substrates as predicted by the purity plots (Fig. 8.3a-e).

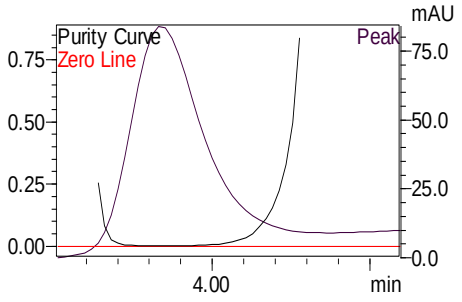

a. Peak purity plot of CHZ at 3.92 min

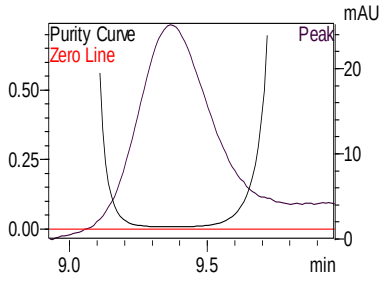

b. Peak purity plot of ATV at 9.43 min

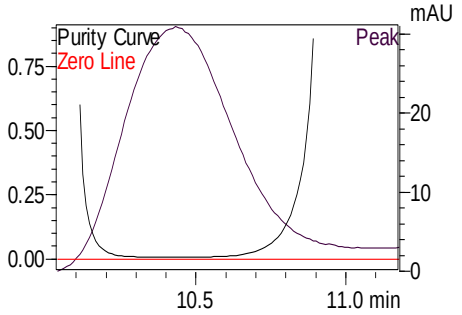

c. Peak purity plot of DIC at 10.56 min

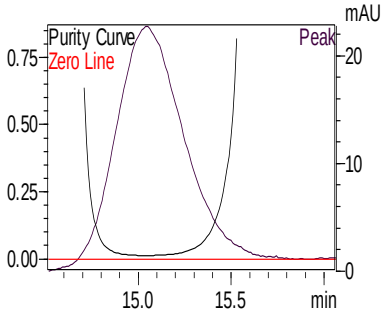

d. Peak purity plot of EFA at 15.09 min

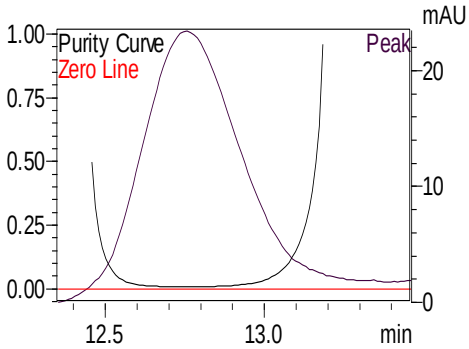

e. Peak purity plot of GLM at 12.83 min

Figure 8.3(a-e) Peak purity plots

8.3.6 Stability:

Freeze and thaw stability: QC microsomes samples at three concentration levels were stored at the storage temperature (−70°C) for 24 h and thawed unassisted at room temperature. When completely thawed, the samples were refrozen for 24 h under the same conditions. The freeze–thaw cycles were repeated twice, and the samples were analyzed after three freeze (−70°C)-thaw (room temperature) cycles;

Short-term temperature stability: QC samples at three concentration levels were kept at room temperature for a period that exceeded the routine preparation time of the samples (around 6 h)

Long-term stability: QC samples at three concentration levels kept at low temperature (−70°C) were studied for a period of one week.

Table 8.10a: Data showing stability in HLM for CHZ (n=2)

QC samples CHZ (µM)	Freeze and thaw stability	Short term stability	Long term stability
19.7	96.5 ± 2.6	98.56 ± 2.1	110.0 ± 2.8
78.85	100.25 ± 1.5	99.63 ± 1.5	105.5 ± 2.4
137.9	98.56 ± 3.2	99.54 ± 1.8	102.4 ± 1.7
Mean	98.43667±2.43	98.910±1.8	105.966±2.3

Table 8.10b: Data showing stability in HLM for ATV (n=2)

QC samples ATV (µM)	Freeze and thaw stability	Short term stability	Long term stability
5.96	97.5 ± 4.6	98.52 ± 1.1	109 ± 3.8
23.86	102.25 ± 1.9	98.63 ± 1.9	98.2 ± 2.2
41.76	98.56 ± 1.8	100.44 ± 2.1	99.4 ± 3.7
Mean	99.436±2.766	99.196±1.7	102.343±3.23

Table 8.10c: Data showing stability in HLM for DIC (n=2)

QC samples DIC (µM)	Freeze and thaw stability	Short term stability	Long term stability
11.23	97.20 ± 4.2	99.56 ± 2.1	106 ± 4.4
44.39	98.43 ± 1.5	97.63 ± 2.5	107.5 ± 3.5
78.63	99.65 ± 3.2	101.54 ± 1.9	109.4 ± 3.7
Mean	98.426±2.966	99.576±2.166	107.63±3.866

Table 8.10d: Data showing stability in HLM for EFV (n=2)

QC samples EFV (µM)	Freeze and thaw stability	Short term stability	Long term stability
10.56	95.4 ± 5.2	98.33 ± 1.2	109 ± 5.8
42.26	100.23 ± 2.1	99.63 ± 1.1	106.5 ± 1.3
73.96	98.76 ± 2.6	102 ± 1.4	102.4 ± 2.8
Mean	97.963±3.3	99.986±1.23	105.96±3.3

8.3.7 System suitability test: Used in determination of instrument performance (e.g., sensitivity and chromatographic retention) by analysis of a reference standard prior to running the analytical batch. System suitability test provide the added assurance that on a specific occasion the method is giving, accurate and precise results. Following parameters were calculated for system suitability of HPLC method.

Table 8.11: System suitability parameters

Parameters	CHZ (µM)	M_1	ATV (µM)	M_2	DIC (µM)	M_3	EFV (µM)	M_4	GLM	
Wavelength (nm)	230	230	247	247	230	230	247	247	230	247
Retention Time (min)	3.99	2.58	9.76	7.92	10.89	4.81	15.58	8.62	13.28	13.28
Theoretical plates per meter± RSD	7622.66	4214.194	6797.575	6936.115	6732.178	5009.014	7692.77	6936.115	8344.215	7654.23
Capacity factor *k'*	2.523	1.983	3.094	2.011	1.862	1.998	2.848	2.009	3.962	2.412
Symmetry factor/Tailing factor *T*	1.599	0.807	1.363	1.363	1.298	1.427	1.303	1.236	1.251	1.195
Resolution *Rs*	2.697	----	4.001	9.013	2.382	3.449	3.678	3.968	4.277	3.864

8.3.8 Analyte recovery from microsomal matrix

Recovery experiments were performed by comparing the analytical results for extracted samples at three concentrations (low, medium, and high) with unextracted standards that represent 100% recovery. The recovery of analytes from the incubation medium was obtained by calculating the ratio of the peak areas of the standard at QC levels and 40 µg/ml IS relative to the peak areas in potassium phosphate buffer. The microsomal matrix contained the same components (i.e., protein, NADPH, $MgCl_2$ and phosphate buffer, etc.) at the concentrations used for incubation. The average recovery was 94.23% for CHZ, 96.43% for ATV, 94.03% for DIC, and 96.24% for EFV.

Table 8.12: Recovery studies

Sr. No.	QC levels (µM)				*Amt found(µM)				*Recovery (%)			
	CHZ	**ATV**	**DIC**	**EFA**	**CHZ**	**ATV**	**DIC**	**EFA**	**CHZ**	**ATV**	**DIC**	**EFA**
1	19.7	5.96	11.23	10.56	18.8	5.99	10.23	9.44	95.43	100.50	91.10	93.18
2	78.85	23.86	44.39	42.26	75.47	21.87	41.58	41.74	95.71	91.66	93.67	98.77
3	137.9	41.76	78.63	73.96	126.25	40.56	76.52	71.56	91.55	97.13	97.32	96.76
Mean									94.23	96.43	94.03	96.24
± SD									2.33	4.46	3.13	2.82

* Average of two determinations

Table 8.13: Summary of validation parameters

Sr.	Parameters	CHZ	ATV	DIC	EFV
1	Wavelength Nm	230	247	230	247
2	Retention time (substrates)	4.08 min	9.76 min	10.89 min	15.58 min
3	Retention time (metabolites)	2.58 min	4.8 min	7.9 min	8.6 min
4	Linearity range µM	19.70-157.6	5.96-41.73	1.23-89.86	10.56-84.53
5	Accuracy	94.23±2.33	96.43±4.46	94.03±3.13	96.24±2.82
6	Intraday Precision	5.804±0.062	5.327±0.239	3.966±0.032	2.578±0.048
7	Interday Precision	5.108±0.038	3.67±0.16	4.589±0.036	2.703±0.072
8	Regression Equation Intercept Slope Correction coefficient	0.013 0.064 0.999	0.332 0.496 0.999	0.033 0.107 0.999	0.124 0.401 0.998
9	LLOD (µg mL)	1.10	0.92	0.88	0.54
10	LLOQ (µg /mL)	1.98	1.85	1.28	1.25
11	Stability Freeze and thaw stability Short term stability Long term stability	98.43667±2.43 98.910±1.8 105.966±2.3	98.56 ± 1.8 100.44 ± 2.1 99.4 ± 3.7	98.426±2.966 99.576±2.166 107.63±3.866	97.963±3.3 99.986±1.23 105.96±3.3
12	Impurity	Not detected	Not detected	Not detected	Not detected
13	Peak purity	1.00000	0.999991	1.00000	1.00000

8.4 *IN VITRO* METABOLISM OF P450 PROBE SUBSTRATE USING HLM

8.4.1. Protein and Time Curves (Reaction linearity optimization)

The effects of HLM concentration and incubation time were examined by constructing the protein and time curves. A series of concentrations of HLM (0.5 – 1 mg/ml) were incubated with CHZ (final concentration 50 µM), ATV (final concentration 20 µM), DIC (final concentration 50 Mm) and EFV (final concentration 50 µM) at 37 ºC to construct protein curves. Meanwhile, 0.5 mg/ml of HLM were incubated with CHZ (final concentration 50 µM), ATV (final concentration 20 µM), DIC (final concentration 50 µM) and EFV (final concentration 50 µM) at 37ºC for various periods (10 – 60 minutes) to create time curves. Briefly the incubation mixtures consisted of 50mM phosphate buffer (pH 7.4), 10 mM $MgCl_2$, 1 mM EDTA, 1 mM NADPH and 0.5 – 1 mg/ml of microsomal protein. In all experiments, CHZ, ATV, DIC and EFV were dissolved and diluted serially in methanol and then alcohol was removed by evaporating to dryness. The substrates were reconstituted in potassium phosphate buffer (50 mM, pH 7.4) .The tubes were placed into an ice bath and 5 µl of HLM was added and vortexed. Tubes (duplicate) containing the reaction mixture in phosphate buffer and NADPH solution were allowed to equilibrate separately in a shaker incubator at 150 rpm for 5 minutes at 37°C. The reaction was initiated by adding 20 µl of NADPH immediately to the tubes and incubation carried out for for various periods (10 – 60 minutes). The reaction was terminated by the addition of 100 µl ice cold acetonitrile containing GLM as internal standard.

Table 8.14a: Data for reaction linearity plot of CHZ at *0.5mg/ml HLM*

Incubation time (min)	Area of CHZ	Area of GLM(IS)	Area of CHZ/ Area of IS	*Cu_{min}=Au*Cs/As	% Drug remaining	% Drug depleted
0	228157	539987	0.423	50	100	0
10	225123	542759	0.415	49.083	98.166	1.834
30	219741	541205	0.406	48.047	96.095	3.905
60	210852	540986	0.390	46.122	92.245	7.755

*Average of two determinations

Table 8.14b: Data for reaction linearity plot of ATV at *0.5mg/ml HLM*

Incubation time (min)	Area of ATV	Area of GLM(IS)	Area of ATV/ Area of IS	*Cu_{min}=Au*Cs/As	% Drug remaining	% Drug depleted
0	768837	215168	3.573	10	100	0
10	767912	220175	3.488	9.761	97.608	2.392
30	724824	214326	3.382	9.465	94.646	5.354
60	712525	214326	3.324	9.304	93.040	6.960

*Average of two determinations

Table 8.14c: Data for reaction linearity plot of DIC at *0.5mg/ml HLM*

Incubation time (min)	Area of DIC	Area of GLM(IS)	Area of DIC/ Area of IS	*Cu_{min}=Au*Cs/As	% Drug remaining	% Drug depleted
0	454419	539987	0.842	50	100	0
10	433211	542859	0.798	47.4143	94.8286	5.1714
30	421004	541205	0.778	46.2191	92.4381	7.5619
60	418691	538786	0.777	46.1715	92.3430	7.6570

*Average of two determinations

Table 8.14d: Data for reaction linearity plot of EFV at *0.5mg/ml HLM*

Incubation time (min)	Area of EFV	Area of GLM(IS)	Area of EFV/ Area of IS	*Cu_{min}=Au*Cs/As	% Drug remaining	% Drug depleted
0	215193	215168	1.000	20	100	0
10	198876	209875	0.948	18.950	94.748	5.252
30	190786	218787	0.872	17.438	87.192	12.808
60	181234	209954	0.863	17.262	86.311	13.689

*Average of two determinations

Table 8.15a: Data for reaction linearity plot of CHZ at *1 mg/ml HLM*

	Area of CHZ	Area of GLM(IS)	Area of CHZ/ Area of IS	*Cu_{min}=Au*Cs/As	% Drug remaining	% Drug depleted
0	228157	539987	0.423	50	100	0
10	220823	541859	0.408	48.2256	96.4512	3.5488
30	212459	543205	0.391	46.2840	92.5680	7.4320
60	210155	539786	0.389	46.0721	92.1441	7.8559

*Average of two determinations

Table 8.15b: Data for reaction linearity plot of ATV at *1 mg/ml HLM*

Incubation time (min)	Area of ATV	Area of GLM(IS)	Area of ATV/ Area of IS	*Cu_{min}=Au*Cs/As	% Drug remaining	% Drug depleted
0	768837	212168	3.624	10	100	0
10	745912	209875	3.554	9.808	98.078	1.922
30	715814	218787	3.272	9.029	90.287	9.713
60	711455	209954	3.389	9.351	93.512	6.488

*Average of two determinations

Table 8.15c: Data for reaction linearity plot of DIC at *1 mg/ml HLM*

Incubation time (min)	Area of DIC	Area of GLM(IS)	Area of DIC/ Area of IS	*Cu_{min}=Au*Cs/As	% Drug remaining	% Drug depleted
0	454419	539987	0.842	50	100	0
10	413211	542859	0.761	45.225	90.451	9.549
30	401004	541205	0.741	44.023	88.047	11.953
60	398691	538786	0.740	43.966	87.932	12.068

*Average of two determinations

Table 8.15d: Data for reaction linearity plot of EFV at *1 mg/ml HLM*

Incubation time (min)	Area of EFV	Area of GLM(IS)	Area of EFV/ Area of IS	*Cu_{min}=Au*Cs/As	% Drug remaining	% Drug depleted
0	215193	215168	1.000	20	100	0
10	185776	209875	0.885	17.701	88.507	11.493
30	182782	218787	0.835	16.707	83.534	16.466
60	178234	209954	0.849	16.976	84.882	15.118

*Average of two determinations

8.4.2. Detection of metabolite (M_1, M_2, M_3, M_4)

Control incubations were carried out without HLM, NADPH to confirm metabolism. Wherever necessary the volume was made up to 200 µl with buffer. **Figures 8.4(a-h)** suggest that NADPH as a cofactor is necessary for HLM to carry out the *in vitro* metabolism of CHZ, ATV, DIC and EFV respectively. Addition of NADPH to the incubation medium generates metabolite M_1 at 2.58 min for CHZ, M_2 at 4.8 min for DIC, M_3 at 7.9 min for ATV, M_4 at 8.6 min for EFV suggesting that the substrates undergo *in*

vitro hydroxylation. **Figure 8.4(i-l)** shows cocktail incubation at 230nm and 247nm in presence and absence of M_1, M_2, M_3, M_4.

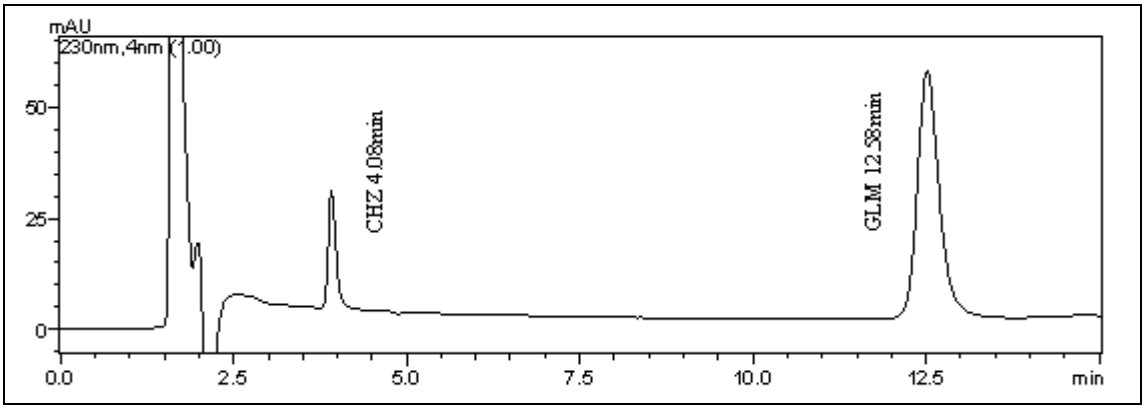

Figure 8.4a. CHZ in NADPH free incubation medium (with HLM)

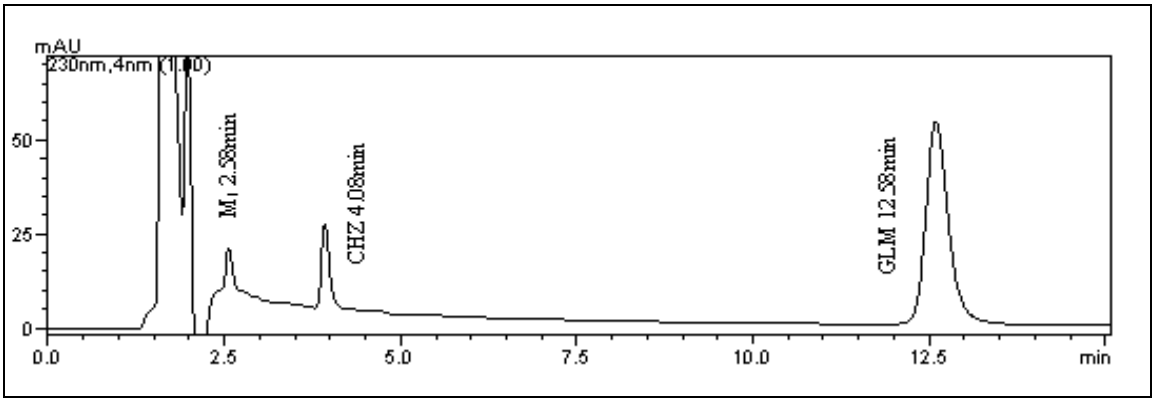

Figure 8.4b. CHZ in microsomal incubation medium (with HLM & NADPH)

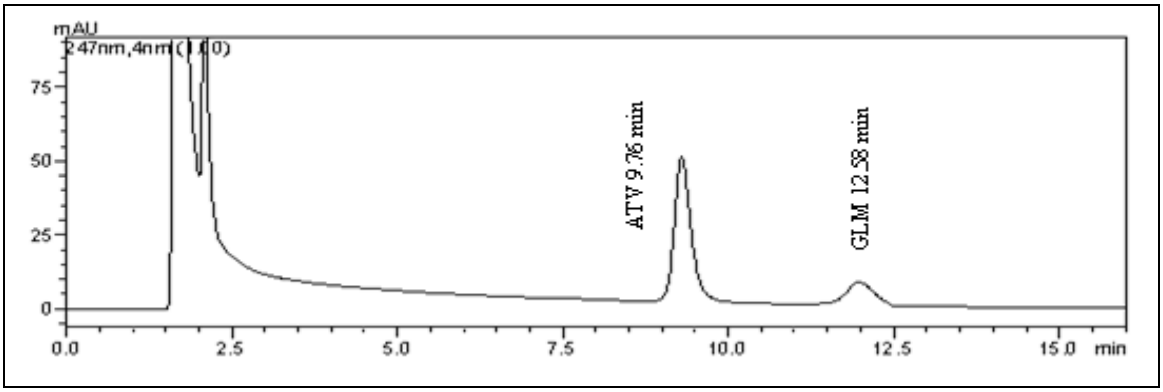

Figure 8.4c. ATV in NADPH free incubation medium (with HLM)

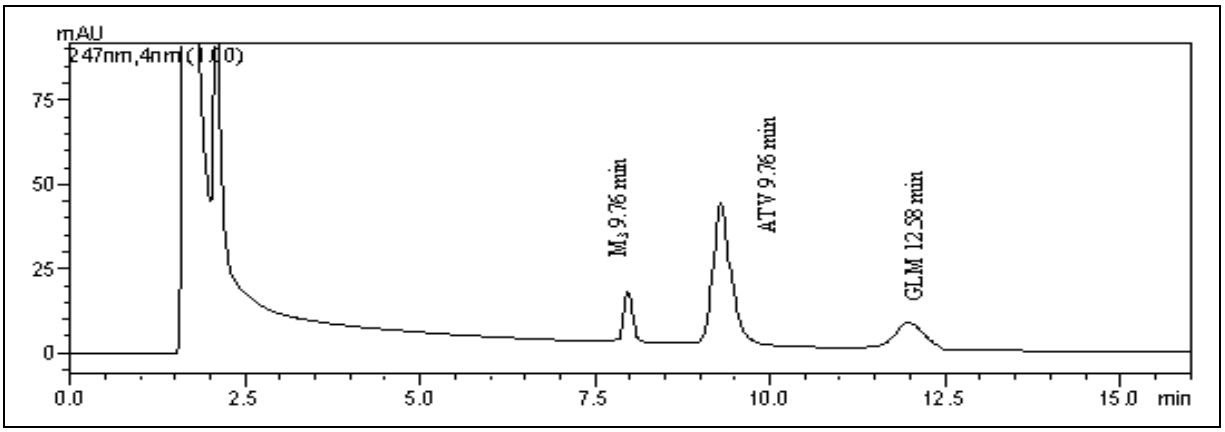

Figure 8.4d. ATV in microsomal incubation medium (with HLM & NADPH)

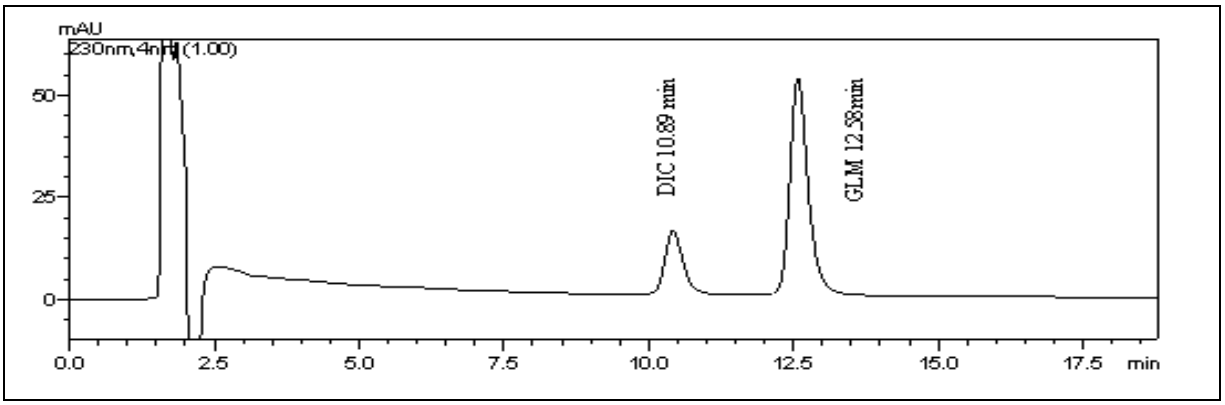

Figure 8.4e. DIC in NADPH free incubation medium (with HLM)

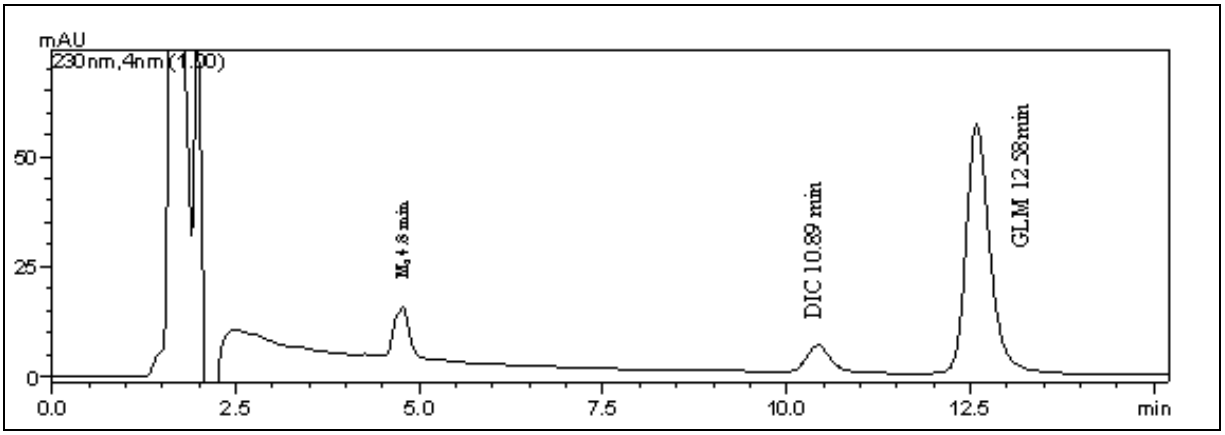

Figure 8.4f. DIC in microsomal incubation medium (with HLM & NADPH)

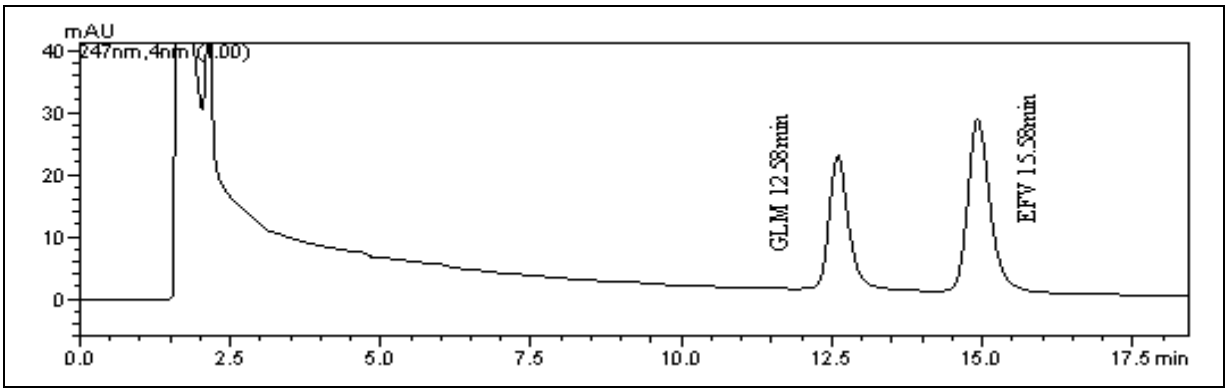

Figure 8.4g. EFV in NADPH free incubation medium (with HLM)

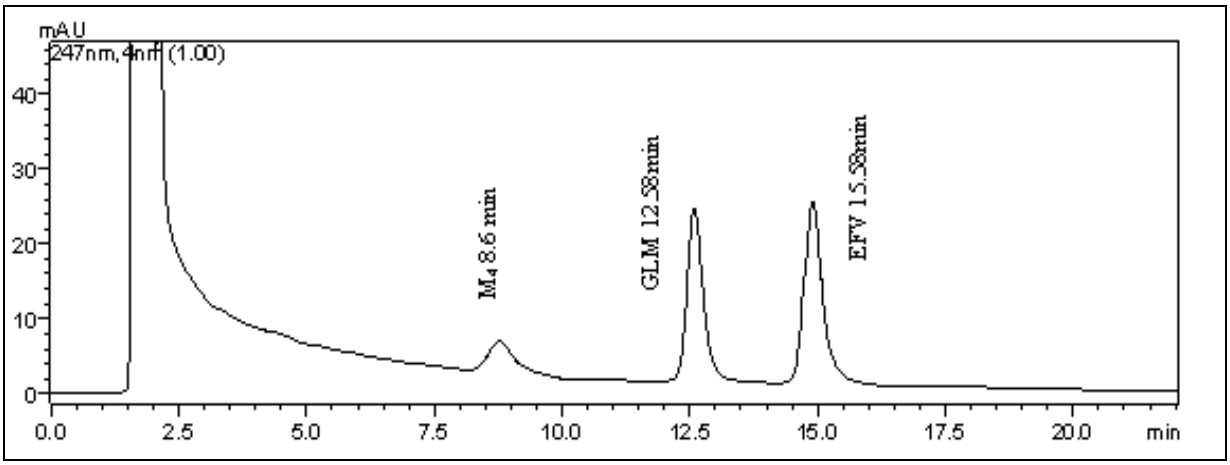

Figure 8.4h. EFV in microsomal incubation medium (with HLM & NADPH)

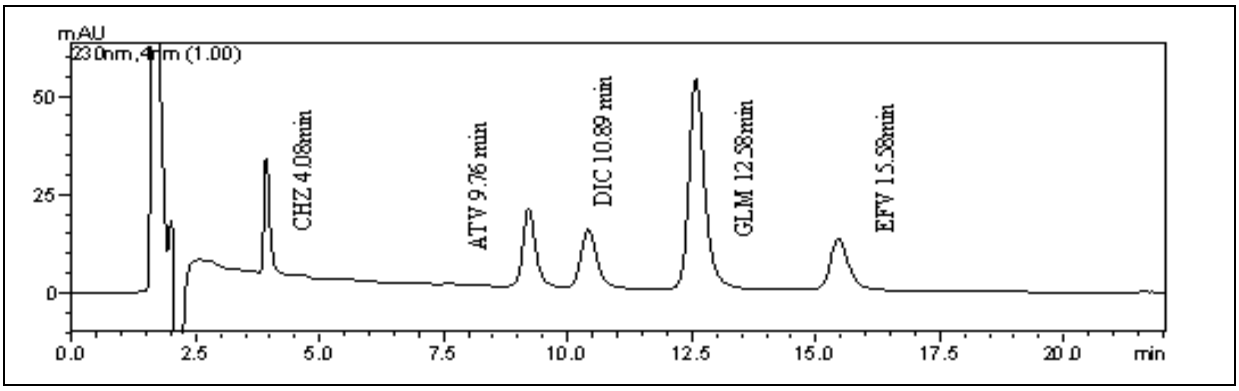

Figure 8.4i. HPLC chromatogram of cocktail incubation of CHZ, ATV, DIC and EFV at 230nm.

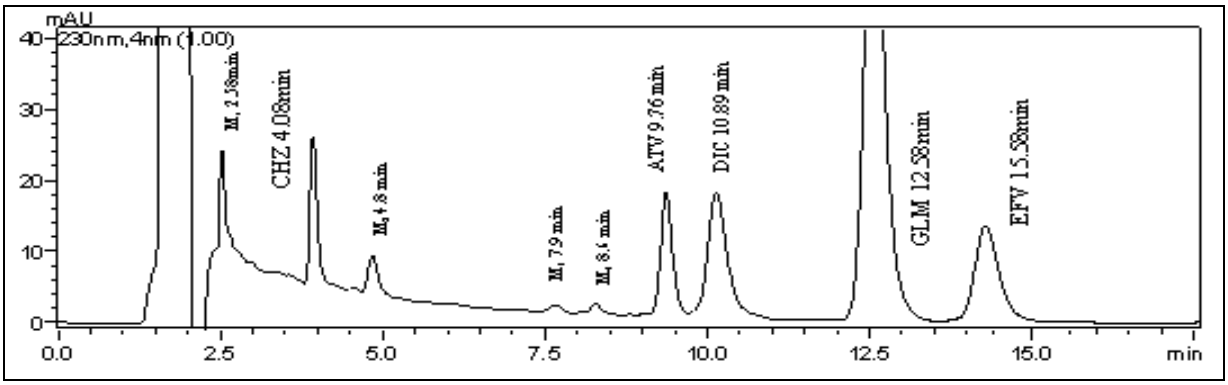

Figure 8.4j. HPLC chromatogram of cocktail incubation of CHZ, ATV, DIC and EFV and their respective metabolites M_1, M_2, M_3, M_4 at 230nm.

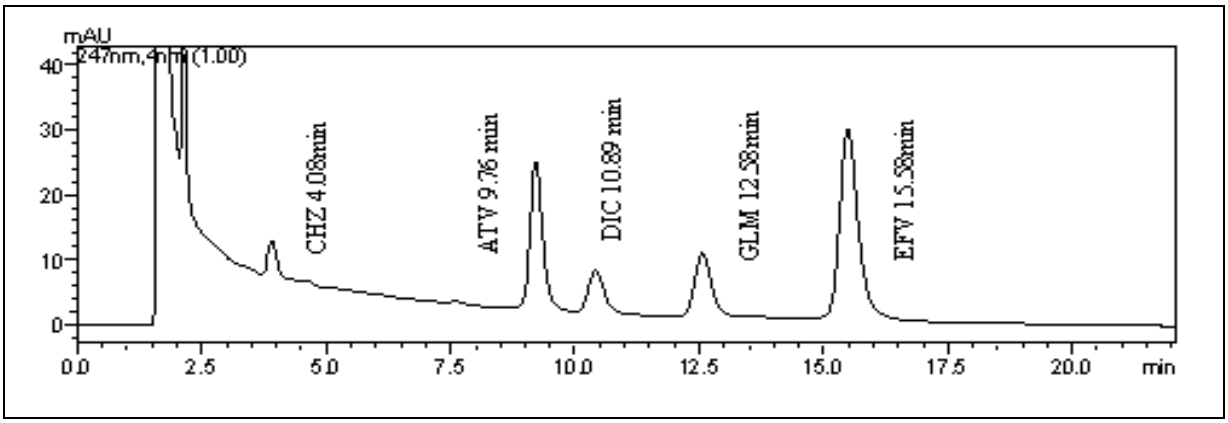

Figure 8.4k. HPLC chromatogram of cocktail incubation of CHZ, ATV, DIC and EFV at 247nm.

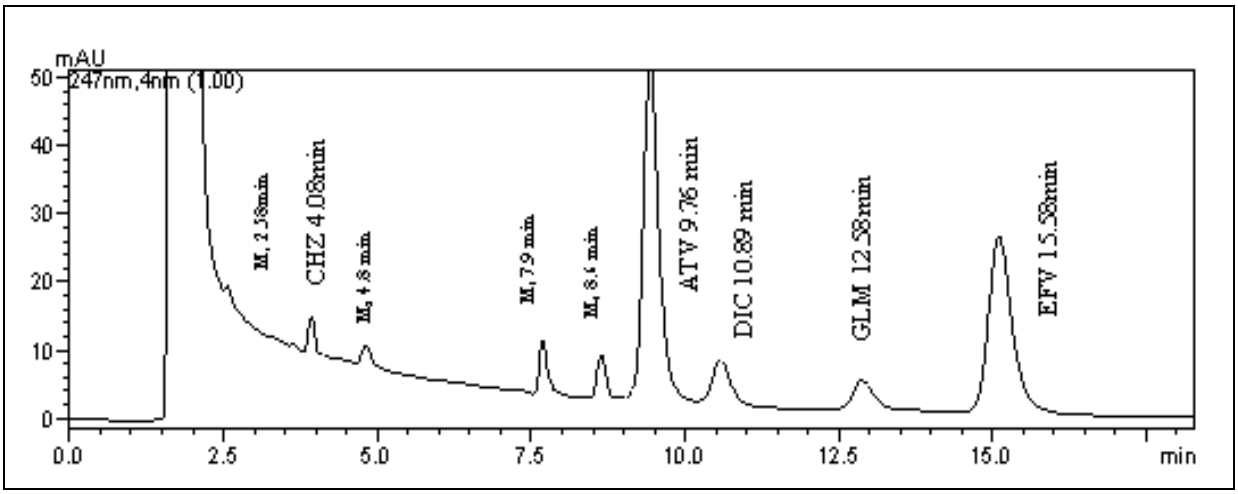

Figure 8.4l. HPLC chromatogram of cocktail incubation of CHZ, ATV, DIC and EFV and their respective metabolites M_1, M_2, M_3, M_4 at 247nm.

8.4.3 Determination of K_m and V_{max} for P450 probe substrate by nonlinear and linear transformations

Preliminary experiments showed that the substrate depletion was linear with respect to incubation time over 30 min and liver microsomal protein concentration of 0.5 mg/ml at 37°C. Kinetic studies were performed by incubating eight concentrations of probe substrate CHZ/ATV/DIC/EFV (5-150 µMole) in duplicate with HLM. For the determination of the apparent Michaelis-Menten constant (K_m) and the maximal velocity of the reaction (V_{max}), plots in relation to the substrate concentration were derived using Graph Pad Prism 5 software. Incubations were performed by incubating HLM with each individual probe substrates alone (Table 8.16(a-d)) and with probe substrates cocktail (Table 8.17(a-d)) to determine whether the cocktail and individual incubations would yield similar results.

Table 8.16a: Michaelis-Menten kinetics data for CHZ *in vitro* incubation with HLM (Individual incubation)

Substrate conc. Cs (µM)	Area of CHZ/ Area of IS 0 min As	Area of CHZ/ Area of IS 30 min Au	Cu_{30min}= Au*Cs/As	$C=Cs_{0min}-Cu_{30min}$	*C/30min/0.5 (µM/min/mg protein)
5	0.068	0.065	4.755	0.245	0.016
10	0.093	0.089	9.577	0.423	0.028
15	0.124	0.118	14.283	0.717	0.048
20	0.166	0.158	19.041	0.959	0.064
50	0.421	0.407	48.337	1.663	0.111
75	0.951	0.926	72.998	2.002	0.133
100	1.386	1.353	97.579	2.421	0.161
150	1.791	1.760	147.457	2.543	0.170

*Average of two experiments

Table 8.16b: Michaelis-Menten kinetics data for ATV *in vitro* incubation with HLM (Individual incubation)

Substrate conc. Cs (µM)	Area of ATV/ Area of IS 0 min As	Area of ATV/ Area of IS 30 min Au	Cu_{30min}= Au*Cs/As	$C=Cs_{0min}-Cu_{30min}$	*C/30min/0.5 (µM/min/mg protein)
5	1.418	1.312	4.625	0.375	0.025
10	3.527	3.230	9.158	0.842	0.056
15	4.507	4.079	13.574	1.426	0.095
20	6.163	5.499	17.845	2.155	0.144
50	15.257	14.135	46.322	3.678	0.245
75	22.830	21.650	71.124	3.876	0.258
100	30.471	29.018	95.233	4.767	0.318
150	45.022	43.430	144.694	5.306	0.354

*Average of two experiments

Table 8.16c: Michaelis-Menten kinetics data for DIC *in vitro* incubation with HLM (Individual incubation)

Substrate conc. Cs (µM)	Area Of DIC/ Area of IS 0 min As	Area of DIC/ Area of IS 30 min Au	Cu_{30min}= Au*Cs/As	$C=Cs_{0min}-Cu_{30min}$	*C/30min/0.5 (µM/min/mg protein)
5	0.223	0.207	4.636	0.364	0.024
10	0.269	0.241	8.970	1.030	0.069
15	0.481	0.411	12.824	2.176	0.145
20	0.663	0.571	17.218	2.782	0.185
50	0.837	0.766	45.734	4.266	0.284
75	2.389	2.214	69.509	5.491	0.366
100	2.944	2.762	93.847	6.153	0.410
150	3.621	3.450	142.908	7.092	0.473

*Average of two experiments

Table 8.16d: Michaelis-Menten kinetics data for EFV *in vitro* incubation with HLM (Individual incubation)

Substrate conc. Cs (µM)	Area of EFV/ Area of IS 0 min As	Area of EFV/ Area of IS 30 min Au	Cu_{30min}= Au*Cs/As	$C=Cs_{0min}-Cu_{30min}$	*C/30min/0.5 (µM/min/mg protein)
5	0.769	0.740	4.807	0.193	0.013
10	0.907	0.839	9.245	0.755	0.050
15	1.216	1.073	13.232	1.768	0.118
20	3.375	2.878	17.056	2.944	0.196
50	4.604	4.168	45.270	4.730	0.315
75	5.980	5.552	69.637	5.363	0.358
100	8.776	8.219	93.655	6.345	0.423
150	13.668	13.030	142.999	7.001	0.467

*Average of two experiments

Table 8.17a: Michaelis-Menten kinetics data for CHZ *in vitro* incubation with HLM (cocktail incubation)

Substrate conc. Cs (µM)	Area of CHZ/ Area of IS 0 min As	Area of CHZ/ Area of IS 30 min Au	Cu_{30min}= Au*Cs/As	$C=Cs_{0min}-Cu_{30min}$	*C/30min/0.5 (µM/min/mg protein)
5	0.065	0.063	4.832	0.168	0.011
10	0.091	0.087	9.533	0.467	0.031
15	0.122	0.116	14.272	0.728	0.049
20	0.163	0.155	19.028	0.972	0.065
50	0.437	0.411	47.019	2.981	0.199
75	0.961	0.923	71.984	3.016	0.201
100	1.336	1.276	95.526	4.474	0.298
150	1.754	1.708	146.071	3.929	0.262

*Average of two experiments

Table 8.17b: Michaelis-Menten kinetics data for ATV *in vitro* incubation with HLM (cocktail incubation)

Substrate conc. Cs (µM)	Area of ATV/ Area of IS 0 min As	Area of ATV/ Area of IS 30 min Au	Cu_{30min}= Au*Cs/As	$C=Cs_{0min} - Cu_{30min}$	*C/30min/0.5 (µM/min/mg protein)
5	1.444	1.344	4.653	0.347	0.023
10	3.549	3.259	9.182	0.818	0.055
15	4.450	4.034	13.601	1.399	0.093
20	6.396	5.722	17.894	2.106	0.140
50	16.213	14.973	46.177	3.823	0.255
75	22.182	20.980	70.936	4.064	0.271
100	31.202	29.725	95.266	4.734	0.316
150	44.522	42.998	144.866	5.134	0.342

*Average of two experiments

Table 8.17c: Michaelis-Menten kinetics data for DIC *in vitro* incubation with HLM (cocktail incubation)

Substrate conc. Cs (µM)	Area Of DIC/ Area of IS 0 min As	Area of DIC/ Area of IS 30 min Au	Cu_{30min}= Au*Cs/As	$C=Cs_{0min}-Cu_{30min}$	*C/30min/0.5 (µM/min/mg protein)
5	0.259	0.250	4.820	0.180	0.012
10	0.343	0.297	8.653	1.347	0.090
15	0.467	0.411	13.193	1.807	0.120
20	0.699	0.629	18.001	1.999	0.133
50	0.896	0.825	46.076	3.924	0.262
75	2.440	2.260	69.457	5.543	0.370
100	2.990	2.811	93.987	6.013	0.401
150	3.432	3.288	143.730	6.270	0.418

*Average of two experiments

Table 8.17d: Michaelis-Menten kinetics data for EFV *in vitro* incubation with HLM (cocktail incubation)

Substrate conc. Cs (µM)	Area of EFV/ Area of IS 0 min As	Area of EFV/ Area of IS 30 min Au	Cu_{30min}= Au*Cs/As	$C=Cs_{0min}-Cu_{30min}$	*C/30min/0.5 (µM/min/mg protein)
5	0.679	0.629	4.632	0.368	0.025
10	0.772	0.695	8.998	1.002	0.067
15	1.169	1.049	13.451	1.549	0.103
20	2.993	2.631	17.582	2.418	0.161
50	4.306	3.983	46.240	3.760	0.251
75	5.803	5.450	70.444	4.556	0.304
100	9.156	8.648	94.445	5.555	0.370
150	12.728	12.192	143.687	6.313	0.421

*Average of two experiments

8.4.4. Data Analysis

In the present study, the disappearance of CHZ, ATV, DIC and EFV in the medium incubated at 37°C with HLM in the presence of the NADPH was determined as the percentage of the initial amount of CHZ, ATV, DIC and EFV in the medium without incubation respectively. The obtained results were expressed as the turnover rate in percentage wherever necessary. Substrate disappearance velocity was calculated as [($C_{0,\ initial}$ - $C_{s,\ t\ min}$) / incubation time /CYP concentration], where $C_{0,\ initial}$ is the substrate concentration at time 0 min and $C_{s,\ t\ min}$ is the substrate concentration after 10, 30, 60 min incubation with 0.5 and 0.75mg/ml protein concentration. Metabolite formation velocity (V) was calculated as ($C_{s,\ t\ min}$ / incubation time / CYP concentration), where Cs, t min was the metabolite concentration after a 10, 30, 60 min incubation.

8.5. RESULTS

8.5.1 Reaction linearity optimization

Linearity of enzyme reactions in the *in vitro* human liver microsomal incubations was assessed by monitoring the effect of incubation time (from 10 to 60 min) and protein concentration (from 0.5 – 1 mg/ml) on metabolite formation of CHZ, ATV, DIC and EFV. Plots in relation to incubation time and HLM concentration were obtained to optimize the turnover of the candidate drugs within the limits of developed assay design such that all subsequent *in vitro* incubations can be performed using the condition that ensures linearity with time and HLM concentration, and less than 20% of the initial substrate is consumed. From figure 8.5(a-d) it is observed that enzyme reactions are linear with 0.5mg/ml HLM concentration and 30 minutes incubation time. Thus a microsomal protein concentration of 0.5 mg/ml and an incubation time of 30 min were chosen as the experimental conditions for assessment of CYP2B6, CYP2C9, CYP2E1 and CYP3A4 activities.

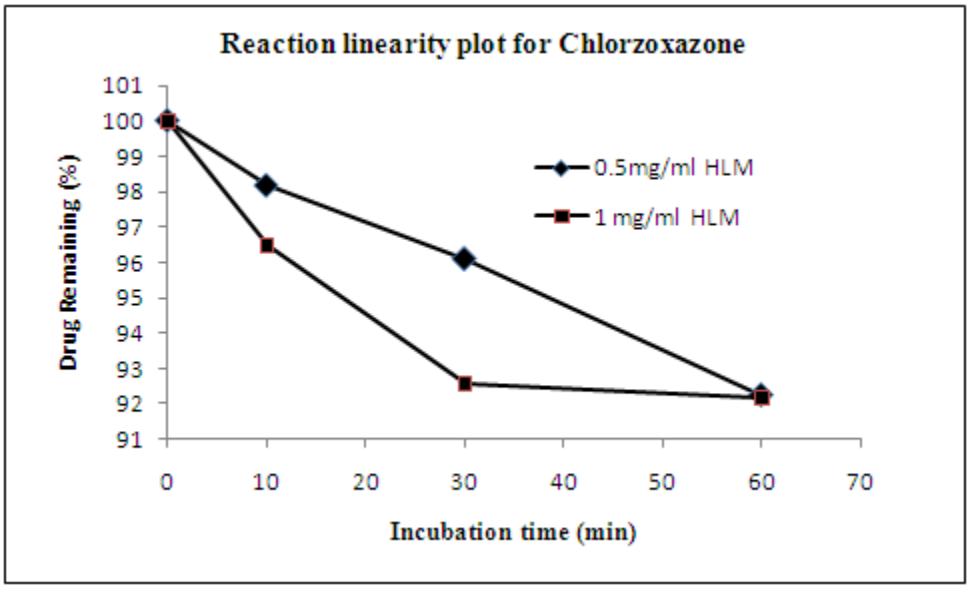

Figure 8.5a. Reaction linearity plot for CHZ.

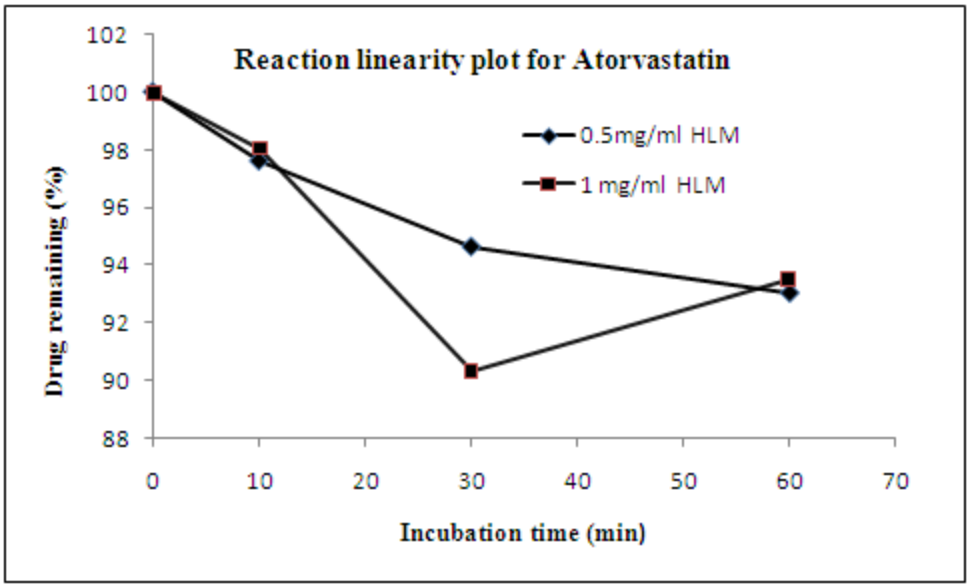

Figure 8.5b. Reaction linearity plot for ATV.

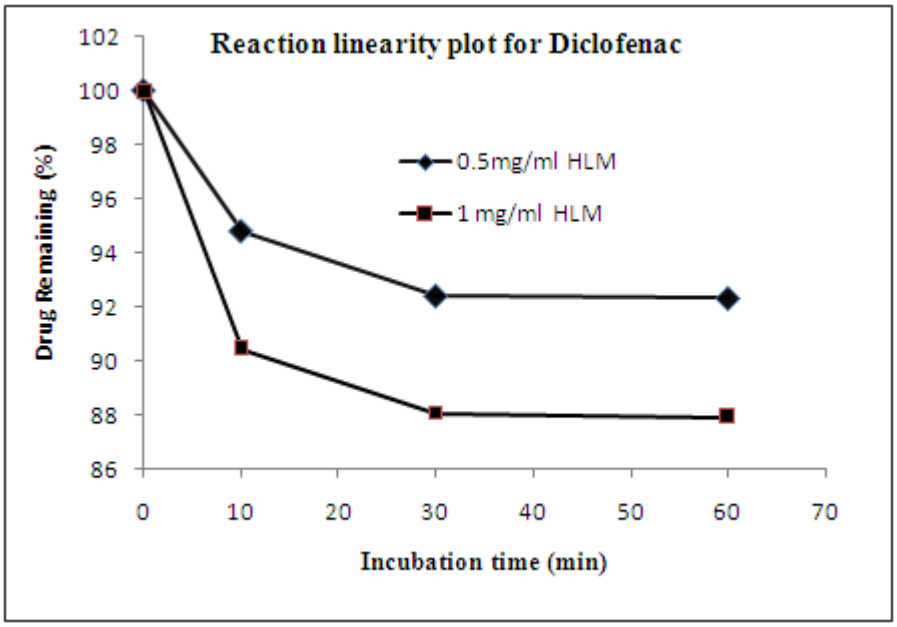

Figure 8.5c. Reaction linearity plot for DIC.

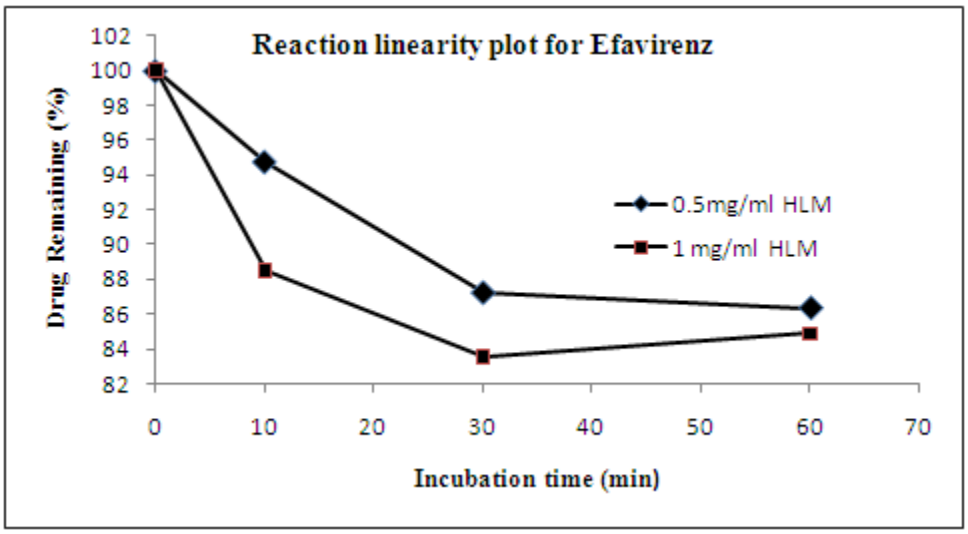

Figure 8.5d. Reaction linearity plot for EFV.

8.5.2. Determination of K_m and V_{max}

Once the optimal conditions (30 min incubation time, 0.5mg/ml HLM) were obtained, the substrate concentration dependence on the rate of metabolite formation was examined. The K_m and V_{max} values for CHZ/ATV/DIC/EFV in individual (Figure 8.6 (a-d)) and

cocktail incubations (Figure 8.7(a-d)) were obtained by nonlinear regression of a plot of enzyme activity versus substrate concentration as shown in Table 8.18. The Michaelis constant, K_m accounts for the concentration of substrate at which half the active sites are filled. Thus, K_m provides a measure of the substrate concentration required for significant catalysis to occur. V_{max} is the rate at which substrate will be converted to product once bound to the enzyme. A substrate concentration around or below the K_m is ideal for determination of competitive inhibitor activity.

Table 8.18. Michaelis Menten constant data (K_m & V_{max}) for CHZ/ATV/DIC/EFV.

Probe Substrates	Individual incubation		Cocktail incubation	
	K_m µMole	V_{max} µMole/min/mg protein	K_m µMole	V_{max} µMole/min/mg protein
CHZ	51.94± 2.15	0.200 ± 0.017	61.22±1.54	0.246±0.013
ATV	57.79 ± 1.09	0.492 ± 0.037	53.81±2.55	0.477±0.037
DIC	62.74 ± 3.45	0.669 ± 0.051	66.62±1.08	0.639±0.065
EFV	64.96 ± 1.19	0.683 ± 0.077	72.41±3.62	0.623±0.044

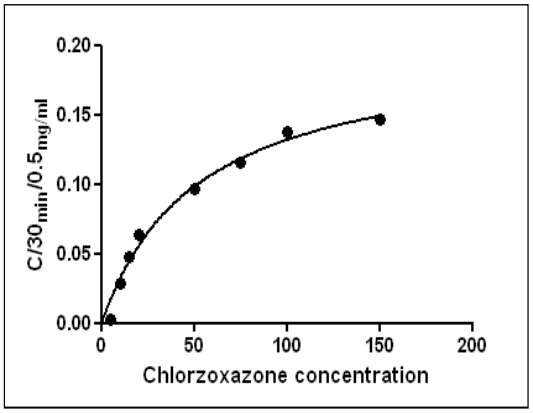

(a)

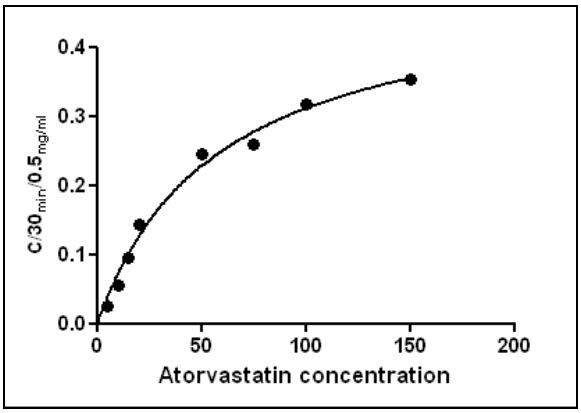

(b)

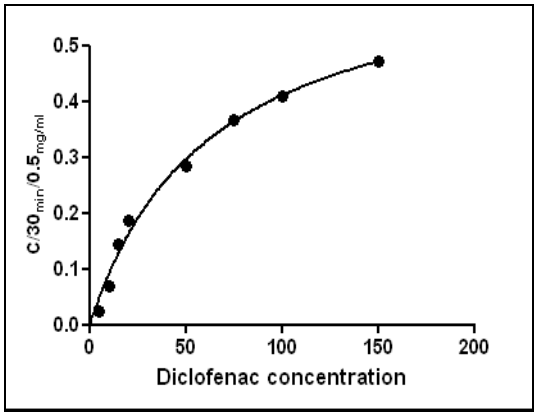

(c)

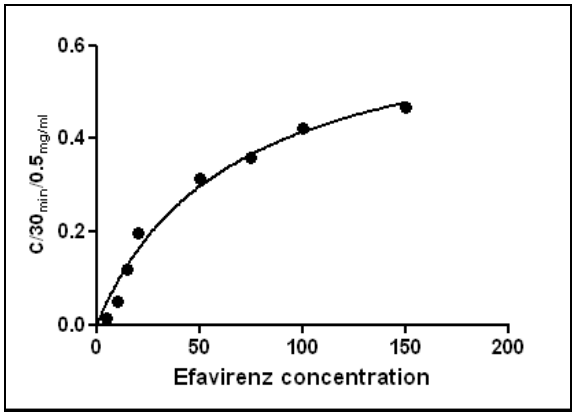

(d)

Figure 8.6(a-d). Michaelis menten plot for a) CHZ b) ATV c) DIC d)EFV with HLM (Individual incubation).

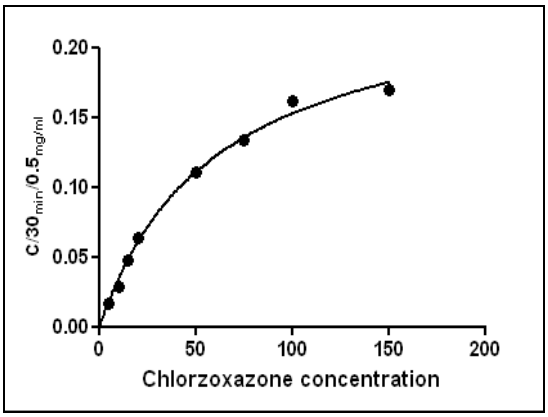

(a)

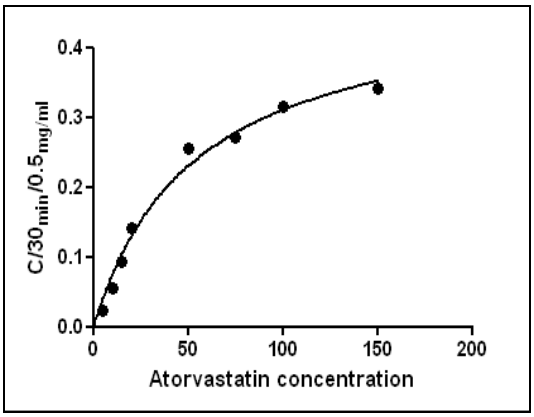

(b)

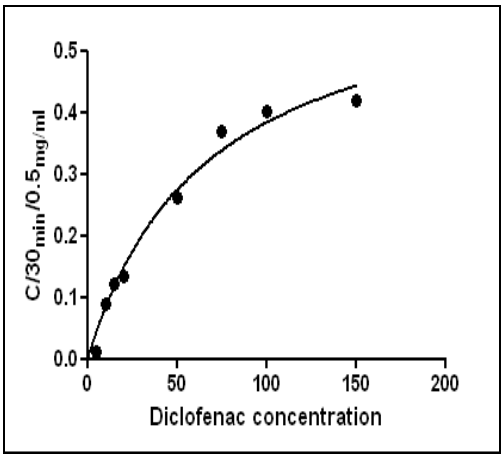

(c)

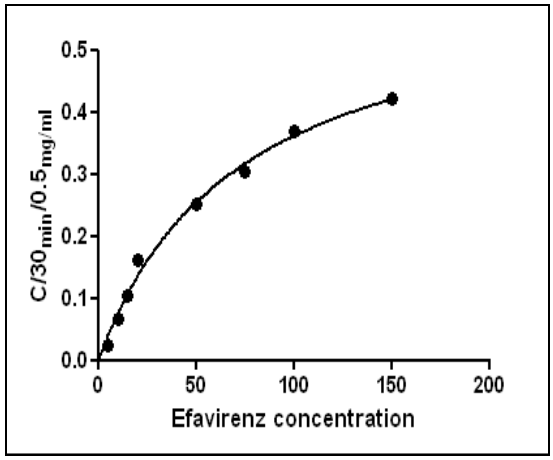

(d)

Figure 8.7(a-d). Michaelis menten plot for a) CHZ b) ATV c) DIC d) EFV with HLM (cocktail incubation).

8.6. DISCUSSION

The probes CHZ/ATV/DIC/EFV to be used in this cocktail approach were chosen based on their CYP specificity, availability and recommendations in regulatory guidance. The probe substrates selected were EFV (CYP2B6), DIC (CYP2C9), CHZ (CYPE1), ATV (CYP3A4). All the substrates were soluble in common solvent methanol and stable during the analysis i.e., no additional interacting peaks of probe substrate were observed in chromatograms after cocktail incubation. All the peaks of probe substrate 4.08 min for CHZ, 9.76 min for ATV, 10.89 min for DIC, 15.58 min for EFV and their respective metabolite M_1 at 2.58 min for CHZ, M_2 at 4.8 min for DIC, M_3 at 7.9 min for ATV, M_4 at 8.6 min for EFV were well resolved.GLM (Glimepiride 40 mcg/ml) was selected as the internal standard of choice as it met all the typical requirements of a compound to be used as an IS, i.e. it was stable during the analysis, readily available, was well resolved from CHZ, ATV, DIC, EFV, its peak shape was good (tailing factor at 230 nm 1.25, tailing factor at 247 nm 1.20), and its elution time (12.58 min) was shorter than that of last eluting analyte peak, EFV (15.58 min) saving run time per sample.

The method showed a linear calibration curve with correlation coefficients greater than 0.999 for the analytes in the investigated concentration range and absolute recoveries of all analytes were >90%. The acceptable intraday and interday precision were <15% relative standard deviation from nominal values. The lower limit of detection (LLOD) was 1.10 μM for CHZ, 0.92 μM for ATV, 0.88 μM for DIC, and 0.54 μM for EFA, respectively. The lower limit of quantitation (LLOQ) was 1.98 μM for CHZ, 1.85 μM for ATV, 1.28 μM for DIC, and 1.25 μM for EFA, respectively.

Linearity of enzyme reactions in the *in vitro* human liver microsomal incubations was assessed by monitoring the effect of incubation time (from 10 to 60 min) and protein concentration (from 0.5 – 1 mg/ml) on metabolite formation of CHZ, ATV, DIC and EFV. The enzyme reactions for assessment of CYP2B6, CYP2C9, CYP2E1 and CYP3A4 activities were linear with 0.5mg/ml HLM concentration and 30 minutes incubation time where less than 20% of the initial substrate was consumed.The K_m and V_{max} values of

CHZ/ATV/DIC/EFV determined using the substrate cocktail were in good agreement with individual substrates.

8.7. CONCLUSION

The developed isocratic LC/UV method has been shown to provide sufficient sensitivity and linear concentration range for the analysis of probe substrate and its metabolites with good resolution from *in vitro* individual incubations as well as cocktail incubations. Overall, the simultaneous development of cocktail substrate assay system for EFV (CYP2B6), DIC (CYP2C9), CHZ (CYPE1), ATV (CYP3A4) is simple, uses conventional instrumentation and provides a scope to analyse all cytochrome P450 combination sets continuously in a single run. Hence can be used to improve throughput and cost-effectiveness in preclinical drug studies. The application of the method allows for fast and simple assessment of any potential inhibition or induction effects drug candidates may have on the metabolism of specific CYP probe substrates. Due to these aspects of specificity, reproducibility and sensitivity, the method can provide not only a reliable *in vitro* approach to rapid screening the inhibitory potential of new molecular entities (NME) but also the reliable data from *in vitro* inhibition studies that can help guide clinical situations. Hence these *in vitro* findings can be extrapolated to carry out P450 probe substrate inhibition assays to determine whether an NME inhibits a particular P450 enzyme activity.

Chapter 8

Part II: Evaluation of cocktail substrate assay system for inhibition screening of CYP2B6, CYP2C9, CYP2E1 & CYP3A4 by MCR-706 and MCR-742

Validation of the method using known P450 enzyme inhibitors (IC50 determinations of known CYP inhibitors**):** Once the *K*m of the probe substrate is established for the test system, an IC50 value of a **known specific P450 inhibitor** can be determined by using the probe substrate concentration at or below the *K*m. The determination of an IC50 value can be used to verify the inhibition experiments by comparing the experimentally obtained IC50 value with known literature values. The rate of the probe substrate turnover is assayed in the presence of various inhibitor concentrations, and the percentage of activity remaining (percentage of the original rate) with respect to inhibitor concentrations are plotted to derive an apparent IC50 value [1]. The limited selectivity of substrates used in the P450 cocktails may lead to deviations in the observed inhibitory activities because various P450 enzymes can be involved in the metabolism of a particular substrate. Hence the method developed for simultaneous evaluation of the activities of four cytochrome P450s (CYP2B6, CYP2C9 and CYP3A4) in human liver microsomes was validated to test the inhibition potential of four CYP isoforms by using their known selective inhibitors (clopidogrel, CYP2B6; fluoxetine, CYP2C9; and ketoconazole, CYP3A4). The IC50(µM) values were determined using the individual substrates and substrate cocktail and compared with literature values to verify the experiment[2]. The inhibitory potential of CYP2E1 using FDA recommended inhibitors could not be evaluated due to unavailability of selective inhibitors (diethyldithiocarbamate, clomethiazole, diallyldisulfide).

8.8 APPLICATION OF THE METHOD

This validated assay was further used to evaluate the inhibition potential of two NME's (New Molecular Entities synthesized in Pharmaceutical Chemistry laboratory of Pharmacy Department of MSU, Baroda, Gujarat).

MCR-706 (NME I) and **MCR-742** (NME II) are proposed to be anticancer drugs. The increased flux of NCEs into drug discovery due to combinatorial chemistry and high-throughput screening techniques has placed an increased demand for speed and efficiency on the CYP inhibition screening methodologies. The use of a cassette incubation of probe substrates with human liver microsomes (HLM), also known as the 'cocktail' approach is becoming a widely accepted approach to determine the interaction of new chemical

entities (NCEs) with cytochrome P450 enzymes (CYP450) in early drug discovery[3,4]. An HPLC-UV method has been developed for the inhibition screening of the major human cytochrome P450 enzymes (CYP2B6, CYP2C9, CYP2E1, and CYP3A4) using an in vitro substrate cocktail. The inhibition potential of NME I and NME II towards four major human hepatic CYP450 enzymes (CYP2B6, CYP2C9, CYP2E1, and CYP3A4) was investigated via cassette dosing of four probe substrates (efavirenz, diclofenac, chlorzoxazone and atorvastatin) in human liver microsomes. In the incubation study of these cocktails, the reaction mixtures were pooled and analyzed simultaneously using developed HPLC method.

8.9 EXPERIMENTAL

8.9.1 Chemicals and Reagents

Clopidogrel bisulphate(CLP) was received as gift sample from Torrent Pharmaceuticals, Gujarat. Ketoconazole(KET) was supplied as gift sample from Sun Pharmaceutical Laboratories Limited, Mumbai and Fluoxetine(FLX) was procured as gift sample from Sun Pharmaceuticals Ltd., Baroda, India. All other chemicals and reagents used in this study were of analytical grade and were procured as described under section 5.1.1.

8.9.2 Inhibitor selection

The inhibitors to be used for validation of this cocktail approach were chosen based not only on their CYP specificity, but also on their availability and recommendations in regulatory guidance [2]. The inhibitor drugs and doses in this cocktail were chosen to be selective for individual CYP isoforms, with the expectation of no or minimal interference with other probe substrates.

Inhibitor for each P450 enzyme was selected based on a representative list of preferred and acceptable in vitro probe inhibitors recommended by FDA [2]. The probe inhibitors selected for each P450 enzyme were as follows: clopidogrel (CYP2B6), fluoxetine (CYP2C9), ketoconazole (CYP3A4). CYP2E1 inhibition activity could not validated as the recommended inhibitors could not be procured inspite of best efforts. Clopidogrel (CLP), Fluoxetine (FLX) and ketoconazole (KET), (Figure.8.8a-c) met all the typical requirements of a compound to be used as probe inhibitor for the simultaneous evaluation of the inhibitory activities of three cytochrome P450s (CYP2B6, CYP2C9, and CYP3A4)

in human liver microsomes. All the inhibitors were soluble in common solvent methanol, which was evaporated during analysis. All the peaks of probe substrate, their respective metabolites and inhibitors were well resolved in chromatograms obtained after cocktail incubation.

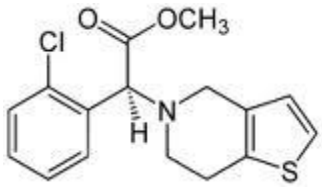

Figure 8.8a. **Clopidogrel**

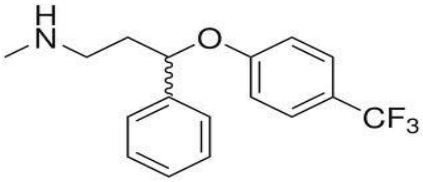

Figure 8.8b. Fluoxetine

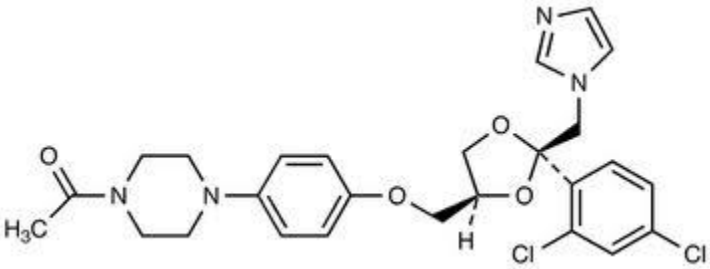

Figure 8.8c. Ketoconazole

8.9.3 Preparation of standard and working solutions

- Preparation of stock solution and working solutions of EFV, DIC, CHZ, ATV: The respective solutions were prepared as described in previous **section 8.2.3.**
- Preparation of stock solution and working solutions of CLP, FLX and ATV: Stock solution**,** 1mg/ml of CLP, FLX and ATV were prepared by dissolving 6.5mg, 5mg, and 10.34 mg in 5 ml of methanol in a volumetric flask to yield a concentration of 3.11mM, 3.23mM, and 0.895mM. **Working solution**, 0.1mg/ml

were prepared by transferring 1.0 ml from stock solution to 10 ml volumetric flask and diluted to the mark with MeOH.

- Preparation of stock solution and working solutions of **MCR-706** (NME I) and **MCR-742** (NME II) **: Stock solution** was prepared by dissolving a precisely weighed 5 mg of **MCR-706** in 5 ml of methanol in a volumetric flask to yield a concentration of 10mM. A series of working solutions were produced by adding appropriate amount of **MCR-706** to the incubation solution to yield 50, 75 and 100 µM of **MCR-706** for inhibition experiment. Same procedure was followed for **MCR-742** (NME II).

8.9.4 Microsomal incubations:

8.9.4.1 Inhibitory effect of CLP/FLX/KET on EFV/DIC/ATV respectively (IC50 Determination).

The potential inhibitory effect of known **specific** P450 inhibitors **CLP/FLX/KET** on the activity of human CYP was evaluated using developed model substrate reaction for efavirenz (CYP2B6), diclofenac (CYP2C9) and atorvastatin (CYP3A4) respectively.

Varying concentrations of **CLP** (0–10µM),**FLX** (0–100µM) and **KET**(0-10 µM) were dissolved and diluted serially in methanol and then alcohol was removed by evaporating to dryness**.** The residue was reconstituted in 140µl potassium phosphate buffer (50 mM, pH 7.4). Similarly probe substrates at fixed concentration of 20µM EFV, 50µM DIC, 50µM CHZ and 10µM ATV (probe substrate concentration at or below their respective Km) were separately dissolved in methanol, allowed to evaporate and reconstituted in 35µl phosphate buffer. The tubes containing inhibitors were placed into an ice bath and 5µl of HLM was added and vortexed. Tubes (duplicate) containing the reaction mixture in phosphate buffer and NADPH solution were allowed to equilibrate separately in a shaker incubator at 150 rpm for 5 min at 37°C. The 35µl reconstituted probe substrate in buffer solution was added to the tubes containing test article where the total volume was 180 µl. The reaction was initiated by adding 20µl of NADPH immediately to the tubes and incubation was carried out for 30 min. The reaction was terminated by the addition of 100 µl ice cold acetonitrile containing 40 mcg/ml of glimepiride as internal standard. Then the samples were subjected to centrifugation on a cooling laboratory centrifuge

(Sigma, 3K30; Germany) at 10,000 rpm (4°C; 10min), and aliquots of the supernatant were directly injected into an HPLC system. The inhibitory effect of CLP/FLX/KET on its selective substrate EFV, DIC and ATV metabolism was expressed as a percentage of the residual activity compared with the control in absence of inhibitor respectively (Table 6.3). Each assay was performed in duplicate for individual and cocktail incubations.

8.9.4.2 Inhibitory effect of MCR-706 and MCR-742 (IC50 Determination).

The potential inhibitory effect of these two NME's, **MCR-706 and MCR-742** on the activity of four human CYP was evaluated by incubating its varying concentrations (0–100 µM) and following the same above procedure described in 8.10.4.1. The inhibitory effect of **MCR-706 and MCR-742** on CHZ/ATV/DIC/EFV metabolism was expressed as a percentage of the residual activity compared with the control in absence of inhibitor respectively. Each assay was performed in duplicate for individual and cocktail incubations.

The proposed inhibitors (MCR-706 and MCR-742) were incubated with substrate cocktail and with individual substrates alone to determine whether the cocktail and individual incubations would yield similar results.

8.9.5 Chromatographic condition:

The same optimized mobile phase (described earlier in 8.2.3), ACN: Ammonium Formate (0.1% FA):: 52:48 (%v/v) was suitable for in vitro evaluation of inhibition potencies of CLP, FLX, KET, MCR-706, MCR-742 on EFV, DIC, ATV and CHZ because it was found to ideally resolve all the substrates, metabolite and inhibitor peaks. Quantification was performed by comparing the peak areas at 230nm for diclofenac 4'-hydroxylation and at 247nm for efavirenz 8-hydroxylation and atorvastatin *o*-hydroxylation in presence and absence of their specific inhibitors. The individual and cocktail incubation showed substrate peaks at 4.08min for CHZ, 9.76 for ATV, 10.89 for DIC, 15.58 for EFV and metabolite peaks M_1 at 2.58 min for CHZ, M_2 at 4.8 min for DIC, M_3 at 7.9 min for ATV and M_4 at 8.6 min for EFV (Figure .8.9e, 8.10e). KET, FLX, CLP specific inhibitor of ATV, DIC, EFV when co incubated in individual as well as

cocktail substrate incubations showed peaks at 3.00 min, 3.4 min and 22.8min respectively (Fig. 8.9(a-f) to 8.12(a-b)).

Similarly MCR-706 and MCR-742 when co incubated in individual as well as cocktail substrate incubations showed peaks at 3.4 min, and 19.8min respectively (Figure 8.13(a-l) to 8.14(a-d)).

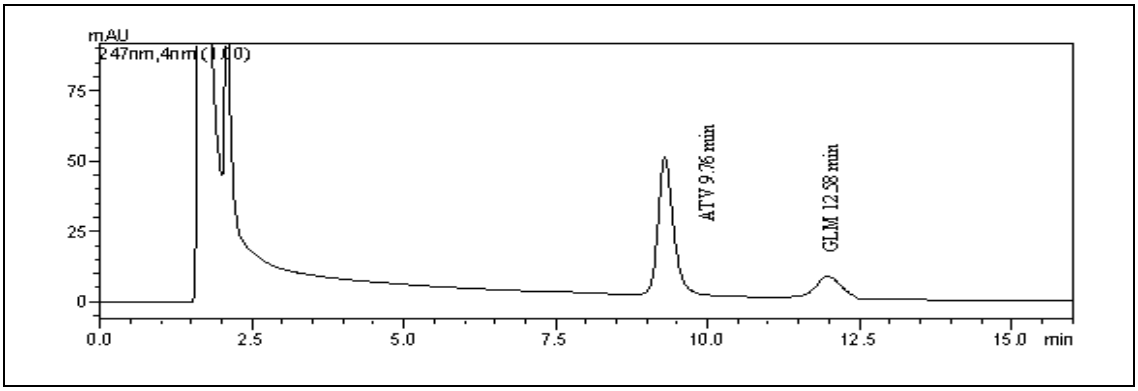

Figure 8.9a. HPLC chromatogram of individual incubation of ATV at 247nm (0 min)

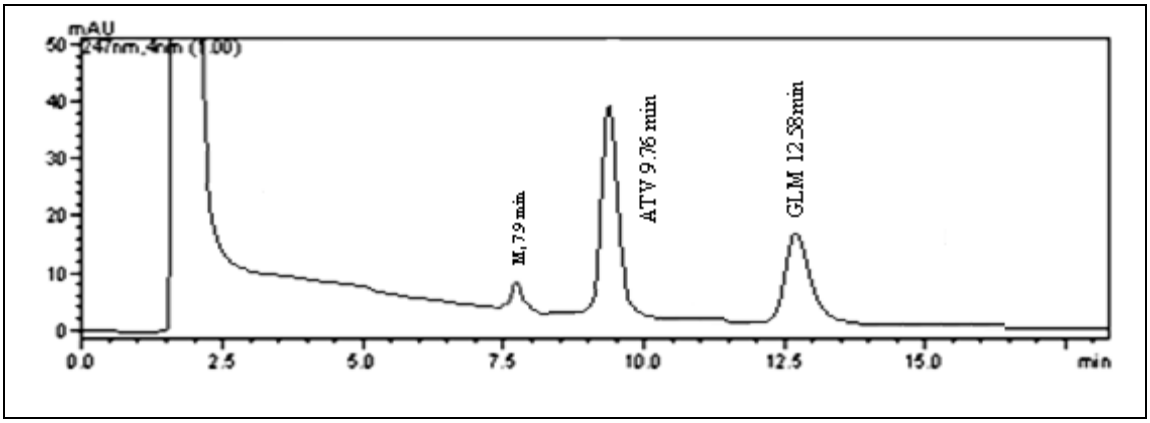

Figure 8.9b. HPLC chromatogram of individual incubation of ATV at 247nm (30 min).

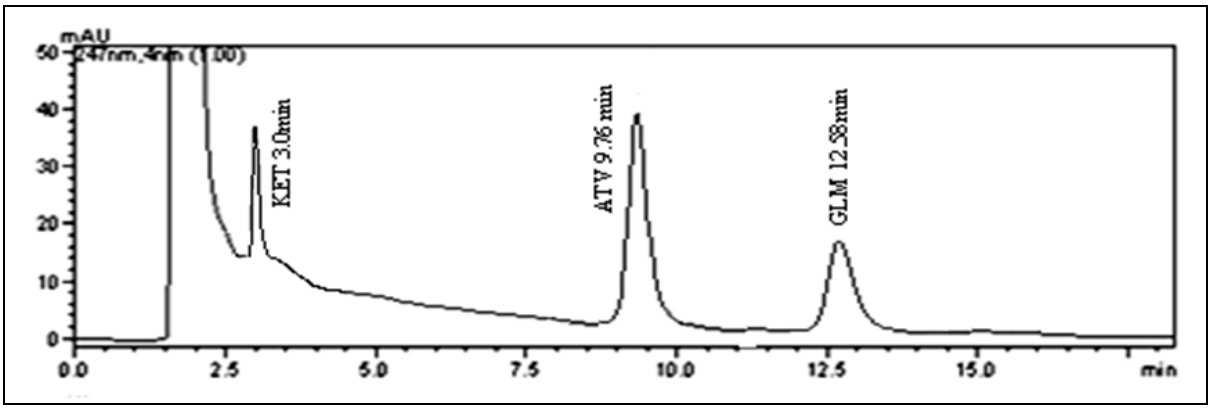

Figure 8.9c. HPLC chromatogram of individual incubation of ATV in presence of KET as inhibitor at 247nm(0 min).

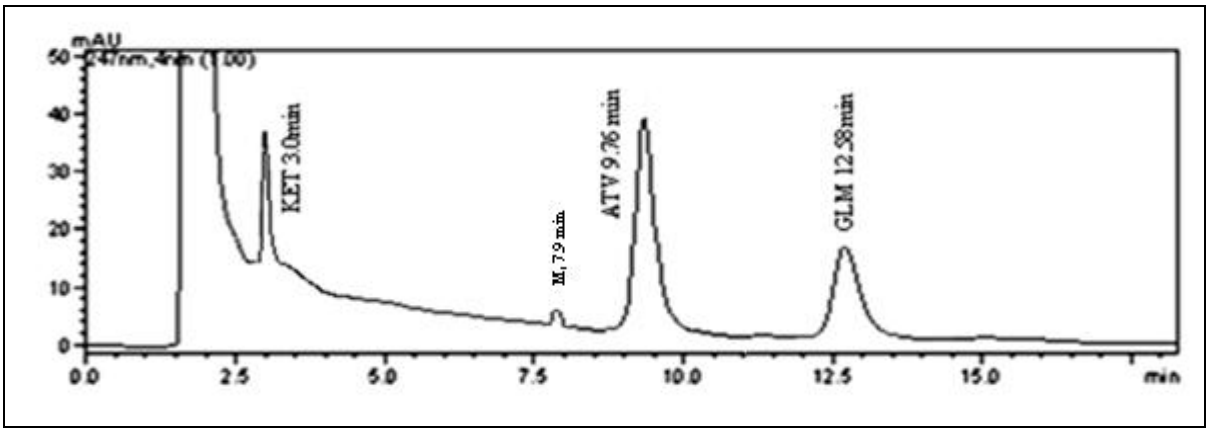

Figure 8.9d. HPLC chromatogram of individual incubation of ATV and its metabolite M_3 in presence of KET as inhibitor at 247nm (30 min).

Fig.8.9(a-d) shows HPLC chromatograms of individual incubation of ATV(9.76 min) in absence and presence of KET(3.0 min) as inhibitor at 247nm (0min and 30min respectively). The incubation carried out at 30 min proves metabolite peak of ATV(M_3) at 7.3min. In presence of KET as inhibitor area of ATV is increased and inhibition of its metabolism to some extent is observed.

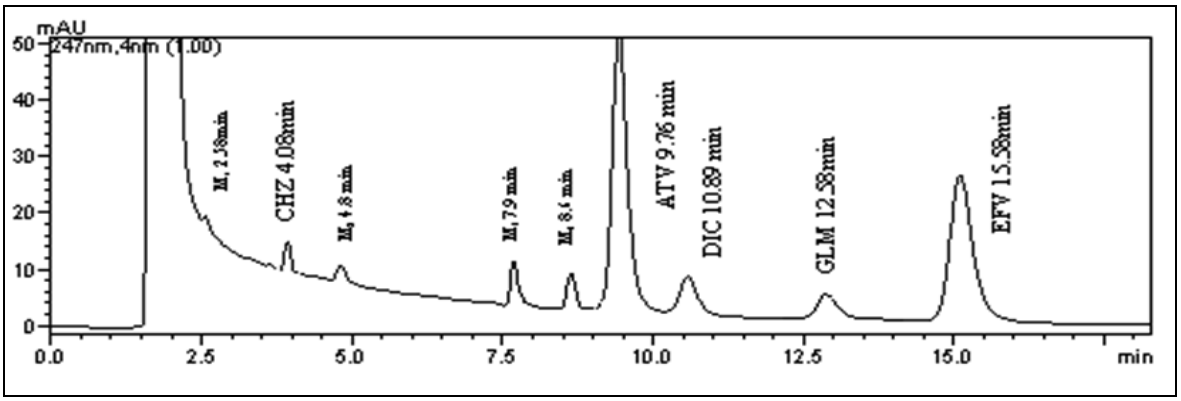

Figure 8.9e. HPLC chromatogram of cocktail incubation of CHZ, ATV, DIC, EFV and their respective metabolites M_1, M_2, M_3, M_4 at 247nm (30 min).

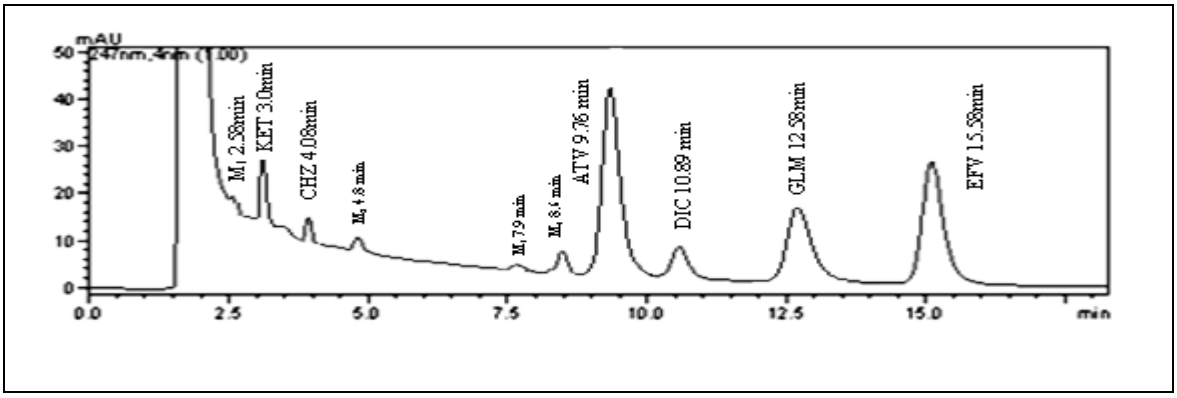

Figure 8.9f. HPLC chromatogram of cocktail incubation of CHZ, ATV, DIC, EFV and their respective metabolites M_1, M_2, M_3, M_4 in presence of KET as inhibitor (for ATV) at 247nm(30 min).

Fig.8.9(e-f) shows HPLC chromatograms of cocktail incubation of CHZ(4.08min),ATV(9.76 min),DIC(10.89min),EFV(13.28min) and their respective metabolites M_1(2.58min), M_3(7.9 min), M_2(4.8min), M_4(8.6min) in absence and presence of KET(3.0 min) as inhibitor carried out for 30min at 247nm. The incubation carried out at 30 min proves metabolite peak of ATV(M_3) at 7.3min. In presence of KET as inhibitor area of ATV is increased and inhibition of its metabolism to some extent is observed.

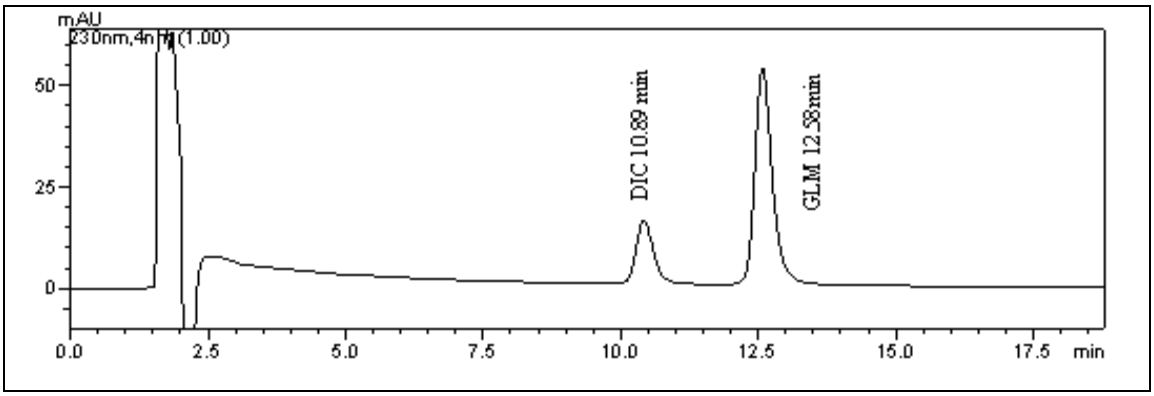

Figure 8.10a. HPLC chromatogram of individual incubation of DIC at 230nm (0 min).

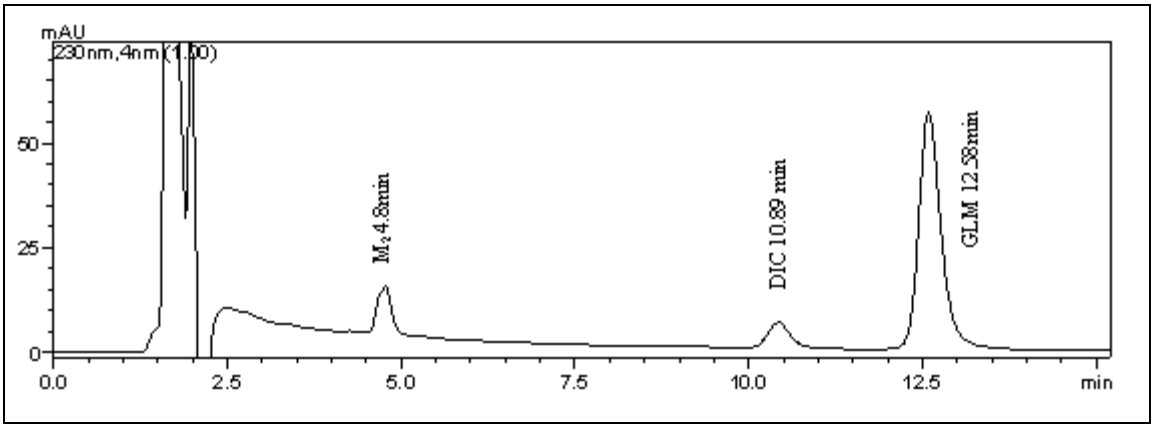

Figure 8.10b. HPLC chromatogram of individual incubation of DIC at 230nm (30 min).

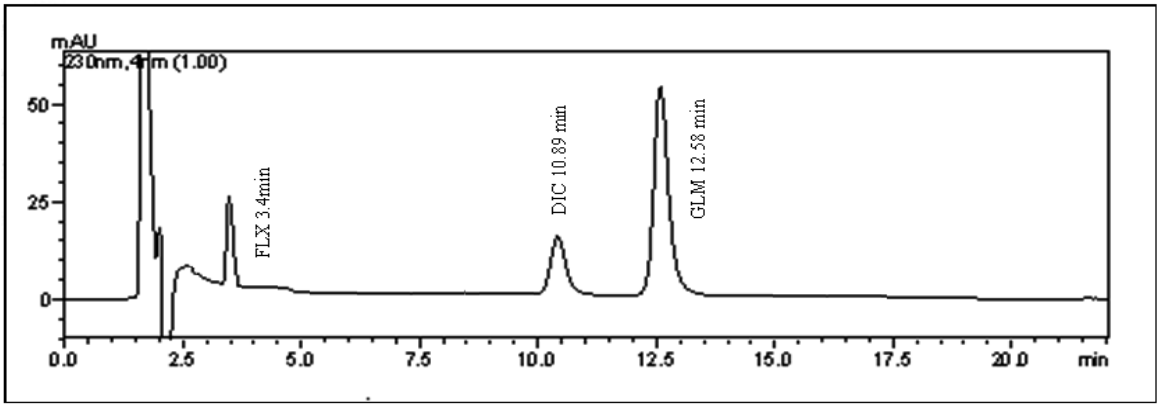

Figure 8.10c. HPLC chromatogram of individual incubation of DIC in presence of FLX as inhibitor at 230nm (0 min).

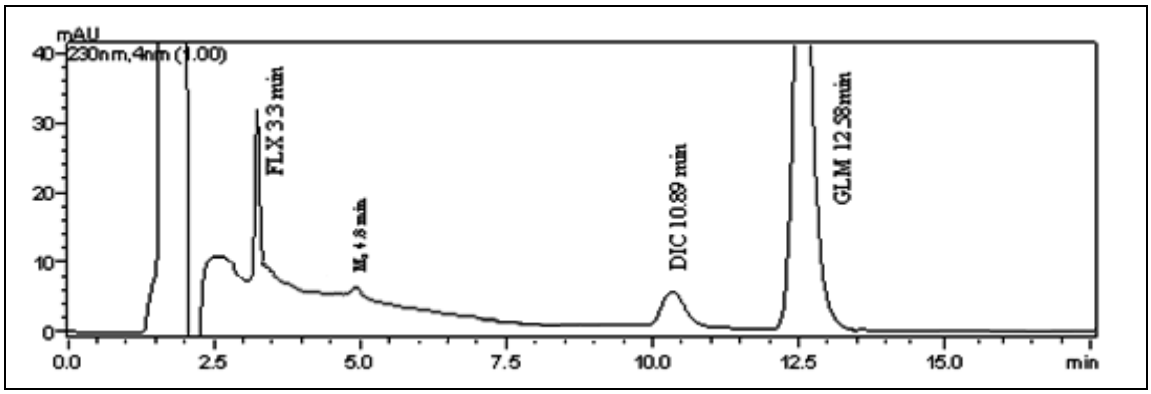

Figure 8.10d. HPLC chromatogram of individual incubation of DIC and its metabolite M_2 in presence of FLX as inhibitor at 230nm (30 min).

Fig.8.10(a-d) shows HPLC chromatograms of individual incubation of DIC (10.89 min) in absence and presence of FLX(3.4 min) as inhibitor at 230nm (0min and 30min respectively). The incubation carried out at 30 min proves metabolite peak of DIC(M_2) at 4.8min. In presence of KET as inhibitor area of DIC is increased and inhibition of its metabolism to some extent is observed.

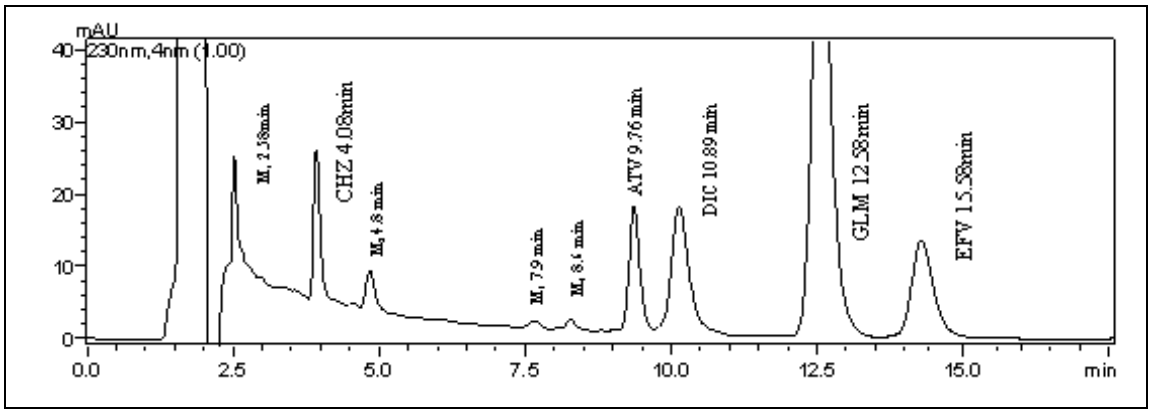

Figure 8.10e. HPLC chromatogram of cocktail incubation of CHZ, ATV, DIC, EFV and their respective metabolites M_1, M_2, M_3, M_4 at 230nm (30 min).

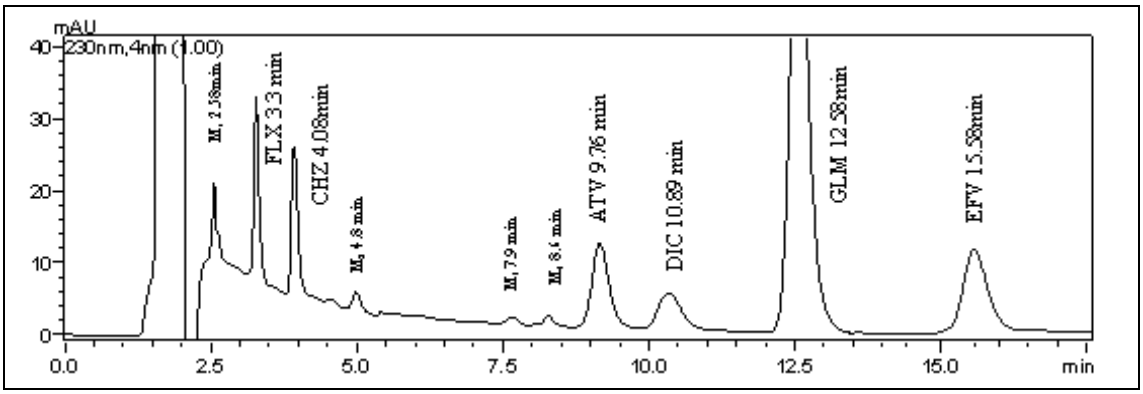

Figure 8.10f. HPLC chromatogram of cocktail incubation of CHZ, ATV, DIC, EFV and their respective metabolites M_1, M_2, M_3, M_4 in presence of FLX as inhibitor (for DIC) at 230nm (30 min).

Fig.8.10(e-f) shows HPLC chromatograms of cocktail incubation of CHZ(4.08min),ATV(9.76 min),DIC(10.89min),EFV(13.28min) and their respective metabolites M_1(2.58min), M_3(7.9 min), M_2(4.8min), M_4(8.6min) in absence and presence of FLX(3.4min) as inhibitor carried out for 30min at 230nm. The incubation carried out at 30 min proves metabolite peak of ATV(M_2) at 4.8min. In presence of FLX as inhibitor area of DIC is increased and inhibition of its metabolism to some extent is observed.

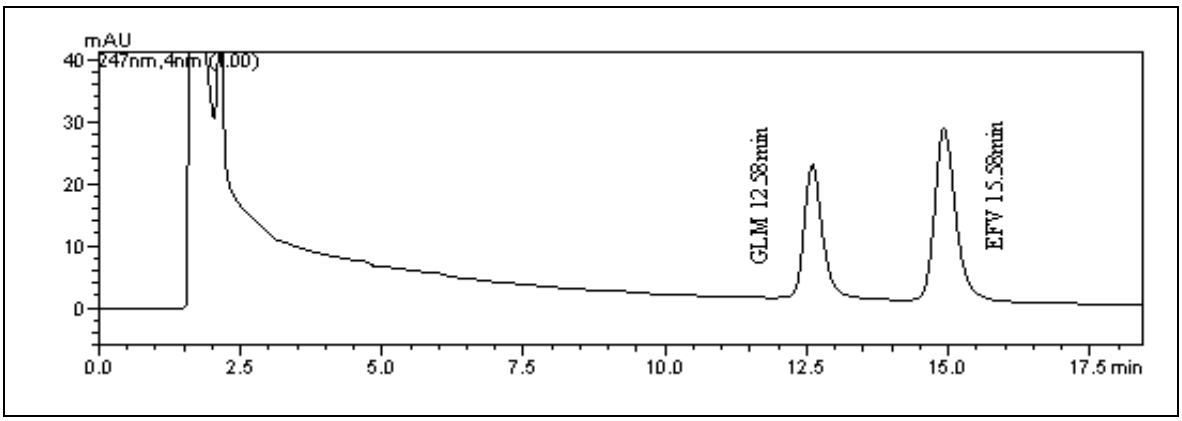

Figure 8.11a. HPLC chromatogram of individual incubation of EFV at 247nm (0 min).

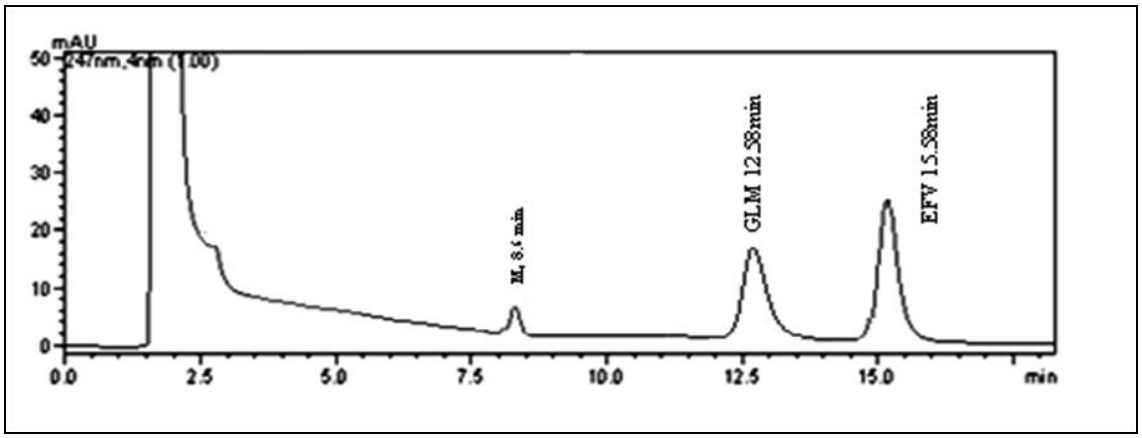

Figure 8.11b. HPLC chromatogram of individual incubation of EFV at 230nm (30 min).

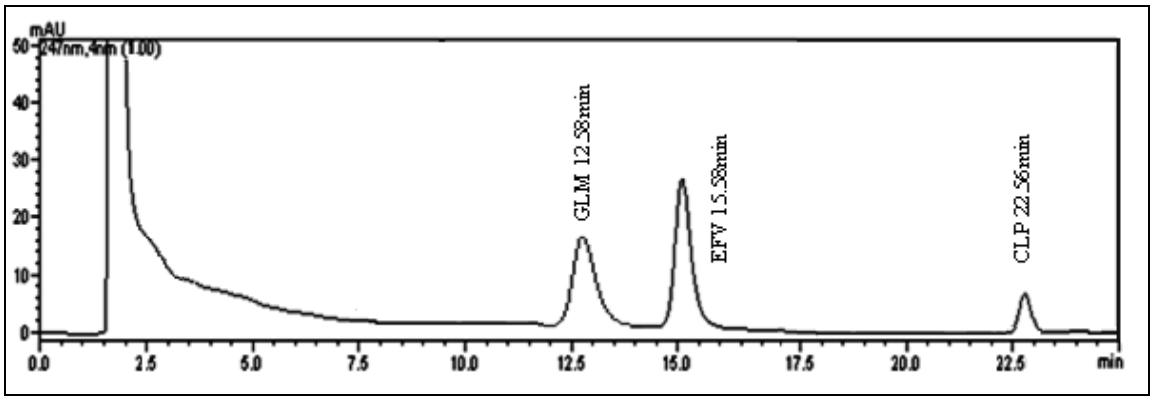

Figure 8.11c. HPLC chromatogram of individual incubation of EFV in presence of CLP as inhibitor at 247nm (0 min).

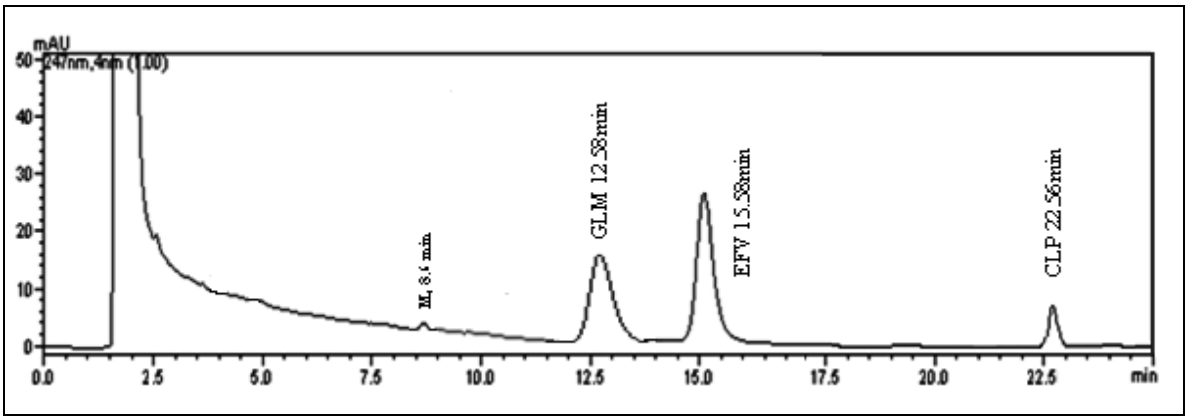

Figure 8.11d. HPLC chromatogram of individual incubation of EFV and its metabolite M_4 in presence of CLP as inhibitor at 247nm (30 min).

Fig.8.11(a-d) shows HPLC chromatograms of individual incubation of EFV(15.58 min) in absence and presence of CLP (22.56min) as inhibitor at 247nm (0min and 30min respectively). The incubation carried out at 30 min proves metabolite peak of EFV (M_4) at 8.6min. In presence of CLP as inhibitor area of EFV is increased and inhibition of its metabolism to some extent is observed.

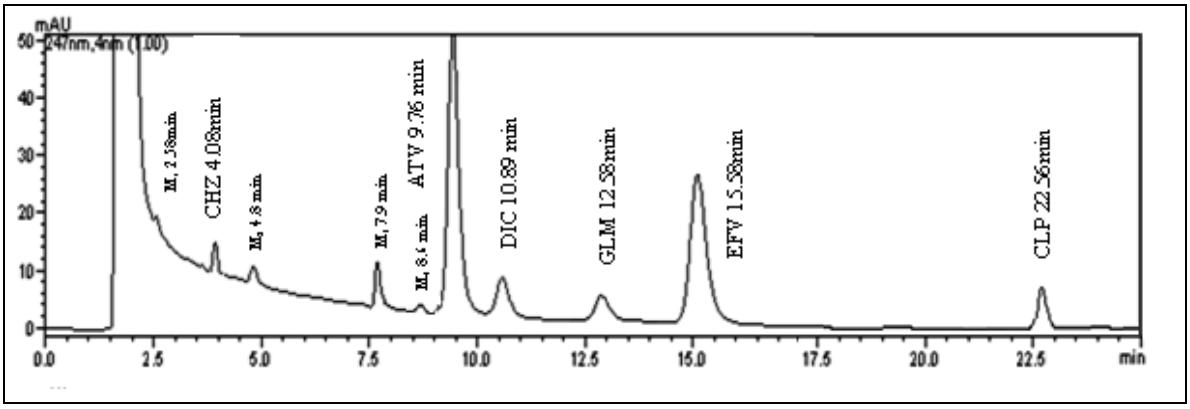

Figure 8.11e. HPLC chromatogram of cocktail incubation of CHZ, ATV, DIC, EFV and their respective metabolites M_1, M_2, M_3, M_4 in presence of CLP as inhibitor (for EFV) at 247nm(30 min).

Fig.8.11(e) shows HPLC chromatograms of cocktail incubation of CHZ(4.08min),ATV(9.76 min),DIC(10.89min),EFV(13.28min) and their respective metabolites M_1(2.58min), M_3(7.9 min), M_2(4.8min), M_4(8.6min) in presence of CLP(22.56min) as inhibitor carried out for 30min at 247nm. The incubation carried out at

30 min proves metabolite peak of EFV(M_4) at 8.6min. In presence of CLP as inhibitor area of EFV is increased and inhibition of its metabolism to some extent is observed.

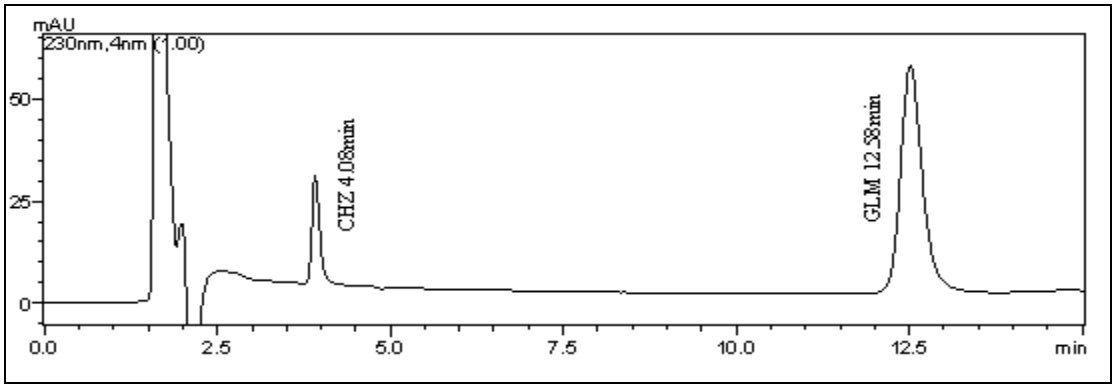

Figure 8.12a. HPLC chromatogram of individual incubation of CHZ at 230nm (0 min).

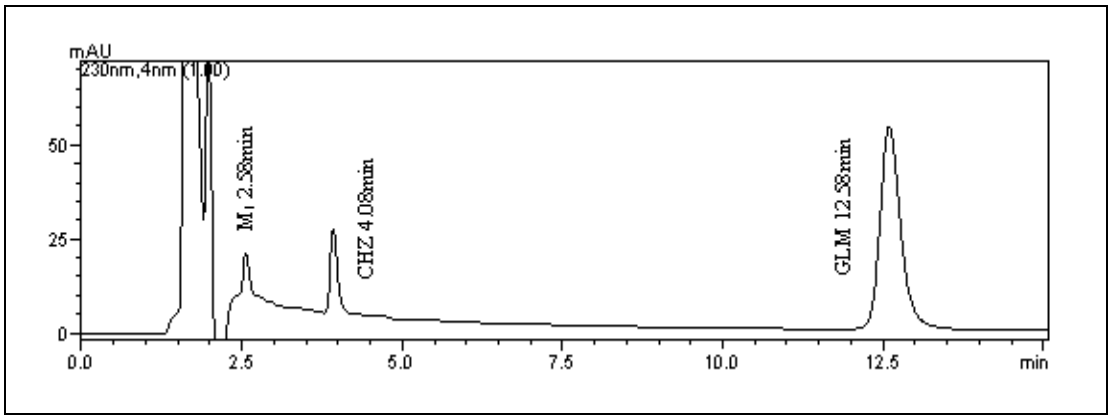

Figure 8.12b. HPLC chromatogram of individual incubation of CHZ at 230nm (30 min).

Fig.8.12(a-b) shows HPLC chromatograms of individual incubation of CHZ (4.08 min) at 230min (0min and 30min respectively). The incubation carried out at 30 min proves metabolite peak of CHZ(M_1) at 2.58min. The selective inhibitor for CHZ was not available, hence inhibition potential for CHZ metabolism using selective inhibitor was not evaluated.

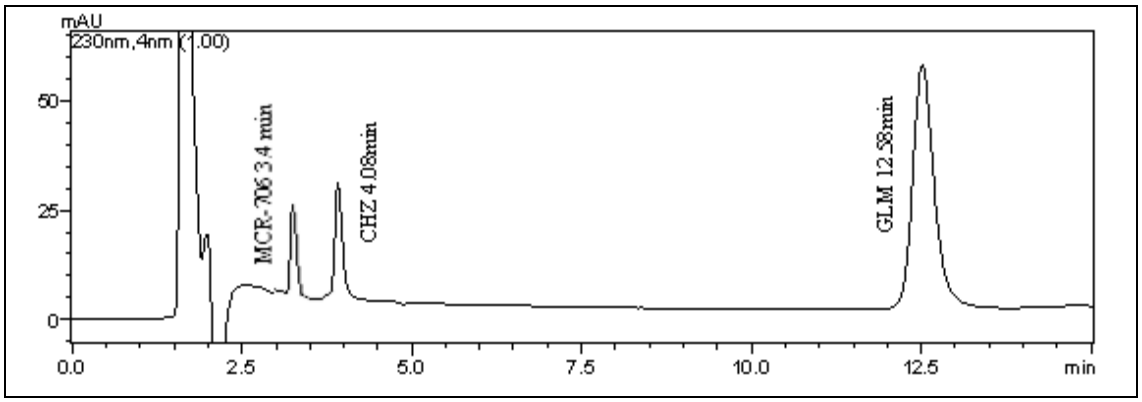

Figure 8.13a. HPLC chromatogram of individual incubation of CHZ in presence of MCR-706 as inhibitor (0 min).

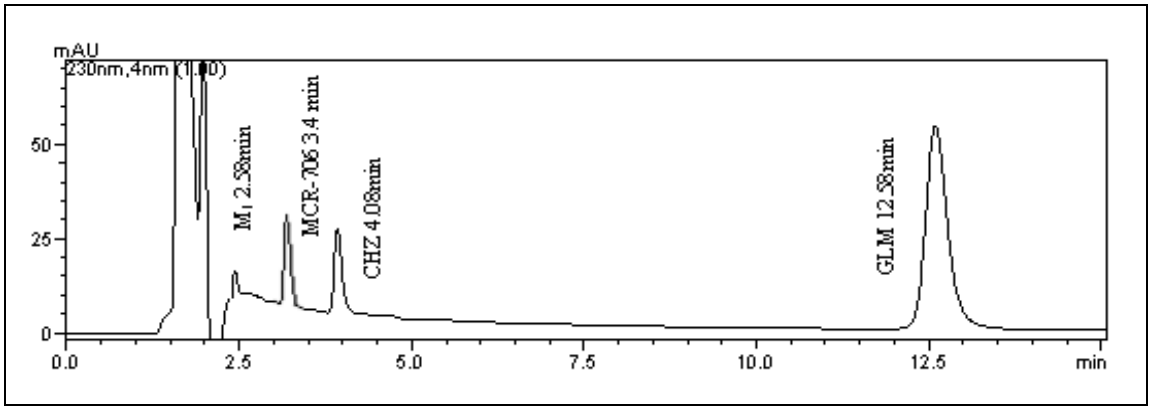

Figure 8.13b. HPLC chromatogram of individual incubation of CHZ and its metabolite M_1 in presence of MCR-706 as inhibitor at 230nm (30 min).

Fig.8.13(a-b) shows HPLC chromatograms of individual incubation of CHZ (4.08 min) in absence and presence of MCR-706 (3.4min) as inhibitor at 230nm (0min and 30min respectively). In presence of MCR-706 as inhibitor area of CHZ is increased and inhibition of its metabolism to some extent is observed.

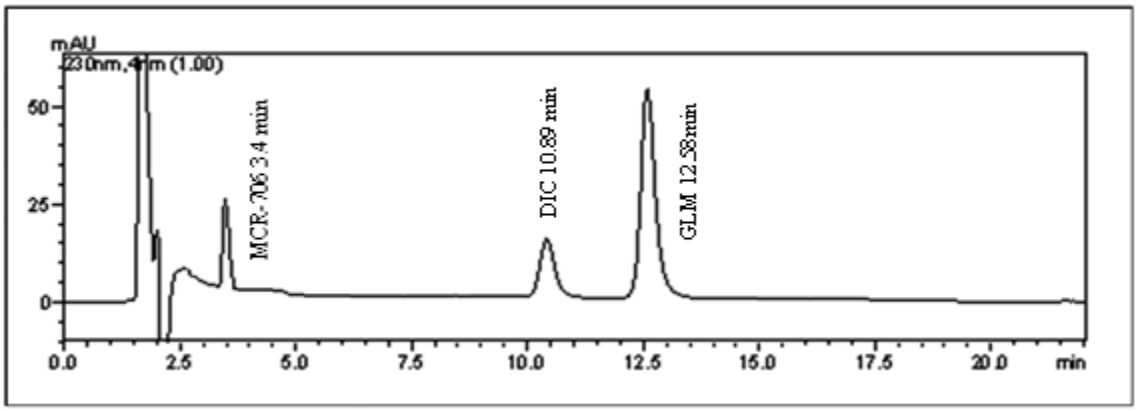

Figure 8.13c. HPLC chromatogram of individual incubation of DIC in presence of MCR-706 as inhibitor (0 min).

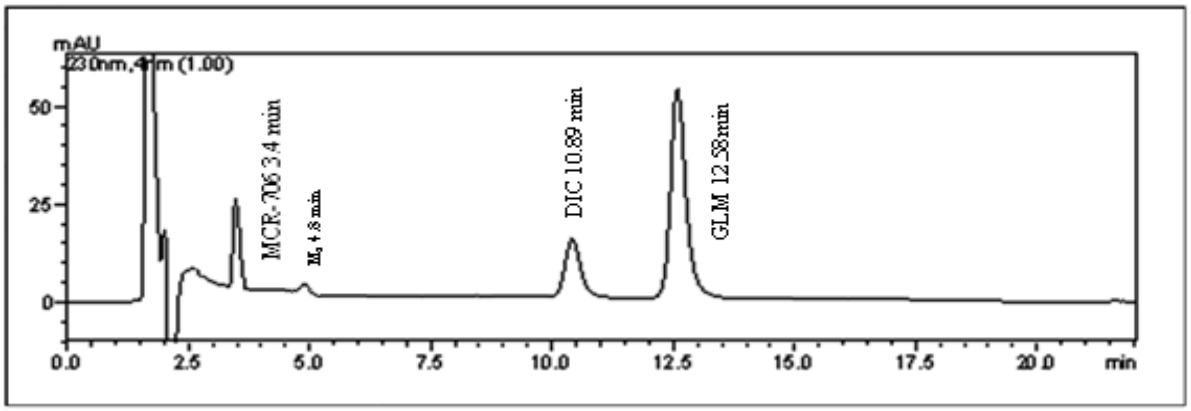

Figure 8.13d. HPLC chromatogram of individual incubation of DIC and its metabolite M_2 in presence of MCR-706 as inhibitor at 230nm (30 min).

Fig.8.13(c-d) shows HPLC chromatograms of individual incubation of DIC(10.89 min) in absence and presence of MCR-706 (3.4min) as inhibitor at 230nm (0min and 30min respectively). In presence of MCR-706 as inhibitor area of DIC is increased and inhibition of its metabolism to some extent is observed.

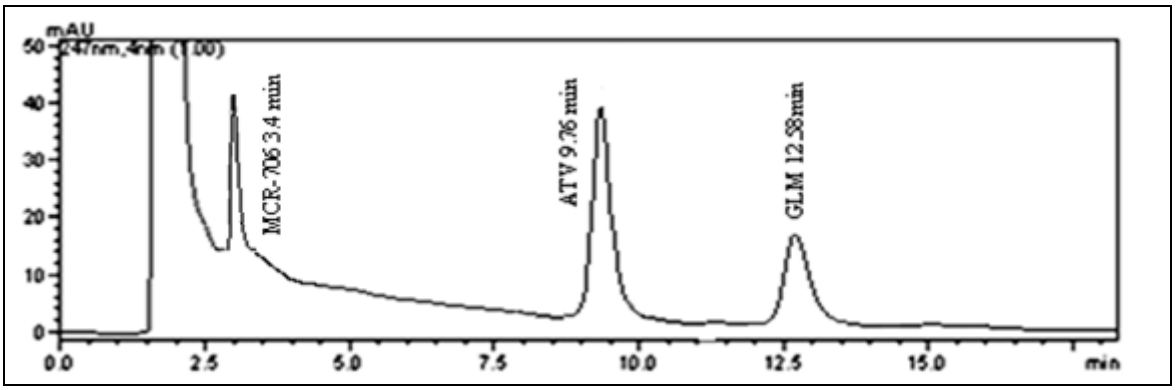

Figure 8.13e. HPLC chromatogram of individual incubation of ATV in presence of MCR-706 as inhibitor (0 min).

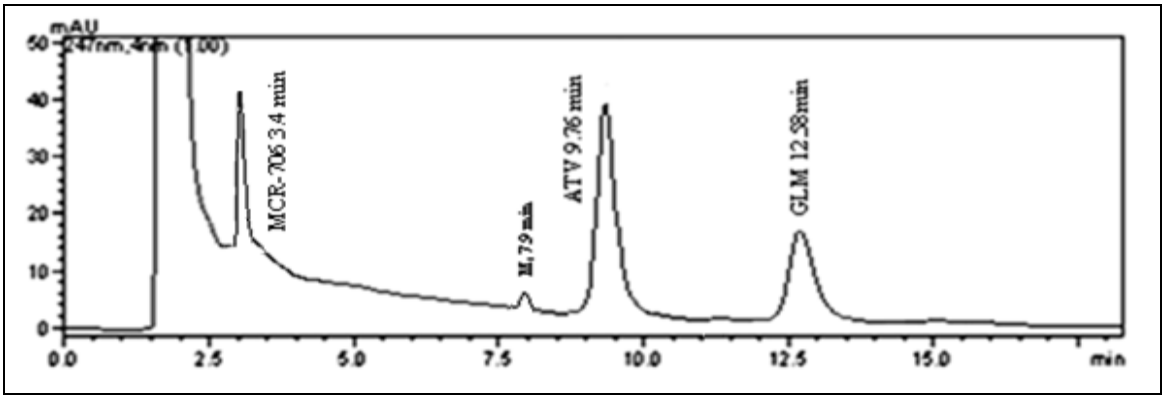

Figure 8.13f. HPLC chromatogram of individual incubation of ATVand its metabolite M_3 in presence of MCR-706 as inhibitor at 230nm (30 min).

Fig.8.13(e-f) shows HPLC chromatograms of individual incubation of ATV(9.76 min) in absence and presence of MCR-706 (3.4min) as inhibitor at 247nm (0min and 30min respectively). In presence of MCR-706 as inhibitor area of ATV is increased and inhibition of its metabolism to some extent is observed.

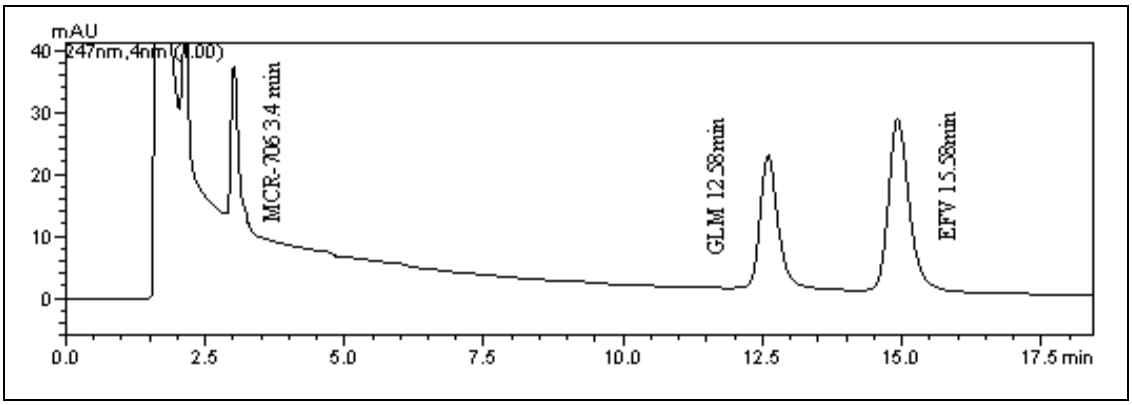

Figure 8.13g. HPLC chromatogram of individual incubation of EFV in presence of MCR-706 as inhibitor (0 min).

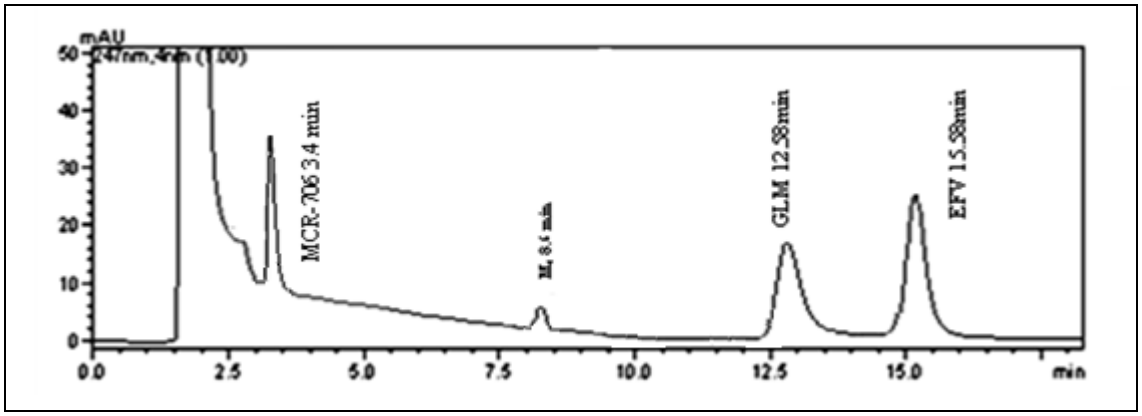

Figure 8.13h. HPLC chromatogram of individual incubation of EFV and its metabolite M_4 in presence of MCR-706 as inhibitor at 247nm (30 min).

Fig.8.13(g-h) shows HPLC chromatograms of individual incubation of EFV(10.89 min) in absence and presence of MCR-706 (13.28min) as inhibitor at 247nm (0min and 30min respectively). In presence of MCR-706 as inhibitor area of EFV is increased and inhibition of its metabolism to some extent is observed

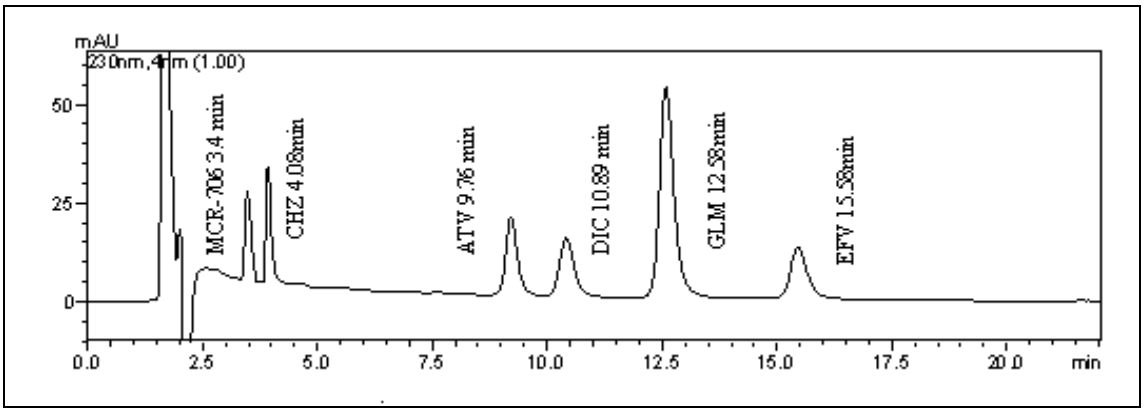

Figure 8.13i. HPLC chromatogram of cocktail incubation of CHZ, ATV, DIC and EFV at 230nm with MCR-706 (0min).

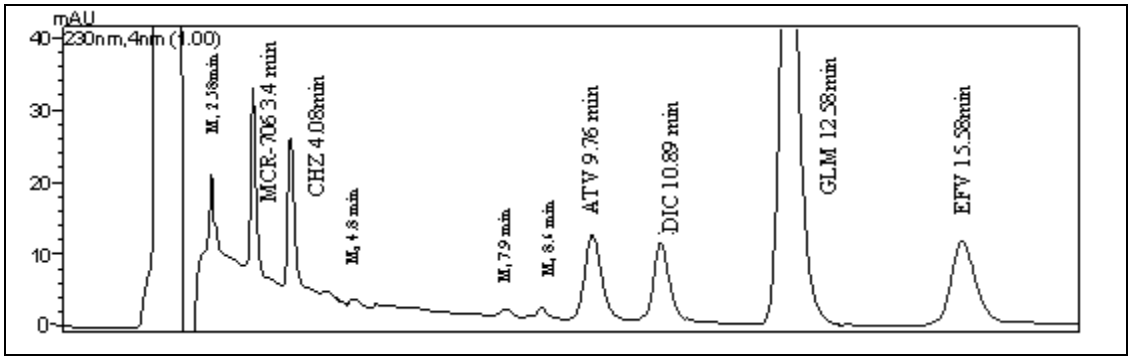

Figure 8.13j. HPLC chromatogram of cocktail incubation of CHZ, ATV, DIC, EFV and their respective metabolites M_1, M_2, M_3, M_4 in presence of MCR-706 as inhibitor at 230nm(30 min).

Fig.8.13(i-j) shows HPLC chromatograms of cocktail incubation (carried out for 0min and 30min) of CHZ(4.08min), ATV(9.76 min), DIC(10.89min), EFV(13.28min) and their respective metabolites M_1(2.58min), M_3(7.9 min), M_2(4.8min), M_4(8.6min) in presence of MCR-706 (13.28min) as inhibitor at 230nm. The incubation carried out at 30 min shows that metabolite peak of DIC(M_2 ,4.8min) is reduced to large extent as compared to CHZ (M_1,2.58min) and area of DIC(10..89) is increased as compared to CHZ(4.08min) .

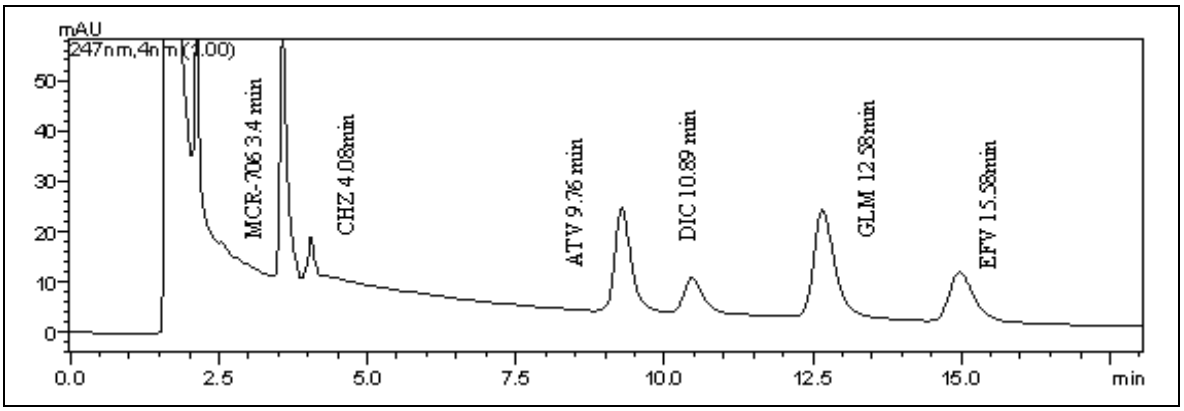

Figure 8.13k. HPLC chromatogram of cocktail incubation of CHZ, ATV, DIC and EFV at 247nm with MCR-706 (0min).

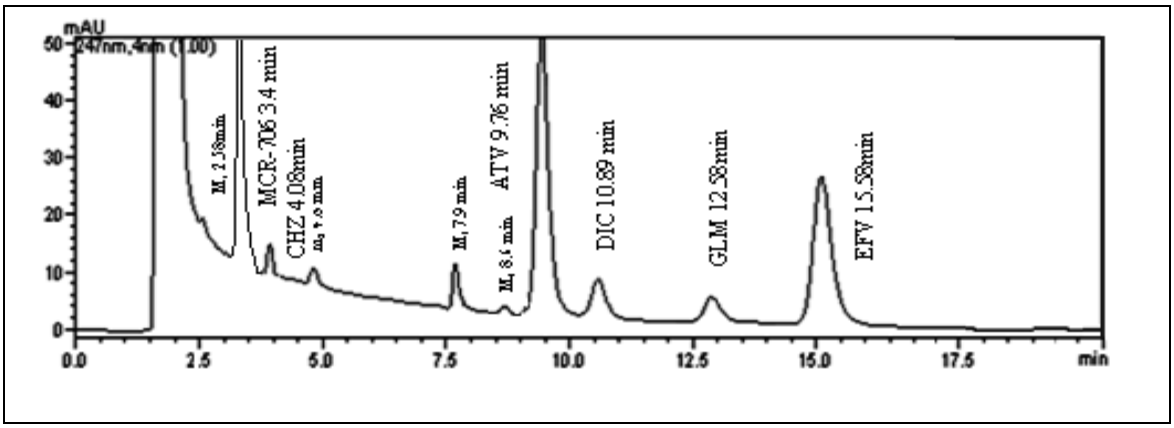

Figure 8.13l. HPLC chromatogram of cocktail incubation of CHZ, ATV, DIC, EFV and their respective metabolites M_1, M_2, M_3, M_4 in presence of MCR-706 as inhibitor at 247nm(30 min).

Fig.8.13(k-l) shows HPLC chromatograms of cocktail incubation (carried out for 0min and 30min) of CHZ(4.08min), ATV(9.76 min), DIC(10.89min), EFV(13.28min) and their respective metabolites M_1(2.58min), M_3(7.9 min), M_2(4.8min), M_4(8.6min) in presence of MCR-706 (13.28min) as inhibitor at 247nm. The incubation carried out at 30 min shows that metabolite peak of ATV(M_3 ,7.9min) is reduced to some extent as compared to metabolite peak of EFV (M_4,8.6min) and area of ATV(9.76min) is increased as compared to EFV(13.28min).

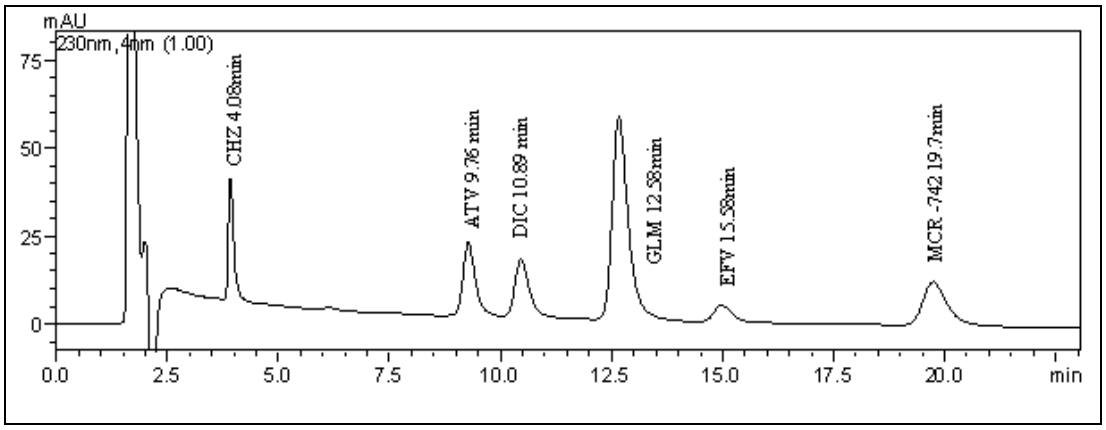

Figure 8.14a. HPLC chromatogram of cocktail incubation of CHZ, ATV, DIC and EFV at 230nm with MCR-742 (0min).

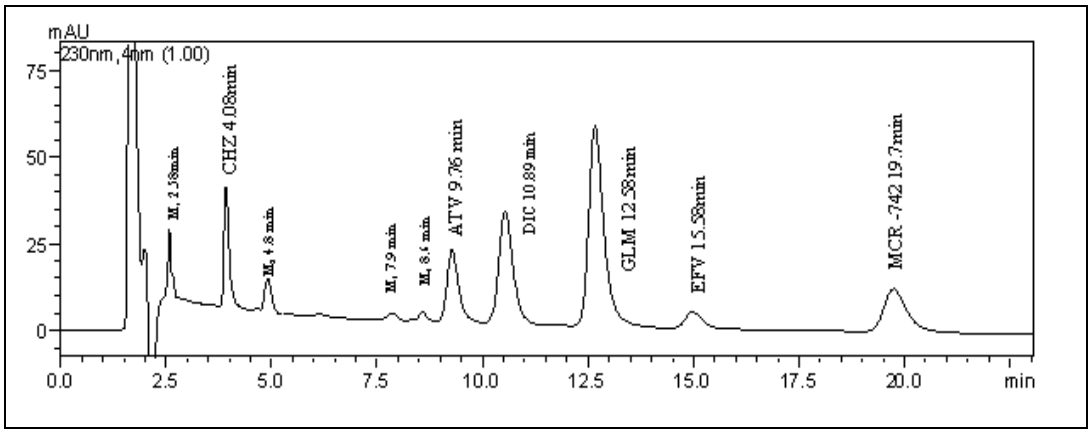

Figure 8.14b. HPLC chromatogram of cocktail incubation of CHZ, ATV, DIC, EFV and their respective metabolites M_1, M_2, M_3, M_4 in presence of MCR-742 as inhibitor at 230nm(30 min).

Fig.8.14(a-b) shows HPLC chromatograms of cocktail incubation (out for 0min and 30min) of CHZ(4.08min), ATV(9.76 min), DIC(10.89min), EFV(13.28min) and their respective metabolites M_1(2.58min), M_3(7.9 min), M_2(4.8min), M_4(8.6min) in presence of MCR-742(13.28min) as inhibitor carried at 230nm. The incubation carried out at 30min shows that metabolite peaks of CHZ(M_1) and DIC(M_2) are not reduced in presence of MCR-742.

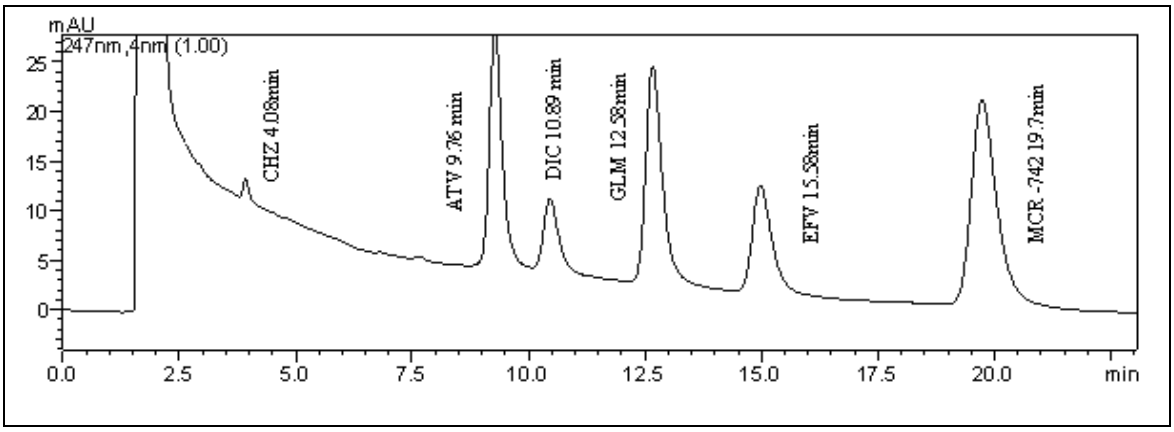

Figure 8.14c. HPLC chromatogram of cocktail incubation of CHZ, ATV, DIC and EFV at 247nm with MCR-742 (0min).

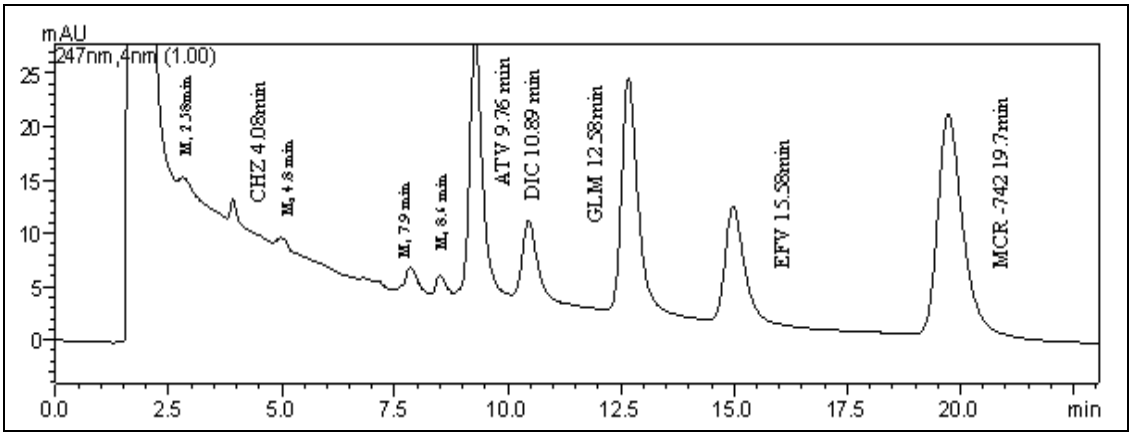

Figure 8.14d. HPLC chromatogram of cocktail incubation of CHZ, ATV, DIC, EFV and their respective metabolites M_1, M_2, M_3, M_4 in presence of MCR-742 as inhibitor at 247nm (30 min).

Fig.8.14(c-d) shows HPLC chromatograms of cocktail incubation (carried out for 0min and 30min) of CHZ(4.08min), ATV(9.76 min), DIC(10.89min), EFV(13.28min) and their respective metabolites M_1(2.58min), M_3(7.9 min), M_2(4.8min), M_4(8.6min) in presence of MCR-742(13.28min) as inhibitor at 247 nm. The incubation carried out at 30min shows that metabolite peaks of ATV(M_1) and EFV(M_2) are not reduced in presence of MCR-742.

8.9.6 Data Analysis

The inhibitory effect of KET, FLX, CLP on ATV/DIC/EFV and **MCR-706 and MCR-742** on CHZ/ATV/DIC/EFV metabolism was expressed as a percentage of the residual activity compared with the control in absence of inhibitor (Table 8.19(a-c) to 8.24(a-d)). Each assay was performed in duplicate. A sigmoid shaped curve was fitted to the data, and the enzyme inhibition parameter IC_{50} was calculated using a nonlinear least square regression analysis of the plot of percent control activity versus concentration of test inhibitor using Graphpad Prism 5 software. Ki value was also estimated using the formula **$Ki= IC_{50}/(1+[S]/Km)$** as described in section 6.1.6.2.

Table 8.19a: Inhibitory effect of varying concentrations of FLX on 50µM DIC (IC50 determination in individual incubation)

FLX (µM)	DIC conc. Cs (µM)	Area of DIC/ Area of IS 0 min As	Area of DIC/ Area of IS 30 min Au	Cu_{30min}= Au*Cs/As	$C=Cs_{0min}-Cu_{30min}$	*C/30min/0.5 (µM/min/mg protein)	*Residual Activity (%)
0	50	0.818	0.753	46.013	3.987	0.266	100.000
25	50	0.819	0.776	47.366	2.634	0.176	66.065
50	50	0.819	0.793	48.448	1.552	0.103	38.925
100	50	0.813	0.797	48.986	1.014	0.068	25.437

*Average of two experiments

Table 8.19b: Inhibitory effect of varying concentrations of CLP on 20µM EFV (IC50 determination in individual incubation)

CLP (µM)	EFV conc. Cs (µM)	Area of EFV / Area of IS 0 min As	Area of EFV / Area of IS 30 min Au	Cu_{30min}= Au*Cs/As	C=Cs_{0min}-Cu_{30min}	*C/30min/0.5 (µM/min/mg protein)	*Residual Activity (%)
0	20	2.955	2.862	19.366	0.634	0.042	100.000
1	20	2.962	2.917	19.694	0.306	0.020	48.286
5	20	2.967	2.936	19.787	0.213	0.014	33.552
10	20	2.967	2.946	19.860	0.140	0.009	22.051

*Average of two experiments

Table 8.19c: Inhibitory effect of varying concentrations of KET on 10µM ATV (IC50 determination in individual incubation)

KET (µM)	ATV conc. Cs (µM)	Area of ATV/ Area of IS 0 min As	Area of ATV/ Area of IS 30 min Au	Cu_{30min}= Au*Cs/As	C=Cs_{0min}-Cu_{30min}	*C/30min/0.5 (µM/min/mg protein)	*Residual Activity (%)
0	10	3.221	2.945	9.143	0.857	0.057	100.000
1	10	3.217	3.102	9.642	0.358	0.024	41.768
3	10	3.206	3.133	9.770	0.230	0.015	26.836
10	10	3.227	3.185	9.869	0.131	0.009	15.278

*Average of two experiments

Table 8.20a: Inhibitory effect of varying concentrations of FLX on 50µM DIC (IC50 determination in cocktail incubation)

FLX (µM)	DIC conc. Cs (µM)	Area of DIC/ Area of IS 0 min As	Area of DIC/ Area of IS 30 min Au	Cu_{30min}= Au*Cs/As	C=Cs_{0min}-Cu_{30min}	*C/30min/0.5 (µM/min/mg protein)	*Residual Activity (%)
0	50	0.815	0.735	45.084	4.916	0.328	100.000
25	50	0.812	0.760	46.781	3.219	0.215	65.474
50	50	0.812	0.775	47.720	2.280	0.152	46.385
100	50	0.814	0.794	48.773	1.227	0.082	24.948

*Average of two experiments

Table 8.20b: Inhibitory effect of varying concentrations of CLP on 20µM EFV (IC50 determination in cocktail incubation)

CLP (µM)	EFV conc. Cs (µM)	Area of EFV / Area of IS 0 min As	Area of EFV / Area of IS 30 min Au	Cu_{30min}= Au*Cs/As	C=Cs_{0min}-Cu_{30min}	*C/30min/0.5 (µM/min/mg protein)	*Residual Activity (%)
0	20	2.952	2.855	19.343	0.657	0.044	100.000
1	20	2.949	2.901	19.675	0.325	0.022	49.495
5	20	2.954	2.922	19.784	0.216	0.014	32.937
10	20	2.957	2.934	19.844	0.156	0.010	23.715

*Average of two experiments

Table 8.20c: Inhibitory effect of varying concentrations of KET on 10µM ATV (IC50 determination in cocktail incubation)

KET (µM)	ATV conc. Cs (µM)	Area of ATV / Area of IS 0 min As	Area of ATV / Area of IS 30 min Au	Cu_{30min}= Au*Cs/As	C=Cs_{0min}-Cu_{30min}	*C/30min/0.5 (µM/min/mg protein)	*Residual Activity (%)
0	10	3.273	2.989	9.134	0.866	0.058	100.000
1	10	3.268	3.140	9.609	0.391	0.026	45.106
3	10	3.272	3.202	9.787	0.213	0.014	24.606
10	10	3.269	3.233	9.889	0.111	0.007	12.793

*Average of two experiments

Table 8.21a: Inhibitory effect of varying concentrations of MCR-706 on 50µM CHZ (IC50 determination in individual incubation)

MCR-706 (µM)	CHZ conc. Cs (µM)	Area of CHZ/ Area of IS 0 min As	Area of CHZ/ Area of IS 30 min Au	Cu_{30min}= Au*Cs/As	C=Cs_{0min}-Cu_{30min}	*C/30min/0.5 (µM/min/mg protein)	*Residual Activity (%)
0	50	0.472	0.416	44.088	5.912	0.394	100.000
50	50	0.475	0.442	46.484	3.516	0.234	59.475
75	50	0.474	0.446	47.091	2.909	0.194	49.207
100	50	0.478	0.454	47.462	2.538	0.169	42.923

*Average of two experiments

Table 8.21b: Inhibitory effect of varying concentrations of MCR-706 on 10µM ATV (IC50 determination in individual incubation)

MCR-706 (µM)	ATV conc. Cs (µM)	Area of ATV/ Area of IS 0 min As	Area of ATV/ Area of IS 30 min Au	Cu_{30min}= Au*Cs/As	C=Cs_{0min}-Cu_{30min}	*C/30min/0.5 (µM/min/mg protein)	*Residual Activity (%)
0	10	3.450	3.202	9.281	0.719	0.048	100.000
50	10	3.474	3.350	9.644	0.356	0.024	49.489
75	10	3.437	3.350	9.747	0.253	0.017	35.240
100	10	3.466	3.396	9.798	0.202	0.013	28.090

*Average of two experiments

Table 8.21c: Inhibitory effect of varying concentrations of MCR-706 on 50µM DIC (IC50 determination in individual incubation)

MCR-706 (µM)	DICconc. Cs (µM)	Area of DIC/ Area of IS 0 min As	Area of DIC/ Area of IS 30 min Au	Cu_{30min}= Au*Cs/As	C=Cs_{0min}-Cu_{30min}	*C/30min/0.5 (µM/min/mg protein)	*Residual Activity (%)
0	50	0.803	0.726	45.207	4.793	0.320	100.000
50	50	0.801	0.772	48.203	1.797	0.120	37.480
75	50	0.801	0.777	48.482	1.518	0.101	31.675
100	50	0.800	0.780	48.754	1.246	0.083	25.988

*Average of two experiments

Table 8.21d: Inhibitory effect of varying concentrations of MCR-706 on 20µM EFV (IC50 determination in individual incubation)

MCR-706 (µM)	EFVconc. Cs (µM)	Area of EFV/ Area of IS 0 min As	Area of EFV/ Area of IS 30 min Au	Cu_{30min}= Au*Cs/As	C=Cs_{0min}-Cu_{30min}	*C/30min/0.5 (µM/min/mg protein)	*Residual Activity (%)
0	20	2.982	2.839	19.040	0.960	0.064	100.000
50	20	2.999	2.897	19.319	0.681	0.045	70.931
75	20	2.967	2.886	19.451	0.549	0.037	57.155
100	20	2.967	2.901	19.559	0.441	0.029	45.976

*Average of two experiments

Table 8.22a: Inhibitory effect of varying concentrations of MCR-706 on 50µM CHZ (IC50 determination in cocktail incubation)

MCR-706 (µM)	CHZ conc. Cs (µM)	Area of CHZ/ Area of IS 0 min As	Area of CHZ/ Area of IS 30 min Au	Cu_{30min}= Au*Cs/As	C=Cs_{0min}-Cu_{30min}	*C/30min/0.5 (µM/min/mg protein)	*Residual Activity (%)
0	50	0.474	0.415	43.782	6.218	0.415	100.000
50	50	0.474	0.440	46.369	3.631	0.242	58.393
75	50	0.476	0.446	46.897	3.103	0.207	49.899
100	50	0.474	0.448	47.300	2.700	0.180	43.424

*Average of two experiments

Table 8.22b: Inhibitory effect of varying concentrations of MCR-706 on 10µM ATV (IC50 determination in cocktail incubation)

MCR-706 (µM)	ATV conc. Cs (µM)	Area of ATV/ Area of IS 0 min As	Area of ATV/ Area of IS 30 min Au	Cu_{30min}= Au*Cs/As	C=Cs_{0min}-Cu_{30min}	*C/30min/0.5 (µM/min/mg protein)	*Residual Activity (%)
0	10	3.460	3.246	9.381	0.619	0.041	100.000
50	10	3.448	3.352	9.722	0.278	0.019	44.916
75	10	3.437	3.356	9.762	0.238	0.016	38.384
100	10	3.456	3.404	9.849	0.151	0.010	24.367

*Average of two experiments

Table 8.22c: Inhibitory effect of varying concentrations of MCR-706 on 50µM DIC (IC50 determination in cocktail incubation)

MCR-706 (µM)	DICconc. Cs (µM)	Area of DIC/ Area of IS 0 min As	Area of DIC/ Area of IS 30 min Au	Cu_{30min}= Au*Cs/As	C=Cs_{0min}-Cu_{30min}	*C/30min/0.5 (µM/min/mg protein)	*Residual Activity (%)
0	50	0.795	0.728	45.792	4.208	0.281	100.000
50	50	0.795	0.769	48.339	1.661	0.111	39.472
75	50	0.798	0.776	48.661	1.339	0.089	31.817
100	50	0.796	0.780	48.961	1.039	0.069	24.701

*Average of two experiments

Table 8.22d: Inhibitory effect of varying concentrations of MCR-706 on 20µM EFV (IC50 determination in cocktail incubation)

MCR-706 (µM)	EFVconc. Cs (µM)	Area of EFV/ Area of IS 0 min As	Area of EFV/ Area of IS 30 min Au	Cu_{30min}= Au*Cs/As	C=Cs_{0min}-Cu_{30min}	*C/30min/0.5 (µM/min/mg protein)	*Residual Activity (%)
0	20	3.021	2.830	18.733	1.267	0.084	100.000
50	20	3.022	2.892	19.137	0.863	0.058	68.117
75	20	2.991	2.879	19.249	0.751	0.050	59.263
100	20	2.995	2.910	19.433	0.567	0.038	44.754

*Average of two experiments

Table 8.23a: Effect of varying concentrations of MCR-742 on 50µM DIC in individual incubation.

MCR-742	DIC conc. Cs (µM)	Area of DIC/ Area of IS 0 min As	Area of DIC/ Area of IS 30 min Au	Cu_{30min}= Au*Cs/As	C=Cs_{0min}-Cu_{30min}	*C/30min/0.5 (µM/min/mg protein)	*Residual Activity (%)
0	50	0.690	0.629	45.635	4.365	0.291	100.000
25	50	0.691	0.638	46.128	3.872	0.258	88.686
50	50	0.690	0.628	45.533	4.467	0.298	102.336
100	50	0.689	0.630	45.729	4.271	0.285	97.831

*Average of two experiments

Table 8.23b: Effect of varying concentrations of MCR-742 on 50µM ATV in individual incubation.

MCR-742	DIC conc. Cs (µM)	Area of ATV/ Area of IS 0 min As	Area of ATV/ Area of IS 30 min Au	Cu_{30min}= Au*Cs/As	C=Cs_{0min}-Cu_{30min}	*C/30min/0.5 (µM/min/mg protein)	*Residual Activity (%)
0	50	2.030	1.884	9.280	0.720	0.048	100.000
25	50	2.011	1.882	9.358	0.642	0.043	89.231
50	50	1.968	1.828	9.287	0.713	0.048	99.010
100	50	1.940	1.784	9.196	0.804	0.054	111.774

*Average of two experiments

Table 8.23c: Effect of varying concentrations of MCR-742 on 50µM CHZ in individual incubation.

MCR-742 (µM)	CHZ conc. Cs (µM)	Area of CHZ/ Area of IS 0 min As	Area of CHZ/ Area of IS 30 min Au	Cu_{30min}= Au*Cs/As	C=Cs_{0min}-Cu_{30min}	*C/30min/0.5 (µM/min/mg protein)	*Residual Activity (%)
0	50	0.563	0.517	45.931	4.069	0.271	100.000
50	50	0.563	0.517	45.835	4.165	0.278	102.375
75	50	0.564	0.522	46.270	3.730	0.249	91.672
100	50	0.563	0.516	45.784	4.216	0.281	103.617

*Average of two experiments

Table 8.23d: Effect of varying concentrations of MCR-742 on 50µM EFV in individual incubation.

MCR-742	EFV conc. Cs (µM)	Area of EFV/ Area of IS 0 min As	Area of EFV/ Area of IS 30 min Au	Cu_{30min}= Au*Cs/As	C=Cs_{0min}-Cu_{30min}	*C/30min/0.5 (µM/min/mg protein)	*Residual Activity (%)
0	50	3.019	2.762	18.297	1.703	0.114	100.000
25	50	3.031	2.779	18.336	1.664	0.111	97.708
50	50	3.007	2.755	18.324	1.676	0.112	98.439
100	50	3.016	2.751	18.239	1.761	0.117	103.430

*Average of two experiments

Table 8.24a: Effect of varying concentrations of MCR-742 on 50µM DIC in cocktail incubation.

MCR-742	DIC conc. Cs (µM)	Area of DIC/ Area of IS 0 min As	Area of DIC/ Area of IS 30 min Au	Cu_{30min}= Au*Cs/As	C=Cs_{0min}-Cu_{30min}	*C/30min/0.5 (µM/min/mg protein)	*Residual Activity (%)
0	50	0.670	0.635	47.417	2.583	0.172	100.000
25	50	0.671	0.640	47.678	2.322	0.155	89.898
50	50	0.671	0.636	47.340	2.660	0.177	102.958
100	50	0.670	0.636	47.464	2.536	0.169	98.148

*Average of two experiments

Table 8.24b: Effect of varying concentrations of MCR-742 on 50µM ATV in cocktail incubation.

MCR-742	DIC conc. Cs (µM)	Area of ATV/ Area of IS 0 min As	Area of ATV/ Area of IS 30 min Au	Cu_{30min}= Au*Cs/As	C=Cs_{0min}-Cu_{30min}	*C/30min/0.5 (µM/min/mg protein)	*Residual Activity (%)
0	50	2.076	1.949	9.387	0.613	0.041	100.000
25	50	2.068	1.955	9.456	0.544	0.036	88.769
50	50	2.078	1.946	9.366	0.634	0.042	103.456
100	50	2.077	1.939	9.336	0.664	0.044	108.265

*Average of two experiments

Table 8.24c: Effect of varying concentrations of MCR-742 on 50µM CHZ in cocktail incubation.

MCR-742 (µM)	CHZ conc. Cs (µM)	Area of CHZ/ Area of IS 0 min As	Area of CHZ/ Area of IS 30 min Au	Cu_{30min}= Au*Cs/As	C=Cs_{0min}-Cu_{30min}	*C/30min/0.5 (µM/min/mg protein)	*Residual Activity (%)
0	50	0.562	0.519	46.176	3.824	0.255	100.000
50	50	0.557	0.511	45.869	4.131	0.275	108.023
75	50	0.557	0.514	46.202	3.798	0.253	99.304
100	50	0.556	0.508	45.711	4.289	0.286	112.145

*Average of two experiments

Table 8.24d: Effect of varying concentrations of MCR-742 on 50µM EFV in cocktail incubation.

MCR-742	EFV conc. Cs (µM)	Area of EFV/ Area of IS 0 min As	Area of EFV/ Area of IS 30 min Au	Cu_{30min}= Au*Cs/As	C=Cs_{0min}-Cu_{30min}	*C/30min/0.5 (µM/min/mg protein)	*Residual Activity (%)
0	50	2.969	2.722	18.336	1.664	0.111	100.000
25	50	2.958	2.707	18.301	1.699	0.113	102.092
50	50	2.970	2.736	18.422	1.578	0.105	94.830
100	50	2.971	2.705	18.207	1.793	0.120	107.749

*Average of two experiments

8.10 RESULTS

Experimentally the inhibition reactions were evaluated via two approaches

I. individual dosing of a substrate (CHZ,ATV,DIC,EFV) and of an inhibitor (KET,FLX,CLP,MCR-706,MCR-742).
II. cassette dosing of substrates (CHZ,ATV,DIC,EFV) combined with individual dosing of inhibitor (KET,FLX,CLP,MCR-706,MCR-742).

8.10.1 IC_{50} determinations of known CYP inhibitors:

The method was validated by incubating known CYP inhibitors (clopidogrel, CYP2B6; fluoxetine, CYP2C9 and ketoconazole, CYP3A4; with the individual substrate they were known to inhibit (EFV; DIC; and ATV respectively) and with the substrate cocktail. The inhibition curves obtained from these experiments are shown in Table 8.25(a-c) and Figure 8.15(a-c) for individual incubation and in Table 8.26(a-c) and Fig. 8.16 (a-c) for cocktail incubation. The IC_{50} values measured by two approaches are summarized in Table 8.26a and 8.26b. Both the approaches generated similar IC_{50} values for each CYP isozyme and all measured IC_{50} values were compared with the literature values [5-7] as shown in Table 8.26c.

CLP, FLX, KET at 1, 50 and 1 µM caused 48.28, 38.92 and 41.76% inhibition of EFV, DIC, and ATV hydroxylation respectively in individual incubation while in cocktail incubation it showed 49.49, 46.385 and 45.106% inhibition respectively. The IC_{50} values of 1.51, 37.95 and 0.88 µM determined with the individual substrates were in good agreement with the IC_{50} values of 1.58, 41.8 and 0.90 µM using the substrate cocktail of EFV/DIC/ATV as shown in Table 8.26c.The IC_{50} values determined using the individual substrates agreed with the values determined using substrate cocktail. Generally a good agreement should also exist between the IC_{50} values (individual & cocktail) and known literature values. Exception to this agreement with published IC50 values of 0.046, 33, and 0.72 µM is observed for CLP/FLX/KET in this study. This could be due to the use of different substrates or expressed enzyme versus human liver microsomes.

The Ki values were also estimated (using the formula Table 8.26d and 8.26e) using obtained IC50 values of CLP, FLX, and KET when co incubated with their respective substrate at fixed concentration (at fixed or below its Km values) in individual and cocktail incubation. Table 8.30a and 8.30b summarizes the Graphpad Prism data stating

the best fit values of IC50 for standard error, 95% confidence intervals and goodness of fit CLP, FLX, KET.

Table 8.25a: Inhibitory effect of varying concentrations (log) of FLX on DIC in individual incubation (IC50 determination).

FLX (µM)	FLX log conc. Cs (µM)	Residual Activity (%)
0	0.000	100.000
25	1.398	66.065
50	1.699	38.925
100	2.000	25.437

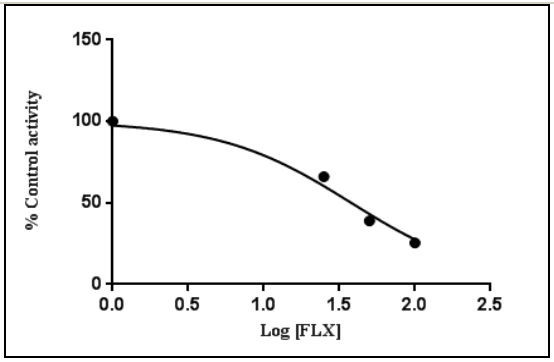

Fig.8.15a. Inhibitory effect of FLX on DIC in individual incubation.

Table 8.25b: Inhibitory effect of varying concentrations (log) of CLP on EFV in individual incubation (IC50 determination)

CLP (µM)	CLP log conc. (µM)	Residual Activity (%)
0.0	---	100.000
1.0	0.000	48.286
5.0	0.699	33.552
10.0	1.000	22.051

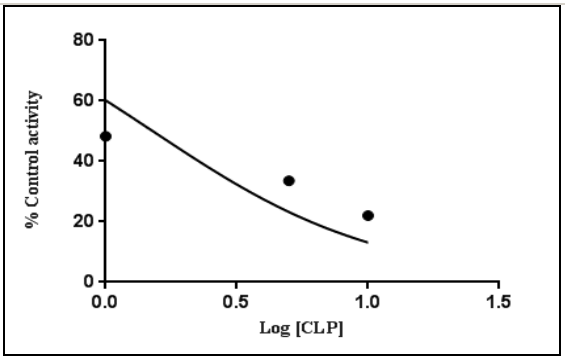

Fig.8.15b. Inhibitory effect of CLP on EFV in individual incubation

Table 8.25c: Inhibitory effect of varying concentrations (log) of KET on ATV in individual incubation (IC50 determination)

KET (µM)	KET log conc. (µM)	Residual Activity (%)
0	---	100
1	0.000	41.768
3	0.477	26.836
10	1.000	15.278

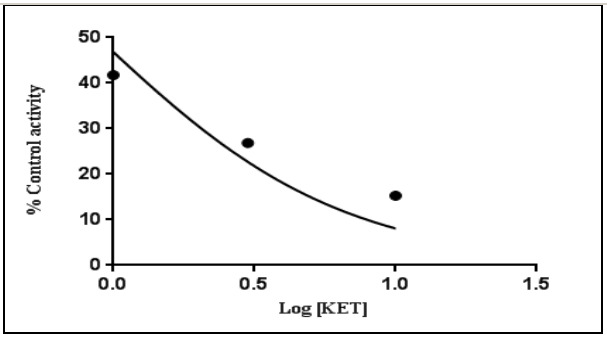

Fig.8.15c . Inhibitory effect of KET on ATV in individual incubation

Table 8.26a: Inhibitory effect of varying concentrations (log) of FLX on DIC in cocktail incubation (IC50 determination)

FLX (µM)	FLX log conc. (µM)	Residual Activity (%)
0	---	100.000
25	1.398	65.474
50	1.699	46.385
100	2.000	24.948

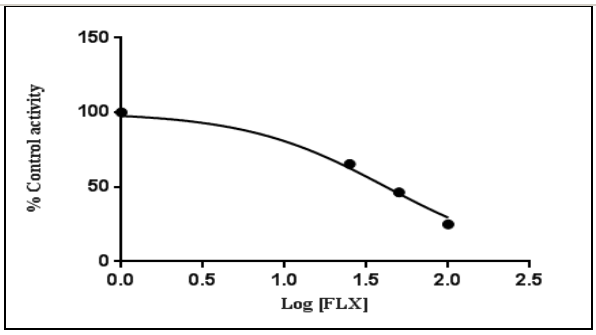

Fig.8.16a. Inhibitory effect of FLX on DIC in cocktail incubation.

Table 8.26b: Inhibitory effect of varying concentrations (log) of CLP on EFV in cocktail incubation (IC50 determination)

CLP (µM)	CLP log conc. (µM)	Residual Activity (%)
0.0	---	100.000
1.0	1.398	49.495
5.0	1.699	32.937
10.0	2.000	23.715

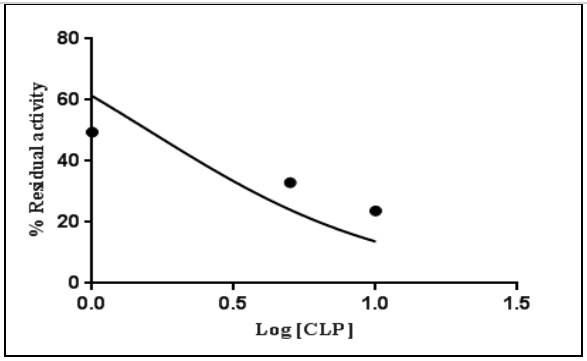

Fig.8.16b Inhibitory effect of CLP on EFV in cocktail incubation.

Table 8.26c: Inhibitory effect of varying concentrations (log) of KET on ATV in cocktail incubation (IC50 determination)

KET (µM)	KET log conc. (µM)	Residual Activity (%)
0	---	100.000
1	0.000	45.106
3	0.477	24.606
10	1.000	12.793

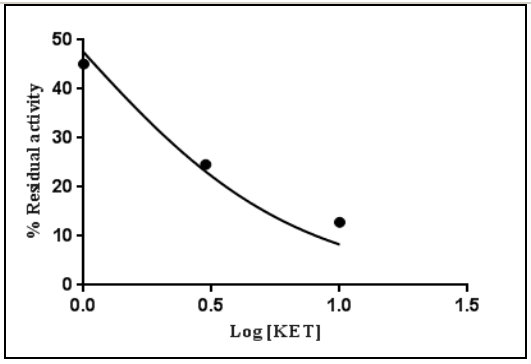

Fig.8.16c. Inhibitory effect of KET on ATV in cocktail incubation

Table 8.26d: Estimation of Ki from individual incubation data.

Probe Substrates	Conc. (µM)	Km from individual plot (µM)	[S]/Km	Inhibitors	IC50 for inhibitors from individual plot (µM)	Ki = IC50/(1+[S]/Km) (µM)
DIC	50	51.94	0.963	**FLX**	**37.95**	**21.12**
ATV	10	57.79	0.173	**KET**	**0.88**	**0.75**
EFV	20	64.96	0.308	**CLP**	**1.51**	**1.16**
CHZ	--	--	--	NA	--	--

NA: Not applicable

Table 8.26e: Estimation of Ki from cocktail incubation data.

Probe Substrates	Conc. (µM)	Km from cocktail plot (µM)	[S]/Km	Inhibitors	IC50 for inhibitors from cocktail plot (µM)	Ki = IC50/(1+[S]/Km) (µM)
DIC	50	61.22	0.963	**FLX**	**41.8**	**23.01**
ATV	10	53.81	0.173	**KET**	**0.90**	**0.76**
EFV	20	66.62	0.308	**CLP**	**1.58**	**1.24**
CHZ	--	--	--	NA	--	--

NA: Not applicable

Table 8.26f: Comparison of IC50s obtained using individual and cocktail substrate incubations with literature value.

CYP enzyme	Inhibitor	IC50 (µM)		
		Individual substrate	Cocktail	Literature[5-7]
3A4	Ketoconazole	0.88	0.90	0.72
2B6	Clopidogrel	1.51	1.58	0.046
2C9	Fluoxetine	37.95	41.8	33
2E1	NA	--	--	--

NA: Not applicable

8.10.2 IC_{50} determinations of NME's (MCR-706 & MCR-742) as inhibitors:

The validated method was used to assess the inhibition potential of two NME's, MCR-706 and MCR-742. The method was evaluated by incubating MCR-706 and MCR-742 separately with the substrate's CHZ, ATV, DIC and EFV. The individual incubation as well as cocktail incubation was carried out for both the NME's. The inhibition curves obtained for MCR-706 from these experiments are shown in Table 8.27(a-d) and Fig. 8.18(a-d) for individual incubation and in Table 8.28(a-d) and Fig. 8.19 (a-d) for cocktail incubation.

For MCR-706, the IC_{50} values of 32.99, 43.44, 73.80 and 99.74 µM determined with the individual substrates were in good agreement with the IC_{50} values of 33.63, 40.34, 73.94 and 97.4 µM using the substrate cocktail of DIC/ATV/CHZ/EFV as shown in Table 8.29a and 8.29b.The IC_{50} values determined using the individual substrates agreed with the values determined using substrate cocktail.

The combined plot (Figure 8.20a.) of inhibitory effect of MCR-706 on DIC, ATV, CHZ and EFV shows that MCR-706 had a lowest IC50 value of 32.99 µM for DIC as well as Ki value of 33.95 µM in individual incubation. Similarly in cocktail incubation also MCR-706 showed a lowest IC50 value of 33.63µM for DIC as well as Ki value of 34.45

µM. This suggests that MCR-706 has highest inhibition potential for CYP2C9 isoform which predicts that MCR-706 is a **selective inhibitor** of CYP2C9. A Bar graph (Figure 8.20c.) of the Ki values of MCR-706 for CYP2C9(DIC), CYP3A4(ATV), CYP2E1(CHZ) and CYP2B6 (EFV) shows that the values obtained in individual incubation are in close agreement with cocktail incubation.

Thus the potential inhibitory activity of MCR-706 on DIC, ATV, CHZ and EFV hydroxylation can be judged as **CYP2C9>CYP3A4>CYP2E1>CYP2B6**.That is MCR-706 has lowest inhibition potential for CYP2B6 isoform with highest IC_{50} value of 99.74 and 97.4 µM respectively in individual as well as cocktail incubation. Table 8.30c and 8.30d summarizes the Graphpad Prism data stating the best fit values of IC50 for standard error, 95% confidence intervals and goodness of fit for DIC, ATV, CHZ and EFV.

In case of MCR-742 it was observed that in spite of being treated as a inhibitor in incubation medium, there was continuous decrease in area of probe substrates as is depicted in Table 8.23(a-d) for individual and in Table 8.24(a-d) for cocktail incubation. Hence IC50 values and Ki values for MCR-742 against DIC, ATV, CHZ and EFV hydroxylation were not estimated. The observations for MCR-742 shows that it is still undergoing metabolism suggesting it does not have significant inhibitory effect on any of these CYP2C9, CYP3A4, CYP2E, CYP2B6 isoforms. This may be a possibility that MCR-742 itself undergoes metabolism or it does have inhibition potential towards CYP isoforms other than those used in the study.

Table 8.27a: Inhibitory effect of varying concentrations (log) of MCR-706 on CHZ in individual incubation (IC50 determination)

MCR-706 (µM)	MCR-706 (µM)	Residual Activity (%)
0	0	100.000
50	1.699	59.475
75	1.875	49.207
100	2.000	42.923

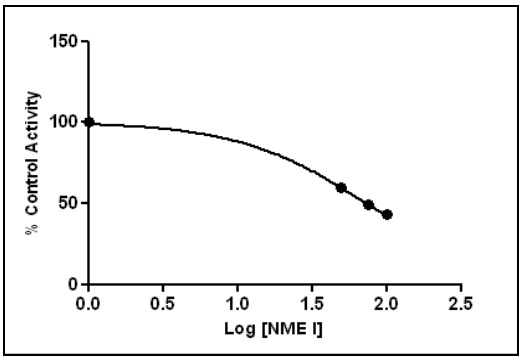

Fig.8.17a. Inhibitory effect of MCR-706 on CHZ in individual incubation.

Table 8.27b: Inhibitory effect of varying concentrations (log) of MCR-706 on ATV in individual incubation (IC50 determination)

MCR-706 (µM)	MCR-706 log conc. Cs (µM)	*Residual Activity (%)
0	0	100.000
50	1.699	49.489
75	1.875	35.240
100	2.000	28.090

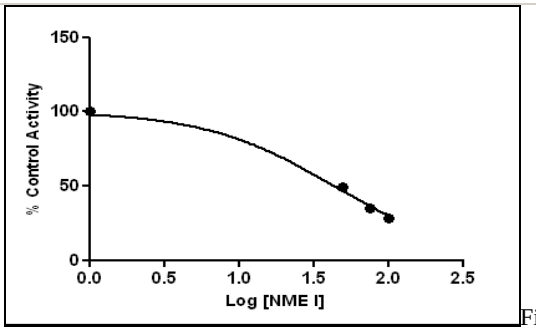

Fig.8.17b. Inhibitory effect of MCR-706 on ATV in individual incubation.

Table 8.27c: Inhibitory effect of varying concentrations (log) of MCR-706 on DIC in individual incubation (IC50 determination)

MCR-706 (µM)	MCR-706 log conc. Cs (µM)	Residual Activity (%)
0	0	100.000
50	1.699	37.480
75	1.875	31.675
100	2.000	25.988

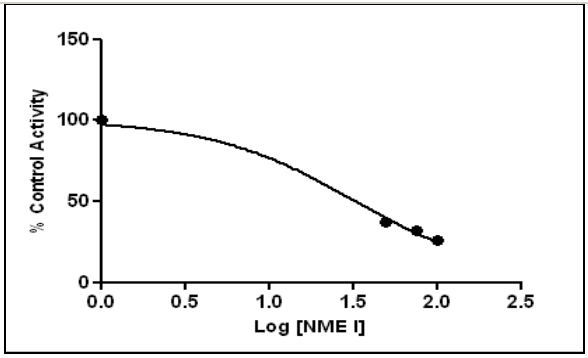

Fig.8.18c. Inhibitory effect of MCR-706 on DIC in individual incubation.

Table 8.27d: Inhibitory effect of varying concentrations (log) of MCR-706 on EFV in individual incubation (IC50 determination)

MCR-706 (µM)	MCR-706 log conc. Cs (µM)	Residual Activity (%)
0	0	100.000
50	1.699	70.931
75	1.875	57.155
100	2.000	45.976

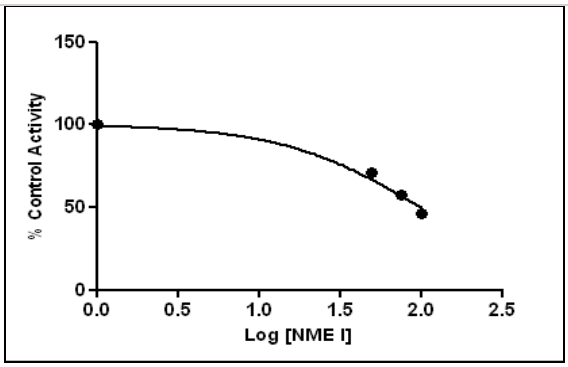

Fig.8.18d. Inhibitory effect of MCR-706 on EFV in individual incubation

Table 8.28a: Inhibitory effect of varying concentrations (log) of MCR-706 on CHZ in cocktail incubation (IC50 determination)

MCR-706 (µM)	MCR-706 log conc. Cs (µM)	Residual Activity (%)
0	0	100.000
50	1.699	58.393
75	1.875	49.899
100	2.000	43.424

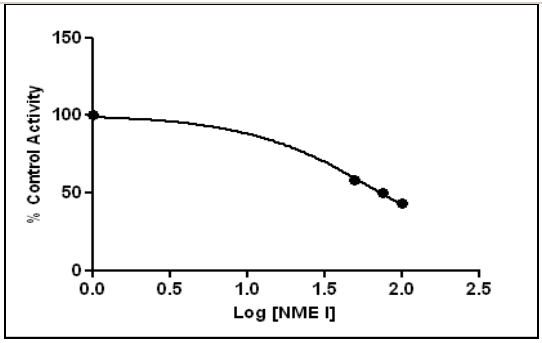

Fig.8.19a. Inhibitory effect of MCR-706 on CHZ in cocktail incubation.

Table 8.28b: Inhibitory effect of varying concentrations (log) of MCR-706 on ATV in cocktail incubation (IC50 determination)

MCR-706 (µM)	MCR-706 log conc. Cs (µM)	Residual Activity (%)
0	0	100.000
50	1.699	44.916
75	1.875	38.384
100	2.000	24.367

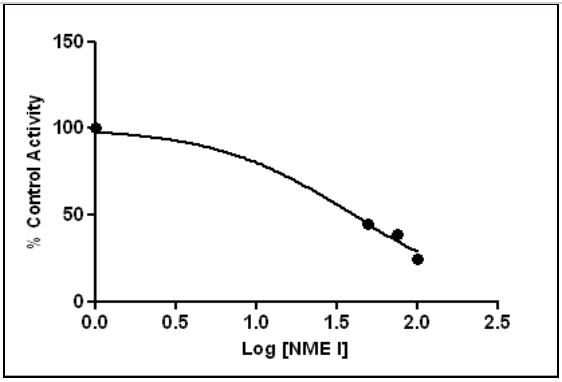

Fig.8.19b. Inhibitory effect of MCR-706 on ATV in cocktail incubation

Table 8.28c: Inhibitory effect of varying concentrations (log) of MCR-706 on DIC in cocktail incubation (IC50 determination)

MCR-706 (µM)	MCR-706 log conc. Cs (µM)	Residual Activity (%)
0	0	100.000
50	1.699	39.472
75	1.875	31.817
100	2.000	24.701

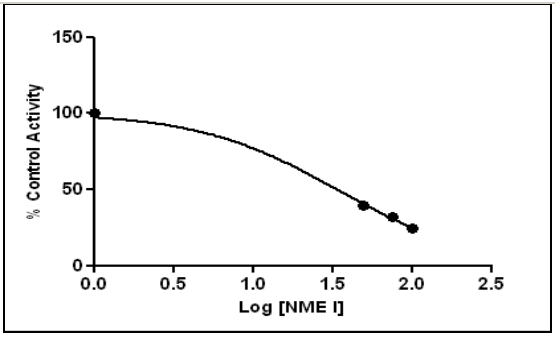

Fig.8.19c. Inhibitory effect of MCR-706 on DIC in cocktail incubation.

Table 8.28d: Inhibitory effect of varying concentrations (log) of MCR-706 on EFV in cocktail incubation (IC50 determination)

MCR-706 (µM)	MCR-706 log conc. Cs (µM)	Residual Activity (%)
0	0	100.000
50	1.699	68.117
75	1.875	59.263
100	2.000	44.754

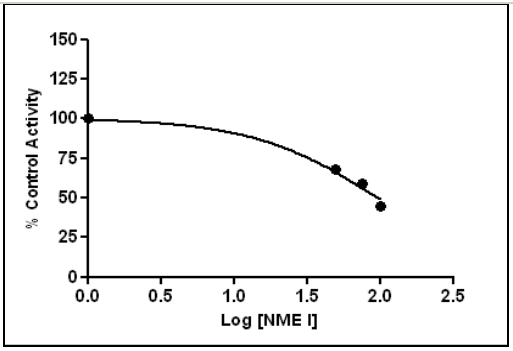

Fig.8.19d. Inhibitory effect of MCR-706 on EFV in cocktail incubation

Table 8.29a: Estimation of Ki for MCR-706 from individual incubation data.

Probe Substrates	Conc. (µM)	IC50 for MCR-706 from individual plot (µM)	Km from individual plot (µM)	[S]/Km	Ki = IC50/(1+[S]/Km) (µM)
DIC	50	**32.99**	51.94	0.963	33.95
ATV	10	**43.44**	57.79	0.173	43.61
CHZ	50	**73.80**	62.74	0.797	74.60
EFV	20	**99.74**	64.96	0.308	100.05

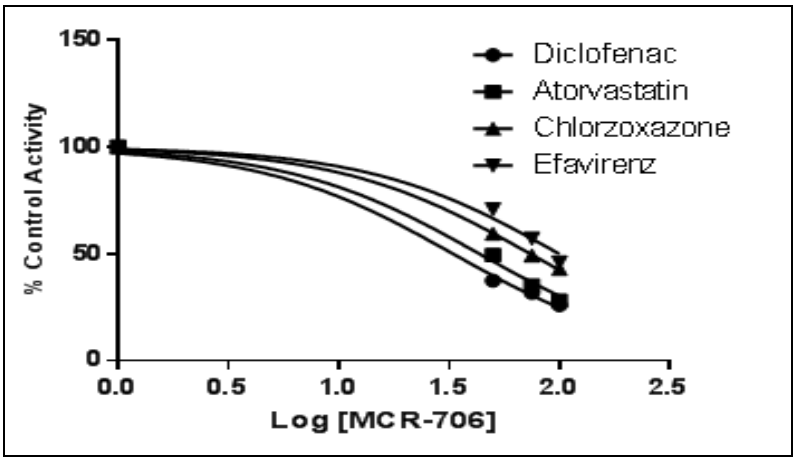

Figure 8.20a. Combined plot of inhibitory effect of MCR-706 on DIC, ATV, CHZ, EFV in individual incubation.

Table 8.29b: Estimation of Ki for MCR-706 from cocktail incubation data.

Probe Substrates	Conc. (µM)	IC50 for MCR-706 from cocktail plot (µM)	Km from cocktail plot (µM)	[S]/Km	Ki = IC50/(1+[S]/Km) (µM)
DIC	50	**33.63**	61.22	0.817	34.45
ATV	10	**40.34**	53.81	0.186	40.53
CHZ	50	**73.94**	66.62	0.751	74.69
EFV	20	**97.4**	72.41	0.276	97.68

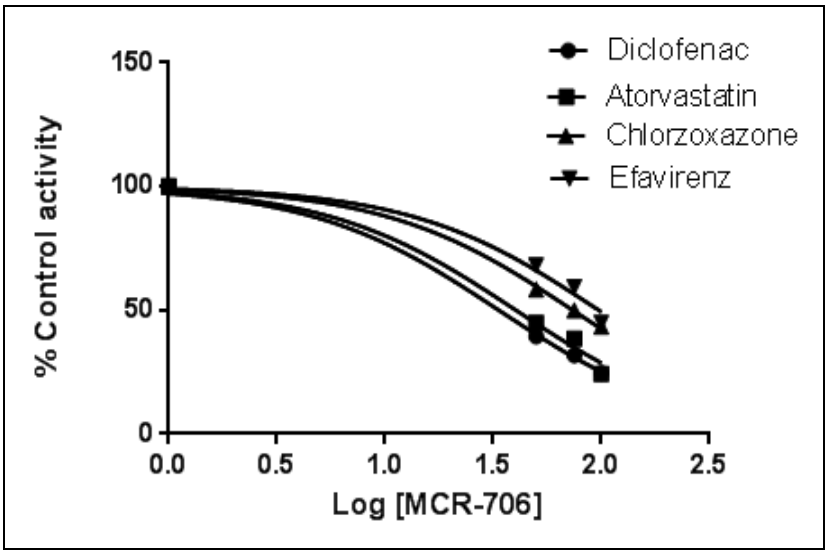

Figure 8.20b. Combined plot of inhibitory effect of MCR-706 on DIC, ATV, CHZ, EFV in cocktail incubation.

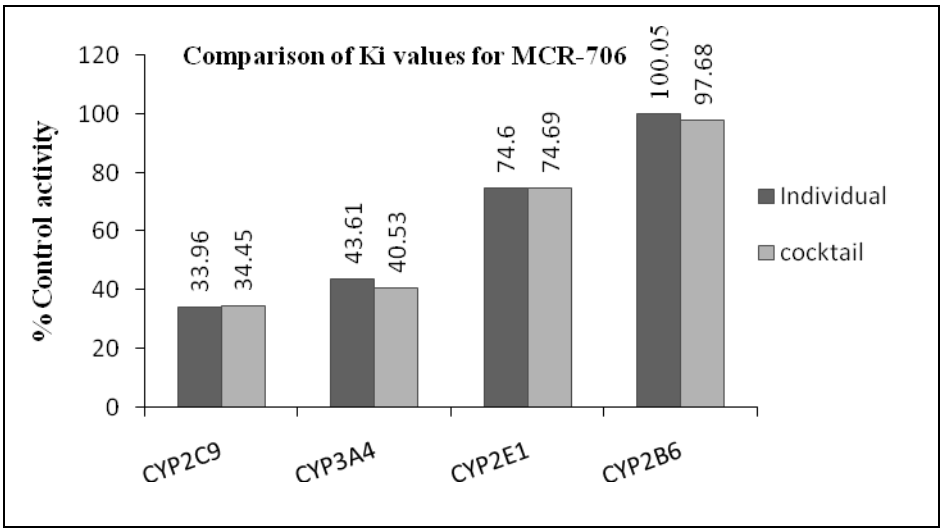

Figure 8.20c. Comparison of the Ki values of MCR-706 on CYP2C9(DIC),CYP3A4(ATV), CYP2E1 (CHZ) and CYP2B6 (EFV) showing that the values obtained in individual incubation are in close agreement with cocktail incubation.

Table 8.30a:Graphpad Prism data of log(inhibitor) vs. normalized response for ATV, EFV and DIC in individual incubation.

log(inhibitor) vs. normalized response	Ketoconazole (Atorvastatin hydroxylation)	Clopidogrel (Efavirenz hydroxylation)	Fluoxetine (Diclofenac hydroxylation)
Best-fit values			
LogIC50(µM)	-0.05512	0.1799	1.579
IC50(µM)	0.8808	1.513	37.95
Std. Error			
LogIC50(µM)	0.09514	0.1739	0.04974
95% Confidence Intervals			
LogIC50(µM)	-0.4645 to 0.3543	-0.5686 to 0.9284	1.421 to 1.737
IC50(µM)	0.3432 to 2.261	0.2700 to 8.480	26.36 to 54.63
Goodness of Fit			
Degrees of Freedom	0.7325	2	3
R square	94.37	0.05157	0.9809
Points analysed	3	3	3

Table 8.30b: Graphpad Prism data of log(inhibitor) vs. normalized response for ATV, EFV and DIC in cocktail incubation.

log(inhibitor) vs. normalized response	Ketoconazole (Atorvastatin hydroxylation)	Clopidogrel (Efavirenz hydroxylation)	Fluoxetine (Diclofenac hydroxylation)
Best-fit values			
LogIC50(µM)	-0.04344	0.2001	1.621
IC50(µM)	0.9048	1.585	41.8
Std. Error			
LogIC50(µM)	0.05148	0.1704	0.03713
95% Confidence Intervals			
LogIC50(µM)	-0.2649 to 0.1781	-0.5331 to 0.9333	1.503 to 1.739
IC50(µM)	0.5433 to 1.507	0.2930 to 8.577	31.85 to 54.88
Goodness of Fit			
Degrees of Freedom	2	2	3
R square	0.9476	0.06524	0.9885
Points analysed	3	3	3

Table 8.30c: Graphpad Prism data of log(inhibitor) vs. normalized response for DIC, ATV, EFV and CHZ in individual incubation.

log(inhibitor) vs. normalized response	MCR-706 (on Diclofenac hydroxylation)	MCR-706 (on Atorvastatin hydroxylation)	MCR-706 (on Chlorzoxazone hydroxylation)	MCR-706 (on Efavirenz hydroxylation)
Best-fit values				
LogIC50(µM)	1.518	1.638	1.868	1.999
IC50(µM)	32.99	43.44	73.8	99.74
Std. Error				
LogIC50(µM)	0.0274	0.02861	0.008698	0.03593
95% Confidence Intervals				
LogIC50(µM)	1.431 to 1.606	1.547 to 1.729	1.840 to 1.896	1.885 to 2.113
IC50(µM)	26.99 to 40.32	35.22 to 53.56	69.24 to 78.65	76.65 to 129.8
Goodness of Fit				
Degrees of Freedom	3	3	3	3
R square	0.9954	0.9934	0.9989	0.9784
Points analysed	4	4	4	4

Table 8.30d: Graphpad Prism data of log(inhibitor) vs. normalized response for DIC, ATV, EFV and CHZ in cocktail incubation.

log(inhibitor) vs. normalized response	MCR-706 (on Diclofenac hydroxylation)	MCR-706 (on Atorvastatin hydroxylation)	MCR-706 (on Chlorzoxazone hydroxylation)	MCR-706 (on Efavirenz hydroxylation)
Best-fit values				
LogIC50(µM)	1.527	1.606	1.869	1.989
IC50(µM)	33.63	40.34	73.94	97.4
Std. Error				
LogIC50(µM)	0.02104	0.03854	0.01222	0.03507
95% Confidence Intervals				
LogIC50(µM)	1.460 to 1.594	1.483 to 1.728	1.830 to 1.908	1.877 to 2.100
IC50(µM)	28.82 to 39.23	30.42 to 53.51	67.61 to 80.87	75.33 to 125.9
Goodness of Fit				
Degrees of Freedom	3	3	3	3
R square	0.9972	0.9889	0.9978	0.9793
Points analysed	4	4	4	4

8.11 CONCLUSION

A HPLC-PDA method has been developed for the inhibition screening of the four major human CYP enzymes (CYP2B6, CYP2C9, CYP3A4, CYP2E1) using an *in vitro* individual substrate and substrate cocktail. The IC_{50} values of selective CYP inhibitors (ketoconazole, CYP3A4; fluoxetine, CYP2C9; clopidogrel, CYP2B6) and two new molecular entities (MCR-706 and MCR 742) determined using the substrate cocktail were in good agreement with individual substrates. The assay uses human liver microsomes and four probe substrates for the major CYP enzymes at concentrations around the estimated K_m values. The developed assay offers a reliable and sensitive screening method for the prediction of the P450 inhibitory potential of new molecular entities using individual and cocktail substrate incubation approach. It uses well characterized, readily available CYP substrates that are very specific for the particular enzyme probed. The simultaneous assay of four enzymes in a single small volume sample conserves both microsomes and putative inhibitors (both which may be limited in quantity). The developed method has the potential to be used for the characterization of P450 enzyme activity in human liver microsomal preparations. In addition, a P450 inhibition profile using this screening method can allow a number of new molecular entities to be screened rapidly for P450 inhibitory potential, which can help in selection of potential drug candidates, and can guide the quantitative prediction of clinical drug interactions.

8.12 REFERENCES

1. Bjornsson D, Callaghan T, Einolf J, Fischer V, Gan L, Grimm S, Kao J, King P, Miwa G, Ni L, Kumar G, McLeod J, Obach S, Roberts S, Roe A, Shah A, Snikeris F, Sullivan T, Tweedie D, Vega M, Walsh J, Wrighton A; The conduct of *in vitro* and *in vivo* drug-drug interaction studies: A Pharmaceutical Research and Manufacturers of America (PHRMA) perspective. Drug metab Dispos 2003, 31; 815-832.

2. FDA (2006) Guidance for Industry: Drug Interaction Studies-Study Design, Data Analysis, and Implications for Dosing and Labelling [http://www.fda.gov/downloads/Drugs/GuidanceComplianceRegulatoryInformation/Guidances/ucm072101.pdf.]

3. Lahoz A, Donato MT, Castell JV, Gómez- Lechón MJ. Strategies to in vitro assessment of major human CYP enzyme activities by using liquid chromatography tandem mass spectrometry. Curr Drug Metab. 2008 Jan;9(1):12-9.

4. Zientek M, Youdim K. Simultaneous Determination of Multiple CYP Inhibition Constants using a Cocktail-Probe Approach. Methods Mol Biol. 2013;987:11-23.

5. Robert L. Walsky and R. Scott Obach. A Comparison of 2-Phenyl-2-(1-piperidinyl)propane (PPP), 1,1,1" Phosphinothioylidynetrisaziridine (ThioTEPA), Clopidogrel, and Ticlopidine as Selective Inactivators of Human Cytochrome P450 2B6. Vol. 35, No. 1, DMD 35:2053–2059, 2007.

6. Tepy Usia, Tadashi Watabe, Shigetoshi Kadota, and Yasuhiro Tezuka. Potent CYP3A4 Inhibitory Constituents of *Piper cubeba.* American Chemical Society and American Society of Pharmacognosy.2005.

7. Obach RS, Walsky RL, Venkatakrishnan K, Gaman EA, Houston JB, Tremaine LM.The utility of in vitro cytochrome P450 inhibition data in the prediction of drug-drug interactions. J Pharmacol Exp Ther. 2006 Jan;316(1):336-48.

Chapter 9
Summary
&
Conclusion

The overall study was initiated in order to investigate the formation kinetics of the metabolites from parent drug *in vitro* and to predict the specific enzymes involved in its metabolic pathway and possible metabolism based Drug/Drug and Drug/Food interactions as well as to develop a cocktail probe substrate assay system for inhibition screening of multiple CYP isoforms by NME *in vitro* using human liver micrososmes. All these methods and there results are summarized in the following section.

- The study **"*In vitro* oxidative biotransformation of GLM as a model substrate for CYP450''** conclusively demonstrates the use of a 3^3 factorial design in the optimization of initial velocity conditions affecting turnover of GLM. P450 reaction phenotyping is defined as a set of experiments that aim to define which human cytochrome P450 enzyme(s) is involved in a given metabolic transformation. Such data are useful in the prediction of pharmacokinetic drug-drug interactions and interpatient variability in drug exposure. Any prolonged incubation in a closed *in vitro* system such as liver microsomes can cause formation of secondary metabolites from the primary metabolites of a drug. Inactivation or denaturation of enzymes can become significant over time in the *in vitro* systems. Thus it is of critical importance that initial velocity conditions are defined.
- This study examines the effects of the main control factors and attempts to enhance the turnover rate of GLM's oxidative biotransformation by optimizing these factors using full factorial design. The derived reduced polynomial equation, contour plot and response surface plot aid in predicting the values of selected independent variables. Contour plots obtained by applying a computerized optimization process suggested a level of 30 minute incubation time (X2) and 0.5mg/ml protein (X3) as an ideal condition. At this level the turnover rate (%Y) was found to be ranging from 18.91% to 19.91%. Thus the rate of GLM disappearance was linear at the chosen concentrations of substrate using the assay conditions and detection system. However, a decrease in the level of incubation time and protein concentration below the selected level, typically yield nonlinear initial velocities of enzyme activity. Once the optimal conditions (30 min incubation time, 0.5mg/ml HLM) were obtained, the substrate concentration

dependence on the rate of metabolite formation was examined. The K_m (28.9 ± 2.97 µMole) and V_{max} (0.559 ± 0.017 µMole/min/mg protein) values were determined by nonlinear regression of a plot of enzyme activity versus substrate concentration. The Michaelis constant, K_m accounts for the concentration of substrate at which half the active sites are filled. Thus, K_m provides a measure of the substrate concentration required for significant catalysis to occur. V_{max} is the rate at which substrate will be converted to product once bound to the enzyme. A substrate concentration around or below the K_m is ideal for determination of competitive inhibitor activity. The Cl_{int} value as predicted after *in vitro* studies was found to be 0.019 µl/min/mg suggesting a direct measure of enzyme activity towards glimepiride. Hence further inhibition studies are needed to confirm the performance of GLM's oxidative biotransformation *in vitro*.

- It was possible to optimize the turnover of the candidate drugs within the limits of developed assay design such that all subsequent *in vitro* incubations can be performed using the condition that ensures linearity with time and HLM concentration, and less than 20% of the initial substrate is consumed. Thus the precise information about the effects of each factor on metabolism can be used to flexibly adjust the system performance. The best estimates of K_m and V_{max} values were obtained with linear (Michaelis Menten plot) as well as nonlinear transformation (Lineweaver Burk plot) for the enzymatic assay of GLM under initial velocity conditions. The low Km value of GLM (28.9 µMole) as compared to literature value of tolbutamide (50 µMole) for CYP2C9 suggest that enzyme has a high affinity for the substrate GLM. Thus GLM can be used as a alternative probe substrate for CYP2C9 reaction phenotyping of new molecular entities.

- The study ***"In vitro* Evaluation of the Pharmacokinetic Alterations Caused by SMZ on GLM Hydroxylation"** evaluated the inhibitory effects of sulfonamides on GLM metabolism mediated by CYP2C9. With concentrations ranging from 30 to 1100 µMole, SMZ exhibited a selective inhibitory effect on CYP2C9-mediated GLM-hydroxylation with an apparent IC_{50} value of 400 µMole and Ki value of 290 µMole. The pattern of inhibition was found to be competitive as K_m value was

increased (32.26 ±4.31 µMole) and V_{max} (0.526 ± 0.031) almost remain unaffected as predicted by Michaelis Menten plot and Lineweaver Burk plot. Also the Ki value obtained by Dixon plot to the left of the ordinate (-290 µMole) suggests competitive inhibition. *IVIVC* findings suggest that AUC of GLM was increased around or more than 1.5 fold by SMZ**.** This predicted increase in plasma concentration of GLM is high, suggesting the risk of hypoglycemia when SMZ is coadministered with GLM.

- Caution must be exercised as sulfamethoxazole can potentiate the hypoglycemic effect of glimepiride when given in combination as is predicted by the *in vitro IVIVC* study. Hence coadministration of sulfamethoxazole with glimepiride (to avoid hypoglycemic attack) and CYP2C9 substrates with narrow therapeutic ranges such as phenytoin (an antiepileptic) and warfarin (an anticoagulant) should be monitored. The study also demonstrated that GLM and SMZ can be used as a probe substrate and selective inhibitor of CYP2C9 respectively, which can provide a reliable *in vitro* approach for kinetic studies.
- This interaction study predicts that coadministration of sulfamethoxazole with glimepiride and CYP2C9 substrates with narrow therapeutic ranges such as phenytoin (an antiepileptic) and warfarin (an anticoagulant) should be monitored closely as sulfonamides can potentiate the hypoglycemic effect of sulfonylurea agents when given in combination.

- The study ***"In vitro* assessment of PIJ and POJ on CYP2C9 mediated GLM metabolism *in vitro*"** investigated that pineapple as well as pomegranate juice affected the CYP2C9 activity *in vitro* which suggests the possible interaction of juices with substrates of CYP2C9 in humans. At concentrations 0.5% v/v the percentage inhibition was 61.26% and at 1.5% v/v it was 22.42% for pineapple juice. Similarly for pomegranate juice, at concentrations 0.5% v/v the percentage inhibition was 77.05% and at 1.5% v/v it was 53.98%. Pineapple juice was found to be a potent inhibitor of human CYP2C9 as compared to pomegranate juice. In human liver microsomes, the mean 50% inhibitory concentrations (IC_{50}) for PIJ and POJ versus CYP (glimepiride hydroxylation) were 1.50 ± 0.233 µl and 4.25 ±

0.532µl respectively. Thus, POJ does not significantly alter metabolism of glimepiride as compared to PIJ which suggests its beneficial effects in subjects with type 2 diabetes. From the comparative study or results of Km and Vmax for GLM alone (27.98 ± 2.77 µM, 0.564 ± 0.015 µM/min/mg protein), Km, Vmax and IC_{50} for GLM in presence of PIJ (47.50 ± 10.99 µM, 0.492 ± 0.038 µM/min/mg protein, 1.50 ± 0.23 µl (0.75% v/v)) Km, Vmax and GLM in presence of POJ (34.00 ± 4.96 µM, 0.50 ± 0.021 µM/min/mg protein, 4.25 ± 0.53µl (2.12% v/v)), it was observed that PIJ exerts significant competitive inhibitory effect than POJ on GLM metabolism.Our results supports the surprising finding by Aviram that the sugars contained in POM juice although similar in content to those found in other fruit juices did not worsen diabetes disease parameters in patients but in fact reduced the risk for atherosclerosis. This is because in most juices, sugars are present in free and harmful forms but in POJ juice however the sugars are attached to unique antioxidants, which make these sugars protective against diabetes and atherosclerosis.

- This study demonstrated that the metabolism of GLM was altered by PIJ and POJ. Addition of 10 µl (5% v/v) of pineapple juice resulted in almost complete inhibition. Amongst the fruits evaluated, PIJ showed strong inhibition towards CYP2C9 activity while POJ appears to make minor contributions to the oxidative metabolism of GLIM. One of the ways to control diabetes mellitus is through the diet and it is here that pomegranate juice can play a part. The low inhibitory potential of pomegranate towards GLM *in vitro* metabolism suggests beneficial effects in subjects with type 2 diabetes. Pomegranate juice may be considered as a healthy fruit juice and awaits additional clinical research to further strengthen for its unique antidiabetic effect.
- Pomegranate juice may be considered as a healthy fruit juice and awaits additional clinical research to further strengthen for its unique antidiabetic effect. Although our *in vitro* evidence in favor of using pomegranate juice for diabetics is very promising, extensive studies are required to fully understand its possible contribution to human health before recommending its regular consumption. In addition, the effects of fruit juices on pharmacokinetics of drugs *in vitro* may not

be consistent with those in humans. Therefore further investigations in humans are necessary to elaborate our findings.

- The *in vitro* drug fruit interaction study predicts that pineapple juice is more inhibitory in nature as compared to pomegranate juice. Hence coadministration of juices should be closely monitored in diabetic patients.
- The study **"Simultaneous method development of cocktail substrate assay system for EFV (CYP2B6), DIC (CYP2C9), CHZ (CYPE1), ATV (CYP3A4)"** describes HPLC-PDA method development and its validation in the presence of HLM. The probes CHZ/ATV/DIC/EFV to be used in this cocktail approach were chosen based on their CYP specificity, availability and recommendations in regulatory guidance. The probe substrates selected were EFV (CYP2B6), DIC (CYP2C9), CHZ (CYPE1), ATV (CYP3A4). All the substrates were soluble in common solvent methanol and stable during the analysis i.e., no additional interacting peaks of probe substrate were observed in chromatograms after cocktail incubation. All the peaks of probe substrate 4.08 min for CHZ, 9.76 min for ATV, 10.89 min for DIC, 15.58 min for EFV and their respective metabolite M_1 at 2.58 min for CHZ, M_2 at 4.8 min for DIC, M_3 at 7.9 min for ATV, M_4 at 8.6 min for EFV were well resolved. Glimepiride (40 mcg/ml) was selected as the internal standard of choice as it was stable during the analysis, readily available, was well resolved from CHZ, ATV, DIC, EFV, its peak shape was good (tailing factor at 230 nm 1.25, tailing factor at 247 nm 1.20), and its elution time (12.58 min) was shorter than that of last eluting analyte peak, EFV (15.58 min) saving run time per sample. The method showed a linear calibration curve with correlation coefficients greater than 0.999 for the analytes in the investigated concentration range and absolute recoveries of all analytes were >90%. The acceptable intraday and interday precision were <15% relative standard deviation from nominal values. The lower limit of detection (LLOD) was 1.10 μM for CHZ, 0.92 μM for ATV, 0.88 μM for DIC, and 0.54 μM for EFA, respectively. The lower limit of quantitation (LLOQ) was 1.98 μM for CHZ, 1.85 μM for ATV, 1.28 μM for DIC, and 1.25 μM for EFA, respectively. The enzyme reactions for assessment of CYP2B6, CYP2C9, CYP2E1 and CYP3A4 activities were linear

with 0.5mg/ml HLM concentration and 30 minutes incubation time where less than 20% of the initial substrate was consumed. The K_m and V_{max} values of CHZ/ATV/DIC/EFV determined using the substrate cocktail were in good agreement with individual substrates.

- The developed isocratic LC/UV method has been shown to provide sufficient sensitivity and linear concentration range for the analysis of probe substrate and its metabolites with good resolution from *in vitro* individual incubations as well as cocktail incubations. Overall, the simultaneous development of cocktail substrate assay system for efavirenz (CYP2B6), diclofenac (CYP2C9), chlorzoxazone (CYPE1), atorvastatin (CYP3A4) is simple, uses conventional instrumentation and provides a scope to analyse all cytochrome P450 combination sets continuously in a single run.
- The developed method can be used to improve throughput and cost-effectiveness in preclinical drug studies. Hence these *in vitro* findings can be extrapolated to carry out P450 probe substrate inhibition assays to determine whether an NME inhibits a particular P450 enzyme activity.
- The study **"Evaluation of cocktail substrate assay system for inhibition screening of CYP2B6, CYP2C9, CYP2E1 & CYP3A4 by MCR-706 and MCR-742."** describes that inhibition reactions were evaluated via two approaches i) individual dosing of a substrate (CHZ, ATV, DIC, EFV) and of an inhibitor (KET, FLX, CLP, MCR-706, MCR-742). ii) cassette dosing of substrates (CHZ,ATV,DIC,EFV) combined with individual dosing of inhibitor (KET,FLX,CLP,MCR-706,MCR-742).The method was validated by incubating known CYP inhibitors (clopidogrel, CYP2B6; fluoxetine, CYP2C9 and ketoconazole, CYP3A4; with the individual substrate they were known to inhibit (EFV; DIC; and ATV respectively) and with the substrate cocktail. Both the approaches generated similar IC_{50} values for each CYP isozyme and all measured IC_{50} values were compared with the literature values. CLP, FLX, KET at 1, 50 and 1 µM caused 48.28, 38.92 and 41.76% inhibition of EFV, DIC, and ATV hydroxylation respectively in individual incubation while in cocktail incubation it showed 49.49, 46.385 and 45.106% inhibition respectively. The IC_{50} values of

1.51, 37.95 and 0.88 µM determined with the individual substrates were in good agreement with the IC_{50} values of 1.58, 41.8 and 0.90 µM using the substrate cocktail of EFV/DIC/ATV. The IC_{50} values determined using the individual substrates agreed with the values determined using substrate cocktail. Exception to this agreement with published IC50 values of 0.046, 33, and 0.72 µM is observed for CLP/FLX/KET in this study. This could be due to the use of different substrates or expressed enzyme versus human liver microsomes. The Ki values were also estimated using obtained IC50 values of CLP, FLX, and KET when co incubated with their respective substrate at fixed concentration (at fixed or below its Km values) in individual and cocktail incubation.

- A HPLC-PDA method has been developed for the inhibition screening of the four major human CYP enzymes (CYP2B6, CYP2C9, CYP3A4, CYP2E1) using an *in vitro* individual substrate and substrate cocktail. The IC_{50} values of selective CYP inhibitors (ketoconazole, CYP3A4; fluoxetine, CYP2C9; clopidogrel, CYP2B6) and two new molecular entities (MCR-706 and MCR 742) determined using the substrate cocktail were in good agreement with individual substrates.The developed assay offers a reliable and sensitive screening method for the prediction of the P450 inhibitory potential of new molecular entities using individual and cocktail substrate incubation approach.
- The developed method has the potential to be used for the characterization of P450 enzyme activity in human liver microsomal preparations. In addition, a P450 inhibition profile using this screening method can allow a number of new molecular entities to be screened rapidly for P450 inhibitory potential, which can help in selection of potential drug candidates, and can guide the quantitative prediction of clinical drug interactions.

Publications/ Presentations

1. Optimization of the *in vitro* oxidative biotransformation of glimepiride as a model substrate for cytochrome P450 using factorial design. Dipti B Ruikar and Sadhana J Rajput: DARU Journal of Pharmaceutical Sciences 2012, 20:38; page 1-8.

2. Study Of *In vitro* Pharmacokinetic Behavior Of Glimepiride As A Model Substrate For CYP450 System. Dipti Ruikar , Sadhana Rajput. Presented at NIPER, Mohali, Punjab.

3. *In vitro* evaluation of glimepiride as a model substrate for CYP2C9 system: Preferential inhibition by sulfamethoxazole. Ruikar DB, Rajput SJ. Presented at pharmacy department, NIRMA university, ahmedabad, Gujrat. (**Awarded FIRST prize**)

4. Invitro Evaluation of the Pharmacokinetic Alterations Caused by Sulfamethoxazole on Glimepiride Hydroxylation: Prediction Of The Invivo Drug Drug Interaction From Invitro Data.
D. Deshmukh , S. Rajput , R. Jain, G. Deshmukh , D. Desai. Presented at AAPS, Washigton, USA.

Ruikar and Rajput *DARU Journal of Pharmaceutical Sciences* 2012, **20**:38
http://www.darujps.com/content/20/1/38

DARU Journal of Pharmaceutical Sciences

RESEARCH ARTICLE Open Access

Optimization of the *in vitro* oxidative biotransformation of glimepiride as a model substrate for cytochrome p450 using factorial design

Dipti B Ruikar and Sadhana J Rajput*

Abstract

Background and purpose of the study: Glimepiride (GLM) was chosen as a model substrate in order to determine the kinetic parameters for *in vitro* metabolism via human liver microsomes (HLM). We aimed to optimize the turnover of the substrate by the test system in relation to incubation time and HLM concentration in such a way that it was linearly dependent on time and less than 20% of the substrate was consumed which utilized the lowest amount of the HLM. Further we aimed to report K_m and V_{max} values for GLM.

Methods: Linearity of enzyme reactions in microsomal incubations was assessed by monitoring the effect of incubation time (from 5 to 60 min) and HLM concentration (from 0.2 to 0.75 mg/ml) on metabolite formation of GLM. The ideal conditions for turnover of GLM were justified using 3x3 factorial design. F value was calculated to confirm the omission of insignificant terms from the full-model to derive a reduced- model polynomial equation. The regression equation was used to develop a contour plot that showed turnover rate within the limits of this design. The optimized reaction velocity data was extrapolated to carry out the kinetic studies *in vitro* to generate a saturation curve for the determination of K_m and V_{max} values.

Results: The reaction was found to be linear with respect to both incubation time between 24 and 50 min and HLM concentration between 0.3 to 0.65 mg/ml. The K_m and V_{max} values obtained by nonlinear least squares regression method was found to be 28.9 ± 2.97 μMole and 0.559 ± 0.017 μMole respectively. Lineweaver-Burk plot was also used to estimate K_m and V_{max} which yield value of 29.411 ± 1.25 μMole and 0.571 ± 0.020 μMole/min/mg protein respectively.

Major conclusion: The statistical approach successfully allows for the optimization of reaction time course experiments. The results obtained with linear as well as the nonlinear transformation were found to be in close agreement with each other which shows the best precision for estimates of K_m and V_{max}.

Keywords: Incubation time, Human liver microsomes, Substrate, Turnover rate, Contour plot

* Correspondence: sjrajput@gmail.com
Quality Assurance Laboratory, Centre Of Relevance And Excellence In Novel Drug Delivery System, Pharmacy Department, G. H. Patel Pharmacy Building, Donor's Plaza, The Maharaja Sayajirao University Of Baroda, Fatehgunj, Vadodara 390 002, Gujarat, India

Background

For most drugs, biotransformation is the major route of elimination, and oxidative metabolism by cytochrome P450 (CYP450) enzymes is a common metabolic pathway [1]. More than 90% of oxidative metabolic reactions (phase I) of drugs are catalyzed by enzymes of the CYP450 family present in liver [2]. In order to investigate drug metabolism prior to human exposure, there are a number of options ranging from *in vitro* screening with human enzymes to *in vivo* assessment in experimental animals. Although animal models can provide information about the biochemical potential for drug biotransformation (i.e. identifying the metabolite(s) that can be formed), such models may only indicate what is biologically possible, not what is biologically relevant for human drug exposure? This is due to the well documented interspecies differences in both expression and substrate specificity of drug metabolizing enzyme. Thus human tissue systems called as human liver microsomes have been developed to address the limitations of animal models of drug metabolism [3,4]. The Pharmaceutical Research and Manufacturers of America Perspective (PhRMA) and U.S. Food and Drug Administration (USFDA) guidelines address the specific designs of the studies, to define a minimal best practice for *in vitro* and *in vivo* pharmacokinetic studies targeted to the development [5,6].

Determinations of the initial velocity conditions are important for the accurate investigation of enzyme kinetic parameters. To determine the kinetic parameters for CYP450 substrate metabolism, the turnover of the substrate by the test system needs to be optimized such that it is linearly dependent on time and less than 20% of the substrate is consumed. Also it is desirable to utilize the lowest amount of enzyme in the incubation that yields readily quantifiable metabolite concentrations. A concentration of below 0.5 mg/ml microsomal protein is suggested as the low enzyme concentration would help maintain minimal enzyme binding. The initial rates of drug disappearance in *in vitro* metabolism are to be measured for minimizing any discrepancy caused by the difference in drug concentrations at the start and at the time of measurement [7]. Once the initial velocity conditions have been established, the substrate concentration should be varied to generate a saturation curve for the determination of K_m (substrate affinity of the enzyme) and V_{max} (maximum reaction rate) values.

To evolve an ideal incubation condition it is important to understand the complexity of enzymatic reactions in a more systematic way using established statistical tools such as full factorial design. Thus the usual approach was to start with a screening design including all controllable factors that may possibly influence the experiment, identify the most important ones and proceed with a 3X3 experimental optimization design [8,9].

GLM belongs to second generation sulphonylurea which is being used for the treatment of non-insulin dependent diabetes mellitus (NIDDM), to achieve appropriate control of blood glucose level. In addition, it maintains a better physiological regulation of insulin secretion than other sulphonylurea during physical exercise. GLM has been shown to undergo hepatic oxidative biotransformation via CYP450 system and its metabolism also has been reported using CYP specific species of seven CYP2C9 variants found in Japanese subjects [10-12].

Liquid chromatography with ultraviolet (LC/UV) [13,14], fluorescence [15,16] or mass spectrometry (MS) detection [17,18] has been commonly used for quantitative determination of CYP probe substrates. LC/MS has the advantages of high sensitivity, selectivity and speed. However, LC/MS instrumentation is costly and may not be available for routine analysis in every research laboratory. In addition, the LC/MS-based assays often require the use of different ionization and ion detection modes due to the diverse structure of CYP probe substrate, which creates difficulty and complexity in developing LC/MS methods for simultaneous analysis. Fluorescence and UV are conventional and inexpensive detectors for LC. Fluorescence detectors are very sensitive but respond only to the few analytes that fluoresce. In contrast, many compounds can absorb ultraviolet light. Therefore, LC with UV detection can be used for the analysis of CYP probe substrates and metabolites [19]. The drawback of UV detection is its relatively low sensitivity and selectivity. However, our preliminary results show that the sensitivity of LC/UV is sufficient for the detection of GLM oxidative biotransformation resulting from normal microsomal incubations.

The present investigation justifies using GLM as a model substrate to statistically optimize its oxidative biotransformation *in vitro* within the limits of developed assay design.

Methods

Chemicals and reagents

GLM was received as a gift sample from Cadila Healthcare Ltd., Ahmedabad, India. Nicotinamide Adenine Dinucleotide Phosphate, reduced tetra sodium salt (NADPH), Magnesium chloride ($MgCl_2$) was purchased from Himedia laboratories, India. Ethylene diamine tetra acetic acid (EDTA), dipotassium hydrogen phosphate and potassium dihydrogenphosphate were purchased from S.d Fine-Chem Limited, India. Methanol and Acetonitrile of HPLC grade were purchased from Spectrochem India. All other chemicals and reagents used in this study were of analytical grade.

Microsomal source

A pool of the 50 HLM (0.5 ml at 20 mg/ml), mixed gender, in a suspension medium of 250 mM sucrose was obtained from Xenotech LLC., USA and stored at −80°C in a deep freezer. The frozen microsomes were thawed by placing the vial under cold running water and kept in an ice water bath until use. The total CYP450 content, protein concentrations, and specific activity of each CYP450 isoforms were as supplied by the manufacturer.

Factorial design and optimization

Based on the results obtained in the preliminary experiments, drug concentration, HLM concentration and incubation time were found to be major variables affecting metabolism of GLM. Hence 3X3 factorial design was applied to find the optimized condition for carrying out a reaction time course experiment for GLM's oxidative biotransformation. In all the experiments NADPH concentration was 1 mM and buffer concentration was 50 mM. In this experimental design, GLM in the presence of HLM was incubated in 27 different combinations.

Effect of variables

To study the effect of variables, different batches were prepared by using 3X3 factorial design. Drug concentration (X1), incubation time (X2) and HLM concentration (X3) were selected as three independent variables. The independent variable and their levels are shown in Table 1. The turnover rate (Y1%) was taken as a response parameter as the dependent variable. These three factors were evaluated each at 3 levels and experimental trials were performed for all 27 possible combinations as reflected from Table 2. The values of the factors were transformed to allow easy calculation of co-efficient in polynomial equation. Interactive multiple regression analysis and F statistics were utilized in order to evaluate the response. The regression equation for the response was calculated using the following equation-Response:

$$Y1(\%) = \beta_0 + \beta_1 X1 + \beta_2 X2 + \beta_3 X3 + \beta_4 X1^2 + \beta_5 X2^2 + \beta_6 X3^2 + \beta_8 X1X2 + \beta_9 X1X3 + \beta 10X2X3 + \beta_{11} X1X2X3$$

where Y1 (%) is turnover rate and indicates the quantitative effect of the independent variables X1, X2 and X3, which represent the drug concentration, incubation time and HLM concentration respectively, β0 is the intercept while β1- β11 represents the regression coefficient of the system. To identify the significant terms, the variables having p value > 0.05 in the full model were discarded and then the reduced model was generated for the independent variables [20,21].

The multiple regression was applied using Microsoft excel 2007 in order to deduce the factors having a significant effect on the enzymatic reaction and the best fitting mathematical model was selected. Two dimensional contour plot and three dimensional response surface plot resulting from the equations were obtained by the NCSS software.

Table 1 Factors, their levels, and coded values

	Levels		
Variables	**Low**	**Medium**	**High**
Drug concentration (X1)	10 μmole	20 μmole	30 μmole
Incubation time (X2)	10 min	35 min	60 min
HLM concentration (X3)	0.25 mg/ml	0.5 mg/ml	0.75 mg/ml
Coded values	−1	0	+1

Incubation conditions

To define the optimal conditions for incubation and HPLC analysis, GLM (10 – 30 μMole) was incubated with HLM for 10 to 60 min across a range of microsomal enzyme concentrations (0.25 – 0.75 mg/ml). Briefly the incubation mixtures consisted of 50 mM phosphate buffer (pH 7.4), 10 mM $MgCl_2$, 1 mM EDTA, 1 mM NADPH and 0.5 mg/ml of microsomal protein. In all experiments, GLM was dissolved and diluted serially in methanol and then alcohol was removed by evaporating to dryness. GLM was reconstituted in potassium phosphate buffer (50 mM, pH 7.4) .The tubes were placed into an ice bath and 5 μl of HLM was added and vortexed. Tubes (duplicate) containing the reaction mixture in phosphate buffer and NADPH solution were allowed to equilibrate separately in a shaker incubator at 150 rpm for 5 min at 37°C. The reaction was initiated by adding 20 μl of NADPH immediately to the tubes and incubation carried out for 30 min. The reaction was terminated by the addition of 100 μl ice cold acetonitrile. The tubes were centrifuged at 10,000 rpm (4°C; 10 min), and aliquots of the supernatant were directly injected into an HPLC system. Control incubations were also carried out without HLM, NADPH to confirm metabolism. Wherever necessary the volume was made up to 200 μl with buffer.

HPLC analysis

A reported HPLC method with UV detection [22] was modified to measure GLM in microsomal incubates. The HPLC system consisted of Shimadzu LC 20 AT pump and SPD 20A UV detector, a rheodyne 7725 fixed injector loop (20 μl), Thermo scientific C18 Hypersil BDS column (4.6 x 250 mm, 5 μm) and a Phenomenex C18 guard column (4 × 3 mm). The mobile phase was composed of acetonitrile and 0.1% formic acid (55; 45 v/v). The operating temperature was ambient and flow rate was 1 ml/min. The column eluent was monitored at a wavelength of 228 nm. Under these chromatographic conditions GLM and its metabolite M1 were eluted at 3.6 and 9.3 min, respectively.

Table 2 Different batches with their experimental coded level of variables for full factorial design

Batch no.	X1	X2	X3	X_1^2	X_2^2	X_3^2	X_1X_2	X_1X_3	X_2X_3	$X_1X_2X_3$	% Turnover rate ± (SEM)†
1	−1	−1	−1	1	1	1	1	1	1	−1	5.01(0.44)
2	−1	−1	0	1	1	0	1	0	0	0	6.5(0.21)
3	−1	−1	1	1	1	1	1	−1	−1	1	8.9(0.41)
4	−1	0	−1	1	0	1	0	1	0	0	8.92(0.25)
5	−1	0	0	1	0	0	0	0	0	0	19.91(0.69)
6	−1	0	1	1	0	1	0	−1	0	0	18.01(0.48)
7	−1	1	−1	1	1	1	−1	1	−1	1	33.4(0.76)
8	−1	1	0	1	1	0	−1	0	0	0	37.69(0.91)
9	−1	1	1	1	1	1	−1	−1	1	−1	38.81(0.56)
10	0	−1	−1	0	1	1	0	0	1	0	4.4(0.84)
11	0	−1	0	0	1	0	0	0	0	0	6.1(0.58)
12	0	−1	1	0	1	1	0	0	−1	0	8.45(0.76)
13	0	0	−1	0	0	1	0	0	0	0	8.05(0.51)
14	0	0	0	0	0	0	0	0	0	0	18.91(0.62)
15	0	0	1	0	0	1	0	0	0	0	15.05(0.65)
16	0	1	−1	0	1	1	0	0	−1	0	31.75(0.53)
17	0	1	0	0	1	0	0	0	0	0	38.45(1.03)
18	0	1	1	0	1	1	0	0	1	0	38.15(0.89)
19	1	−1	−1	1	1	1	−1	−1	1	1	3.8(0.75)
20	1	−1	0	1	1	0	−1	0	0	0	5.24(0.92)
21	1	−1	1	1	1	1	−1	1	−1	−1	7.91(0.72)
22	1	0	−1	1	0	1	0	0	0	0	7.56(0.55)
23	1	0	0	1	0	0	0	0	0	0	19.08(0.78)
24	1	0	1	1	0	1	0	0	0	0	14.32(0.43)
25	1	1	−1	1	1	1	1	−1	−1	−1	30.56(0.67)
26	1	1	0	1	1	0	1	0	0	0	35.91(0.48)
27	1	1	1	1	1	1	1	1	1	1	36.42(0.34)

†n = 2.

In vitro metabolism of GLM using HLM

Preliminary experiments showed that the substrate depletion was linear with respect to both time over 50 min and liver microsomal protein concentration (0.3-0.65 mg/ml) at 37°C. Thus a 30 min incubation time and 0.5 mg/ml microsomal protein concentration was selected. Kinetic studies were performed by incubating eight concentrations of GLM (0-100 μMole) in duplicate with HLM.

Determination of K_m and V_{max} for GLM metabolism by nonlinear and linear transformations

For the determination of the apparent Michaelis-Menten constant (K_m) and the maximal velocity of the reaction (V_{max}), plots in relation to the substrate concentration were derived using GraphPad Prism 5 software.

A number of ways of re-arranging the Michaelis-Menten equation ($V = V_{max}\ [S]/K_m + [S]$) have been devised to obtain linear relationships which permit more precise fitting to the experimental points, and estimation of the values of K_m and V_{max}. Hence data for reaction velocities was also evaluated by double reciprocal plot (Lineweaver-Burk equation, $1/V = K_m/V_{max} * 1/[S] + 1/V_{max}$). The intersection points were determined graphically using Microsoft Excel 2007.

Data analysis

In the present study, the disappearance of GLM in the medium incubated at 37°C with HLM in the presence of the NADPH was determined as the percentage of the initial amount of GLM in the medium without incubation. The obtained results were expressed as the turnover rate in percentage wherever necessary. Substrate disappearance velocity was calculated as $[(C_{0,\ initial} - C_{s,\ t\ min})/$ incubation time/CYP concentration], where $C_{0,\ initial}$ is the substrate concentration at time 0 min and $C_{s,\ t\ min}$

is the substrate concentration after 10, 35, 60 min incubation with 0.25, 0.5 and 0.75 mg/ml protein concentration. Metabolite formation velocity (V) was calculated as ($C_{s,\ t\ min}$/incubation time/CYP concentration), where Cs, t min was the metabolite concentration after a 10, 35, 60 min incubation.

Results

Reaction linearity optimization by factorial design

Linearity of enzyme reactions in the *in vitro* human liver microsomal incubations was assessed by monitoring the effect of incubation time (from 10 to 60 min) and protein concentration (from 0.25 – 0.75 mg/ml) on metabolite formation of GLM. Using 3X3 factorial design as shown in Table 2, 27 batches were prepared varying three independent variables such as drug concentration (X1), incubation time (X2) and HLM concentration (X3). The turnover rates as response are recorded in Table 2. The results of the regression output and response of full model and reduced model are represented in Table 3. The equations for full and reduced model are given below.

Full model

$$\begin{aligned} Y1(\%) = {} & 16.522 - 0.903X1 + 14.707X2 + 2.891X3 \\ & - 0.042X1^2 + 6.541X2^2 - 3.107X3^2 \\ & - 0.288X1X2 - 0.263X1X3 \\ & + 0.468X2X3 + 0.02875X1X2X3 \end{aligned} \quad (1)$$

Reduced model

$$\begin{aligned} Y = {} & 16.522 + 14.707X2 + 2.891X3 + 6.541X2^2 \\ & - 3.107X3^2 \end{aligned} \quad (2)$$

As the model was generated by taking only the significant terms from the full model, the results are deduced by interpreting the reduced model. The positive sign for coefficient of X2 and X3 in equation 1 shows that the rate of metabolism increases with increase in incubation time and HLM concentration.

The results of the Analysis of variance (ANOVA) of the second order polynomial equation are given in Table 4. F statistics of the result of ANOVA of full and reduced model confirmed omission of non-significant terms of equation 1. Since the calculated F value (0.6841) was less than the tabled F value (2.74) ($\alpha = 0.05$, V1 = 6 and V2 = 16), it was concluded that the neglected terms do not significantly contribute in the prediction [23]. The goodness of fit of the model was checked by the determination coefficients (R^2). In this case, the values of the determination coefficients (adj R^2) were very high (>90%), which indicates a high significance of the model. All the above considerations indicate an adequacy of the regression model [24,25].

Contour plot

Contour plots are a diagrammatic representation of the values of the response. They are helpful in explaining the relationship between independent and dependent variables. The reduced models were used to plot two dimension contour plot at a fixed level of 0 for X1 respectively, and the values of X2 and X3 were computed between −1 and +1 at predetermined values of the turnover rate.

Figure 1 shows the contour plot drawn at 0 level of X_1 (20 μMole), for a prefixed turnover rate of GLM ranging from 4.0% to 34.6%. The plot was found to be linear for approximate values of 17.60%, 21.00% and 24.40% whereas the approximate values of 10.80%, 14.20% and 17.60% showed somewhat linearly curved segments. The approximate values 7.40% and 34.60% showed inconsistent segments signifying nonlinear

Table 3 Response of Full Model and Reduced Model

	Turnover rate (%)			
Response	Full model		Reduced model	
	X coefficient	P value	X coefficient	P value
X1	−0.903	0.093963003	-	-
X2	14.707	2.935912E-15†	14.708	1.92E-19
X3	2.891	3.72138E-05†	2.921	4.63E-06
$X1^2$	−0.042	0.962269567	-	-
$X2^2$	6.541	1.39313E-06†	6.541	9.21E-08
$X3^2$	−3.107	0.0027451†	−3.107	0.001253
X1X2	−0.288	0.648852013	-	-
X1X3	−0.263	0.706627127	-	-
X2X3	0.468	0.46193583	-	-
X1X2X3	0.028	0.970329444	-	-
Intercept	16.522	7.07592E-11	16.49481481	5.84E-15

†significant terms at p > 0.05.

Table 4 Analysis of variance (ANOVA) for full and reduced models of GLM metabolism

	DF	SS	MS	*F*†	R	R^2	Adj. R^2
			Regression				
FM	10	4380.932	438.0932	94.570	0.9916	0.9834	0.9730
RM	4	4361.916	1090.479	257.590			
			Error				
FM	16	74.119(E1)	4.632				
RM	22	93.134(E2)	4.233				

†SSE2-SSE1 = 93.134 − 74.119 = 19.015.
No. of the parameters omitted = 6.
MS of error (full model) =4.632.
F calculated = (SSE2 −SSE1/no. of parameters omitted)/MS of error (full model) = (19.015/6)/4.632 = 0.684189.
Tabled *F* value = 2.74 ($\alpha = 0.05$, V1 = 6 and V2 = 16).
Where DF indicates degrees of freedom; SS sum of square; MS mean sum of square and *F* is Fischer's ratio.

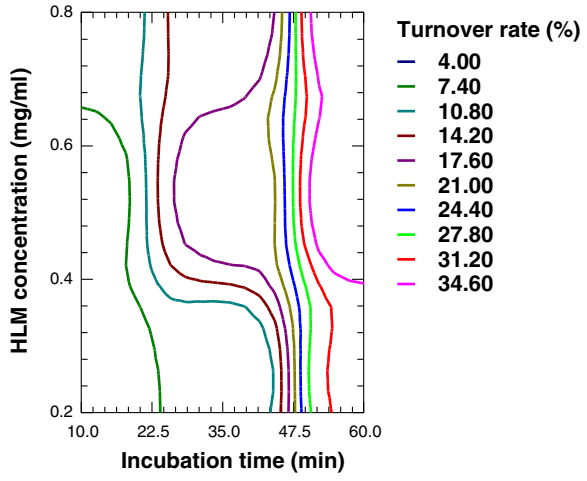

Figure 1 Contour plot for GLM oxidative biotransformation showing effect on turnover rate at 0 level of drug concentration (X1).

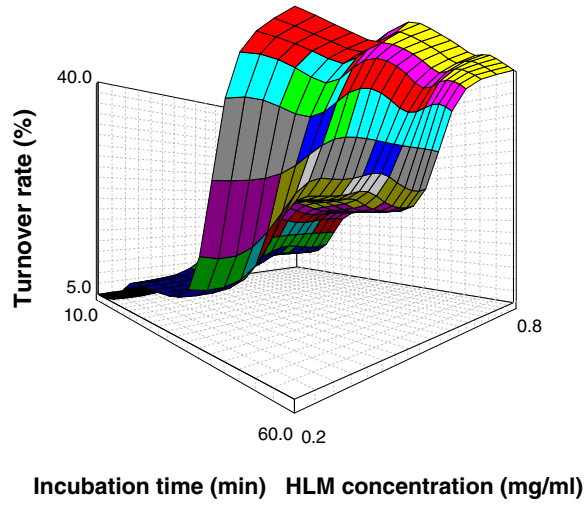

Figure 2 Response surface plot for GLM oxidative biotransformation showing effect on turnover rate at 0 level of X1.

relationship between X_2 and X_3 variables. It was determined from the contour that maximum turnover of about 34.60% could be obtained with X_2 range at 54.4 to 60 min and X_3 at 0.4 to 0.8 mg/ml of protein concentration. As per the PhRMA and USFDA guidelines, it was observed that up to 20% metabolism of the substrate within the limits of this design could be obtained with incubation time (X_2) from 24 to 50 min and protein concentration (X3) from 0.3 to 0.65 mg/ml. Hence for further study, 0.5 mg/ml protein and 30 min incubation time was optimized.

Response surface plot

Three dimensional response surface plot generated by NCSS software represented in Figure 2, depicts the turnover rate of GLM as a substrate. It shows an increase in turnover of the substrate with increase in the protein concentration and incubation time.

Determination of K_m and V_{max} for GLM metabolism by nonlinear and linear transformations

GLM metabolism in the presence of HLM followed Michaelis-Menten kinetics. K_m and V_{max} values obtained by nonlinear least squares regression method was found to be 28.9 ± 2.97 μMole and 0.559 ± 0.017 μMole/min/mg protein respectively. From Lineweaver-Burk plot the K_m and V_{max} values were found to be 29.411 ± 1.25 μMole and 0.571 ± 0.020 μMole/min/mg protein respectively (Figure 3). Thus the values obtained with nonlinear as well as a linear transformation of the data were found to be in close agreement with each other. Each data

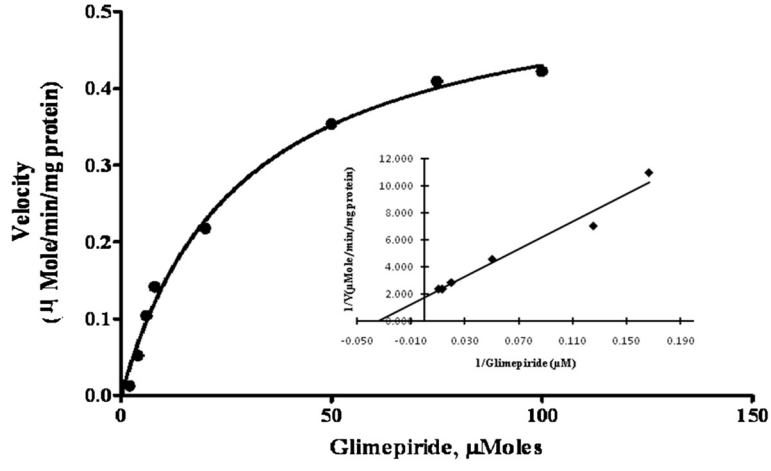

Figure 3 Michaelis-Menten plot for GLM oxidative biotransformation in HLM.

point represents an average of at least two parallel incubations.

Discussion

P450 reaction phenotyping is defined as a set of experiments that aim to define which human cytochrome P450 enzyme(s) is involved in a given metabolic transformation. Such data are useful in the prediction of pharmacokinetic drug-drug interactions and interpatient variability in drug exposure. Any prolonged incubation in a closed *in vitro* system such as liver microsomes can cause formation of metabolites from the primary metabolites of a drug. Inactivation or denaturation of enzymes can become significant over time in the *in vitro* systems. Thus it is of critical importance that initial velocity conditions are defined [7].

The present study conclusively demonstrates the use of a 3X3 factorial design in the optimization of initial velocity conditions affecting turnover of GLM. The derived reduced polynomial equation, contour plot and response surface plot aid in predicting the values of selected independent variables. Contour plot (Figure 1) obtained by applying a computerized optimization process suggested a level of 30 min incubation time (X2) and 0.5 mg/ml protein (X3) as an ideal condition. At this level the turnover rate (%Y) was found to be ranging from 18.91% to 19.91%. Thus the rate of GLM disappearance was linear at the chosen concentrations of substrate using the assay conditions and detection system. However, a decrease in the level of incubation time and protein concentration below the selected level, typically yield nonlinear initial velocities of enzyme activity.

Once the optimal conditions were obtained, the substrate concentration dependence on the rate of metabolite formation was examined. The K_m and V_{max} value was determined by nonlinear regression of a plot of enzyme activity versus substrate concentration. The Michaelis constant, K_m accounts for the concentration of substrate at which half the active sites are filled. Thus, K_m provides a measure of the substrate concentration required for significant catalysis to occur. V_{max} is the rate at which substrate will be converted to product once bound to the enzyme. A substrate concentration around or below the K_m is ideal for determination of competitive inhibitor activity. Hence further inhibition studies are needed to confirm the performance of GLM's oxidative biotransformation *in vitro*.

Conclusions

This study examines the effects of the main control factors and attempts to enhance the turnover rate of GLM's oxidative biotransformation by optimizing these factors using full factorial design. It was possible to optimize the turnover of the candidate drugs within the limits of developed assay design such that all subsequent *in vitro* incubations can be performed using the condition that ensures linearity with time and HLM concentration, and less than 20% of the initial substrate is consumed. Thus the precise information about the effects of each factor on metabolism can be used to flexibly adjust the system performance. The best estimates of K_m and V_{max} values were obtained with linear as well as nonlinear transformation for the enzymatic assay of GLM under initial velocity conditions.

Abbreviations

GLM: Glimepiride; HLM: Human liver microsomes; NADPH: Nicotinamide Adenine Dinucleotide Phosphate, reduced tetra sodium salt; EDTA: Ethylene diamine tetra acetic acid; $MgCl_2$: Magnesium chloride; CYP450: Cytochrome P450; PhRMA: Pharmaceutical Research and Manufacturers of America Perspective; USFDA: U.S. Food and Drug Administration; NIDDM: Non-insulin dependent diabetes mellitus; LC/UV: Liquid chromatography with ultraviolet; LC/MS: Liquid chromatography with mass spectrometry; K_m: Michaelis-Menten constant; V_{max}: Maximal velocity of the reaction; ANOVA: Analysis of variance.

Competing interests

The authors declare that they have no competing interests.

Authors' contributions

DBR carried out the *in vitro* kinetic studies, participated in its design and coordination, performed the statistical analysis and drafted the manuscript. SJR has made substantial contributions for acquisition of data, its interpretation and involved in drafting the manuscript and revising it critically for important intellectual content. All authors read and approved the final manuscript.

Acknowledgements

This work was supported by the research grant provided by All India Council for Technical Education (AICTE - NDF), New Delhi, India. The authors would like to thank Cadila Healthcare Ltd., Ahmedabad, Gujrat, INDIA for providing gift sample of glimepiride.

Received: 29 June 2012 Accepted: 29 August 2012
Published: 10 September 2012

References

1. Rendic S: **Summary of information on human CYP enzymes: human P450 metabolism data.** *Drug Metab Rev* 2002, **34**:83–448.
2. Guengerich F: **Human cytochrome P450 enzymes**. In *Cytochrome P450—Structure, Mechanism, and Biochemistry*. Edited by Paul R. New York: Kluwer; 2005:377–530.
3. Boobis R: **Prediction of inhibitory drug-drug interactions by studies *in vitro***. In *Advances in drug metabolism in man*. Edited by Pacifici M, Fracchia N. Luxembourg: Office for the Official Publications of the European Communities; 1995:513–39.
4. Guillouzo A, Langouët S, Morel F, Fardel O, Abdel-Razzak Z, Corcos L: **The isolated human cell as a tool to predict *in vivo* metabolism of drugs**. In *Advances in drug metabolism in man*. Edited by Pacifici M, Fracchia N. Luxembourg: Office for the Official Publications of the European Communities; 1995:756–82.
5. Bjornsson D, Callaghan T, Einolf J, Fischer V, Gan L, Grimm S, Kao J, King P, Miwa G, Ni L, Kumar G, McLeod J, Obach S, Roberts S, Roe A, Shah A, Snikeris F, Sullivan T, Tweedie D, Vega M, Walsh J, Wrighton A: **The conduct of *in vitro* and *in vivo* drug-drug interaction studies: a Pharmaceutical Research and Manufacturers of America (PHRMA) perspective.** *Drug Metab Dispos* 2003, **31**:815–832.
6. FDA: *Guidance for Industry: Drug Interaction Studies-Study Design, Data Analysis, and Implications for Dosing and Labelling*. 2006. http://www.fda.gov/downloads/Drugs/GuidanceComplianceRegulatoryInformation/Guidances/ucm072101.pdf.

7. Youngill K: *Handbook of essential pharmacokinetics, pharmacodynamics and drug metabolism for industrial scientists*. Springer street New York: Springer; 2001.
8. Bournique B, Petry M, Gousset G: **Usefulness of statistic experimental designs in enzymology: example with recombinant *hCYP3A4* and 1A2.** *Anal Biochem* 1999, **276:**18–26.
9. Niemeijer R, de Boer JH, Gerding K, de Zeeuw A: **Optimisation of the *in vitro* glucuronidation of ibuprofen using factorial design.** *Pharmaceutisch. weekblad. Scientific edition* 1989, **11:**232–235.
10. Kirchheiner J, Roots I, Goldammer M, Rosenkranz B, Brockmöller J: **Effect of genetic polymorphisms in cytochrome p450 *CYP2C9* and *CYP2C8* on the pharmacokinetics of oral antidiabetic drugs.** *Clinical Relevance Clin Pharmacokinet* 2005, **44:**1209–1225.
11. Suzuki K, Yanagawa T, Shibasaki T, Kaniwa N, Hasegawa R, Tohkin M: **Effect of *CYP2C9* genetic polymorphisms on the efficacy and pharmacokinetics of glimepiride in subjects with type 2 diabetes.** *Diabetes Res Clin Pract* 2006, **72:**148–54.
12. Keiko M, Noriko H, Emiko S, Masahiro T, Su-Ryang K, Nahoko K, Noriko K, Ryuichi H, Kazuki Y, Kei K, Toshiyuki M, Yoshiro S, Jun-ichi S: **Substrate-Dependent Functional Alterations of Seven CYP2C9 Variants Found in Japanese Subjects.** *Drug Metab Dispos* 2009, **37:**1895–1903.
13. Frye F: **Stiff: determination of chlorzoxazone and 6-hydroxychlorzoxazone in human plasma and urine by high-performance liquid chromatography.** *J Chromatogr B Biomed Sci Appl* 1996, **686:**291–296.
14. Hansen L, Brosen K: **Quantitative determination of tolbutamide and its metabolites in human plasma and urine by high-performance liquid chromatography and UV detection.** *Ther Drug Monit* 1999, **21:**664–671.
15. Bendriss K, Markoglou N, Wainer W: **High-performance liquid chromatography assay for simultaneous determination of dextromethorphan and its main metabolites in urine and in microsomal preparations.** *J Chromatogr B Biome. Sci Appl* 2001, **754:**209–215.
16. Rege B, March C, Sarkar A: **Development of a rapid and sensitive high-performance liquid chromatographic method to determine CYP2D6 phenotype in human liver microsomes.** *Biomed Chromatogr* 2002, **16:**31–40.
17. Ayrton J, Plumb R, Leavens J, Mallett D, Dickins M, Dear J: **Application of a generic fast gradient liquid chromatography tandem mass spectrometry method for the analysis of cytochrome P450 probe substrates.** *Rapid Commun Mass Spectrom* 1998, **12:**217–224.
18. Yin H, Racha J, Li Y, Olejni N, Satoh H, Moore D: **Automated high throughput human CYP isoform activity assay using SPE-LC/MS method: application in CYP inhibition evaluation.** *Xenobiotica* 2000, **30:**141–154.
19. Tianyi Z, Yongxin Z, Chandrani G: **Simultaneous determination of metabolites from multiple cytochrome P450 probe substrates by gradient liquid chromatography with UV detection.** *Current. Separations* 2003, **20:**87–91.
20. Adinarayana K, Ellaiah P: **Response surface optimization of the critical medium components for the production of alkaline protease by a newly isolated Bacillus sp.** *J Pharm. Pharmaceut. Sci* 2002, **5:**281–287.
21. Huang B, Tsai H, Lee H, Chang S, Wu C: **Optimization of pH independent release of nicardipine hydrochloride extended-release matrix tablets using response surface methodology.** *Int J Pharm* 2005, **289:**87–95.
22. Khan U, Aslam F, Ashfaq M, Asghar N: **Determination of glimepiride in pharmaceutical formulations using HPLC and first-derivative spectrophotometric methods.** *J. Anal. Chem* 2009, **64:**171–175.
23. Bolton S, Bon C: *Pharmaceutical Statistics: Practical and Clinical Applications*. New York: Marcel Dekker; 1997.
24. Cochran W, Cox G: *Experimental Designs*. New York: John Wiley and Sons; 1957.
25. Box G, Hunter W, Hunter J: *Statistics for experimenters: design, innovation, and discovery*. New York: Wiley Interscience; 2005.

doi:10.1186/2008-2231-20-38
Cite this article as: Ruikar and Rajput: Optimization of the *in vitro* oxidative biotransformation of glimepiride as a model substrate for cytochrome p450 using factorial design. *DARU Journal of Pharmaceutical Sciences* 2012 **20**:38.

NIPER Poster Presentation

Study Of *Invitro* Pharmacokinetic Behavior Of Glimepiride As A Model Substrate For CYP450 System

Dipti Ruikar , Sadhana J. Rajput

Abstract

Glimepiride(GLM) is a widely used sulfonylurea drug and indicated as an adjunct to diet and exercise to improve glycemic control in adults with type 2 diabetes mellitus. The drug is completely metabolized by oxidative biotransformation after either IV or oral dose. It undergoes hepatic oxidative biotransformation via CYP450 system *invivo.*In this study glimepiride was chosen as a model substrate to determine the kinetic parameters for invitro metabolism via human liver microsomes. Linearity of enzyme reactions in *invitro* human liver microsomal incubations was assessed by monitoring the effect of incubation time (from 5 to 60 min) and protein concentration (from 0.2 to 1mg/ml) on metabolite formation of GLM.For subsequent analysis , an incubation time of 30 min and 0.5mg/ml protein concentration was used. Under these conditions the reaction is linear with respect to both incubation time and protein concentration. The overall metabolism of GLM was determined as disappearance of parent drug from an incubation mixture using HPLC with UV detection. In addition it is desirable to determine the initial rates during the early time points, when a significant decrease in enzyme activity is expected over time. Thus construction of Michaelis Menten plot is necessary to determine reaction kinetics in terms of Km and Vmax. Reaction rate was determined at different drug concentrations , typically spanning a range from 2µM to 100µM. The Km and Vmax values obtained by non linear least squares regression method were found to be 28.9 ± 4.3 µmole and 0.559 ± 0.031 µmole/min/mg protein. The double reciprocal plot (Lineweaver Burk plot) was also used to estimate the Km and Vmax values which were found to be 29.411 µMole and 0.571 µMole/min/mg protein. Thus the values obtained with nonlinear as well as linear transformation of the data were found to be nearly close.

NIRMA poster presentation

Invitro evaluation of glimepiride as a model substrate for CYP2C9 system: Preferential inhibition by sulfamethoxazole

Ruikar DB, Rajput SJ

Abstract

Accumulating evidence indicates that CYP2C9 ranks amongst the most important drug metabolizing enzymes in humans. Due to the role of CYP2C9 in drug metabolism, it is important to evaluate the kinetic behavior of CYP2C9 substrates and their potential to undergo inhibiton with concomitant drugs. Glimepiride (GLM) is a widely used sulfonylurea drug which undergoes oxidative biotransformation via CYP450 (2C9) after either IV or oral dose. In this study glimepiride was chosen as a model substrate to determine the kinetic parameters for *invitro* metabolism via human liver microsomes. The present study also investigates and compares the impact of GLM as a substrate and sulfamethoxazole (SMZ) as inhibitor on *invitro* kinetic parameters, namely Km,Vmax, IC50 and Ki on the prediction accuracy of the reported tolbutamide-sulfamethoxazole *invitro* drug interaction model. Thus the clinical significance of potential CYP2C9-mediated drug–drug interaction of glimepiride with sulfamethoxazole in presence of human liver microsomes was established. The overall metabolism of GLM in presence and absence of SMZ was determined as disappearance of parent drug from an incubation mixture using HPLC with UV detection at 228nm. The Km and Vmax values obtained by non linear least squares regression method were found to be 28.9 ± 4.3 µmole and 0.559 ± 0.031 µmole/min/mg protein. Further the studies conducted by using constant concentration of SMZ on the MM kinetics of glimepiride were used to assess the nature of inhibition. The findings suggested the competitive nature of inhibition as Km was increased (32.26 µMole)and Vmax (0.526 µMole/min/mg protein) almost remained unaffected.

AAPS poster presentation

Invitro Evaluation of the Pharmacokinetic Alterations Caused by Sulfamethoxazole on Glimepiride Hydroxylation: Prediction Of The *In vivo* Drug Drug Interaction From *In vitro* Data.

R Jain[1], D. Deshmukh (Ruikar)[1] , S. Rajput[1] , G. Deshmukh[2] , D. Desai[1]

1 Maharaja Sayajirao University of Baroda, 2 Sumandeep Vidyapeeth

Abstract

Purpose.
To evaluate the use of glimepiride as a model substrate and sulfamethoxazole as an inhibitor for CYP2C9 invitro using human liver microsomes and establish invivo clinical significance of potential CYP2C9 mediated drug-drug interaction of glimepiride with sulfamethoxazole from invitro data.

Methods.
Linearity of enzyme reactions in invitro human liver microsomal incubations was assessed by monitoring the effect of incubation time (5 to 60 min) and protein concentration (0.2 to 1 mg/ml) on metabolite formation of Glimepiride. An incubation time of 30 min and 0.5mg/ml protein concentration was found to be linear with respect to both incubation time and protein concentration. Incubation mixtures contained 100mM potassium phosphate buffer (pH 7.4), 1Mm EDTA,0.5mg/ml protein and NADPH. Reactions were initiated by adding 10mM NADPH after a 5 min incubation at 37°C. After 30 min , the reactions were terminated using 100µl ice cold acetonotrile. The samples were centrifuged and supernatant was directly injected for LC/UV analysis at 228nm. The overall metabolism of glimepiride in presence and absence of sulfamethoxazole was determined as disappearance of parent drug from an incubation mixture.

Results.
Km and Vmax values for glimepiride metabolism obtained by nonlinear least squares regression method were found to be 28.9(4.3) µMole and 0.559 (0.031) µMole/min/mg protein respectively. The results of present study showed that sulfamethoxazole compeitvely inhibited CYP2C9 mediated metabolism of glimepiride with a Ki value of 297.17 µMole. With concentrations ranging from 50 to 500 µMole , sulfamethoxazole exhibited a selective inhibitory effect on CYP2C9 mediated glimepiride metabolism with an apparent IC50 value of 400 µMole and Ki value of 297.17 µMole in human liver microsomes.

Conclusion.
Results suggested the competitive nature of inhibition by sulfamethoxazole as Km was increased (32.26 µMole) and Vmax (0.526 µMole/min/mg protein) almost remained unaffected. The present study also investigates and compares the impact of glimepiride as a substrate and sulfamethoxazole as inhibitor on invitro kinetic parameters, namely Km,Vmax, IC50 and Ki on the prediction accuracy of the reported tolbutamide-sulfamethoxazole invitro drug interaction model.